FINAL REPORT ON THE

WINTER 1981 TRAFFICABILITY TESTS OF THE USCGC POLAR SEA

ICE INDUCED VIBRATION MEASUREMENTS AND DEVELOPMENT OF A MODEL FOR ICEBREAKING EXCITATION FORCES

VOLUME IXB - CALCULATIONS AND ANALYSIS

10 March 1982

by

I.F. Glen
I. Majid
G. Tam
B. Menon

Sumbitted to

TRANSPORTATION DEVELOPMENT CENTRE
1000 Sherbrooke Street, West
Montreal, Quebec, H3A 2R3

Submitted by

ARCTEC CANADA LIMITED
311 Leggett Drive
Kanata, Ontario, K2K 1Z8

Library and Information Centre/ Centre de Documentation (GSLA) LE
SEP 6 1983
Transport Canada / Transports Canada

The Project Team consisted of:

°I. Glen
°I. Majid
°B. Menon
°G. Tam
°D. Blair

The contents of this report reflect the views of the contractor and not necessarily the official views of the Transportation Development Centre.

REPORT DOCUMENTATION FORM

1. Transport Canada Report No.	2. TDC Project No.	3. Recipient's Catalogue No.
TP 4081E	4254, 4255, 4256	

4. Title and Subtitle
Winter 1981 Trafficability Tests of the USCGC POLAR SEA, Volume IXB: Ice Induced Vibration Measurements and Development of a Model for Icebreaking Excitation Forces - Calculations and Analysis

5. Report Date
MARCH 1982

6. Performing Organization Report No.
792C

7. Author(s)
I.F. Glen, I. Majid, G. Tam and B. Menon

8. Transport Canada File No.
D1460-156-2

9. Performing Organization Name and Address
Arctec Canada Ltd.
311 Leggett Drive
Kanata, Ontario
K2K 1Z8

10. DSS File No.
17ST.T8200-0-0516

11. DSS or Transport Canada Contract No.
1ST80-00073

12. Sponsoring Agency Name and Address
Transportation Development Centre (TDC)
1000 Sherbrooke Street West
P.O. Box 549, Place de l'aviation
Montreal, Quebec H3A 2R3

13. Type of Report and Period Covered
Final Nov.1980-Oct. 1981

14. Sponsoring Agency Code
TDC 4254, 4255, 4256

15. Supplementary Notes
(i) Volume IXA - Final Report
(ii) Volume IXC - Records & Data

16. TDC Project Officer
I.M. Bayly

17. Abstract

The vibratory response of the USCGC POLAR SEA to ice induced loads during the trafficability tests of winter 1981 is presented. Vibratory trials were carried out from 6 January to 11 February 1981. The data recorded on magnetic and video tapes consists of vertical, athwartship and fore and aft accelerations at various locations within the ship, strain measurements at frames 161 and 171, ship's speed, ice conditions, etc. Post trail analysis includes calculation of the fundamental frequencies of the hull girder up to the 5th and 6th modes, comparison of calculated frequencies with those recorded by the accelerometers, assessing the propulsion train vibrations in the longitudinal mode and formulation of a mathematical model for extracting the forcing function causing the ship board vibrations. A procedure for retrieving the raw data collected during the trails is also presented.

18. Key Words	19. Distribution Statement
Full scale trials, Ice induced vibrations, Mathematical model icebreakers	Limited number of copies available from TDC

20. Security Classification (of this report)	21. Security Classification (of this page)	22. No. of Pages	23. Price
nil	nil	52	nil

FORMULE DE DOCUMENTATION POUR RAPPORT

1. Nº du rapport Transports Canada	2. Nº de l'étude — CDT	3. Nº de catalogue du destinataire
TP 4081E	4254, 4255, 4256	

4. Titre et sous-titre	5. Date du rapport
Winter 1981 Trafficability Tests of the USCGC POLAR SEA, Volume IX B: Ice Induced Vibration Measurements and Development of a Model for Icebreaking Excitation Forces - Calculations and Analysis	mars 1982
	6. Nº du rapport de l'organisme exécutant: 792C

7. Auteur(s)	8. Nº de dossier Transports Canada
I.F. Glen, I. Majid, G. Tam and B. Menon	D1460-156-2

9. Nom et adresse de l'organisme exécutant	10. Nº de dossier — ASC
Arctec Canada Limitée 311 Leggett Drive Kanata, Ontario K2K 1Z8	17ST.T8200-0-0516
	11. Nº de contrat — ASC ou Transports Canada: 1ST80-00073

12. Nom et adresse de l'organisme parrain	13. Genre de rapport et période visée
Centre de développement des transports (CDT) 1000 o., rue Sherbrooke C.P. 549, Place de l'aviation Montréal, Québec H3A 2R3	Final nov.1980-oct. 1981
	14. Code de l'organisme parrain: CDT 4254, 4255, 4256

15. Remarques additionnelles	16. Agent de projet — CDT
(i) Volume IXA - Final Report (ii) Volume IXC - Records & Data	I.M. Bayly

17. Résumé

Ce rapport décrit le comportement vibratoire sous l'action des glaces de la coque du brise-glace américain Polar Sea lors de son périple dans les glaces arctiques durant la période du 6 janvier au 11 février 1981. Les données recueillies lors des essais du comportement vibratoire ont été enregistrées sur bandes magnétiques et vidéo, notamment les accélérations verticales, longitudinales et transversales en divers endroits de la coque, les déformations au droit des membrures 161 et 171, les vitesses, les conditions de glace, etc. L'analyse qui a suivi ces essais comporte le calcul des fréquences de résonance de la coque jusqu'au 5e et 6e modes de vibration, la comparaison des fréquences calculées et celles effectivement enregistrées, l'évaluation des vibrations longitudinales du système de propulsion et d'entraînement du navire et l'élaboration d'un modèle mathématique permettant de connaître les fonctions sous lesquelles se présentent les forces variables à l'origine des vibrations ressenties à bord. Enfin, une méthode permettant de se retrouver dans la masse de données brutes recueillies à bord est présentée dans le rapport.

18. Mots-clés	19. Diffusion
Essais en vraie grandeur, vibrations sous l'action des glaces, modèle mathématique, brise-glace	Nombre limité de copies disponibles au CDT

20. Classification de sécurité (de ce rapport)	21. Classification de sécurité (de cette page)	22. Nombre de pages	23. Prix
aucune	aucune	52	aucun

TABLE OF CONTENTS

VOLUME IXB

DETAILS OF CALCULATIONS AND ANALYSIS

APPENDIX A - THE PROPOSED TEST PLAN

APPENDIX B - NATURAL FREQUENCIES AND MODE SHAPES

- B.1 - Introduction
- B.2 - Verification of GBRP
- B.3 - Free Vibration Analysis of Ship Hull
- B.4 - Estimation of Propulsion System Longitudinal Vibration Frequencies
- B.5 - Input Preparation for GBRP
- B.6 - References

APPENDIX C - FULL SCALE DATA REDUCTION

- C.1 - Objectives
- C.2 - Methodology
- C.3 - Results of Data Reduction
- C.4 - Procedure for Accessing Data

APPENDIX D - ANALYSIS OF ACCELERATION DATA

- D.1 - Acceleration Profiles of Hull Structure
- D.2 - Acceleration Spectrum Analysis
- D.3 - Conclusions

APPENDIX E - METHOD OF EXTRACTING FORCE SPECTRA FROM MEASURED RESPONSE SPECTRA

- E.1 - Basic Theoretical and Physical Considerations
- E.2 - Derivation of Force from Response Based on Modal Analysis
- E.3 - Example Calculation
- E.4 - Need for Experimental Validation of Transfer Function
- E.5 - Softwares and Input Data for Computation
- E.6 - Selection of Cases and Data Reduction
- E.7 - Results of Analysis
- E.8 - References

APPENDIX A

THE PROPOSED TEST PLAN

The test plan as originally planned and set out is included herein as a reference when assessing the degree to which objectives have been met.

A.1 THE PROPOSED TEST PLAN

Recordings are to be made in both open water and in ice-covered waters. In open water, a section of recording in calm seas is desirable to serve as a 'reference level' to compare with response when in ice. Data points at several propeller speeds and/or pitches are required. Since the bollard tow tests must be carried out in relatively light seas, and since a number of speeds will be employed, it is anticipated that this will serve as a useful exercise from the vibratory response point of view. Other conditions may present themselves in the calm waters of Puget Sound and the Strait of Juan de Fuca, provided that rudder movements are kept to a minimum, and the very thin grease and pancake ice forming just below the ice edge will suppress the sea without offering any external source of vibratory excitation.

It is also intended to gather data in a heavy seaway during the first part of the trip. The North Pacific, and particularly areas such as Unimak Pass can usually be relied upon to provide suitable conditions at that time of year. Some slamming may be expected to occur, providing a different type of excitation for comparison with that provided by ice encounter.

The most important data will be taken in ice-covered waters. Three specific types of encounter may be defined:

i. "white noise" excitation during level icebreaking.
ii. "unit impulse" excitation during discrete encounters with floes or ridges, where such parameters as vessel speed, impact location, and characteristics of impacted ice may be well defined.
iii. excitation at "blade rate" provided by propeller ice milling.

Although intentional ice milling incidents and imprudent encounters with multi-year floes or other ice features will not be undertaken, it is expected that they will occur as a matter of course during transit from the southern ice edge to Point Barrow and beyond. Level icebreaking opportunities should also be plentiful, and during the planned controlled tests to measure icebreaking resistance (to be carried out by ARCTEC Inc.), systematic variation of such parameters as shaft speed and propeller pitch, vessel speed, ice thickness, etc. will provide opportunities to assess the dependence of the vibratory response on these various inputs.

From the time the ice edge is encountered, the recorders will be run continuously, as long as the vessel is underway. (Due to the many conflicting requirements placed upon the vessel, the average daily steaming time is unclear). Pauses will be made only to change magnetic tapes, which can be accomplished in approximately ten minutes. In so far as is possible, tape changes will be timed so as not to miss important data.

Limited use will be made of the oscillograph aboard the vessel, since time domain analysis of the acceleration data without the benefit of significant post-test processing and filtering is somewhat futile. The major use of this device may be to ensure correct operation of accelerometers, and to display the strain gauge or propulsion system signals. Judicious use should be made of the oscillograph, however, since continuous recording would be of limited value and in fact would consume far greater quantities of expensive light-sensitive paper than have been provided for.

Instead, our experience has underlined the importance of a well-planned and carefully kept logging system, from which the incidents of most interest can be quickly extracted during analysis. The use of the Systron Donner time code reader and search unit greatly facilitates this task. Sample data sheets, test execution outline and test sheets for the proposed tests follow.

USCGC POLAR SEA
TEST EXECUTION OUTLINE

TEST NO.	TITLE
T-1	Level Ice Continuous Motion Operations
T-2	Response While Turning in Level Ice
T-3	Vibratory Response Backing and Ramming
T-4	Response During Impact
0.1	Open Water Vibration Response - Calm Water
0.2	Open Water Vibration Response - Bollard
0.3	Open Water Response Seaway
0.4	High Power Crash Reversal
0.5	Response While Turning in Open Water
C-1	Calibration of Masthead and Aft Overside LLTV
C-2	TV Overside Camera Calibration

TEST NO. T-1

CHECK COMPLETED

USCGC POLAR SEA

TEST EXECUTION OUTLINE

TITLE

Level Ice Continuous Motion Operations

OBJECTIVE

To measure the vibratory response of the vessel while proceeding at steady forward speed and course in various level ice conditions.

PROCEDURE

Record for as long as possible when ship breaking level ice in continuous mode.
At least 3 significantly different ship powers are desired in at least 3 ice thicknesses. (If possible, obtain photos of track behind ship from helicopter.)
Masthead TV on one VTR alternate side TV's on other VTR to provide ice thickness measure and snow cover.
Operation of portable analyzer required.
Note on log (one voice channel) any significant changes in ice conditions (e.g. ridge frequency increase, leads) or action which would increase likelihood of milling. Note (subjectively) personal observation of ship motion during tests.

SHIP REQUIREMENTS

Steady power setting for reasonable period. At least 3 speeds in 1m ice thickness. Minimum rudder angle.

REMARKS

This is a key test. It will happen in the middle of continuous recording. Identification in log of voice tape, when the ship enters relatively level rigid-free ice, will greatly assist analysis.

TEST NO. T-2

CHECK
COMPLETED

USCGC POLAR SEA

TEST EXECUTION OUTLINE

TITLE

Response While Turning in Level Ice

OBJECTIVE

To record response in turning in ice when symmetry is destroyed.
and probability of milling of ice increases.

PROCEDURE

As for C-1.
Note demanded rudder angle.
Note time rudder commands given.
Record other observations such as
- heel angle
- observe track for milling
portable analyzer to be used on shaft system, etc.

SHIP REQUIREMENTS

Steady power in turn.
At least 90° head change.
Steady rudder angle.

REMARKS

This test was done on an opportunity basis with ARCTEC Incorporated.

TEST NO. T-3

CHECK COMPLETED

USCGC POLAR SEA

TEST EXECUTION OUTLINE

TITLE	Vibratory Response to Backing and Ramming
OBJECTIVE	To note the hull vibration during difficult icebreaking rams.
PROCEDURE	Record continuously as we are interested in response throughout the cycle (backing, acceleration, etc.). On some runs go outboard, observe and record ice milling during backing. Note obvious engine-generated vibration (note times when boosts occur). Record with portable pick-up during at least 5 typical sequential rams. Obtain good sample of head-on and oblique rams.
SHIP REQUIREMENTS	Controlled rams (ridges, etc.) as stated in ARCTEC Incorporated test requirements. Steady speed.
REMARKS	Anticipate different response during back-up, acceleration.

TEST NO. T-4

CHECK
COMPLETED

USCGC POLAR SEA

TEST EXECUTION OUTLINE

TITLE

Response During Impact

OBJECTIVE

To record the response during impact with (multi-year) floes, etc.

PROCEDURE

Continuous recording, noting situations when ship is proceeding at speed in thin ice or open water and strikes ice edge or ridge obliquely or ahead.
Ship should attempt to strike such features on side of TV camera at different locations on hull from stem to midships and at different speeds.
Reflected (double impacts)of value.
Set VTR to 1 hour setting just prior to ram.
Record using portable recorder during several impacts and reflections.

SHIP REQUIREMENTS

Controlled impact with ice features at various speeds and locations.

REMARKS

This is a key set of data.
Obtain as much as possible.

TEST NO. 0.1

CHECK COMPLETED

USCGC POLAR SEA

TEST EXECUTION OUTLINE

TITLE

Open Water Vibration Response - Calm Water

OBJECTIVE

To establish the ice-free vibratory response of the ship at a number of ship speeds in calm water.

PROCEDURE

With the ship proceeding on a straight course at steady speed in open water (less than SS2-calm) record the response of the accelerometers over a period of 15 minutes.
The portable vibration pick-up should also be deployed to the shaft and thrust bearings.
This to be performed at each of at least 3 RPM settings up to full power.

SHIP REQUIREMENTS

Steady power and speed.
No throttle changes during reading.
Minimum rudder movement.
Any change in operating condition to be reported to test team and logged.

RPM settings of 20%, 50%, 70%, and 100% full speed desirable.
Repeat during Bollard Tests also highly desirable (see separate sheet).
With diesels only and repeat with all prime movers (gas turbines) desirable.

REMARKS

Use voice channel to note any unusual events, sea state, wind direction.
Have bridge liaison to assess rudder usage.
Side video not necessary.

TEST NO. 0.2

CHECK
COMPLETED

USCGC POLAR SEA

TEST EXECUTION OUTLINE

TITLE

Open Water Vibration Response - Bollard

OBJECTIVE

To establish the vibratory response of the ship in the overload condition in ice-free water.

PROCEDURE

During the bollard tow tests when steady thrust is obtained, record the response for 15 minutes. Record populsion system response with portable system or as long as constant thrust is held.
Record for each power setting tested.

SHIP REQUIREMENTS

1. As required for bollard tests.
2. To report any changes in steady state operating conditions.

REMARKS

Note any unusual external influences including any 'snatching' in tow line, etc.

I believe the Bollard Test has been completed and so this test will not be done.

TEST NO. 0.3

CHECK COMPLETED

USCGC POLAR SEA

TEST EXECUTION OUTLINE

TITLE	Open Water Response Seaway
OBJECTIVE	To measure the base vibratory response in a seaway.
PROCEDURE	Record for a period of at least 15 minutes during transit in open water with a sea running. Note sea conditions, heading, rudder use, etc. Repeat for as many sea states, speeds as possible. Note any slamming or excessive motions which may cause propeller emergence.
SHIP REQUIREMENTS	Steady power and speed. No throttle changes. Minimum rudder movement.
REMARKS	On an opportunity basis.

TEST NO. 0.4

CHECK
COMPLETED

USCGC POLAR SEA

TEST EXECUTION OUTLINE

TITLE	High Power Crash Reversal
OBJECTIVE	To measure the ice-free response at low speed and high power.
PROCEDURE	Record everything including portable pick-up at several points during a number of open-water crash reversals throughout cycle including 10 minutes minimum record before astern thrust is ordered.
SHIP REQUIREMENTS	Proceeding at full power (preferred) in open water. Apply sudden astern power as in emergency crash reversal. When vessel is stationary, apply full ahead power until steady speed is obtained. Repeat at several initial power settings and astern power settings.
REMARKS	Must be introduced via ARCTEC Incorporated during Seattle - Nome leg.

TEST NO. 0.5

CHECK
COMPLETED

USCGC POLAR SEA

TEST EXECUTION OUTLINE

TITLE

Response While Turning in Open Water

OBJECTIVE

To record response while turning in open water.

PROCEDURE

Record during steady turn.
Note demanded rudder angle.
Observe sea state, wind direction, heel angle, etc.
Use portable analyzer

SHIP REQUIREMENTS

Steady power in turn.
At least 90° heading change.
Steady rudder angle.

REMARKS

This test was done on an opportunity basis with ARCTEC Incorporated.

TEST NO. C-1

CHECK
COMPLETED

USCGC POLAR SEA

TEST EXECUTION OUTLINE

TITLE	Calibration of Masthead & aft overside CCTV
OBJECTIVE	To record calibration of ARCTEC Incorporated TV Systems.
PROCEDURE	During calibrations of ARCTEC Incorporated TV Systems record on tape. Make voice channel notation as required. Produce overlay grid for masthead monitor for use onboard.
SHIP REQUIREMENTS	As stated by ARCTEC Incorporated, but must include being stationary in level ice.
REMARKS	If this is not scheduled during ACL onboard phase, it will be acquired after trials from ARCTEC Incorporated tapes.

TEST NO. C-2

CHECK COMPLETED

USCGC POLAR SEA

TEST EXECUTION OUTLINE

TITLE	TV Overside Camera Calibration
OBJECTIVE	To develop a grid with which to assess, via the TV film, the location of ice impacts.
PROCEDURE	With the ship stationary in level ice proceed to the ice and mark out using a tape and any suitable TV visible line/rod, a grid of one ice lines which are perpendicular to the ship centreline. At points measured from the bow (frame on displacement stations), record this calibration on video tape as well as marking on a screen overlay a line parallel to the ship $\mathbb{C}_L$ and some constant distance off should also be drawn. The waterline (if hidden) must be marked by moving a pole against the hull and measuring distance to point on pole that is visible on screen.
SHIP REQUIREMENTS	Stationary close alongside level ice of sufficient thickness to support personnel. Minimum ice disturbance on side being calibrated. Personnel to assist. Two-way communication with lab.
REMARKS	May be done in dark using flashlight shone to camera so long as communications are good. See reverse for illustration.

T.V. MONITOR

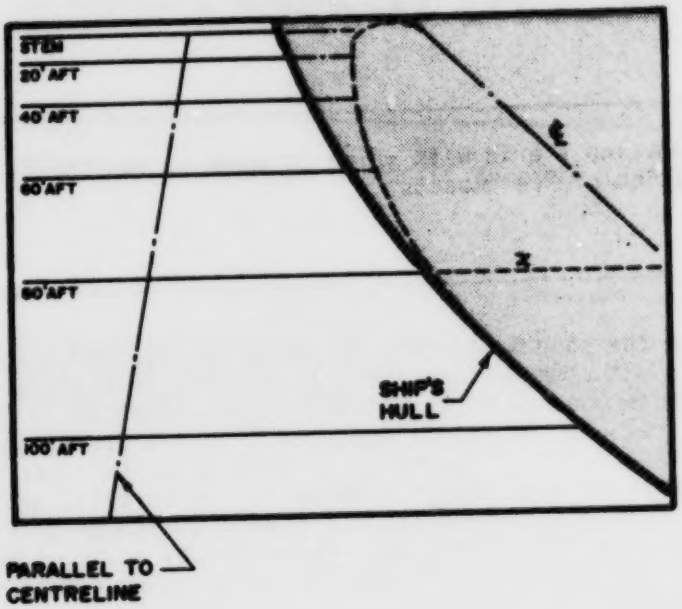

WATERLINE OFFSETS (π)

DRAFT	DISTANCE FROM STEM *					
24						
28						
30						
32						

* STEM IS POINT WHERE BOW CUTS ICE AT THE WATERLINE AT WHICH SHIP IS SITTING.

APPENDIX B

NATURAL FREQUENCIES AND MODE SHAPES

B.1 INTRODUCTION

As a result of the rapid development of high-speed automatic digital computer systems, a number of computer programs have been developed, in the past several years, for ship vibration analysis. Reed and Burnside [1], in their paper presented a comprehensive review on the computer techniques and general information on computer programs for use in ship vibration analysis and design.

In this study, the computer program GBRP (General Bending Response Program) developed at the US Naval Ship Research and Development Center was used for the free vibration analysis of the ship. The choice of this program is due to its availability and the recommendation from the Defence Research Establishment Atlantic.

Briefly, the program solves a system of finite-difference equations which approximate the boundary-value problem representing the motion of a vibrating non-uniform mass-spring system such as a ship hull or shafting in bending. The program calculates natural frequencies and mode shapes and the response to specified harmonic driving forces and moments.

The ship hull is assumed to vibrate like a non-uniform, continuous, free-free beam with equivalent mass, elastic and inertial properties per unit length. The physical parameters for completely defining the system are the cross-sectional elastic properties including mass per unit length, bending compliance, and shear compliance. These physical parameters are calculated from the ship plans and other information.

This section presents the free vibration analysis of ship hull and the shafting for USCGC POLAR SEA using the finite-difference computer program GBRP. In the analysis of the ship hull, the treatment included vertical, horizontal as well as longitudinal vibration. As for the propeller shafting, only the longitudinal mode vibration was examined.

B.2 VERIFICATION OF GBRP

The computer program GBRP (General Bending Response Program) was developed by US Naval Ship Research and Development Center. Verifications of this program code were reported in References [2 and 3].

The computer program was installed on Control Data NOS Cyber 70 Series computer systems. Although it was not our main objective to verify the program code, it is always a good practice to test the program in order to establish some level of confidence.

Forced (Nonharmonic) Vibration Application:

i. Problem 1: Simple Harmonic Oscillator, Response to Rectangular Impulse
ii. Problem 2: Response of a Spring-Mass System to Rectangular Impulse.

Longitudinal Natural Frequency Calculation:

iii. Problem 3: Uniform Free/Free Beam
iv. Problem 4: Uniform Fixed/Free Beam.

The first two problems considered were identical to those Henderson [1] used to test the GBRP capability for transient response. The purpose of these re-runs is to check the validity of the reallocated code. The next two problems were to test the GBRP capability for natural frequency calculations.

Sample Problem 1

For convenience the following physical details have been reproduced from Reference [2]. The mechanical system is shown in Figure B.1(a). The transient force, $F(t)$, represents a constant 0.5 lb force acting on the system for 0.2 seconds. The mass,

$$M = 1.0 \frac{\text{lb.in}}{\text{sec}^2}$$

the spring constant, k = 3.4 lbs/in., the damping constant,

$$c = 0.6 \frac{\text{lb-sec}}{\text{in}}$$

and the natural frequency of this system is

$$\frac{1}{2\pi}\sqrt{\frac{k}{m}} = 0.4613\text{Hz.} \qquad (m \text{ denotes mass/unit length})$$

The input data for the GBRP was prepared through the use of standard GBRP data formats as provided in Reference [2] and is shown in Exhibit B.1. We have successfully reproduced the same results as those presented in Reference [2]. The program results are included in Annex 2, Volume IXC.

The analytical solution for this problem can be obtained from the formula:

$$Z(t) = \frac{F_o}{MW_o^2}\left[\Psi(t) - \Psi(t-\tau)\, U(t-\tau)\right] \qquad (B.1)$$

where F_o = magnitude of the force
M = mass
$W_o = \sqrt{k/m}$
$\Psi(t) = 1 - e^{-bt}\left[\cos \omega t + \frac{b}{\omega} \sin \omega t\right]$
with $b = c/2M$

$$U(t-\tau) = \begin{cases} 0 , & t < \tau \\ 1 , & t > \tau \end{cases}$$

with τ is the impulse duration

FIGURE B.1

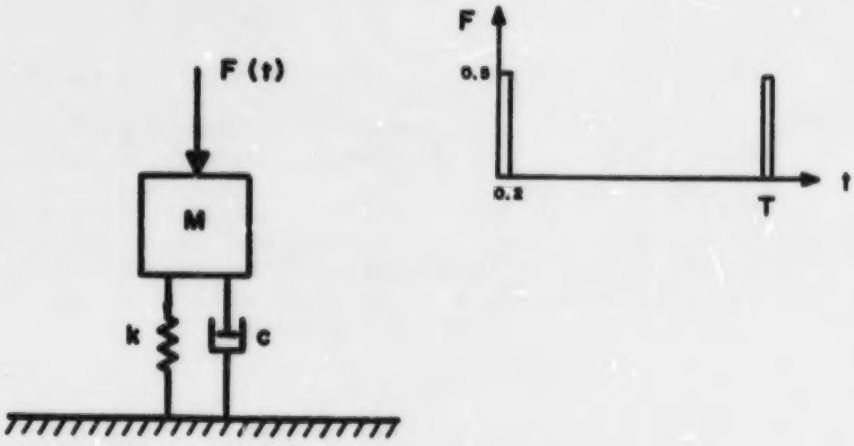

(a) SIMPLE HARMONIC OSCILLATOR

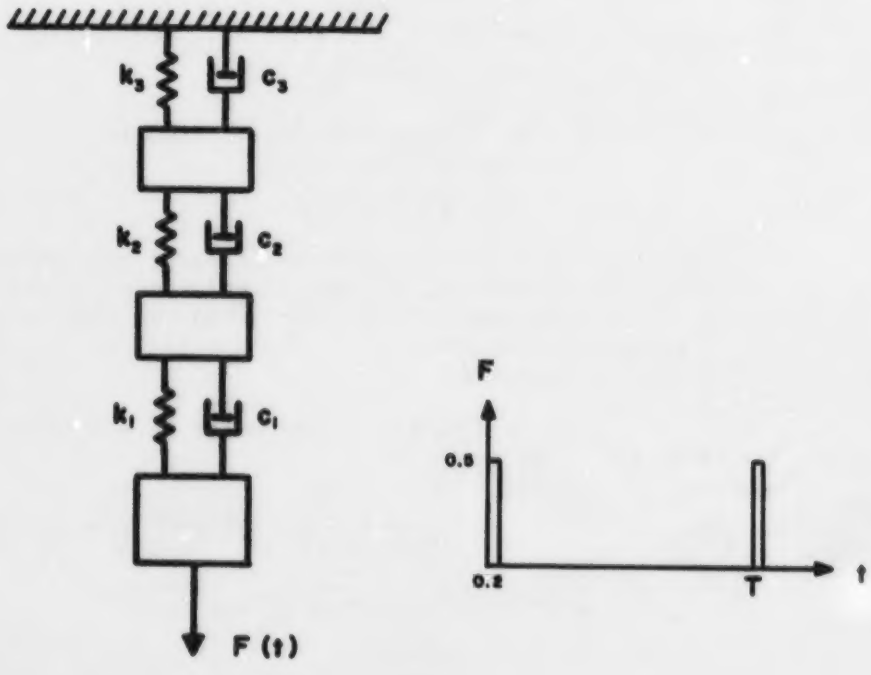

(b) SYSTEMS OF SPRINGS AND MASSES

EXHIBIT B. 1 GBRP INPUT DATA FOR SAMPLE PROBLEM 1

```
2
  100  100 0300 0001
 2048  300      1   300   1   1   2    0.04      4.0  20.0   2 2 2 2 1
001057005001001
            SIMPLE HARMONIC OSCILLATOR
00900110012001300132014101430151 0153
001000      RESPONSE TO RECTANGULAR FORCING FUNCTION
00200000              0003                    3
00300001.000001     14.950.05
0032  00101
00410000     00011.0
00430001     00011.0
0051         00011.0       1.0
00530001000000018.4         0.6
0099
```

EXHIBIT B.2 GBRP INPUT DATA FOR SAMPLE PROBLEM 2

```
2
  100  016 0500 1501
 2048  100      1   500   3   1   2    0.04      4.0  30.0   2 2 2 2 1
003057005001000
            MULTI-SECTION SYSTEM
00900110012001300132014103430151 0353
001000      RESPONSE TO RECTANGULAR FORCING FUNCTION
00200000              0003                    3
00300003.000001 16.63317.0333333
0032  00101
00410000     00011.0
00430001     00011.0
00430002     00011.0
00430003     00012.0
0051         00011.0       1.0
00530001000200012000.    100.
00530002000300014000.    200.
00530003000000016000.   0300.
0099
```

A comparison between the GBRP results and the analytical solution for the oscillator response computed for 4 seconds of duration is shown in Figure B.2. The good agreement of the two solutions is obvious.

Sample Problem 2

Once again, the physical details of the spring-mass system considered are reproduced from Reference [2]. The system configuration is given in Figure B.1(b). The values of M and k are from Biggs [4]. The values of the damping constants are assumed to be 5 percent of the respective spring constants which they are associated. They are given as follows:

$$M_1 = 1 \frac{\text{lb.sec}^2}{\text{in}} \qquad k_{1,2} = 2000 \frac{\text{lb}}{\text{in}} \qquad c_{1,2} = 100 \frac{\text{lb.sec}}{\text{in}}$$

$$M_2 = 1 \frac{\text{lb.sec}^2}{\text{in}} \qquad k_{2,3} = 4000 \frac{\text{lb}}{\text{in}} \qquad c_{2,3} = 200 \frac{\text{lb.sec}}{\text{in}}$$

$$M_3 = 2 \frac{\text{lb.sec}^2}{\text{in}} \qquad k_{3,0} = 6000 \frac{\text{lb}}{\text{in}} \qquad c_{3,0} = 300 \frac{\text{lb.sec}}{\text{in}}$$

The transient rectangular impulse is the same used with the first sample problem.

The input data for the GBRP is shown in Exhibit B.2 and the computed responses of the system are provided in Annex 2. The responses of the respective masses predicted by GBRP for a 3-second time window are shown in Figures B.3, B.4 and B.5 in dots.

Biggs [4] has provided an analytical solution for this problem using Laplace Transform technique. The results are also included in the figures (shown in solid line) for comparison. The program results agree well with the Laplace transform solution.

Sample Problem 3

In this example the free vibration of an uniform beam in the longitudinal mode was examined. The end condition of the beam were considered free-free. The physical data of the beam is given as:

Mass (M) = 378.634 ton-sec^2/ft

Cross section area (A) = 13 ft^2

length (L) = 352 ft

elastic modulus (E) = 1.93×10^6 ton/ft^2

FIGURE B. 2

SIMPLE HARMONIC OSCILLATOR,
COMPARISON OF GBRP AND ANALYTICAL SOLUTIONS

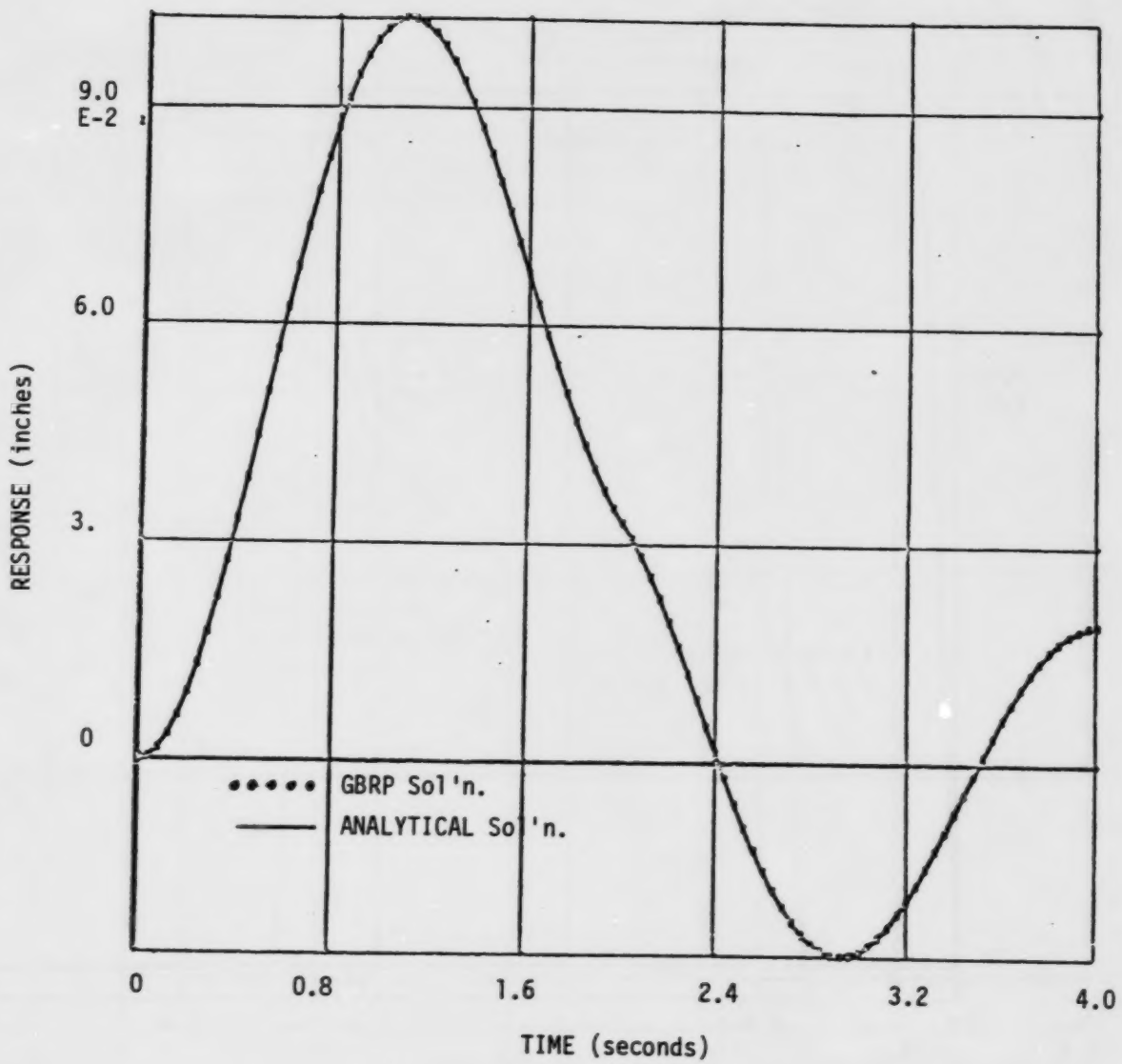

FIGURE B.3

RESPONSE OF MASS 1 TO A TRANSIENT
RECTANGULAR IMPULSE

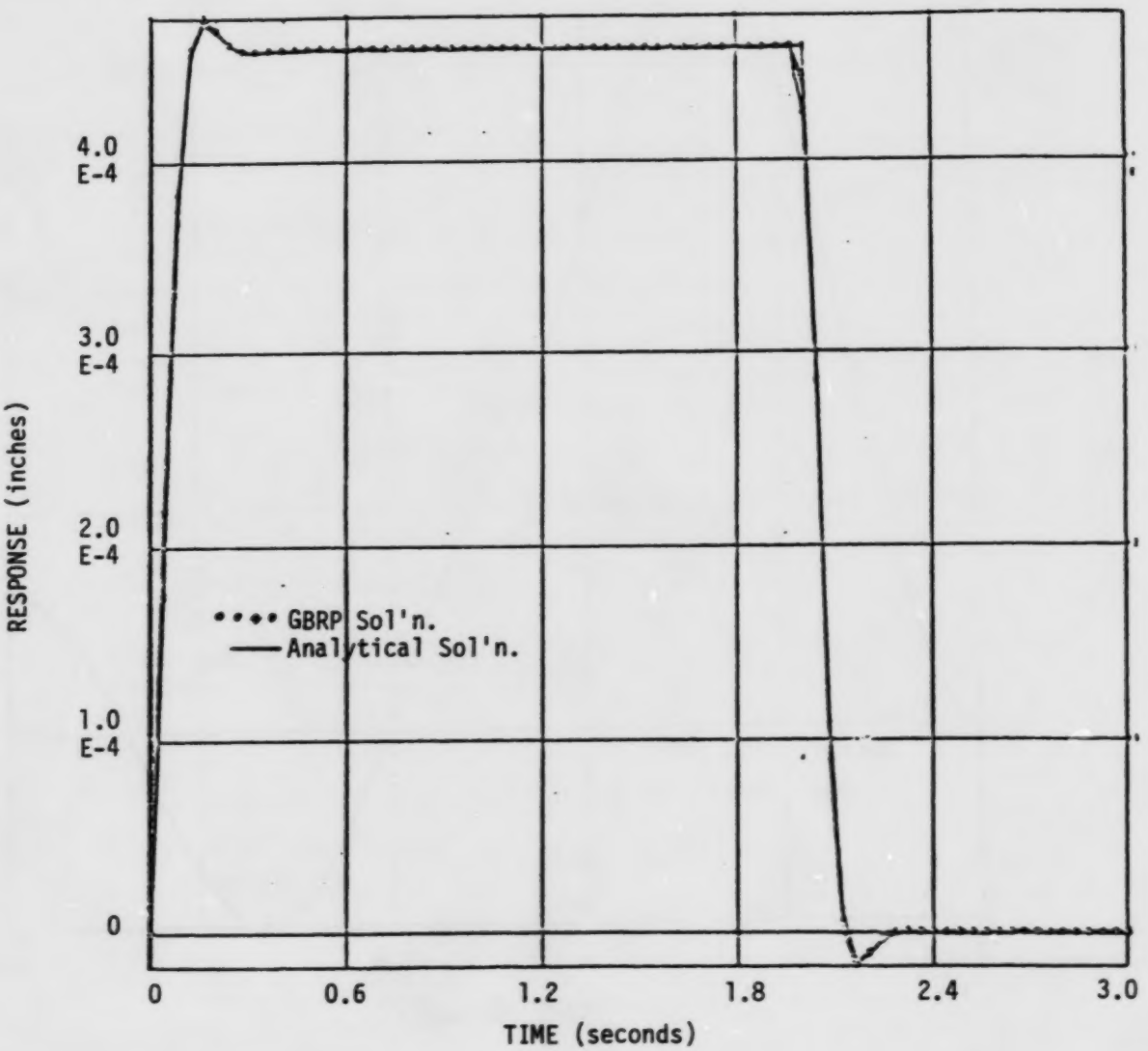

FIGURE B.4

RESPONSE OF MASS 2 TO A TRANSIENT RECTANGULAR IMPULSE

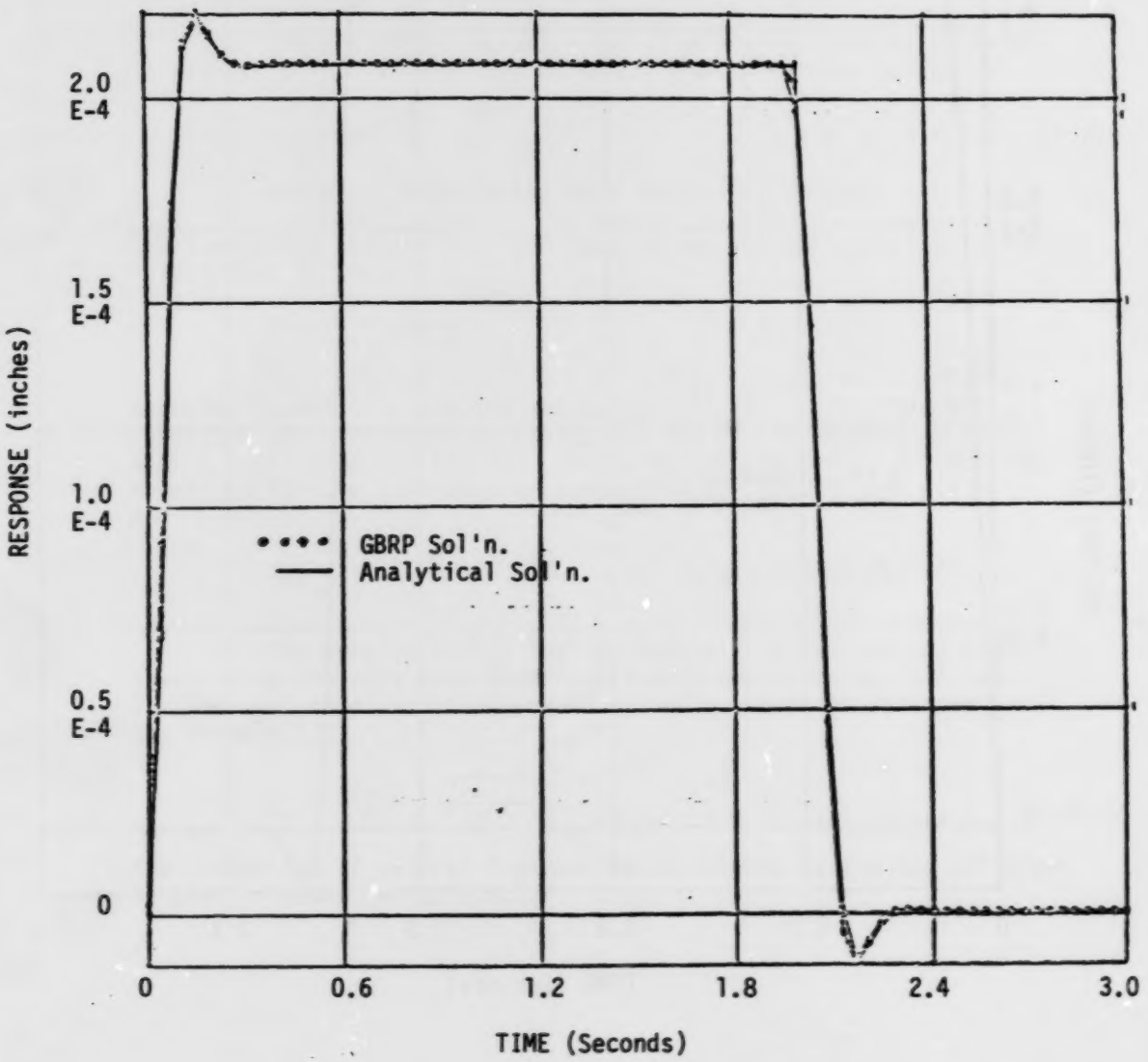

FIGURE B.5

RESPONSE OF MASS 3 TO A TRANSIENT RECTANGULAR IMPULSE

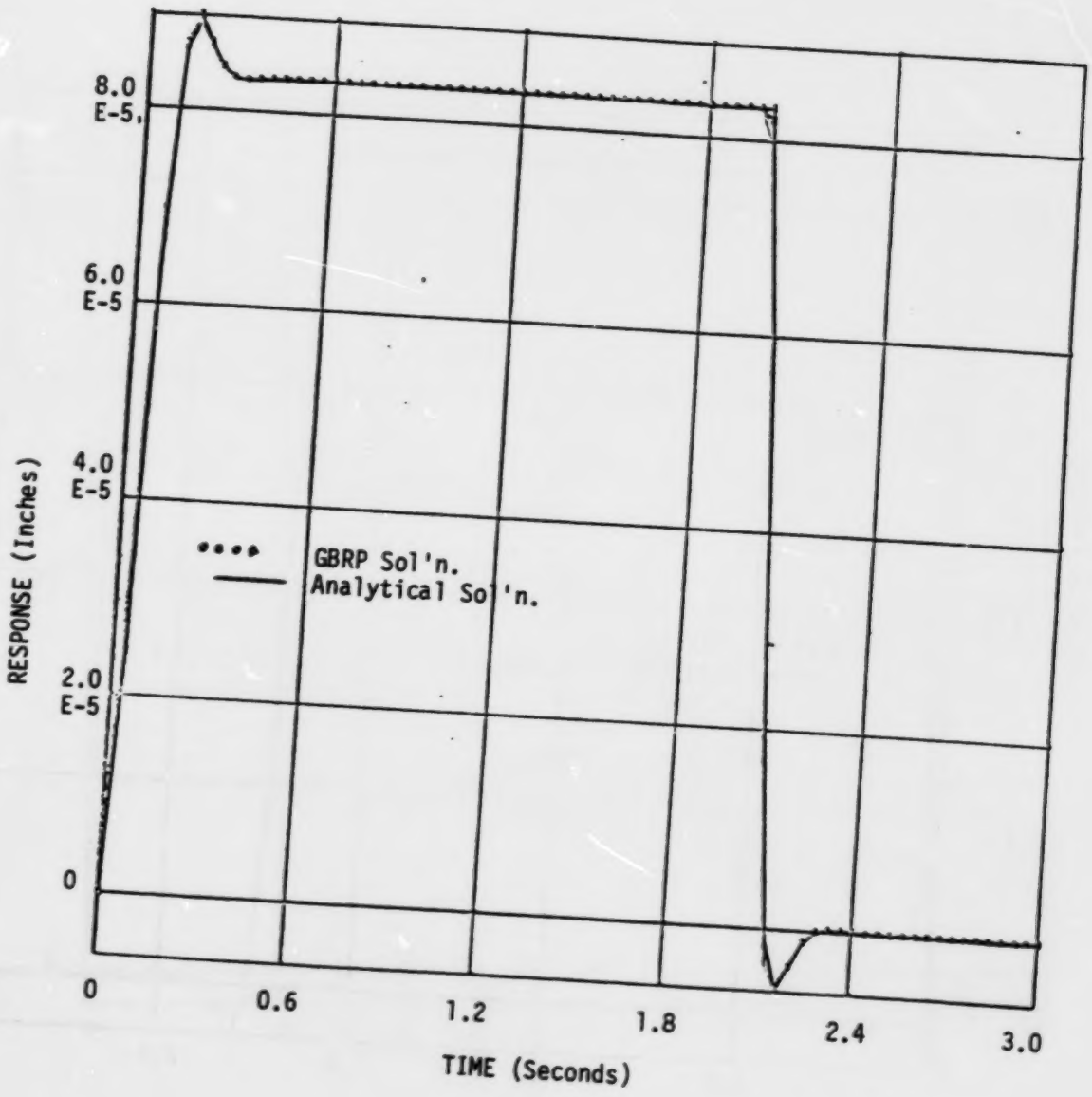

This longitudinal vibration problem can be solved using the GBRP program by dividing the beam into sections connected by springs, thus reducing the model to a mass-spring system. The spring constant was evaluated by dividing the product of E and A by the sectional length (ΔX). Consider dividing the beam into 20 equal sections (Figure B.6), the following sectional properties are derived:

sectional mass = 18.932 ton-sec^2/ft
sectional length = 17.6 ft
spring constant = 1.4256 x 10^6 ton/ft.

The program was then exercised to calculate the natural frequencies and mode shapes from the zero-mode to the fourth mode. The program results are included in Annex 2.

The analytical solution for this problem considered here is available in standard text books [5] and is represented by:

$$f_n = \frac{n}{2} \quad \frac{EA}{mL^2} \qquad n = 1, 2, 3, \ldots\ldots \quad \text{(B.2)}$$

where m = distributed mass (mass/unit length).

The comparison between the GBRP results and the analytical solution is illustrated in Table B.1.

Sample Problem 4

This problem uses the same system considered in previous example, except that one end was assumed fixed. This fixed end condition was treated by attaching one end of the beam to "ground" with a heavily damped spring. The values of the spring and damping constants for the last section connecting to "ground" are given as:

$$k_{20,0} = 500 \times 10^6 \ \frac{\text{ton}}{\text{ft}} \qquad c_{20,0} = 5000 \ \frac{\text{ton-sec}}{\text{ft}}$$

The program output for the natural frequencies and mode shapes from the zero mode tothe fourth mode are included in Annex 2. The analytical solution for this configuration is obtained by the formula [5]:

$$f_n = \frac{(2n-1)}{4}\sqrt{\frac{EA}{mL^2}} \quad ; \quad n = 1, 2, 3, \ldots\ldots \quad \text{(B.3)}$$

the comparison of natural frequencies calculated by the two solutions is also included in Table B.1.

FIGURE B.6 LONGITUDINAL MODEL FOR A UNIFORM BEAM

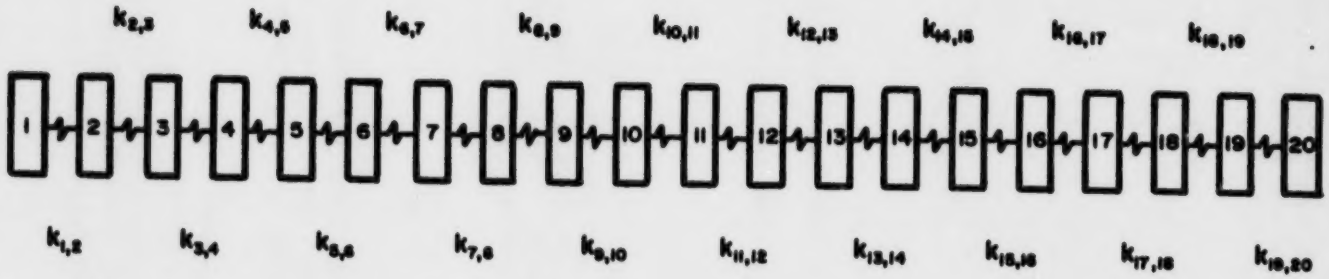

TABLE B.1 LONGITUDINAL NATURAL FREQUENCY CALCULATIONS FOR A UNIFORM BEAM

END CONDITIONS	MODE	NO. OF NODES	GBRP PREDICTION (Hz)	ANALYTICAL SOLUTION (Hz)
FREE/FREE	0	1	6.85	6.86
	I	2	13.66	13.72
	II	3	20.39	20.58
	III	4	26.99	27.44
	IV	5	33.43	34.33
FREE/FIXED	0	1	3.52	3.43
	I	2	10.53	10.29
	II	3	17.47	17.15
	III	4	24.30	24.01
	IV	5	30.97	30.87

B.3 FREE VIBRATION ANALYSIS OF SHIP HULL

The system of differential equations to be satisfied by the ship hull and shafting system in bending [2] is given by:

$$\frac{\partial V}{\partial X} = \mu \frac{\partial^2 y}{\partial t^2} - c \frac{\partial y}{\partial t} + P$$

$$\frac{\partial M}{\partial X} = V + I_{\mu z} \frac{\partial^2 \gamma}{\partial t^2} + Q \qquad \text{(B.4)}$$

$$\frac{\partial y}{\partial x} = \gamma - \frac{V}{KAG}$$

$$\frac{\partial \gamma}{\partial x} = \frac{M}{EI}$$

where x = distance in the longitudinal direction measured from the origin of coordinates

y = displacement normal to x in the plane of bending

t = time variable

γ = angular displacement relative to the Z-axis

V = shearing force in the direction of flexural vibration (y-direction)

M = bending moment

μ = effective mass per unit length

$I_{\mu z}$ = effective rotary inertia per unit length

KAG = shear rigidity

EI = bending rigidity

P = external excitation force

c = damping coefficient

Q = external forcing moment.

By means of finite-difference technique, GBRP program reduce the above system of partial differential equations to a system of finite difference equation.

In the vertical and horizontal mode of vibration, the ship hull is represented by a non-uniform, continuous, free-free beam with mass and elastic properties per unit length being equivalent to those of the actual ship. In the longitudinal mode of vibration the ship hull and shafting are modelled as a mass-spring system.

The ship hull of POLAR SEA was idealized as a 20-section non-uniform beam system and Figure B.7 shows the representation. The problem was then to evaluate the equivalent beam parameters for the ship sectional properties as in puts to the GBRP program. These physical parameters in the form required by the computer code includes:

- °mass per unit length (including added mass) (μ)
- °bending compliance ($\Delta X/EI$)
- °shear compliance ($\Delta X/KAG$)

The longitudinal vibration, the spring constants are required for the springs that made up the spring-mass system.

B.3.1 Procedure for Calculating Vibration Parameters

The following briefly describes the manner in which the tables for the physical parameters, required as input to the GBRP are calculated. A full list of the symbols used, the tables and details of the parameters are included in Annex 1, Volume III.

Table 1: The weight is obtained from the ship's weight curve, station numbers are measured from the after perpendicular (i.e. AP = 0 and FP = 20).

Table 2, 3 & 4: The values of draught (T), half breadth (b) and cross sectional area (S) below the WL were obtained from the ship's body plan and their respective curves are shown in Figures 5, 3 and 9.

The value of J was obtained from Figure 13, and C_V and C_H from Figures 14 and 15 respectively.

Table 5: The values of $\mu_{\nu V}$ and $\mu_{\nu H}$ obtained in Tables 3 and 4 are plotted in Figure 1 for use in Table 5.

Table 6: The horizontal and vertical moments of inertia of all available sections were calculated and plotted and faired curves drawn, as shown in Figure 11. Values I_V and I_H at half-stations were obtained from Figure 11.

FIGURE B.7 IDEALIZATION OF SHIP HULL MODEL FOR GBRP

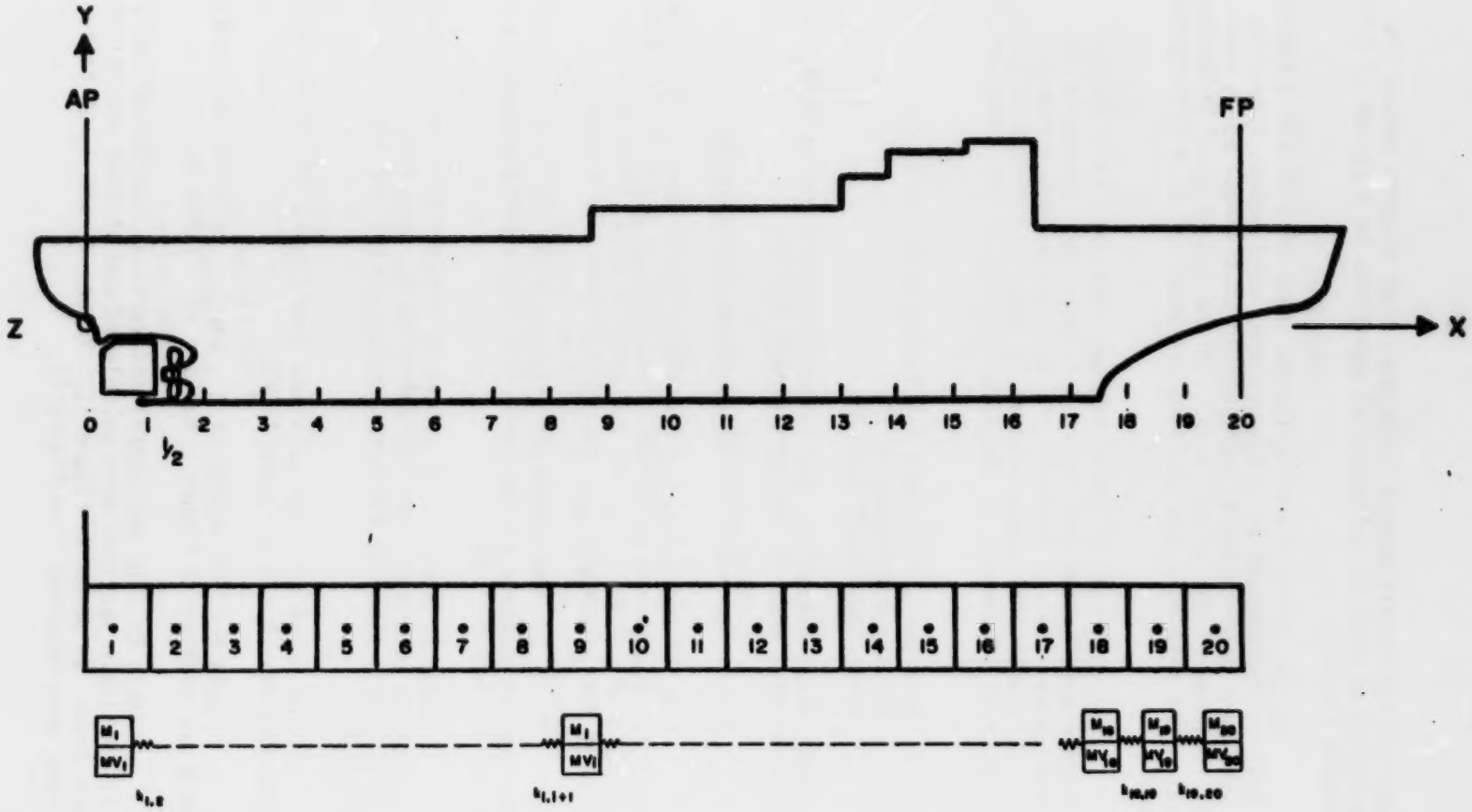

M_I = MASS OF SECTION I

MV_I = VIRTUAL MASS OF ENTRAINED WATER FOR SECTION I

$k_{I,I+1}$ = SPRING OF EQUIVALENT SECTIONAL STIFFNESS

Table 7: Vertical and horizontal areas (A'_V and A'_H) were calculated for all available sections and faired curves drawn as shown in Figure 10. The faired values of A'_V and A'_H were used in Table 7.

Table B.2 summarizes the input parameters furnished for the GBRP for the horizontal and vertical vibration calculations.

For longitudinal vibration the ship hull was idealized as a mass-spring system as shown in Figure B.6. Each of the sectional masses is connected by a spring with equivalent sectional stiffness. The spring constant can be determined by:

$$k = \frac{EA}{\Delta X} \tag{B.5}$$

where E = elastic modulus
A = cross-sectional area
ΔX = length of hull section.

The basic input data required is sectional mass ($\mu\Delta X$) and their associated spring constants ($k_{n,m}$) and they are given in Table B.3

B.3.2. Input Preparation

Once the structural system and its associated beam parameters were defined, the input data required for the GBRP program were then prepared through the use of the standard form as shown in Exhibit B.3. The format is quite self-explanatory. Details of each card required are given in B.5.

Exhibits B.4, B.5 and B.6 represent a reproduction of the sample set of input data for the solution run for the horizontal, vertical and longitudinal free vibration analysis of the ship hull respectively.

TABLE B.2

PHYSICAL PARAMETERS FOR LATERAL VIBRATIONS

FOR GBRP (USCGC POLAR SEA)

L = 352 ft. B = 78.876 ft. ΔX = 17.60 ft.

SECTION NUMBER	VERTICAL MODE			HORIZONTAL MODE		
	$(\mu\Delta X)$ ton-sec²/ft	$(\Delta X/EI) \times 10^{10}$ 1/ton-ft	$(\Delta X/KAG) \times 10^{6}$ ft/ton	$(\mu\Delta X)$ ton-sec²/ft	$(\Delta X/EI) \times 10^{10}$ 1/ton-ft	$(\Delta X/KAG) \times 10^{6}$ ft/ton
1	9.111	17.1904	13.670	13.775	15.7564	6.4143
2	13.997	11.1233	7.5805	17.517	8.96098	4.0186
3	21.023	9.69722	4.7649	21.727	7.62406	2.9413
4	27.602	9.04771	3.1766	24.786	7.00284	2.3489
5	24.804	9.36116	3.6659	18.644	6.63427	1.9280
6	44.804	9.33805	4.3543	34.596	6.24016	2.1519
7	45.904	9.33805	4.6325	31.560	5.74701	2.3163
8	45.157	9.33805	4.5691	27.909	5.08147	2.2236
9	46.903	9.33805	4.2902	27.543	4.81111	2.0717
10	47.151	9.33805	4.0479	26.295	4.28745	2.0463
11	47.588	9.33805	3.7903	26.116	3.67139	1.7694
12	47.828	9.33805	3.5258	26.268	3.05455	1.8226
13	47.202	9.40771	3.3354	25.853	3.08445	1.8738
14	45.579	9.43115	3.1949	25.691	3.58100	1.6846
15	41.535	9.45472	3.0322	25.783	4.44886	1.3504
16	38.103	9.45472	2.8655	27.279	5.52856	1.7463
17	30.890	9.55027	2.6683	24.642	7.41477	2.0978
18	21.052	10.5052	2.8508	19.996	10.8044	2.5657
19	14.974	14.2176	3.8984	17.878	18.9077	3.5110
20	24.771	35.0172		29.699	54.0219	

TABLE B.3

INPUT DATA FOR LONGITUDINAL VIBRATION (USCGC POLAR SEA)

$E = 1.93 \times 10^6$ ton/ft², $\Delta X = 17.6$ ft

STATION NUMBER	$(\mu \Delta X)$ ton-sec²/ft	$*A_{V^1} + A_{H^1}$ ft²	STATION NUMBER	$A_{V^1} + A_{H^1}$ ft²	$(k_{n,m}) \times 10^6$ ton/ft
½	8.853	3.3492	1	5.1947	0.56965
1½	11.357	7.0401	2	8.8651	0.97214
2½	15.391	10.6901	3	12.6791	1.39038
3½	18.802	14.6681	4	16.4589	1.80487
4½	12.660	18.2497	5	17.7713	1.94878
5½	28.612	17.2928	6	16.4863	1.80787
6½	25.928	15.6797	7	15.2901	1.67670
7½	22.365	14.9005	8	15.2764	1.67520
8½	21.911	15.6523	9	16.2333	1.78013
9½	20.575	16.8143	10	17.4978	1.97879
10½	30.308	18.1813	11	18.8307	2.06496
11½	20.548	19.4800	12	19.1246	2.09719
12½	20.221	18.7691	13	19.1656	2.10168
13½	20.235	19.5620	14	21.4212	2.34903
14½	20.415	23.2803	15	22.6447	2.48320
15½	21.911	22.0090	16	20.9837	2.30109
16½	19.098	19.9584	17	19.3843	2.12566
17½	14.012	18.8101	18	16.6708	1.82810
18½	11.806	14.5314	19	12.1323	1.33042
19½	23.891	9.7332			

* Data obtained from Table 7 of Annex 1.

EXHIBIT B.3 GBRP INPUT FORMS FOR FREE VIBRATION ANALYSIS

(SAMPLE DATA TAKEN FROM USCGC POLAR SEA TEST - NATURAL FREQUENCIES IN LONGITUDINAL MODE -- AS FOUND IN APPENDIX IX C)

TITLE NATURAL FREQUENCIES (LONGITUDINAL) PROGRAMMER - DATE -

PROBLEM NO. - PHASE - LABEL [ ] - SHEET - OF -

RUN SELECTION CARD NO PARTICULARS REQUIRED (NPR)

1

DIMENSIONS FOR FAST FOURIER TRANSFORM INTERFACE (NONHARMONIC VIBRATIONS ONLY) NPR

D16 D17 D18 D19

1 4 7 10

DATA FOR FAST FOURIER TRANSFORM INTERFACE (NONHARMONIC VIBRATIONS ONLY) NPR

1 6 11 17 23 27 31 35 43 51 59 61 63 65 67

DIMENSIONS FOR GBRP NPR

D2 D3 D5 D14 D15 D6 D7 D8 D9 D10 D11 D12 D13

1 4 7 10 13 16 19 22 25 28 31 34 37

EXHIBIT B.3. (Con't.)

TITLE NATURAL FREQUENCIES (LONGITUDINAL) PROGRAMMER - DATE -

PROBLEM NO. - PHASE - LABEL - SHEET - OF -

RUN TITLE CARD NPR

ΔΔΔΔΔΔΔΔΔΔΔΔ

DATA CONTROL CARD NPR

(X) TYPE NO TYPE etc.

0090

CASE TITLE CARD NATURAL FREQUENCIES (LONGITUDINAL)

0010ΔΔΔΔΔΔΔΔ

OPTION CONTROL CARD

	OP1	OP2	OP3	OP4	OP5	OP6	OP7	OP8	OP9	OP10
00200000	0	0	0	0	0	0	0	0	0	1

EDIT CONTROL CARD NPR

00210000

GENERAL DATA CARD

	NO SECTIONS	ω_1(CPS)	ω_2(CPS)	$\Delta\omega$(CPS)	h	Power of ω	NPLOTC
0030	20	00.000	2000.000	.500	-	.000	-

SYSTEMS DATA CARDS NPR

	SYSTEMS	RADIUS	INITIAL J	
0031				
0031				

FORCING FUNCTION LOCATION CARD ____ (Used only if forces are nonharmonic)

0032

EXHIBIT B.3 (Con't.)

TITLE NATURAL FREQUENCIES (LONGITUDINAL) PROGRAMMER _____ DATE _____

PROBLEM NO. _____ PHASE _____ LABEL [ ] _____ SHEET ____ OF ____

SECTION DATA CARDS

	SECTION NO. (5–8)	END CONDN. (9–12)	SYSTEM (13–16)	MASS (17–24)	WATER INERTIA (25–32)	$(\Delta X/EI)_n$ (33–40)	$(\Delta X)_{n,n+1}$ (41–48)	$(\Delta X/KAG)_{n,n+1}$ (49–56)	$(I_{\mu z}\Delta X)_{n,n+1}$ (57–64)	P_n (65–72)
REAL PART OF SCALING FACTORS										
00410000		0000	1	1.0000E+00	0	0	0	0	0	0
00410000		0000								
00410000		0000								
IMAGINARY PART OF SCALING FACTORS NPR										
00420000		0000								
00420000		0000								
00420000		0000								
PARAMETER VALUES - UNSCALED										
0043	1	1	1	8.5830E+00	0	0	0	0	0	0
0043	2	0	1	1.1357E+01	0	0	0	0	0	0
0043	3	0	1	1.5391E+01	0	0	0	0	0	0
0043	4	0	1	1.8802E+01	0	0	0	0	0	0
0043	5	0	1	1.2260E+01	0	0	0	0	0	0
0043	6	0	1	2.8612E+01	0	0	0	0	0	0
0043	7	0	1	2.5928E+01	0	0	0	0	0	0
0043	8	0	1	2.2365E+01	0	0	0	0	0	0
0043	9	0	1	2.1911E+01	0	0	0	0	0	0
0043	10	0	1	2.0575E+01	0	0	0	0	0	0
0043	11	0	1	3.0308E+01	0	0	0	0	0	0
0043	12	0	1	2.0548E+01	0	0	0	0	0	0
0043	13	0	1	2.0221E+01	0	0	0	0	0	0
0043	14	0	1	2.0235E+01	0	0	0	0	0	0
0043	15	0	1	2.0415E+01	0	0	0	0	0	0

EXHIBIT B.3. (Con't.)

TITLE NATURAL FREQUENCIES (LONGITUDINAL) PROGRAMMER DATE

PROBLEM NO. PHASE LABEL SHEET OF

5 9 13 17 25 33 41 49 57 65 73

SPECIAL CONNECTION CARDS

	n	m	SYSTEM	$K_{n,m}$	$C_{n,m}$	$C_{n,m}/\omega$	$\Delta X_{n,m}$	$(\Delta X/KAG)_{n,m}$	$(I_{\mu z}\Delta X)_{n,m}$	$Q_{n,m}$	
REAL PART OF SCALING FACTORS											
0051	0000	0000	1	1.000E+06	0	0	0	0	0	0	
0051	0000	0000									
0051	0000	0000									
IMAGINARY PART OF SCALING FACTORS NPR											
0052	0000	0000									
0052	0000	0000									
0052	0000	0000									
PARAMETER VALUES - UNSCALED											
0053	1	2	1	5.6965E-01	0	0	0	0	0	0	
0053	2	3	1	9.7214E-01	0	0	0	0	0	0	
0053	3	4	1	1.3904E+00	0	0	0	0	0	0	
0053	4	5	1	1.8049E+00	0	0	0	0	0	0	
0053	5	6	1	1.9488E+00	0	0	0	0	0	0	
0053	6	7	1	1.8079E+00	0	0	0	0	0	0	
0053	7	8	1	1.8767E+00	0	0	0	0	0	0	
0053	8	9	1	1.6752E+00	0	0	0	0	0	0	
0053	9	10	1	1.7801E+00	0	0	0	0	0	0	
0053	10	11	1	1.9188E+00	0	0	0	0	0	0	

EXHIBIT B.3 (Con't.)

TITLE NATURAL FREQUENCIES (LONGITUDINAL) PROGRAMMER _____ DATE _____

PROBLEM NO. _____ PHASE _____ LABEL [ ] _____ SHEET ____ OF ____

CHARACTRON PLOTTING CHARACTERS NPR

000000	ΔΔΔΔΔΔΔΔΔΔ	+ΔΔΔΔΔΔΔΔΔ	0ΔΔΔΔΔΔΔΔΔ	XΔΔΔΔΔΔΔΔΔ	-ΔΔΔΔΔΔΔΔΔ	•ΔΔΔΔΔΔΔΔΔ	
34	7	17	27	37	47	57	

NATURAL FREQUENCY SELECTION CARD NPR

00700000		
34	9	11

SYSTEMS TO BE PLOTTED (USED ONLY WITH OPTION 6 PLOTTING) NPR

1st	2nd	3rd	4th	5th	6th	
						etc.
1	3	5	7	9	11	

START NEW DATA SET CARD _____

0050
31

END OF DATA CARD _____

0099
34

EXHIBIT B.4 INPUT DATA FOR FREE VIBRATION IN HORIZONTAL MODE

```
1
020057005
          NATURAL FREQUENCIES OF HORIZONTAL VIBRATION
009001100120012101300141204301 70
001000      NATURAL FREQUENCIES OF HORIZONTAL VIBRATION(USCGC POLAR SEA)
00200000                                          0001
002100000001000600100015 0020
003000200.00001 200.0   .05
00410000000000011.0                1.0E-10     1.0  1.0E-6
00430001000100011 3.775          15.7564 17.60   6.4143
00430002     000117.517          8.96098 17.60   4.0186
00430003     000121.727          7.62406 17.60   2.9413
00430004     000124.786          7.00284 17.60   2.3489
00430005     000118.644          6.63427 17.60   1.9280
00430006     000134.596          6.24016 17.60   2.1519
00430007     000131.560          5.74701 17.60   2.3163
00430008     000127.909          5.08147 17.60   2.2236
00430009     000127.543          4.81111 17.60   2.0717
00430010     000126.295          4.28745 17.60   2.0463
00430011     000126.116          3.67139 17.60   1.7694
00430012     000126.268          3.05455 17.60   1.8226
00430013     000125.853          3.08445 17.60   1.8738
00430014     000125.691          3.58100 17.60   1.6846
00430015     000125.783          4.44886 17.60   1.3504
00430016     000127.279          5.52856 17.60   1.7463
00430017     000124.642          7.41477 17.60   2.0978
00430018     000119.996          10.8044 17.60   2.5657
00430019     000117.878          18.9077 17.60   3.5110
00430020000100012 9.699          54.0219 17.60
0070000009
0099
```

EXHIBIT B.5 INPUT DATA FOR FREE VIBRATION IN VERTICAL MODE

```
1
020057005000
          VERTICAL NATURAL FREQUENCY
009001100120012101300141204301 70
001000        NATURAL FREQUENCY IN VERTICAL BENDING
00200000              00000              00000     1
00210000000100060010001500 20
003000200.000001 200.000 0.50
00410000    00011.0                 1.0E-10      1.0  1.0E-6
00430001000100019.111              17.1904 17.60    13.670
00430002    000113.997             11.1233 17.60    7.5805
00430003    000121.023             9.69722 17.60    4.7649
00430004    000127.602             9.04771 17.60    3.1766
00430005    000124.804             9.36116 17.60    3.6659
00430006    000144.804             9.33805 17.60    4.3543
00430007    000145.904             9.33805 17.60    4.6325
00430008    000145.157             9.33805 17.60    4.5691
00430009    000146.903             9.33805 17.60    4.2902
00430010    000147.151             9.33805 17.60    4.0479
00430011    000147.588             9.33805 17.60    3.7903
00430012    000147.828             9.33805 17.60    3.5258
00430013    000147.202             9.40771 17.60    3.3354
00430014    000145.579             9.43115 17.60    3.1949
00430015    000141.535             9.45472 17.60    3.0322
00430016    000138.103             9.45472 17.60    2.8655
00430017    000130.890             9.55027 17.60    2.6683
00430018    000121.052             10.5052 17.60    2.8508
00430019    000114.974             14.2176 17.60    3.8984
00430020000100012 4.771            35.0172 17.60
0070000009
0099
```

EXHIBIT B.6

INPUT DATA FOR FREE VIBRATION

IN LONGITUDINAL MODE

```
1
020057005
              TEST LONG FREQ,  POLAR SEA
009001100120013001412043015119530170
001000        NATURAL FREQUENCIES
0020                                                    0001
00300020.00001   2000.    0.5
00410000     00011.0
00430001000100018.58300
00430002     000111.3570
00430003     000115.3910
00430004     000118.8020
00430005     000112.6600
00430006     000128.6120
00430007     000125.9280
00430008     000122.3650
00430009     000121.9110
00430010     000120.5750
00430011     000130.3080
00430012     000120.5480
00430013     000120.2210
00430014     000120.2350
00430015     000120.4150
00430016     000121.9110
00430017     000119.0980
00430018     000114.0120
00430019     000111.8060
00430020000100000123.8910
0051         00011.0  E+6
00530001000200010.569650
00530002000300010.972140
00530003000400011.39038
00530004000500011.80487
00530005000600011.94878
00530006000700011.80787
00530007000800011.67670
00530008000900011.67520
00530009001000011.78013
00530010001100011.91879
00530011001200012.06496
00530012001300012.09719
00530013001400012.10168
00530014001500012.34903
00530015001600012.48320
00530016001700012.30105
00530017001800012.12566
00530018001900011.82810
00530019002000011.33042
00700000009
0099
```

B.3.3 Results and Discussion

The natural frequencies and the mode shapes of the ship hull in the three distinct modes of vibration (vertical, horizontal and longitudinal) were computed by exercising the GBRP program with the appropriate input data. The output generated is shown in tabular form including a list of the input data and the computed results of deflection and moments (see Annex 2). The calculated deflections are always normalized with respect to the deflection of the first section. In all the present calculations, section 1 is at the stern. The deflection tables at each frequency represent the normal mode shapes of the hull.

In this study, three sets of outputs for the free vibrations in the horizontal, vertical as well as the longitudinal modes were generated and are included in Annex 2. Table B.4 presents a summary of the results. It is seen that in all the principal modes of vibration (Figure B.8, B.9 and B.10) the frequency of vibration in the vertical direction has the lowest value. This indicates that for the same mass distribution, the vertical stiffness distribution is lower than those in the horizontal and longitudinal directions. It may be expected, therefore, that forced responses (i.e. deflections due to ice-induced forces) are likely to be higher in the primary mode in the vertical direction. The frequencies for the rigid body modes have been hand calculated separately. (Details are given in Section E.4 of Appendix E).

It may be noted (Figure B.10) that the lowest mode shape for the longitudinal vibration has only a single node at approximately midship. This means that if the hull is excited longitudinally at this particular frequency, the bow and the stern halves would move in phase opposition and zero vibration amplitude will be observed at midship. As expected for an elastic system with gradual changes in stiffness and inertia, the mode shapes for symmetric vibrations in the three directions are approximate periodic functions along the hull length.

The fundamental natural frequencies in the vertical and horizontal directions calculated by GBRP have been compared with those calculated using existing empirical formulae. The details of the calculations are given in Annex 2. Table B.5 shows the comparison. It is seen that the fundamental frequency calculated by the two methods agree very closely in the vertical direction. However, the comparison is not that close for horizontal vibrations.

TABLE B.4

NATURAL FREQUENCIES FOR USCGC POLAR SEA SHIP HULL

	HORIZONTAL	VERTICAL	LONGITUDINAL
Zero(th) Mode	0	0.186	0
Primary Mode	4.13	2.74	8.41
Mode 2	7.43	5.00	16.11
Mode 3	10.87	7.26	22.6
Mode 4	14.47	9.46	28.6
Mode 5	17.44	11.52	35.82

TABLE B.5

COMPARISON OF FREQUENCIES CALCULATED BY
GBRP WITH THOSE PREDICTED BY EMPIRICAL FORMULAE

	VERTICAL		HORIZONTAL	
	GBRP	EMPIRICAL	GBRP	EMPIRICAL
FUNDAMENTAL FREQUENCY, Hz	2.74	2.82	4.13	5.12

FIGURE B.8

MODE SHAPES AND NATURAL FREQUENCIES FOR HORIZONTAL VIBRATION (USCGC POLAR SEA)

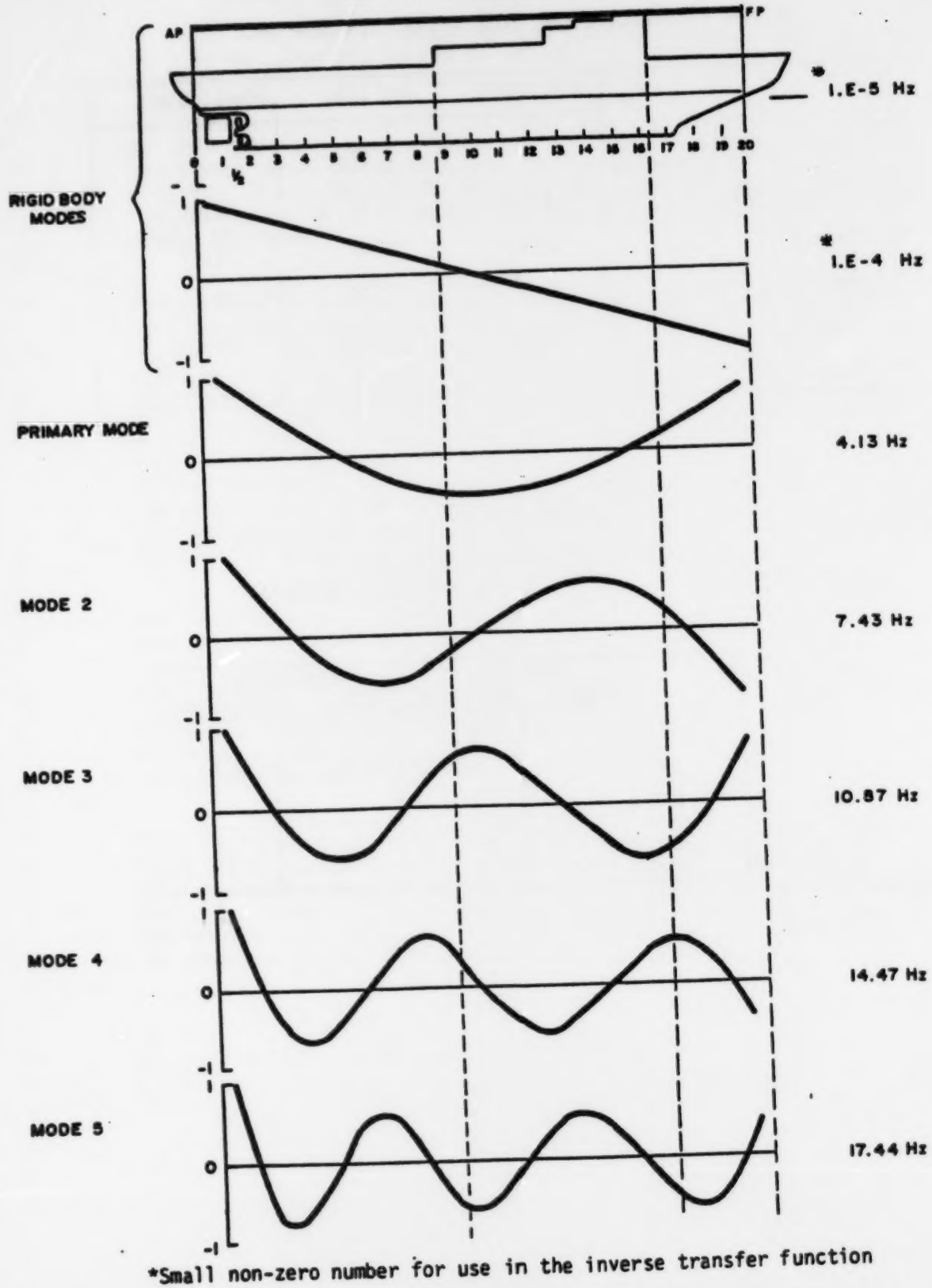

*Small non-zero number for use in the inverse transfer function

FIGURE B.9

MODE SHAPES AND NATURAL FREQUENCIES FOR VERTICAL VIBRATION
(USCGC POLAR SEA)

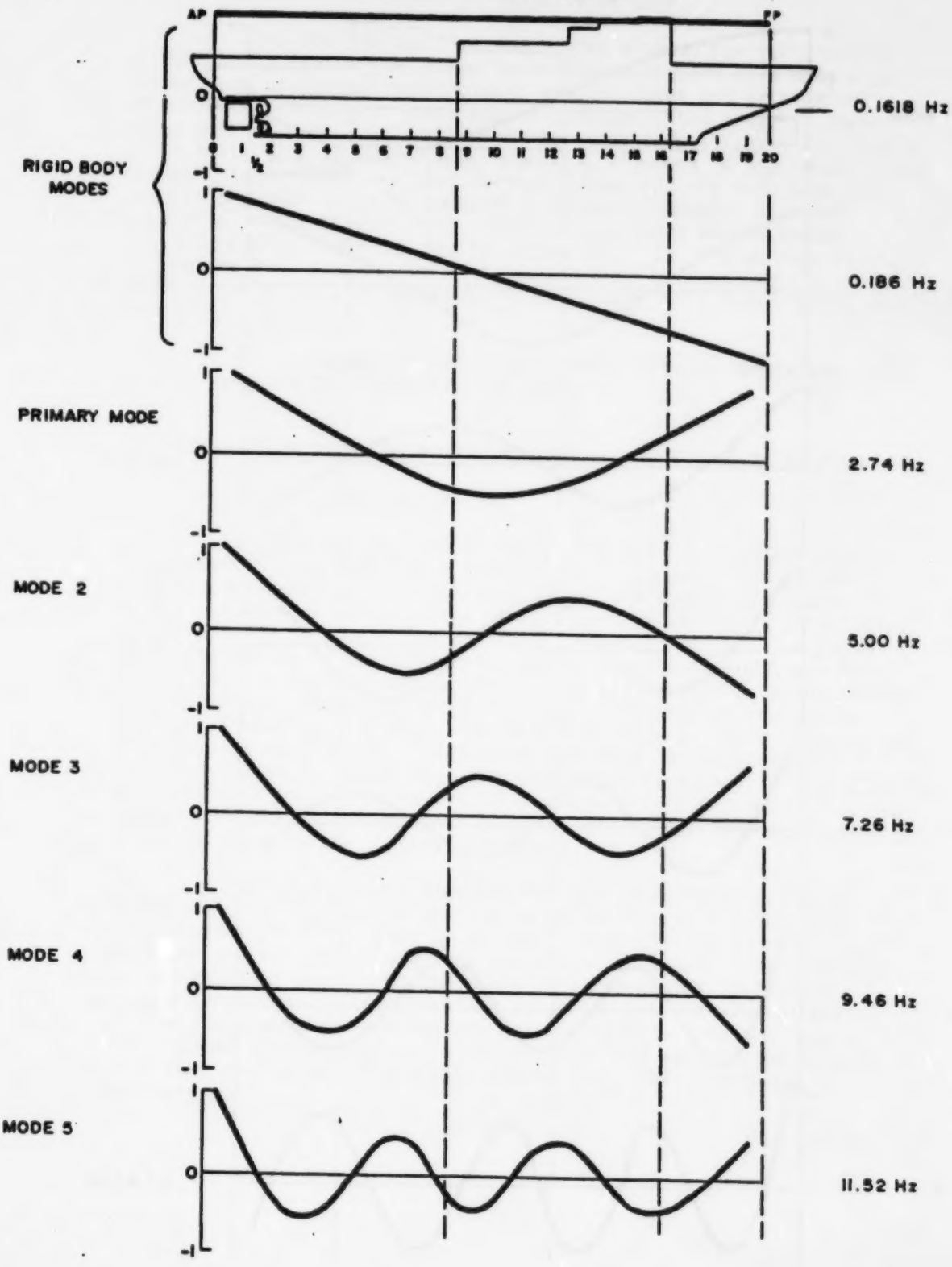

FIGURE B.10

MODE SHAPES AND NATURAL FREQUENCIES FOR LONGITUDINAL VIBRATION (USCGC POLAR SEA)

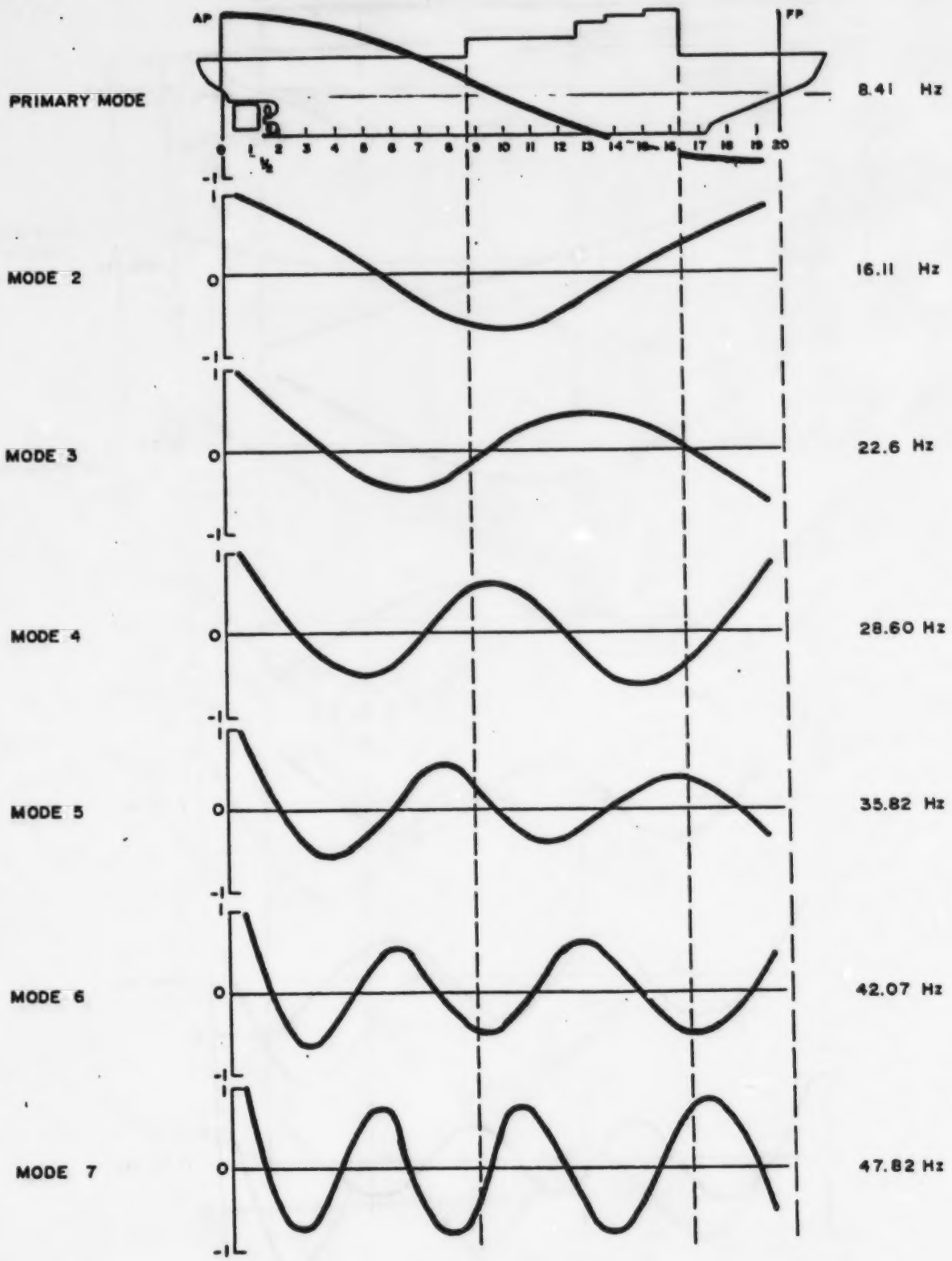

B.3.4 Conclusions on Validity of GBRP

With the limited time and budget allowed for verification of GBRP, only first order comparisons of its results were made with closed form analytical solutions of special cases and predictions of empirical formulae. These comparisons indicated that, in these cases GBRP computes the frequencies and mode shapes fairly accurately. It is felt that, for achieving complete confidence in the capabilities of GBRP, it is necessary that further comparisons be made with the results of other existing computer programs. Examples of other available models of ship hull vibration are those due to Kruppa [6], Misra [7], Kumai [8] and Hylarides [9]. It is also necessary to compare GBRP predictions with experimental data of Townsin [10], wherein the effects of hydrodynamic added mass have been clearly identified.

It is estimated that an additional fifteen sample runs will be required to accomplish the above task.

B.4 ESTIMATE OF PROPULSION SYSTEM LONGITUDINAL VIBRATION FREQUENCIES

B.4.1. Introduction

In general, to keep propeller and hull excitations low, it is desirable to use many blades on the propeller. One of the primary considerations in the selection of the number of blades is the natural frequency of the shafting and propeller in longitudinal vibration. To ascertain the probable frequency that will be found after the design of the propulsion system and its supports are developed, it is useful to have a plot of natural frequency versus foundation stiffness. Using values of the probable range of foundation and thrust bearing stiffness, the probable range of shaft longitudinal frequency is determined. The number of blades in the propeller is chosen so that, preferably, the excitation frequency is less than 80% of a possible propulsion natural frequency. A less desirable, but sometimes necessary, solution is to make the excitation frequency about 30% above the longitudinal natural frequency.

For making these predictions, the approximate propeller diameter, propeller weight and the water inertia associated with longitudinal vibration must be defined. Also the approximate diameter of the tail shaft and line shaft must be known. The simplest procedure is to predict on the basis of a one-degree-of-freedom system consisting of the propeller and water inertia plus a portion of the shaft weight vibrating against the stiffness of the thrust bearing and its foundation. Since the shafting weighs considerably more than the propeller and adds flexibility, this procedure is not very good.

An improved procedure is to model the propeller and shaft as a series of concentrated masses and elastic elements and use a Holzer process for frequency prediction. With this degree of complication it becomes desirable to use a computer.

If a computer is used, many of the complications of defining the mass-elastic system can be avoided by using a finite-difference or finite-element program such as GBRP, STARDYNE, etc. However, a more accurate result can be obtained with less input (and, therefore less chance for error) if the shaft is represented by a continuous mass and elasticity distribution. The results of a computer program for predicting the natural frequencies of propeller and shafting systems defined by concentrated and distributed masses and stiffnesses is presented and discussed below.

Output Information: The results of exercizing the computer program will consist of the natural frequencies and mode shapes. In addition, a plot of natural frequency of the shafting system as a function of the stiffness of the thrust bearing foundation.

Input Information: (1) Shafting arrangement, diameters, and lengths. (2) Propeller mass, diameter, number of blades, pitch, and developed area ratio (or mean width ratio).

Basis for Calculation: The propeller is represented by its weight and the weight of entrained water as given by Lewis and Auslaender [12]. The shaft is represented by a distributed mass and elasticity. The gearing and turbines forward of the thrust bearing are not included in the present analysis, as the shaft coupling aft of each reduction gear is disconnected while on Diesel-Electric (DE) mode of operation.

The computer program employed in the present study is once again GBRP, as its prediction accuracy for the longitudinal mode was verified and found to be acceptable (see Section B.2). In the following sections, the basis for the preparation of input data required for the exercise are detailed.

B.4.2. Thrust Bearing Foundation Stiffness

The propulsion system arrangement for the POLAR Class Icebreakers is depicted in Figure B.11. As can be seen, the thrust bearing for each wing shaft is aft of the main motor, while the thrust bearing for the centerline shaft is between the main motor and the reduction gear. Additionally, the centerline thrust bearing contains an integral radial (steady) bearing. The shaft coupling aft of each reduction gear is disconnected while on the Diesel-Electric Mode and engaged while on Gas Tubine Mode. The present analysis deals with the DE-mode only where stiffnesses and masses of components forward of the thrust bearings can be ignored.

FIGURE B.11

PROPULSION SYSTEM ARRANGEMENT

POLAR CLASS

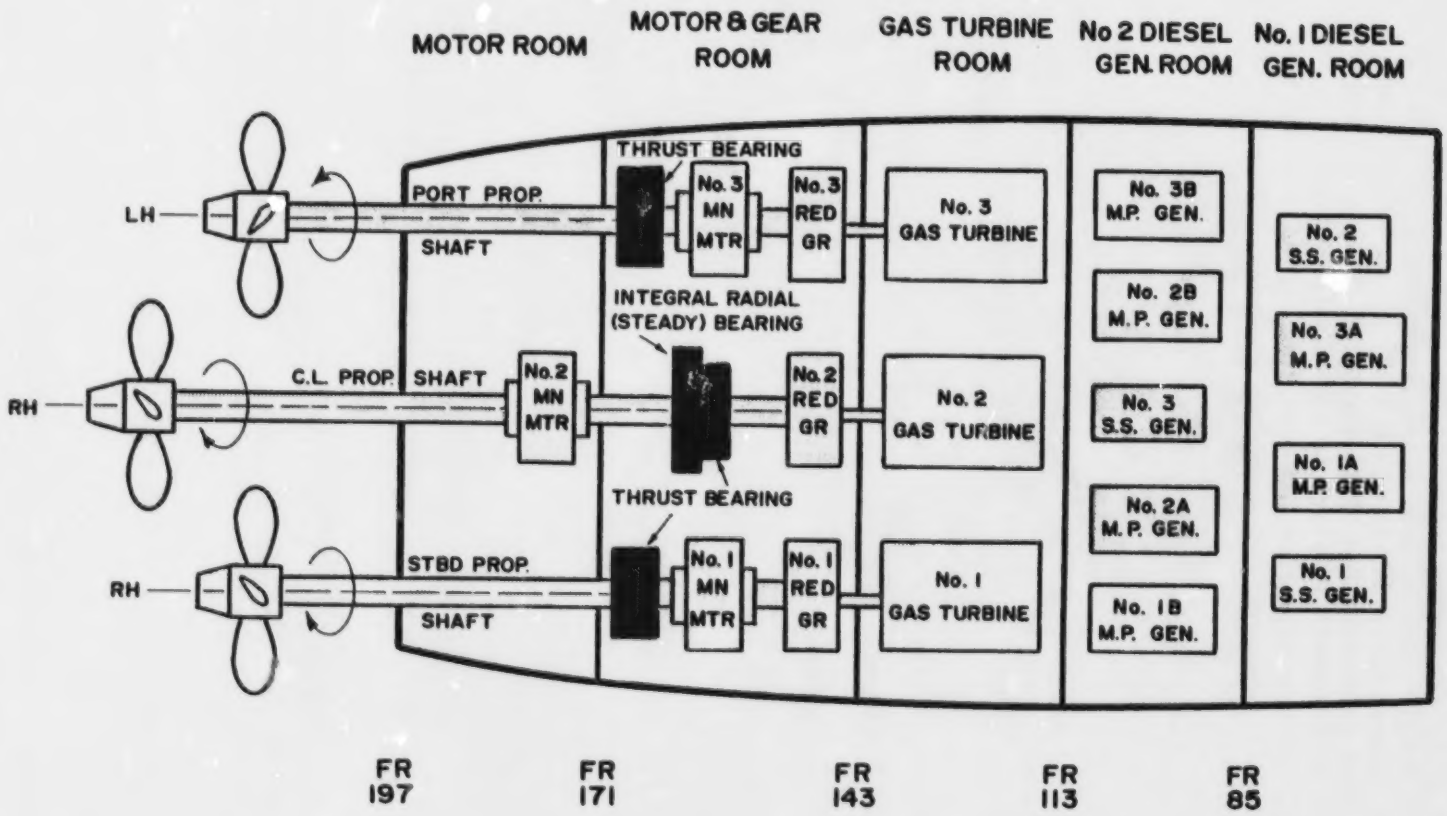

USCG made measurements of the shaft deflections during open water trials. It was noticed that the axial vibratory amplitudes were less than 50% of the steady-state displacements. The possibility of large vibratory amplitudes that could be caused by thrust reversals during propeller ice milling was not considered at that stage. Typical open water centerline shaft axial stiffness varied between 5.5×10^6 and 15.6×10^6 lb/inch [13] (These were calculated using recorded shaft thrust at the bearing and the measured bearing displacement relative to the foundations).

B.4.3 Elements of the Vibratory System

Stiffness: Axial stiffness of the shaft
Thrust bearing
Bearing Housing
Bearing Foundation
Hull Structure

Mass: Propeller inertia
Hydrodynamic inertia
Shaft mass.

An increase in thrust bearing stiffness will reduce off-resonance vibratory response.

Icebreaker propellers operate in a medium which contains large blocks of ice, and the 'milling' of this ice by the propeller blades generates large forces in a wide band of frequency range. In addition, the occurrence of thrust reversals, which result in collar-pad separation in the thrust bearing may cause a reduction of the apparent natural frequencies of the shaft system. This phenomenon, loosely termed 'hammering' of the thrust bearing, is non-linear in character and hence is not amendable to analysis using GBRP and such other computer programs. In order to be able to eliminate the resonance problem in the axial vibration of the shaft, it is necessary that prediction of the occurrence of 'hammering' is possible.

The detailed study carred out for USCG (Reference [13]) provides numerical values of the stiffnesses of the main elastic components of the propulsion system of the Polar Class ships.

Stiffnesses from F.E. Models: (a) Wing thrust bearing foundation (original) - Symmetric loading - 11.17×10^6 lb/inch, Anti-Symmetric - 11.96×10^6. (b) Modified - 12.52×10^6. (c) Reinforced - 24.987×10^6.

Because of the substantial scantlings associated with the reinforced foundations, USCG authorities consider the stiffness figure of 24.0×10^6 lb/inch as an upper bound on the axial stiffness that can be built into these ships, without drastically altering the current configuration of the wing shafting systems.

B.4.4. Thrust Bearing Stiffness

An estimate of the stiffness of the thrust bearing has been made by USCG using standard engineering techniques. The net stiffness of the bearing unit is determined by adding up the individual stiffnesses of the various components in the system from the thrust collar to the flanges. The source of the 'stiffness' or 'flexibility' (reciprocal of stiffness) in each of these units may not be the same, but by studying the mechanical action of each of these units, it is possible to derive approximate stiffness values valid for small amplitudes of vibration. For example, the net flexibility of the thrust collar is obtained by circular plate loaded with a uniformly distributed pressure field over a band in the circumferential direction.

The results are given in the form of deflection versus thrust plots so that the flexibility of each component can be calculated as the slope of the straight line function. The derived stiffnesses of the various components are enumerated in Table B.6 rather than the individual flexibilities, since the former provide a better physical 'feel' for the relative rigidity of the thrust bearing components. The net stiffness of the thrust bearing is found to be 0.105 million tons/ft. It may be noted that the thrust bearing stiffness is approximately twice that of the original foundations. In expressing the stiffness of components which do not exhibit linear elastic characteristics, the numerical values in Table B.6 indicate the approximate linear coefficients which are valid for the design thrust and small fluctuations about the design thrust. This linearization process does not introduce significant errors into the net stiffness calculations as the strongly nonlinear element (namely, the oil film) has a stiffness (at design thrust) which is approximately an order of magnitude lower than that of a linear element such as the thrust shoes. It may also be noted that the thrust pads are the stiffest among the thrust bearing components.

B.4.5. Propeller Shaft and Propeller Particulars

The stiffness of the shaft can be determined in a straight forward manner knowing the diameter, length and the modulus of elasticity.

The axial stiffness, k_s, for a length l_s is given by:

$$k_s = A_s E / l_s \qquad \text{(B.6)}$$

where A_s and E are the cross-sectional area and modulus of elasticity respectively.

TABLE B.6

STIFFNESSES OF THRUST BEARING COMPONENTS [13]

COMPONENT	NATURE OF MECHANICAL ACTION	STIFFNESS 10^6(ton/ft)
Thrust Collar	Linear, elastic	3.91
Oil Film	Nonlinear, viscous	1.0
Thrust Pads	Linear, elastic	50.52
Thrust Buttons	Nonlinear, Hertzian contact	0.51
Levelling Links	Linear, elastic	1.64
Link-to-Link Contact	Nonlinear, Hertzian contact	2.52
Retainer	Linear, elastic	1.46
Front-end to casing contact	Linear, elastic	2.64
Front End	Linear, elastic	1.03
Casing	Linear, elastic	1.20
Flange	Linear, elastic	1.67

The particulars of the wing and center propellers required for hydrodynamic inertia calculations is given in Table B.7.

B.4.6. Hydrodynamic Inertia of Propellers

Kane and McGoldrick [14] have shown that the longitudinal and torsional oscillations of a propulsion shaft are coupled by water inertia and damping. They pointed out that providing the longitudinal frequency is at least twice the frequency of the lowest torsional mode, this coupling is weak. Under such conditions, the longitudinal frequencies can be calculated as if there were no torsional restraint from the shaft system, and torsional frequencies can be calculated as if the system were infinitely rigid in the longitudinal mode. It appears that except in very unusual designs, this condition will always be satisfied. Based on experiments and theoretical considerations, Lewis and Auslaender [12] have come up with empirical expressions for the hydrodynamic added mass and inertia of propellers, applicable to the longitudinal and torsional modes of vibration of the shaft. With slight change in notations:

$$M_a' = \frac{0.21\rho D^3 (\overline{MWR})^2 n}{[1+(p/d)^2]\ (0.3 + \overline{MWR}\ )} \qquad \text{(B.7)}$$

$$M_a = \frac{M_a'}{1 + \frac{p^2 M_a'}{4\pi^2 J}} \qquad \text{(B.8)}$$

$$J_a = 0.02\ M_a' p^2 \qquad \text{(B.9)}$$

where M_a' = Hydrodynamic added mass of a propeller in longitudinal vibration but with its rotation restrained to zero. This is a basic quantity which is not to be used as such in vibration analysis.

M_a = Equivalent added mass of a propeller in longitudinal vibration free to rotate on its shaft. With weak coupling between the longitudinal and torsional modes, M_a is to be used for longitudinal vibration analysis.

J_a = Hydrodynamic added moment of inertia in torsion or rotation. Strictly speaking, this is valid only for cases wherein the shaft is restrained from vibrating in the longitudinal mode. But it is adequate for approximate torsional calculations if the coupling is weak.

TABLE B.7

POLAR CLASS PROPELLER PARTICULARS

Diameter	= 16 ft
Pitch	= 27.3 ft
Developed Area Ratio	= 0.707
Number of Blades	= 4
Propeller mass (metal only)	= 3120 lb sec^2/ft
Propeller Shaft	
Inside diameter	= 10.24 inch
Outside diameter	= 26.0 inch

D = Propeller Diameter

p = Propeller pitch (nominal driving face)

$\overline{MWR}$ = Mean Width ratio

n = Number of blades

ρ = Mass density of water

J = Polar moment of inertia of propeller (metal only)

In the cases where coupling between the longitudinal and torsional vibrational modes is significant, the coupled added mass is given by:

$$C = M'_a p/2\pi \tag{B.10}$$

The numerical values of the parameters required for the calculation of the hydrodynamic added masses of the Polar Class propellers is given in Table B.7.

B.4.7. Mass Distributions

The mass distributions of the wing and centerline shafts required for vibration analysis are shown in Table B.8 and respectively. Masses of the propeller, main motor rotor, thrust bearing and the thrust bearing foundation were obtained from Gulick [15]. The mass distribution for the shaft was calculated knowing the inside and outside diameters and the density of steel. The propeller hydrodynamic added mass was calculated from expressions given in Section B.4.6.

The stiffness distributions for the wing shaft and the center shaft are given in Tables B.9 and B.11. With the above elastic and inertial characteristics in hand, it is possible to represent the propulsion system in longitudinal vibration as shown in Figures B.12 and B.13. It can be seen in both figures that the propulsion train cannot be considered in isolation for longitudinal vibration analysis as the foundation and the hull structure themselves have finite masses and stiffnesses. Three separate cases were, therefore considered. The first is the ideal case of an infinitely rigid thrust bearing foundation. Secondly, the case of a finite foundation wherein the stiffness of the foundation is variable. Three numerical values of the foundation stiffness as enumerated in Section B.4.2 are considered. Finally, the case of longitudinal vibration with the influence of hull structural elements included.

TABLE B.8

WING SHAFT MASS DISTRIBUTION

MASSES	COMPONENT	lb sec²/inch
1*	Propeller + hyd. added mass	416.0
2	Shafting	169.0
3	Shafting	95.6
4	Shafting	50.8
5	O/D shafting	16.8
6	Intermediate shafting	21.0
7	Intermediate Shafting	12.7
8	Intermediate Shafting	25.4
9	Thrust Bearing	63.5
10	Thrust Bearing Foundation	1597.0
11	Shafting	28.8
12	Main Motor Rotor + Shafting	194.0
13	Shafting	23.1
14	Shafting	35.8

* Mass numbers in the first column relate to corresponding numbers in Figure B.12.

TABLE B.9

WING SHAFT STIFFNESS DISTRIBUTION

STIFFNESS	COMPONENT		lb/in, x 10^6
1-2**	Tailshaft		72.0
2-3	Tailshaft		72.0
3-4	Tailshaft		135.0
4-5	O/D Shaft		263.0
5-6	Shafting		263.0
6-7	Shafting		474.0
7-8	Shafting		474.0
8-9	Shafting		233.0
9-10	Thrust Bearing		19.6
10-0*	Thrust Bearing Foundation	11.17, 12.53,	24.0
9-11	Shafting		428.0
11-12	Shafting		259.0
12-13	Shafting		350.0
13-14	Shafting		350.0

* A "0" indicates a grounded spring. The three thrust bearing stiffnesses correspond to the original, the modified and the reinforced foundations respectively.

** Numbers in the first column refer to spring elements in Figure B.12.

TABLE B.10

CENTERLINE SHAFT MASS DISTRIBUTION

MASSES	COMPONENT	lb.sec²/inch
1*	Propeller + Hydrodynamic Added Mass	405.7
2	Tailshaft	176.2
3	Tailshaft	111.9
4	Tailshaft	69.2
5	O/D Shaft	39.1
6	Main Rotor Motor	205.4
7	Intermediate Shafting	67.4
8	Intermediate Shafting	51.0
9	Thrust Bearing	63.7
10	Thrust Bearing Foundation	1194.0
11	Shafting	36.5

* Mass numbers in the first column relate to corresponding numbers in Figure B.13.

TABLE B.11

CENTERLINE SHAFT STIFFNESS DISTRIBUTION

STIFFNESSES	COMPONENT	lb/in. x 10^6
1-2**	Tailshaft	74.6
2-3	Tailshaft	55.9
3-4	Tailshaft	49.3
4-5	O/D Shaft	120.0
5-6	Shafting	203.0
6-7	Shafting	147.8
7-8	Shafting	116.7
8-9	Shafting	184.4
9-10	Thrust Bearing	19.6
10-0*	Thrust Bearing Foundation	11.17, 12.53, 24.0
9-11	Shafting	237.0

* A "0" indicates a grounded spring. The three thrust bearing stiffnesses correspond to the original, the modififed and the reinforced foundations respectively.

** Numbers in the first column refer to spring elements in Figure B.13.

FIGURE B.12

WING PROPULSION SHAFT MODEL FOR LONGITUDINAL VIBRATION ANALYSIS

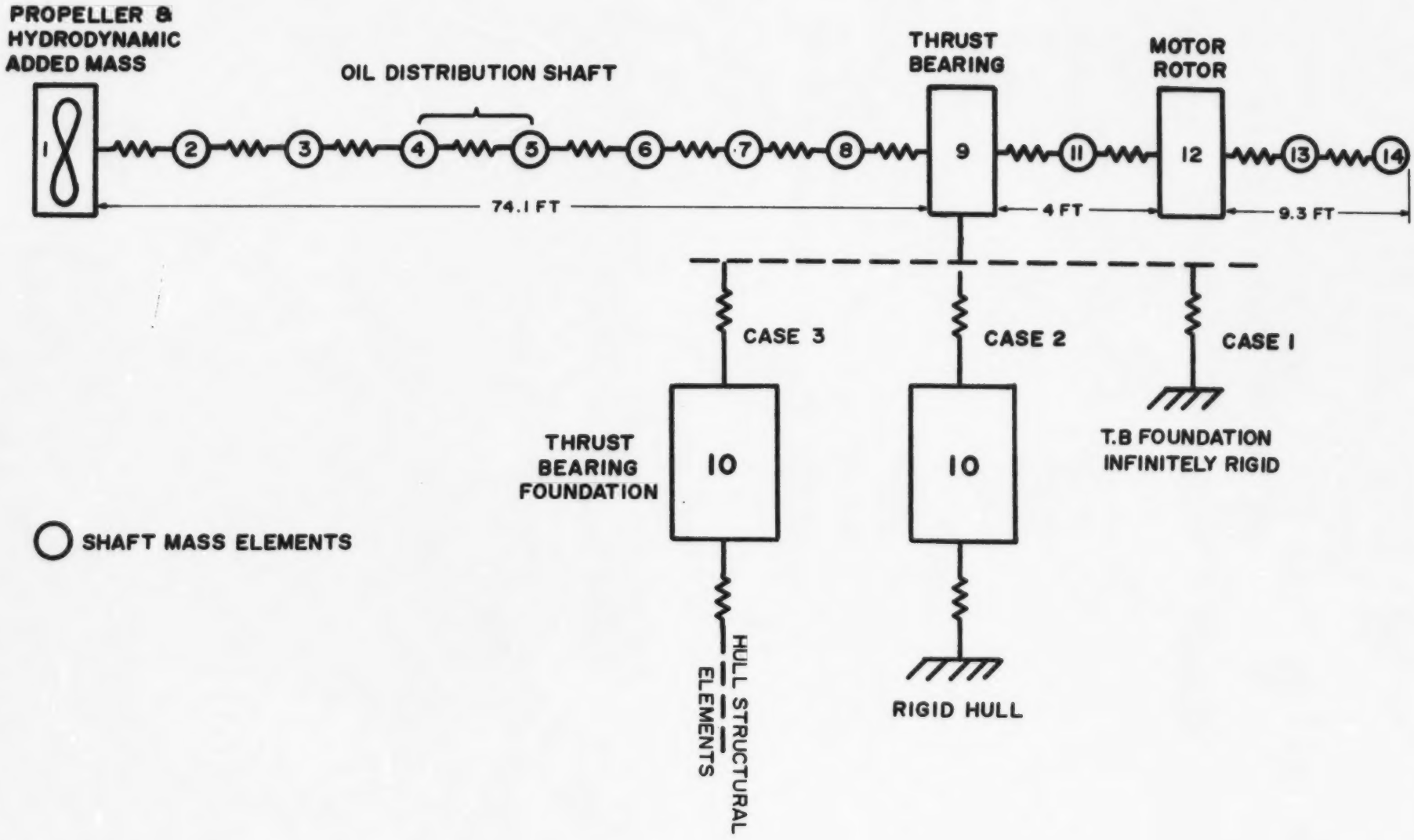

FIGURE B.13

CENTERLINE SHAFT MODEL FOR LONGITUDINAL VIBRATION ANALYSIS

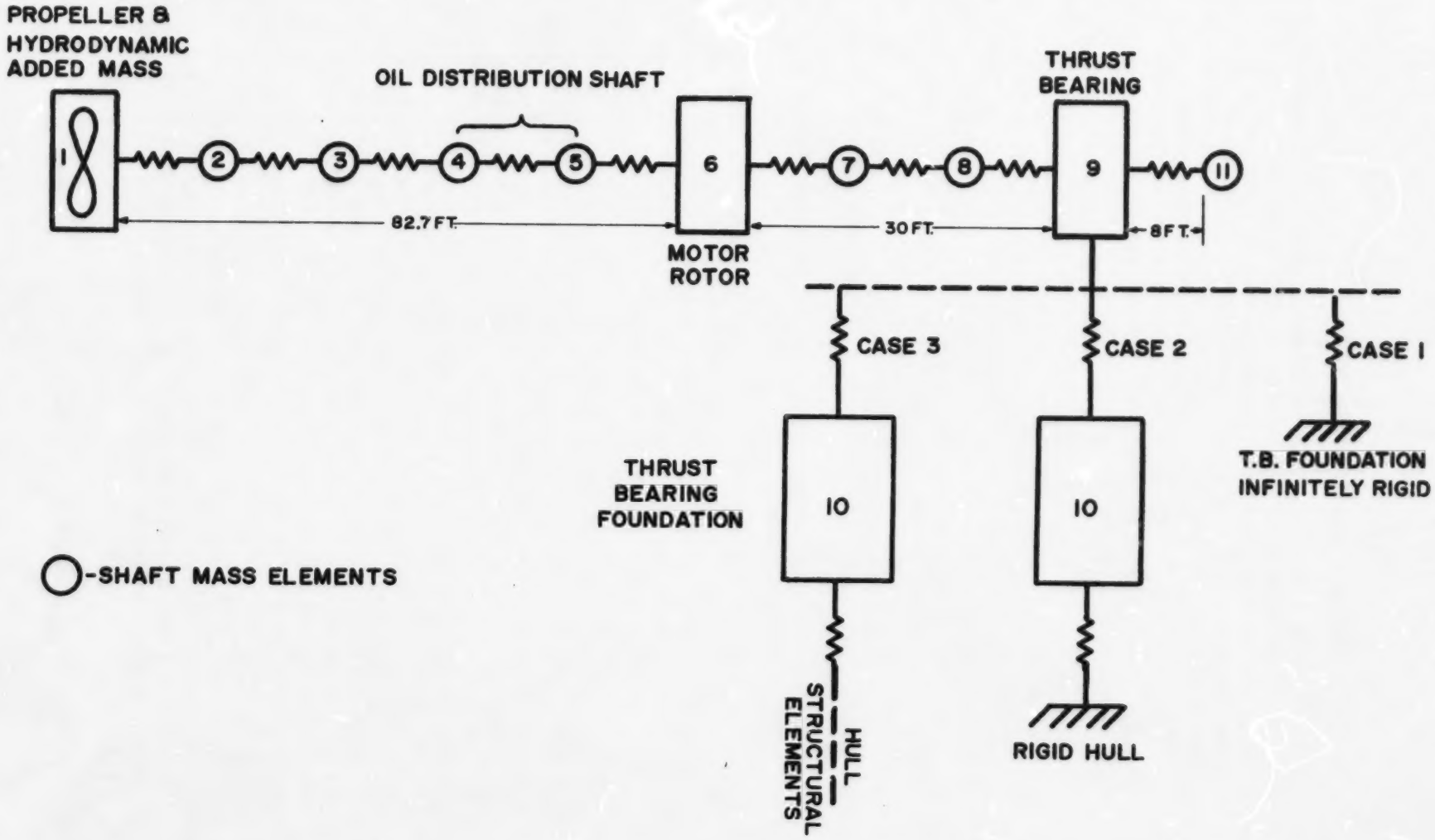

B.4.8. Results of Analysis

In addition to the three thrust bearing foundation stiffnesses given in Section B.4.2 the case of an infinitely stiff (six orders of magnitude higher) foundation was also considered, as a limiting case for which one might expect complete transmission of vibration to the hull structure in the longitudinal mode (Figures B.12 and B.13). Using the stiffness and mass distributions enumerated in Tables B.9, B.10, B.11 and B.12, GBRP was exercised for the eight cases (four of the wing shaft and four of the center shaft). Figure B.14 and B.15 show the output in graphical form for the wing shaft and the center shaft respectively. The mode shapes and frequencies up to the third mode are illustrated. Vibrational modes with frequencies about 130 Hz are not shown as such higher modes are not of immediate interest. In plotting the mode shapes, the modal deflection at mass element 10 (see Figures B.12 and B.13), i.e. the thrust bearing foundation, is excluded as it is part of a parallel array of masses and springs consisting of the hull structure. As expected, the mode shapes for the longitudinal vibrations of the propulsion system are very much unlike those of the hull structure (see Figure B.10). These non-periodic modal functions are characteristic of elastic systems with abrupt changes in inertias and stiffnesses which applies to propulsion train components. Note also that the modes are not numbered on the same basis as those representing hull bending vibrations.

The computed mode shapes are shown for the case of the 'as built' thrust bearing foundation (see case a) as well as for the ideal case of very stiff thrust bearing foundation (case b). The mode shapes for the intermediate stiffnesses are not plotted as they are barely different from those in case (a). From Figure B.14, for case (a), it can be seen that in the zero mode of vibration, the elements of the propulsion system would tend to oscillate almost in phase just as in a single degree-of-freedom system. That is, the effects of the distribution of inertias and stiffnesses are of second order nature for this particular mode. The next vibrational mode has a single node just forward of the main motor rotor and has a fairly high frequency. It is interesting to note that the second mode (49.02 Hz) also possesses only a single node, although shifted further aft and close to the propeller end. The third mode exhibits two nodes and its frequency is more than double that of the second mode. If, for comparison purposes, we also examine the computed modal functions in case (b), it is seen that the increase in foundation stiffness has brought about a peculiar change in the properties of the various vibrational modes. The effect of the distributed inertia and stiffness is more pronounced in the zero mode for this case. This implies that, in the case of an extremely stiff foundation, the vibrational characteristics of the center shaft cannot be modelled as a single spring-mass system. A striking feature of the two cases is that the higher modes (first and higher) exhibit a one-to-one correspondence - the nth mode of case (b) is very nearly similar to the $(n + 1)^{th}$ mode of case (a) in shape as

FIGURE B.14 MODE SHAPES AND FREQUENCIES FOR LONGITUDINAL VIBRATION OF PROPULSION SYSTEM

WING SHAFT

CASE A

T.B. FOUNDATION STIFFNESS = 11.17×10^6 LB/IN

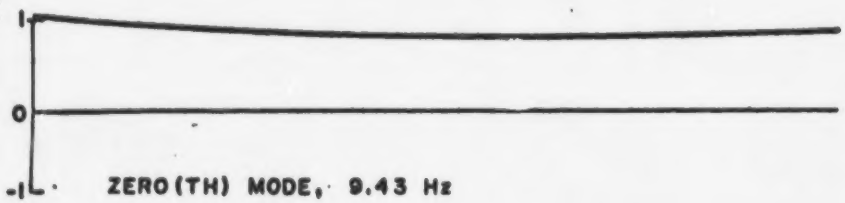

ZERO (TH) MODE, 9.43 Hz

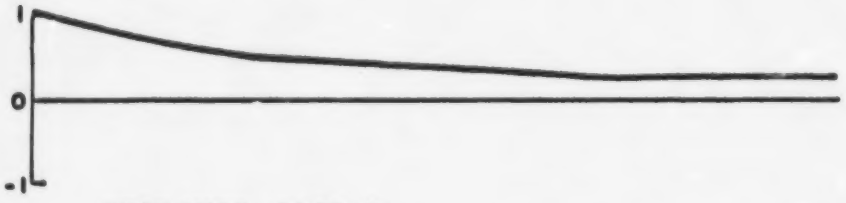

FIRST MODE, 24.88 Hz.

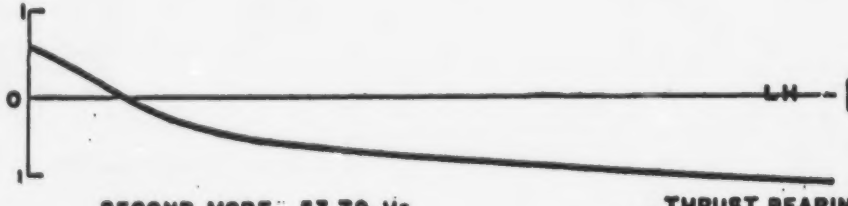

SECOND MODE, 53.79 Hz

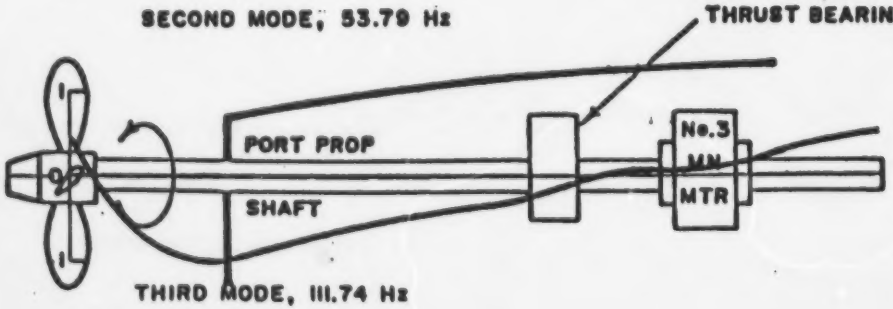

THIRD MODE, 111.74 Hz

CASE B

T. B. FOUNDATION STIFFNESS INFINITE

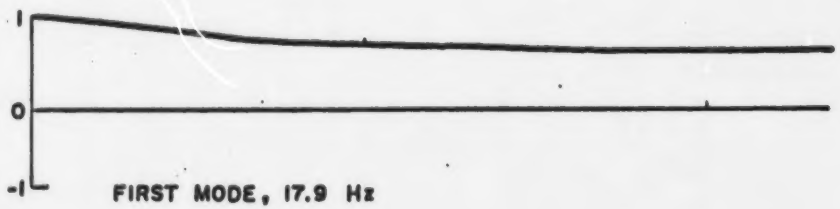

FIRST MODE, 17.9 Hz

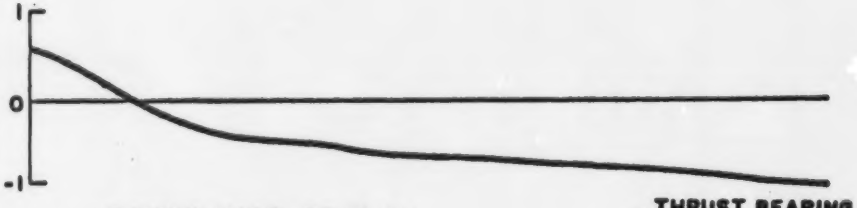

SECOND MODE, 53.01 Hz

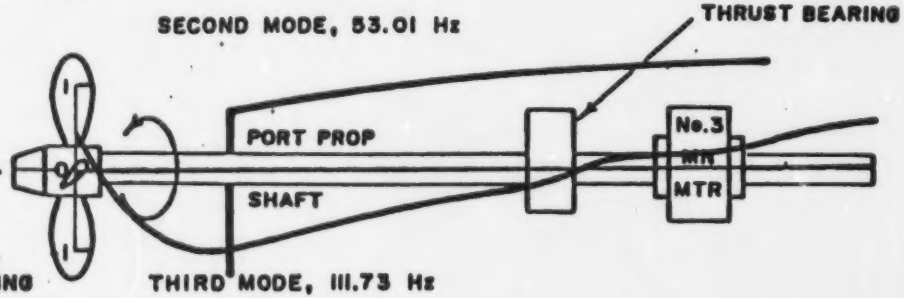

THIRD MODE, 111.73 Hz

well as frequency. It may be inferred that the effect of having an extremely stiff thrust bearing foundation is to completely eliminate the zeroth mode. For stiff thrust bearing foundation stiffnesses, therefore, the propulsion system behaves more like a continuous elastic system with distributed inertias and stiffnesses.

The above reasoning is qualitatively applicable to the case of the center shaft longitudinal mode shapes as well, shown in Figure B.15.

Variation of Frequency with Stiffness: The dependence of the first three longitudinal natural frequencies of the wing shafts as well as the center shaft on the foundation stiffnesses are shown in Figure B.16(a) and (b). The broken lines in (a) and (b) depict the probable variation of the frequencies as the foundation stiffness of 100% over the 'as-built' value, the corresponding increase in the lowest natural frequency is 32% for the wing shafts and 21% for the center shaft. As limiting cases, it can be seen from Figure B.16(a) and (b) that the maximum possible increases in frequencies are approximately 90% and 60% respectively. This means that increasing the foundation stiffness is not always the most practical method of ensuring low levels of propeller-induced vibrations. The number of blades is the next design variable to be considered.

In the case of the Polar Class vessels, the comparison of the lowest natural frequencies of the wing and center shafts with the propeller excitation frequencies (in the Diesel-Electric mode of operation) is shown in Table B.12

TABLE B.12

COMPARISON OF SHAFT FREQUENCIES WITH PROPELLER EXCITATION FREQUENCIES

SHAFT	SHAFT SPEED (rpm)	f_e PROPELLER EXCITATION FREQUENCY, Hz (BLADE FREQ.)	f_n LOWEST LONGITUDINAL FREQUENCY, Hz	f_e/f_n ·/·
WING	110	7.32	9.43	78
CENTERLINE	130	8.68	9.48	92

FIGURE B.15 MODE SHAPES AND FREQUENCIES FOR LONGITUDINAL VIBRATION OF PROPULSION SYSTEM CENTER SHAFT

CASE A

T. B. FOUNDATION STIFFNESS = 11.17 x 10^6 LB/IN

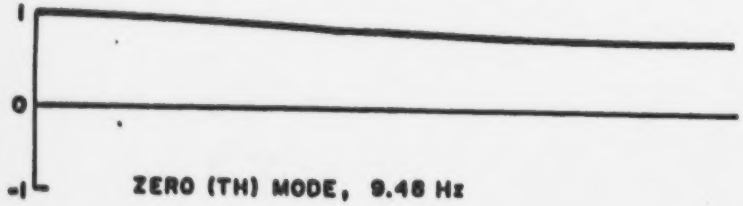

ZERO (TH) MODE, 9.48 Hz

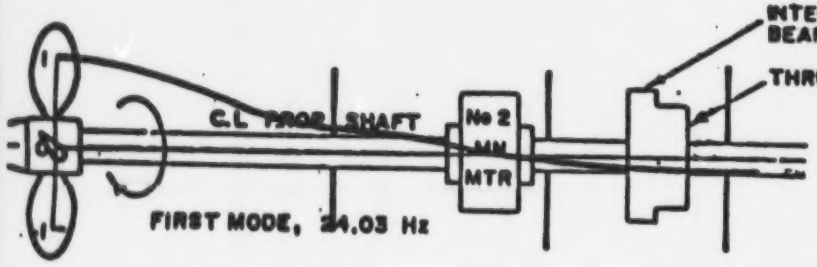

FIRST MODE, 24.03 Hz

SECOND MODE, 49.02 Hz

THIRD MODE, 106.59 Hz

CASE B

T.B. FOUNDATION INFINITELY STIFF

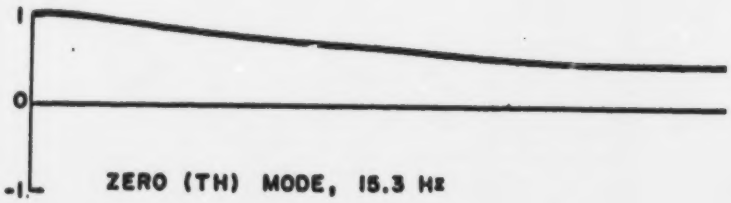

ZERO (TH) MODE, 15.3 Hz

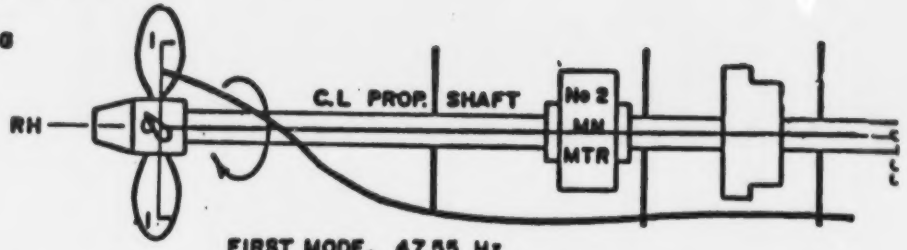

FIRST MODE, 47.55 Hz

SECOND MODE, 106.47 Hz

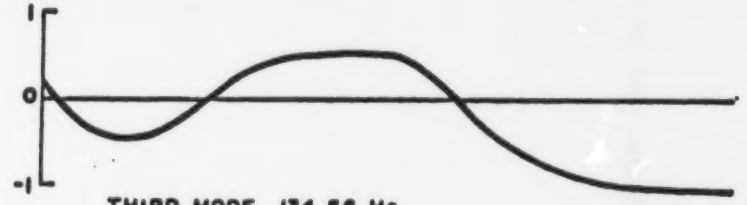

THIRD MODE, 134.56 Hz

FIGURE B.16

VARIATION OF NATURAL FREQUENCIES WITH T.B. FOUNDATION STIFFNESS

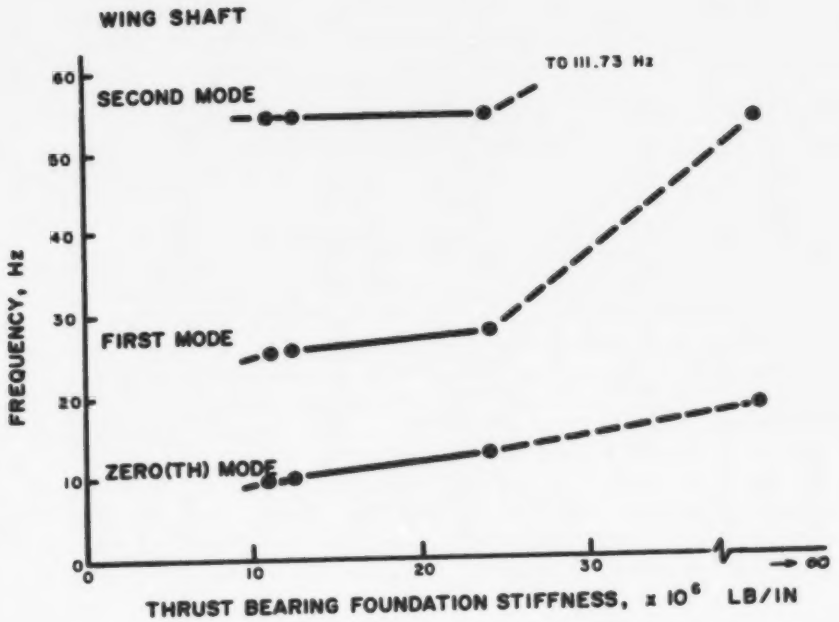

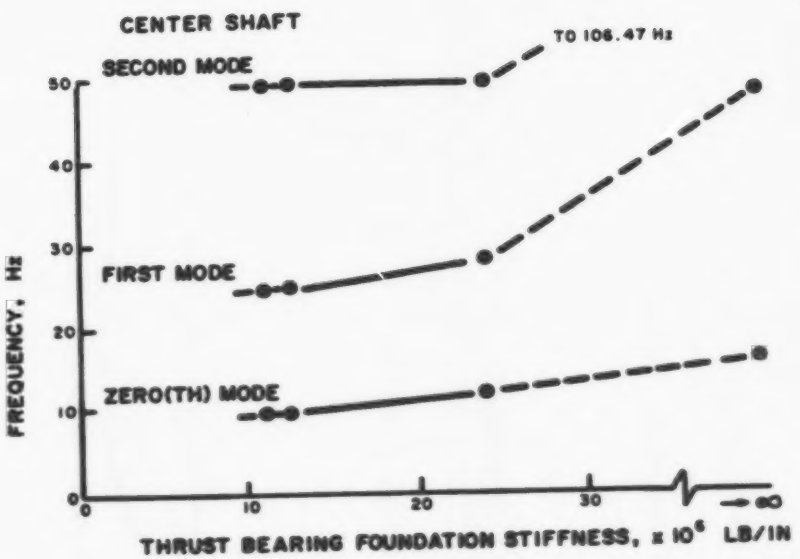

If the general rule given in B.4.1 is applied to the present case, it is seen that the lowest natural frequency of the wing shafts is only marginally adequate for safe operations. At the same time, the natural frequency of the centershaft is too close to the propeller blade frequency at the normal operating shaft speed.

B.4.9 Summary of Results of Propulsion System Vibration Analysis

The propulsion system consists of the line shafting, the thrust block, its foundations as well as the masses pertaining to the machinery. The determination of the parameters essential to this type of analysis involves calculation of the stiffness of the thrust block foundations and double bottom structure which are deduced from Finite Element models. Reports on studies conducted by/for the U.S. Coast Guard are referenced at the appropriate places. Numerical values of the inertial parameters required for vibration analysis were obtained by private communications. By exercising the structural analysis program GBRP, the values of the four lowest natural frequencies of longitudinal vibration have been assessed. In order to study the vibration characteristics of the propulsion system in isolation (independent of the effects of other hull structural elements), it was necessary to consider infinite stiffness for the thrust bearing foundations. The two lowest values of the frequencies are 9.45 and 24.4 Hz which are only marginally above frequencies corresponding to the two lowest harmonics of excitation which could arise from each of the thrust propellers. This confirmed that the possibility of a dynamic amplification of the response to thrust variations is finite. In this respect, it must be emphasized that the adoption, at a later stage, of a 'modified design' for the thrust bearing foundation forward of the bulkhead and below the tanktop is a significant factor in reducing the probability of excessive propeller-induced hull vibration.

APPENDIX B.5

INPUT PREPARATION FOR GBRP

IV. INPUT PREPARATION FOR GBRP

The input data required for the GBRC1 program is that required for setting up the system of difference equations described in Section II. In particular, the following kinds of data can be included for each case:

1) The total number of sections. This must be less than 80.

2) The range of frequency values and the frequency interval for which response curves are required.

3) The system to which each beam section belongs, i.e., whether to the hull, shaft, or some other system.

4) For the hull and/or any other system, for which the J-factor is required for the added or virtual mass calculation, the following data is required:

   a) An initial value for the J-factor

   b) The radius

   c) A water inertia term for each section

5) The mass of each section.

6) The integral over each section of the reciprocal of the bending rigidity, i.e., $(\Delta x/EI)_n$.

7) The integral from the mid-point of each section to the mid-point of the next of the reciprocal of the shear rigidity, i.e., $(\Delta x/KAG)_{n,\,n+1}$ or $(\Delta x/KAG)_{n,\,m}$.

8) The integral of the mass polar moment of inertia from the mid-point of each section to the mid-point of the next, i.e., $(I_{\mu x}\,\Delta x)_{n,\,n+1}$ or $(I_{\mu x}\,\Delta x)_{n,\,m}$.

9) The spring constant and damping coefficient associated with each spring connection.

10) For each set of parameters, for each system a complex scaling factor can be supplied. This allows damping to be introduced in various ways. In particular, a complex scaling factor for the ship mass corresponds to the introduction of a Rayleigh damping coefficient.

For each section and connection a system number between 1 and 80 inclusive must be specified. This number is used to select the scaling factors to be applied to the parameters for that section or connection. It is also used in order that the program can select the set of sections and connections which make up a given system so that the zeros of the displacement of that system can be determined for the calculation of the virtual mass coefficient J. Section numbers for sections which are connected to each other should differ by less than 15.

The input data cards for GBRC1 are laid out as shown in Figures 5 to 10 Section V. The contents of these cards are described in detail below. In general, when a series of problems is being run, only those data cards which contain changes from the previous case are required. The numbers punched in columns 3 and 4 of each card identify the kind of information that card contains. An input deck should begin with a title card, and the set of data for each problem should begin with a data control card (columns 3 and 4 contain 90) which gives, for each type of data card included, the number of such cards. The data cards

for the problem should follow in the same sequence as they are given on the data control card. The last card of the input deck for a set of problems should contain 99 in columns 3 and 4 if no additional problems are to be run, and 98 in columns 3 and 4 if a complete data set for another unrelated problem follows.

Detailed formats for each type of card are given below.

1) Run Title Card

Columns	Contents
7 to 12	(62HΔΔ
13 to 72	These contain whatever title is to be associated with this run.

2) Data Control Card

Columns	Contents
3 to 4	90 (Type of data)
5 to 6 7 to 8	Columns 5, 6 contain number of data cards of type given by columns 7, 8 which follow for this case.
9 to 10 11 to 12	Similar to previous four columns for next data cards for this case.
etc.	

3) Case Title Card

Columns	Contents
3 to 4	10
7 to 12	(62HΔΔ
13 to 72	Title for this case

4) Option Control Card

Columns	Contents
3 to 4	20
9 to 12	Op 1: Added mass option selector. 0 if added mass as specified in input is used, 1 if J water inertia as specified in input is to be used (See Section III)
13 to 16	Op 2: Selector for A-matrix and P-vector setup option. 0 for present.
17 to 20	Op 3: Selector for edit routine to be used at each frequency. 0 for present.
21 to 24	Op 4: Selector for final edit routine. 0 for present.

Columns	Contents	
25 to 28	Op 5:	Selector for A-matrix routine. 0 if A-matrix is not printed; 1 if A-matrix is to be printed.
29-32	Op 6:	≠0 Plot displacements and/or moments versus sections for each frequency. 0 - No plot. 1 - Plot displacements only. 2 - Plot moments only. 3 - Plot displacements and moments.
33-36	Op 7:	≠0 Plot displacements and/or moments versus frequency for selected sections. 0, 1, 2, 3 } Same designation as above.
41-44	Op 9:	Selector to determine if forcing function is to be multiplied by square of frequency (ω). 0 - Force not multiplied. 1 - Force is multiplied.
45-48	Op 10:	Selector for natural frequency search. 0 - Ordinary response is obtained for all frequencies specified. 1 - Natural frequencies and mode shapes are obtained.

5) Edit Control Card

3 to 4	21
9 to 12, 13 to 16, 17 to 20, 21 to 24, 25 to 28	Section numbers for those sections for which displacements and moments are to be tabulated versus frequency.

6) General Data Card

Columns	Contents
3 to 4	30
7 to 8	Number of sections; maximum of 80
9 to 16	Starting frequency in cps
17 to 24	Upper limit for frequency in cps
25 to 32	Frequency interval to be used in cps Note: If a search is being made for natural frequencies, this will be the interval used to isolate individual frequencies.

7) System Data Cards for Added Mass Calculation

3 to 4	31
7 to 8	System number. The hull sections, shafting sections, etc., can be distinguished from each other by assigning a system number to each set of sections. These numbers may be in the range 1-80.
9 to 16	Radius associated with system in the units in which the unscaled distances between adjacent section centers are given.
17 to 24	Initial J-value for use with this system.

8) Section Parameter Cards

Columns	Contents
3 to 4	43
7 to 8	Section number
12	End condition - normally 0. 1 for V(o) = M(o) = 0 2 for X = 0 = FIXED
15 to 16	System number
17 to 24	Ship mass
25 to 32	Water inertia
33 to 40	$(\Delta x/EI)_n$
41 to 48	$(\Delta x)_{n, n+1}$
49 to 56	$(\Delta x/KAG)_{n, n+1}$
57 to 64	$(I_{\mu z} \Delta x)_{n, n+1}$
65 to 72	P_n

9) Scaling Factor Cards for Section Parameters

3 to 4	41 if this card contains real parts of scaling factors. 42 if this card contains the imaginary parts of the scaling factors.
15 to 16	System number for which scaling factors on this card are to be applied.
17 to 72	Scaling factor for each parameter are given in those columns containing that parameter value on the section parameter cards.

10) Special Connection Parameter Cards

Columns	Contents
3 to 4	53
7 to 8 11 to 12	The section numbers for the connection n to m;* if m = 0, this will represent a connection from section n to ground.
15 to 16	System number with which connection is to be associated.
17 to 24	$k_{n,m}$ Spring constant for connection
25 to 32	$c_{n,m}$ Constant damping coefficient for connection
33 to 40	$c_{n,m/\omega}$ Coefficient for frequency dependent damping for connection
41 to 48	$(\Delta x)_{n,m}$
49 to 56	$(\Delta x/KAG)_{n,m}$
57 to 64	$(I_{\mu z}\Delta x)_{n,m}$
65 to 72	$Q_{n,m}$

Note that in general either $k_{n,m}$, $c_{n,m}$ and/or $c_{n,m/\omega}$ or $(\Delta x)_{n,m}$, $\frac{\Delta x}{KAG_{n,m}}$ and $(I_{\mu z}\,\Delta x)_{n,m}$ will be supplied depending on whether sections n and m are connected by a spring or are two adjacent sections of a beam. It is important that the system numbers in these two cases be distinct, if J factors for the virtual mass calculation are to be calculated for the beam.

11) Scaling Factor Cards for Parameters in Special Connections

3 to 4	51: This card contains real parts of scaling factors.
	52: This card contains imaginary parts of scaling factors.

*Absolute value of (m − n) must be less than 15. While in general, the numbers m and n can be entered on the card in the order n, m or m,n, in the case of a ground connection the 0 must be in Column 12.

Columns	Contents
13 to 16	System number with which these scaling factors are to be associated.
17 to 72	Scaling factors for parameters in corresponding locations on special connection parameter cards.

12) Microfilm Recorder Plotting Characters

3 to 4	60
7 to 12	blank
13 to 18	ΔΔΔΔΔ+
19 to 24	ΔΔΔΔΔ0
25 to 30	ΔΔΔΔ ΔX
31 to 36	ΔΔΔΔΔ-
37 to 42	ΔΔΔΔΔ·

13) Natural Frequency Card

3 to 4	70
9 to 10	Number of natural frequencies desired.

14) Begin a complete new set of data

3 to 4	98

15) End of data

3 to 4	99

16) Number of cases

1 to 2	Total number of cases computed in a particular run. This number will be equal to the number of "90" and "98" cards plus one.*

*This card is used only when plotting is required and it is the only data card used with the binary deck (Part II) of the code, see page 67.

Note 1. When setting up data, only columns on any input card type need be punched for which data actually exists. If a card is blank, except for the identifying number, it should be omitted from the data deck. The listing of number and type of each card on the Data Control Card is completely arbitrary; however, once it is punched, the physical lineup of the data cards must follow in exactly this order.

B.6 REFERENCES

1. F.E. Reed and O.H. Burnside, "Computer Techniques for Use in Ship Vibration Analysis and Design", SNAME, paper presented at the Ship Vibration Symposium, Arlington, Va., October 16-17, 1978.

2. F.M. Henderson, "Forced Vibration Calculation Using General Bending Response Program (GBRP) and the Fast Fourier Transform", Naval Ship Research and Development Center Report 4481, August 1974.

3. M.E. Golden and F.M. Henderson, "An Updated Guide to the Use of General Bending Response Program (GBRP)", Naval Ship Research and Development Center, Report 4601, April 1975.

4. J.M. Biggs, "Introduction to Structural Dynamics", McGraw-Hill, Inc., New York, 1964.

5. Meirovitch, L., *Analytical Methods in Vibrations*, The MacMillan Company, New York, 1967.

6. Kruppa, C. (1962), "Beitrag zum Problem der Hydrodynamischen Tragheitsgrossen bei elastischen Schiffsschwingungen," Schiffstechnik, Heft 45, Bd. 9, pp. 38-60.

7. Misra, P.N., "Transverse Vibrations of a Ship Hull in Ideal Fluid, Determined Through Variational Methods", Journal of Ship Research, Vol. 18, No. 3, Sept.1974, pp.185-202.

8. Kumai, T. (1967), "On the Estimation of Natural Frequencies of Vertical Vibration of Ships", Journal of Society of Naval Architects of Japan, 3-3, May, pp. 217-224.

9. Hylarides, S. (1971) "Ship Vibration Analysis by Finite Element Technique," Part II, The Netherland Ship Research Centre, TNO, Report No. 153 S, Delft, May pp. 1-15.

10. Townsin, R.L. (1969), "Virtual Mass Reduction Factors: J Values for Ship Vibration Calculations, Derived from Tests with Beams including Ellipsoids and Ship Models," Trans RINA, Vol. III, No. 3, pp.385-97.

11. Rules for the Design of Propellers, American Bureau of Shipping and Lloyds Register of Ships.

12. Lewis, F.M., and Auslaender, "Virtual Inertia of Propellers", Journal of Ship Research, March 1960, p.37.

13. Vassilopoulos, L. and Hamilton, F.M., "Longitudinal Stiffness Analysis for the Propulsion Shafting Systems of the Polar Class Icebreakers", Paper presented at the American Society of Naval Engineers Conference, May 1980.

14. Kane, J.R., and McGoldrick, R.T., "Longitudinal Vibration of Marine Propulsion-Shafting Systems", Trans. SNAME, Vol. 57, 1949.

15. Lcdr. R.W. Gulick, U.S. Coast Guard, Washington, D.C., Personal Communication.

APPENDIX C

FULL SCALE DATA REDUCTION

C.1 OBJECTIVES

The objectives of reducing the full scale data can be outlined as follows:

i) To select cases of different operating conditions for the spectrum analysis.

ii) To establish the initial conditions of the vessel as well as the environmental data (sea state, ice conditons). In case of ship impact, the location of impact and the post-impact conditions were also included.

iii) To establish a log with clear and complete information as to how the video and analogue data can be accessed for re-examination.

The scenarios of interest cover the following:

i) open water turning
ii) crash reversal
iii) backing in ice
iv) continuous ice transit
v) ramming in level ice
vi) ramming pressure ridge.

The selection of suitable cases was based on a set of criteria that were believed to cover the requirements. The criteria are outlined as:

i) Establishment of data availability,
ii) confident estimation of pre-impact conditions,
iii) evidence of clear, sharp impact,
iv) evidence of uniform ice conditions,
v) clear, visual evidence of motions after impact.

It should be pointed out that during this task of reducing full scale data emphasis was put on the ship impact scenarios rather than open-water operations.

The establishment of data availability involved matching for each case, the visual and oscillograph records to ensure that both records were recording at the time of impact. A review of the video for the case of interest was made to establish the pre- and after-impact conditions. Ship speed just prior to impact was determined by use of the video tape from the forward-looking camera. Ice thickness was estimated by video tape from the side-looking camera mounted on the ship side. If this was not available, daily ice thickness data obtained by the ice team was used.

C.2 METHODOLOGY

During the period of the trial program, a total of 26 magnetic tapes and 16 video tapes were used representing some 100 hours of test data. To ensure successful data reduction, the procedures consists of the following steps:

i) Review both the trafficability data summary obtained from ARCTEC Incorporated and the voyage summary log prepared by ARCTEC CANADA personnel to establish an initial data base (Annex 3).

ii) Review video tape records of the voyages to establish the impact scenario and the initial, after impact conditions.

iii) Review the oscillograph outputs of every acceleration during the corresponding time period for each impact.

iv) Re-examination of both the video and oscillograph records to select representative cases of each scenario for spectrum analysis.

The first step is a 'short cut' to establish an initial data base for further assessment of the suitability of the scenario for selection. Thus, there was no need to review all the video tapes. Once this was done, both the video and oscillograph records were scrutinized to extract representative cases. Initial and post-impact conditions were logged. A calibrated scale for the forward-looking camera was available and it allowed an accurate determination of the length of travel for an ice piece moving across the video screen. An ice piece or edge was first located on the scale and a stopwatch started. Once the ice piece or edge has crossed the screen, the watch was stopped. The distance travelled and the time recorded were then used to calculate the ship speed. Usually, three or four measurements were made and the resulting speeds were averaged. The location of impact was approximated by eye judgement.

Once the first extraction of promising cases was completed, a final decision was made to select representative cases for each scenario under consideration. This involved re-examination of both the detailed video log and the oscillograph outputs. The final selection of representative cases was based on the criteria mentioned in previous section.

C.3 RESULTS OF DATA REDUCTION

The results of the full-scale data reduction were a series of scenarios including ice transiting, ice ramming and open-water operations. A log of the initially extracted promising cases is given in Annex 4. The log consists of the ice conditions as well as the ship's behaviour prior to and after impact. In most cases, the documentation also includes a sketch of ice field and the traced path of the ship before and after impact.

The final selected cases for the spectrum analysis are shown in Table C.1.

TABLE C.1

SELECTED CASES FOR SPECTRUM ANALYSIS

SHIP OPERATING CONDITION	DAY-TIME GROUP	TAPE# COUNT#	IMPACT POSITION	SHIP SPEED (K)	ICE (FT) MAX.	AVE.
Open Water Turning	01:29:10:57	1-1,4022				
Crash Reversal (Gas Turbine)	01:29:13:58	1-2,392		13.0		
Backing in Level Ice	01:31:13:02	1-2,3521			1.5	1.0
Continuous Ice Transit	01:30:23:43	1-2,758	Head-on	9.3	1.5	1.0
Continuous Ice Transit	01:31:14:10	1-2,4160	Head-on	6.0	1.5	
Ramming Level Ice	02:08:02:30	1-9,3797	Oblique	9.0	4.0	3.5
Ramming Level Ice	02:09:06:20	1-10,3241	Oblique	9.0	4.0	3.0
Ramming Level Ice	02:09:06:09	1-10,3133	Head-On	5.3	4.0	3.0
Ramming Level Ice	02:09:14:00	1-11,1833	Head-On	4.0	3.0	2.0
Ramming Pressure Ridge	02:08:02:23	1-0,3732	Oblique	6.0	4.0	3.5
Oblique Impact	02:08:23:50	1-9,4494	Oblique	9.0	2.0	
Oblique Impact	02:09:06:26	1-10,3316	Oblique	7.0	4.0	3.0

PROCEDURE FOR ACCESSING DATA

Data Recorded

The data acquired by ARCTEC CANADA LIMITED during the POLAR SEA trials consists of the following:

(a) General ice conditions
(b) Ice thickness
(c) Ship's speed
(d) Shipboard accelerations
(e) Deck and hull strains
(f) Shaft torque and thrust
(g) Propeller revolutions
(h) Time code

The data were recorded on video and magnetic tapes. Two magnetic tape recorders, each with a 28-channel capability and two low light T.V. cameras were used to make the records. A total of 26 magnetic tapes and 17 video tapes were recorded.

Cataloguing

The four sets of tapes (2 each for magnetic and video recorders) have been sequentially numbered for easy identification.

The Magnetic Tapes are identified by a 6 or 7 character number such as 7921-X or 7922-X where X is a number from 1 to 13. The logic of the number can be explained by the following examples:

7921-8 ← Indicates "reel no: 8"
Indicates "magnetic tape-recorder no: 1"
ARCTEC'S number for this project

Similarly

7922-11 ← Indicates "reel no: 11"
Indicates "magnetic tape recorder no: 2"
ARCTEC'S number for this project

The Video Tapes are identified by a six character number such as: 7923 - X or 7924 - Y where X is a number from 1 to 8 and Y a number from 1 to 9. The logic of the number can be explained by the following examples:

7923-5 ← Indicates "reel no: 5"
Indicates "Port side, over the side downward looking video camera"
ARCTEC'S number for this project

Similarly:

7924-9 ←——— Indicates "reel no: 9"
——— Indicates "Aloft-con forward looking video camera"
——— ARCTEC'S number for this project.

In addition to the above information, the videotape boxes also show the time, date and month that each video tape covers.

The Data Log consists of three distinct sections (see Annex 3):

(*i*) Section 1 shows a diagramatic view of the ship with locations of the various sensors.

(*ii*) Section 2 is *the log* showing the date, time, tape-counters and remarks.

(*iii*) Section 3 is the *channel assignment log* showing the channels (or tape tracks) allocated to the tapes on each of the two magnetic recorders and calibration factors.

Accessing of Data

All the data collected by ARCTEC CANADA LTD on-board team can be accessed through the information recorded in the Data Log.

The starting point may be either the date and time group (DTG) or a specific incident.

Assuming that data is required for a specified date-time-group, the following procedure applies. Example: Feb. 3rd at about 2:30 p.m.

(a) Locate the DTG in the first two columns (headed: SYSTRON DONNER). This is the 3rd row on page no. 4.

(b) Proceed along this row to the columns on the right which show that the information is available on:

(*i*) magnetic tape reel no: 4 of recorder 7921 with tape counter in the neighborhood of 1235.

(*ii*) magnetic tape reel no: 4 of recorder 7922 with tape counter in the neighborhood of 712.

(*iii*) Video tape reel no: 3 of the over-the-side-T.V. camera, recorder no 7923, with tape counter in the neighborhood of 350

(*iv*) Video tape reel no: 3 of the forward looking (ie: aloftcon) T.V. camera (recorder no 7924), with tape counter in the neighborhood of 812.

(c) The last column (headed "Activity") indicates that at this time the ship was "Backing & Ramming".

(d) The *Channel Assignment Log*, sheet 1 in the third section of the Data Log, shows the channel on which the output from each sensor is recorded. For example, if it is desired to examine the accelerations experienced in the vicinity of the "elevator" and the thrust developed by the Port propeller shaft:

(*i*) Section 1 of the Data Log shows that the "Elevator" accelerometers are nos: 2X, 2Y & 2Z.

(*ii*) Channel assignment of recorder number 1 shows that channels nos: 10, 11 & 12 contain these records and that channel 28 is the video time code (slow code). Connect these four channels from the tape recorder to the video display unit (VDU). Examination in the neighborhood of tape counter reading 1235 will replay the recorded accelerations and channel 28 will give a continuous read out of time.

(*iii*) Connect channels 4 and 28 of recorder no: 2 to the VDU and run the tape (no: 7922-4) to the vicinity of counter no: 712. The VDU will now display the Port Shaft Thrust recorded and the time read out.

The two video tapes may be played back to obtain an averall assessment of the prevailing snow/ice/sea conditions, the ship's speed and ice thickness. This can be done by constructing an *overlay grid* for the particular VDU being used. The procedure is as follows:

(a) Select video calibration incidents from the Tape Log Activity column. For example Page 2 row nos: 20, 21 and 22. (Row 20 is the aloftcon and rows 21 & 22 are over-the-side cameras).

(b) Choose video tape no: 7924-1 and run the tape recorder till the counter reads in the neighborhood of 500.

(c) Play back this tape through the VDU. The pictures on the screen & the voice channel explain the "ahead" calibration procedure.

(d) Following this procedure, a grid such as figure C.1 can be prepared on a transparent sheet of mylar.

(e) This overlay can be used to assess the ship's speed by noting a "land mark" in the ice ahead of the ship and the time taken for it to cross the horizontal distance lines on the overlay.

(f) A similar procedure can be followed for tape 7923-1 in the neighborhood of tape counter reading 580. This will produce a grid of distances looking downwards and out from the ship's port side. Such a grid overlay is shown in figure C.2. This grid may be used to measure thicknesses of broken blocks of ice as they turn over and pass by the ship's side.

FIGURE C.1
CALIBRATED GRID FOR FORWARD-LOOKING CAMERA

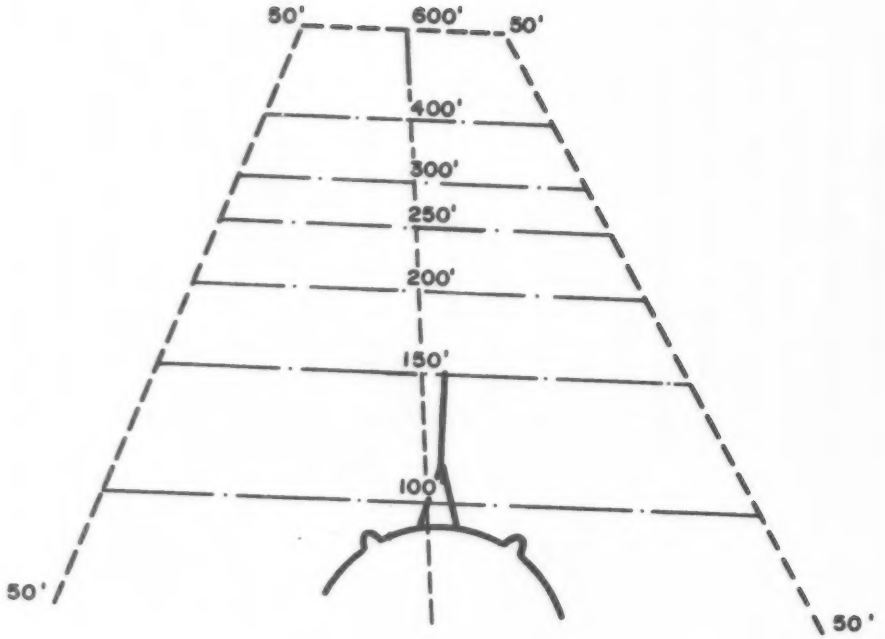

FIGURE C.2

CALIBRATED GRID FOR SIDE-LOOKING CAMERA

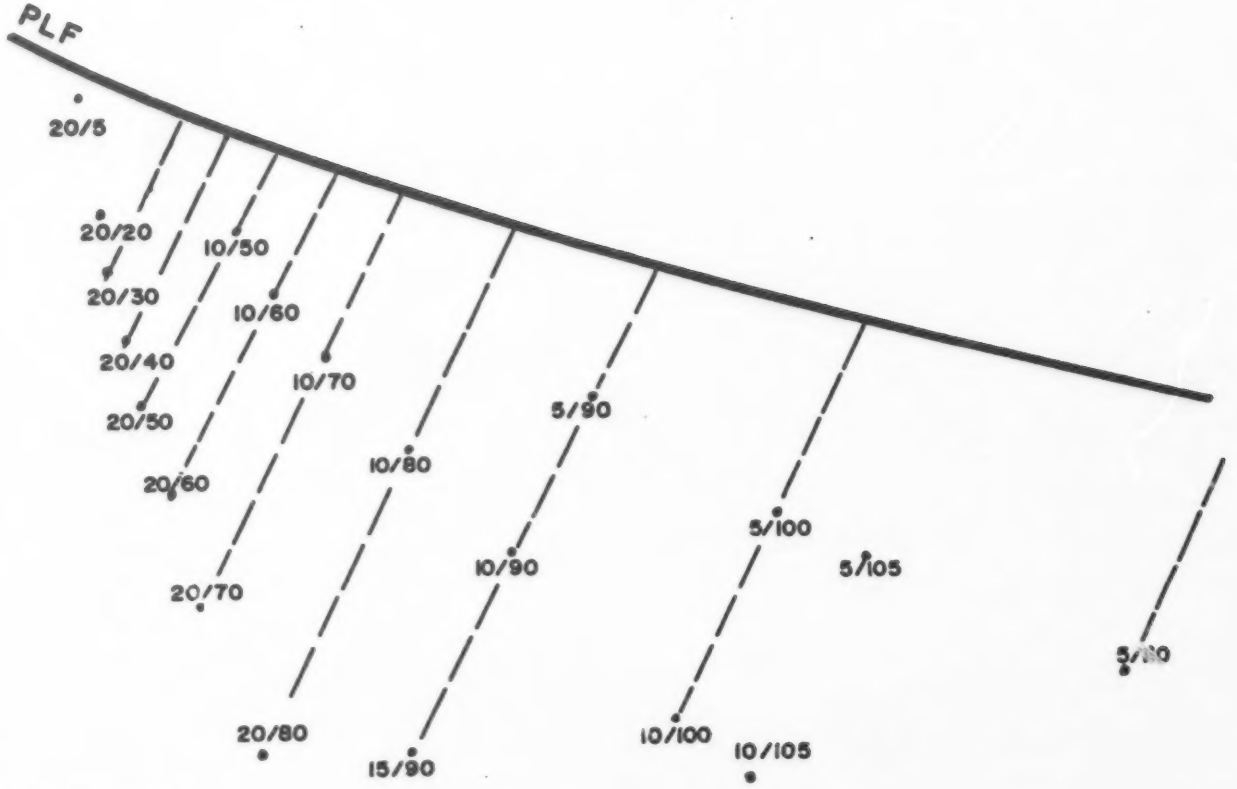

LEGEND

PLF - Portside, looking forward

20/5 - 20' from ship's side at the WL and 5' abaft stem at WL measured parallel to the CL

APPENDIX D

ANALYSIS OF ACCELERATION DATA

D.1 ACCELERATION PROFILES OF HULL STRUCTURES

The objective of this section is to investigate if it is possible to derive the hull deflection curves (vibration shapes) from the measured accelerations

It became necessary to develop a limited amount of new software in order to generate a fairly large number of examples of hull response contours during interaction with ice. The computer program developed for ARCTEC'S HP 9845 machine consisted of two halves:

The first half does the scanning, digitization, sorting and unpacking;

The second part converts the data into engineering units and produces the various plots. Figure D.1 depicts a flowchart of the various steps involved in the procedure.

To assess the usefulness of the recorded acceleration data for purposes of the present analysis, accelerations at positions 1Y and 2Z are plotted out. A quick look at the time-series would indicate intervals where relatively high vibrations were recorded. The vibrations in channels (7, 9, 11, 12, 14, 20, 21, 23, on the 28-channel tape recorder) within these time intervals are plotted out. These channels have acceleration data in the vertical and horizontal directions measured at positions 1Y, 1Z, 2Y, 2Z, 3Y, 5Y, 5Z and 6Y. At specifiefd time intervals, accelerations at each of these locations are plotted out as shown in Figure D.2 (a) and (b).

A large number of such acceleration profiles (see Annex 3) were generated. Careful study of the generated profiles indicated the following:

- The horizontal vibrations of the hull structure are predominantly a combination of the zero(th) and the first modes.
- The vertical vibrations are dominated by the first and second modes.

FIGURE D.1

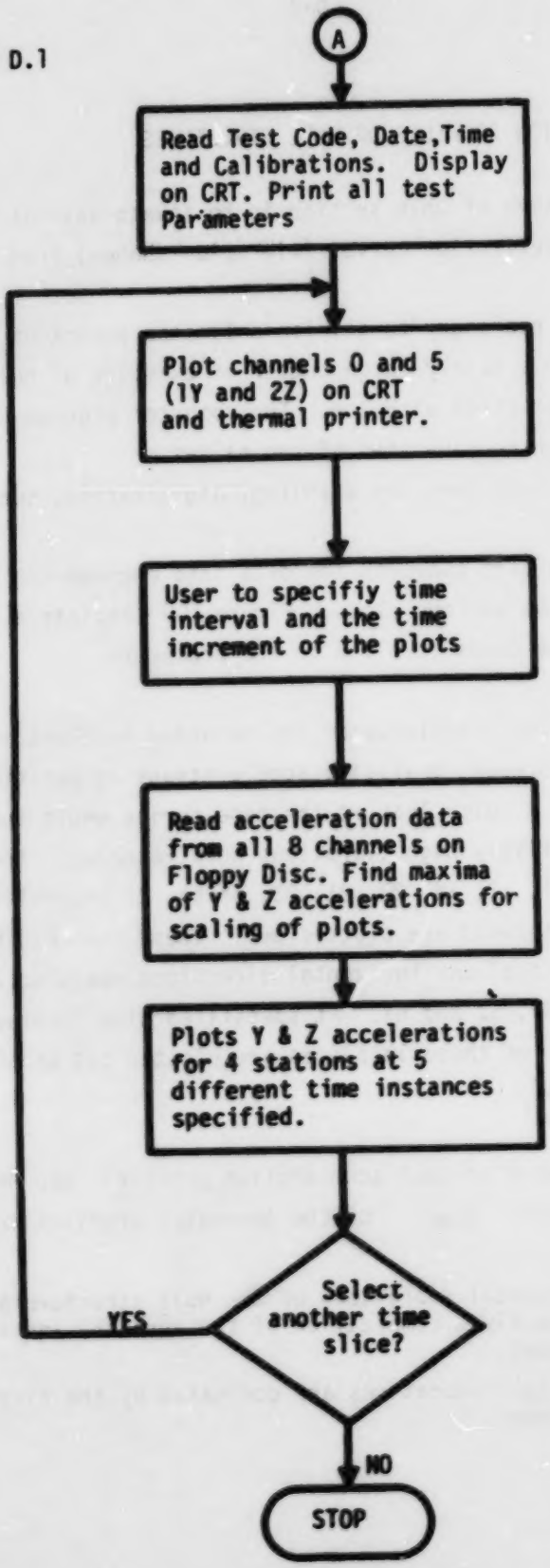
A
Read Test Code, Date,Time and Calibrations. Display on CRT. Print all test Parameters
Plot channels 0 and 5 (1Y and 2Z) on CRT and thermal printer.
User to specifiy time interval and the time increment of the plots
Read acceleration data from all 8 channels on Floppy Disc. Find maxima of Y & Z accelerations for scaling of plots.
Plots Y & Z accelerations for 4 stations at 5 different time instances specified.
Select another time slice?
YES
NO
STOP

User Enters: File Name
Length of Record (sec)
Plot Step Size

Repeat until end of selected time slice.

FIGURE D.2

TYPICAL ACCELERATION PROFILES

(a)

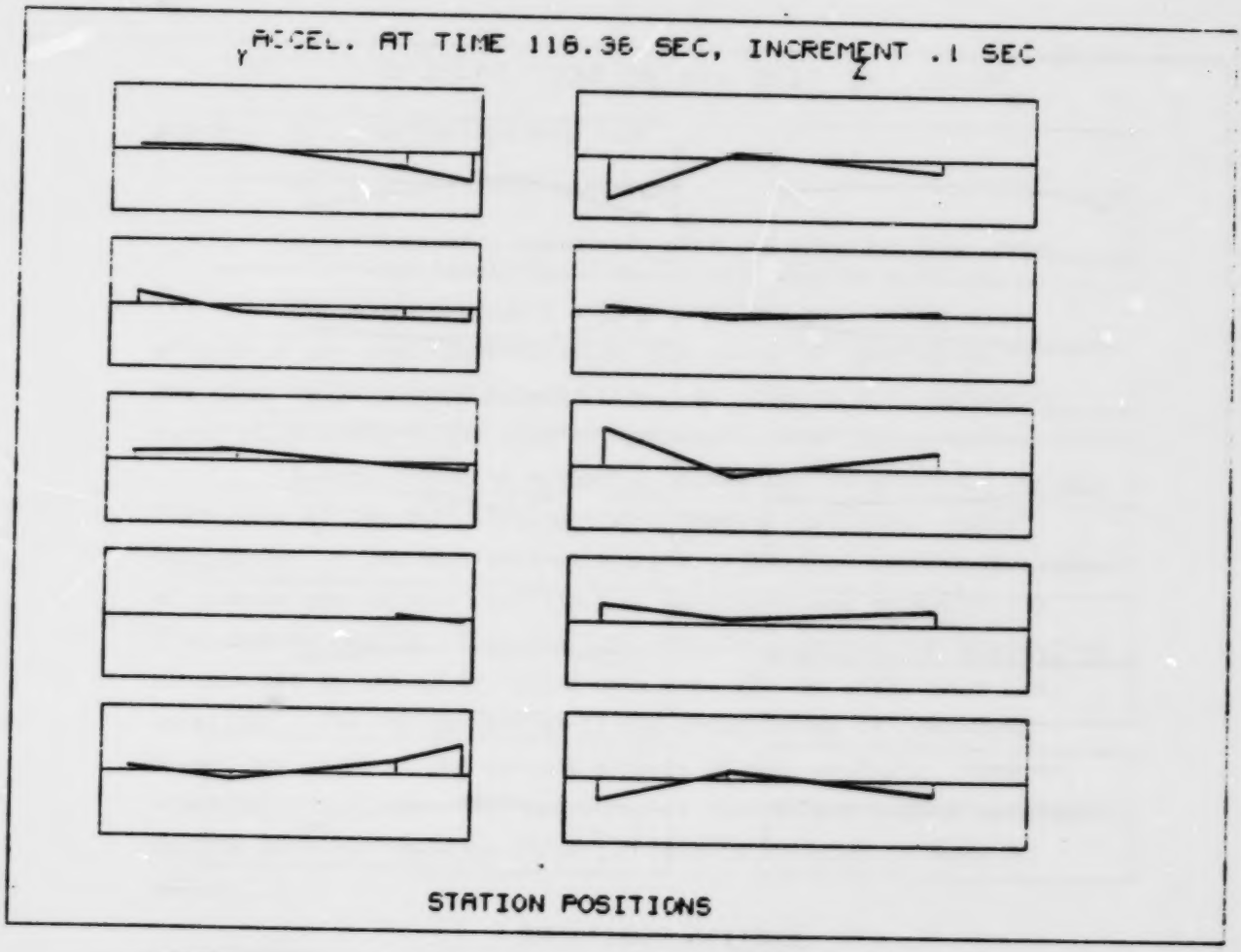

HORIZONTAL **VERTICAL**

LEGEND

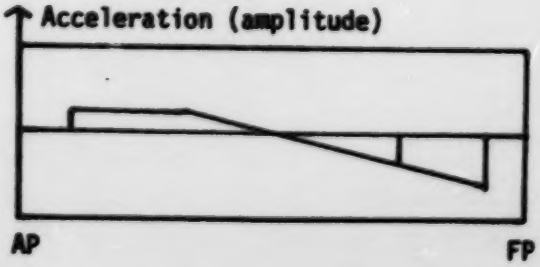

FIGURE D.2

TYPICAL ACCELERATION PROFILES

(b)

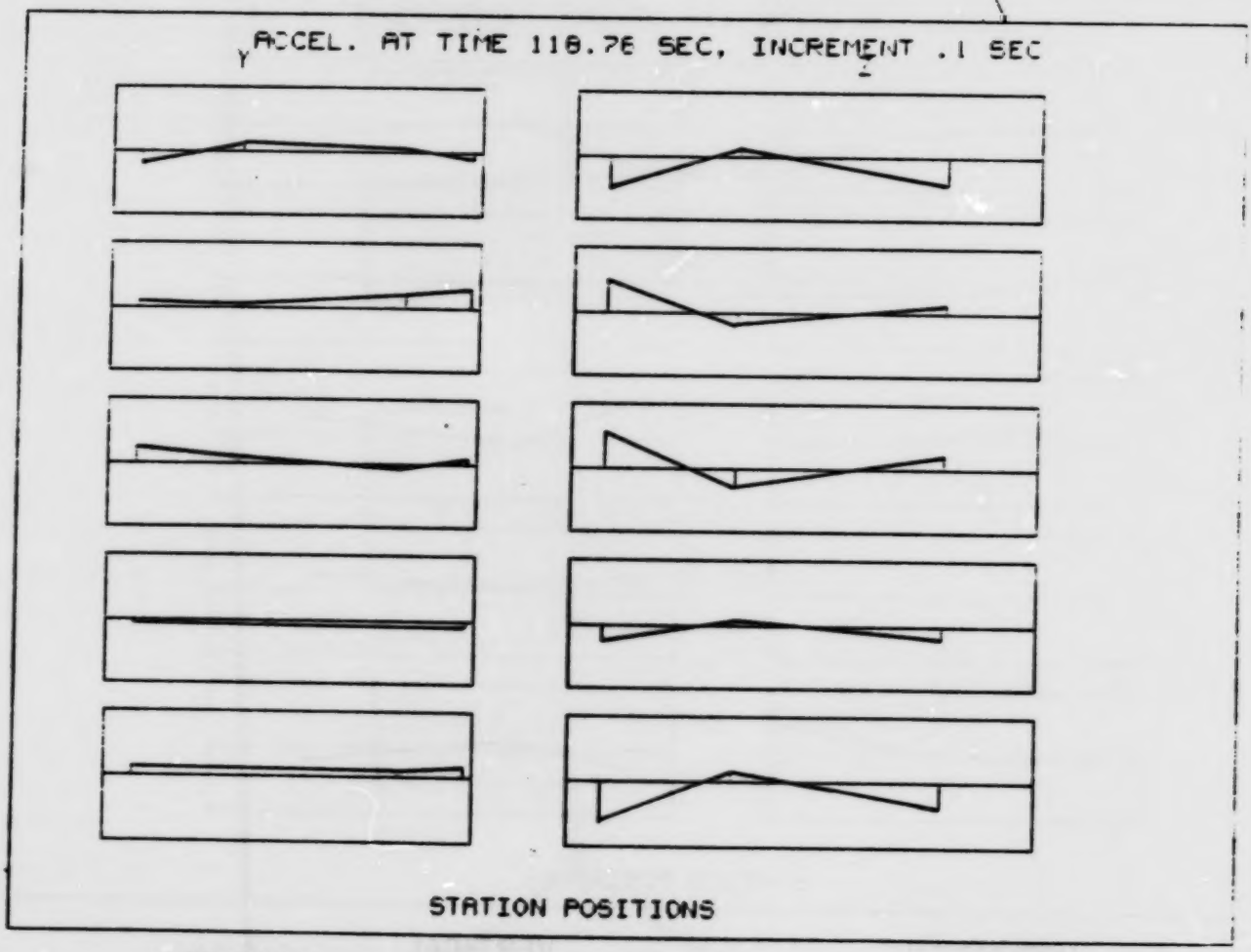

HORIZONTAL **VERTICAL**

The above observations also indicate the dominant frequencies of hull structure response in the horizontal and vertical modes. As a first attempt at deriving the vibratory deflection curve, one might use the acceleration amplitudes along with the apparent dominant frequencies and perform a simple double integration process. The maximum deflection at any transducer location, i, is then given by:

$$X_i^o = A_i^o \omega_n^2 \qquad (D.1)$$

where X_i^o = deflection amplitude

A_i^o = acceleration amplitude

ω_n = frequency associated with the dominant mode shape (n) identified from the acceleration profiles.

The above procedure will provide the peak deflections at each of the transducer location, but yields no information on the phase relationships between them. An accurate hull deflection curve is, therefore, not readily forthcoming from such a method.

A more elaborate method to obtain the instantaneous deflection curve of the hull structure will involve continuous double integration of the acceleration signals. This will require knowledge of appropriate initial conditions of velocities and positions and also require the use of an analogue computer, wherein the integration circuit can be set up to handle data from all the eight transducer locations. The implementation of the above scheme is considered beyond the scope of the present efforts of data analysis. However, a moderate level of effort was directed towards the task of developing the detailed analogue circuit. This is included in Annex 3, Volume III.

D.2 ACCELERATION SPECTRUM ANALYSIS

D.2.1 Introduction

Because of the random nature of the icebreaking process, and their dependence on the ice conditions, the time histories do not often provide detailed information on the vibration of ship structures. In contrast, a frequency (spectrum) analysis of the motion which produces a power spectral density may specify completely the vibratory characteristics of the system. Hence, part of this study is to examine the frequency contents of each acceleration under different operating conditions. This was achieved by performing a spectrum analysis on the time histories of the acceleration using a Fast Fourier Transform (FFT) computing spectrum analyzer. The power spectral density was converted by using a calibration factor to engineering units.

The analysis was performed to fulfill two objectives:

- To ascertain the frequencies which register peak values of acceleration.
- Comparison of the frequencies and their magnitudes between different ship-ice impact scenarios.

The frequency range of greatest interest was 0-50Hz corresponding to the range spanning the five lowest longitudinal natural frequencies of the ship. A frequency range of 0-500Hz was also used in some cases. With a recording speed of 1 7/8 ips on the tape recorder, the corresponding bandwidth was 625 Hz, and a frequency range of 500 Hz was arbitrarily chosen.

The scenarios under consideration include:

- open water turning
- crash reversal
- backing in level ice
- continuous ice transit
- ramming level ice
- ramming pressure ridge

A summary of these cases that were evaluated and the frequency range setting on the analyzer is shown in Table D.1. In this table, the "MODE" is referred as the type of averaging capability in the spectrum analyzer. This is a property of the analyzer and in this case is the number of 8 sec. or 0.8 sec. *peak measurements* that were taken to produce the required time *window*. XXP indicates the number of peak spectra to be averaged. The units in the window are minutes (') and seconds (").

TABLE D.1

SELECTED CASES FOR SPECTRUM ANALYSIS

SHIP OPERATING CONDITIONS	DAY-TIME GROUP	TAPE #, COUNT #	50 Hz		500 Hz	
			MODE	WINDOW	MODE	WINDOW
Open Water Turning	01:29:10:57	1-1, 4022			880P	6'
Crash Reversal	01:29:13:58	1-2, 392			640P	4'30"
Backing In Level Ice	01:31:13:02	1-2, 3521	4P	20"	128P	1'
Continuous Ice Transit, 9-3 kt, Max 1 1/2, Avg. 1'	01:30:23:43	1-2, 758	32P	2'	290P	2'
Continuous Ice Transit 6 kts 1 1/2'ice	01:31:14:10	1-2, 4160	32P	2'	290P	2'
Ramming Level Ice Obli, 9 kt, Ice max 4', Avg 3½'	02:08:02:30	1-9, 3797	4P	20"		
Ramming Level Ice Obli, 9 kt, Max. 4', Avg. 3'	02:09:06:20	1-10, 3241	16P	1'20"		
Ramming Level Ice Head-On 5.33 kt, Max 4', Avg. 3'	02:09:06:09	1-10, 3133	4P	20"		
Ramming Level Ice Head-On 4 kts, Max. 3', Avg. 2'	02:09:14:00	1-11, 1833	16P	1'20"		
Ramming Pressure Ridge Obli. 6 kt., Max. 4', Avg. 3½'	02:08:02:23	1-9, 3732	8P	40"	128P	1'
Oblique Impact Obli. 9 kt., Max. 2'	02:08:23:50	1-9, 4494	4P	20"		
Oblique Impact Obli. 7 kts., Max. 4', Avg. 3'	02:09:06:26	1-10, 3316	16P	1'20"	128P	1'
Open Water prior to Test	02:08:02:23		Inst	8"		
Open Water Prior to Test	02:08:23:50		Inst	8"		

D.2.2 Methodology

The particular case to be analyzed was first located on the magnetic tape. Once the case was identified a decision was made on the time over which the sample would be taken for the spectrum analysis. The spectrum analyzer has a memory of 8 seconds at the 50 Hz frequency range and a memory of 0.8 seconds at the 500 Hz range. These correspond to a frequency resolution of 0.125 Hz and 1.25 Hz respectively. The memory also corresponds to the minimum time scale for sampling. However, the analyzer is also capable of increasing the time scale of sampling by averaging the spectra of a number of successions of time transient. The analyzer was set at the PEAK mode to record a profile of the highest amplitudes. The final decision on the length of time was made by a re-examination of the video record as well as the time histories of the acceleration signal. The time display feature on the spectrum analyzer was used to review the time transient.

After determining the length of time of the sample, the input amplitude sensitivity and spectrum average mode were selected on the analyzer. Then the playback recorder and analyzer were activated simultaneously. When the sampling was completed, an average peak power spectrum would display on the screen. The sharp peaks on the spectrum could be amplified or reduced using a gain setting control on the analyzer allowing a close examination of the spectrum profile. The vertical scale changed considerably from profile to profile resulting in a wide range of vertical scales. This is reflected in the graphical outputs presented in this report. Therefore, examination must be approached with caution by noting the vertical scales.

Finally, an X-Y plotter was then used to trace the spectrum display on the screen of the spectrum analyzer. A cursor was utilized to obtain exact frequency and power magnitudes for many of the peaks of the profile. The power magnitudes were then converted to g' x g'/Hz by means of known calibration factor for each accelerometer.

Because of the large quantity of data recorded it was not practical to analyze all accelerometer data for evey accelerometer location, only the forward accelerometers 1Y and 1Z, the aft accelerometers 7X, 7Y and 7Z, and the center accelerometers 4X, 4Y and 4Z were included.

D.2.3 Results of Spectrum Analysis

The acceleration power spectrum plots for the 12 selected cases as well as two open water cases are shown in Figures 6.1 to 6.19 and the order of presentation is shown in Table D.2. These are presented as Annex 6 in a separate volume.

The spectrum analysis for each case are presented in the following order as marked:

- °forward sway (1Y)
- °forward heave (1Z)
- °surge (4X)
- °sway (4Y)
- °heave (4Z)
- °aft surge (7X)
- °aft sway (7Y)
- °aft heave. (7Z)

It should be noted that the vertical scale tends to change considerably between each plot. Comparison between profiles should be approached with this consideration in mind. This was due to varying sensitivity between each accelerometer as well as the desire to examine more closely the relationship between frequencies with peaks and others without. Significant spikes on the spectra are labelled; the top number being the value of the acceleration power spectral density in "g x g/Hz", while the lower bracketed number being its frequency. The plotter occasionally truncated the spikes which, therefore, do not always appear to scale to the correct 'height' but which are labelled with the correct value.

TABLE D.2

SCENARIO	DAY-TIME GROUP	FIGURES FOR 50 Hz	FIGURES FOR 500 Hz
OPEN WATER TURNING	01:29:10:57		6.1 a - h
CRASH REVERSAL	01:29:13:58		6.2 a - h
BACKING IN LEVEL ICE	01:31:13:02	6.3 a - h	6.4 a - h
CONTINUOUS ICE TRANSIT (9.3 kts, 1.5' thk)	01:30:23:43	6.5 a - h	6.6 a - h
CONTINUOUS ICE TRANSIT (6 kts., 1.5' thk)	01:31:14:10	6.7 a - h	6.8 a - h
RAMMING LEVEL ICE (Oblique, 9 kts, 4' thk)	02:08:02:30	6.9 a - h	
RAMMING LEVEL ICE (Oblique, 9 kts, 4' thk)	02:09:06:20	6.10 a - h	
RAMMING LEVEL ICE (Head-on, 5.33 kts, 4' thk)	02:09:06:09	6.11 a - h	
RAMMING LEVEL ICE (Head-on, 4 kts, 3' thk)	02:09:14:00	6.12 a - h	
RAMMING PRESSURE RIDGE (Oblique, 6 kts., 4' thk)	02:08:02:23	6.14 a - h	6.13 a - h
OBLIQUE IMPACT (9 kts., 2' thk)	02:08:23:50	6.15 a - h	
OBLIQUE IMPACT (7 kts., 4' thk)	02:09:06:26	6.16 a - h	6.17 a - h
OPEN WATER PRIOR TO TEST	02:08:02:23	6.18 a - h	
OPEN WATER PRIOR TO TEST	02:08:23:50	6.19 a - h	

The acceleration spectra presented on the 50 Hz range have a frequency resolution of 0.125 Hz, and 1.25 Hz for a 500 Hz range.

D.2.4 Discussion of Spectra

Turning and Crash Reversal in Open Water

Figures 6.1 a-h and 6.2 a-h show the acceleration power spectra for the accelerometers at the bow, at mid-ship, and at the stern for the POLAR SEA turning and crash reversal respectively. As noted from the turning case, the bow accelerometers did not indicate as many dominant frequencies as those mounted at the stern. As well, the level of energy is more pronounced at the stern than at the bow. It is noted that the vibration energy at the stern is spread from 25 to 95 Hz, with highest vibration for the vertical mode. There is a spike at the lowest frequency of resolution of 1.25 Hz, this would be associated with the rigid body motion. In the case of the crash reversal the difference in vibration between the bow and the stern is rather obvious. Figures 6.2 a and b show that there are two dominant frequencies at 1.25 ~ 2.5 and 11.25 Hz for the bow accelerometers, the first being associated with rigid body motion while the latter undoubtedly being induced by the propeller. In contrast, the stern accelerometers detected many dominant frequencies in the range of 20 to 100 Hz and its total energy level of vibration (mean-square of the power spectra) is an order of magnitude higher than that observed at the bow. It is also interesting to note that the longitudinal stern accelerometer detected a stronger frequency component at 1.25 Hz than the other stern accelerometers. This is logical as the primary motion in the crash reversal was in the surge mode. The dominant frequencies at about 300 - 350 Hz might be induced by the gas turbine.

Backing in Level Ice

This incident was examined both at frequency ranges of 50 and 500 Hz. The peaks at 7.25 and 8.5 Hz for the bow accelerometers (Figures 6.3 a and b) are propeller noise which resulted from a shaft speed of 109 and 128 rpm with a four blade propeller. These two frequency components are of similar magnitude in the surge and heave directions at the stern (Figures 6.3 f, g, h) but are less significant in the overall vibration levels at the stern where the dominant frequency components generally

spread in region between 20 to 34 Hz and in region between 40 to 90 Hz. The vibration level was stronger at stern than at the bow. In the 500 Hz range spectra (Figures 6.4 a-h) the vibration levels at the bow concentrated at the low end,below 10 Hz, while at the stern the dominant frequencies spread from 19 to 120 Hz. In general, the energy of vibration at the stern was at least an order of magnitude larger than recorded at the bow.

Continuous Transit in Level Ice

In a typical icebreaking process, the interaction between the ship and the ice not only includes the ice crushing and fracture at the bow/stem, but also involves multiple loadings on the bow with the side ice cusps. To relate the acceleration spectra with the cusp breaking, estimates of frequency of cusp encounters was made using a hypothetical system. More details are given in section E.7 of Appendix E. Table D.3 shows the frequency of cusp encounters for various ice thicknesses and ship speeds.

Two cases of continuous ice transitting were examined and their response spectra are very much similar. These two cases were both analysed at 50 and 500 Hz ranges (Figures 6.5a - 6.8 h).

As noted in the 500 Hz spectra, the contribution in vibration energy is insignificant for frequencies over 250 Hz. Both the bow and stern vertical accelerometers indicate dominant frequency components at the low end of the spectra, 1.25 to 5 Hz, which were associated with breaking the ice since the resolution was 1.25 Hz (Figures 6.6 b and h and 6.8 b and h). It is interesting to see that the magnitudes of this frequency component for the bow and the stern are of the same order of magnitude. The stern accelerometer did not indicate this frequency component be the most dominant as the bow accelerometer did, but assumed a highest magnitude at 22.5 Hz for the first case and 43.75 Hz for the second case which might be associated with the machinery. Generally speaking, the vibration level is stronger in the vertical direction than in the transverse direction.

The 50 Hz spectra shown in Figures 6.5 a-h and 6.7 a-h provide more details in the low frequency end which is of great interest

TABLE D.3

ESTIMATES OF FREQUENCY OF CUSP ENCOUNTERS

ICE THICKNESS (ft)	CUSP DEPTH Wc	CUSP LENGTH Lc	SHIP SPEED (IN KNOTS)					
			4	6	8	10	12	14
1	5.58	16.74	0.81	1.21	1.61	2.02	2.42	2.82
2	9.84	29.52	0.46	0.69	0.91	1.14	1.37	1.60
3	14.11	42.33	0.32	0.48	0.64	0.80	0.96	1.12
4	18.04	54.12	0.29	0.37	0.50	0.62	0.75	0.87
5	21.33	63.98	0.21	0.32	0.42	0.53	0.63	0.74

IDEALIZED SHIP TRACK

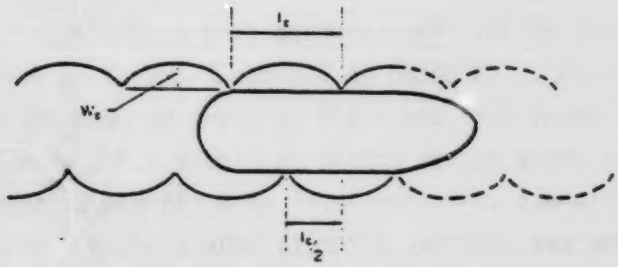

$l_c = 1.0\, W_c \rightarrow 4.0\, W_c$

WE ASSUME $l_c = 3.0\, W_c$

to us. Both the bow and stern accelerometers recorded dominant frequency components at the frequency range of 0.125 to 2Hz and these frequency components are usually the highest in the tranverse direction.The spike at 0.125 Hz is related to local ice impact at the bow, while the spikes at 1.5 Hz in Figure 6.5 a and at 1.375 Hz in Figure 6.7a are associated with the side cusp breaking. The cusp breaking component is usually larger in the tranverse direction and far more pronounced at the bow than at the stern. For the first case the ship was transitting through 1.5 foot thick level ice at a speed of 9.3 knots, from Table D.3 the frequency of side cusp encounter would approximately be 1.47 Hz . The same frequency was found for the peak vibration in Figure 6.5a. The peaks at about 8.625 Hz in figure 6.5 a-h are the propeller noise for a shaft speed of 130 rpm with a four blade propeller. The peaks at 2.875 Hz in the vertical accelerometers might be the resonant vibration in the first mode (two nodes) of the hull.

Ramming in Level Ice

Figures D.4,5 & 6 represent the 8-second window time transients for the bow vertical accelerometers in open water (low degree of concentration of ice rubbles) immediately prior to impact, during impact and the time period when the ship was stuck in ice respectively for the ramming incident at time 81:02:08:02:30. The corresponding acceleration spectra are given by Figures D.7, 8 &9 . As noted in Figures D.7 & 8 the dominant frequency components at about 2.75 and 2.875 Hz might be resonant vibration of the ship's hull as these do not appear in Figure D.9 when the ship was stuck in ice. The highest vibration level at 0.125 Hz was seen only during ice impact and none was detected prior to impact or when ship stuck in ice. This indicates that the acceleration due to ice impact must be associated with frequency below 0.4Hz. The peak at 11.375 Hz in Figure D.9 must be related to the propeller noise. The peaks at 22.75 and 31.65 Hz must be associated with the diesels. The 22.75 Hz frequency component is also noticeable in open water prior to impact.

Figures 6.9 to 6.12 show the acceleration spectra for ramming level ice. The first two sets of spectra, Figures 6.9 a-h and 6.10 a-h, represented the initial contact being oblique, and the last two sets were head-on impact initially. In general the distribution of vibration energy for the bow accelerometers is primarily concentrated in a region below

FIGURE D.4 Time Record for bow vertical accelerometer in open water prior to impact for ramming test at 02:08:02:30. (USCGC POLAR SEA)

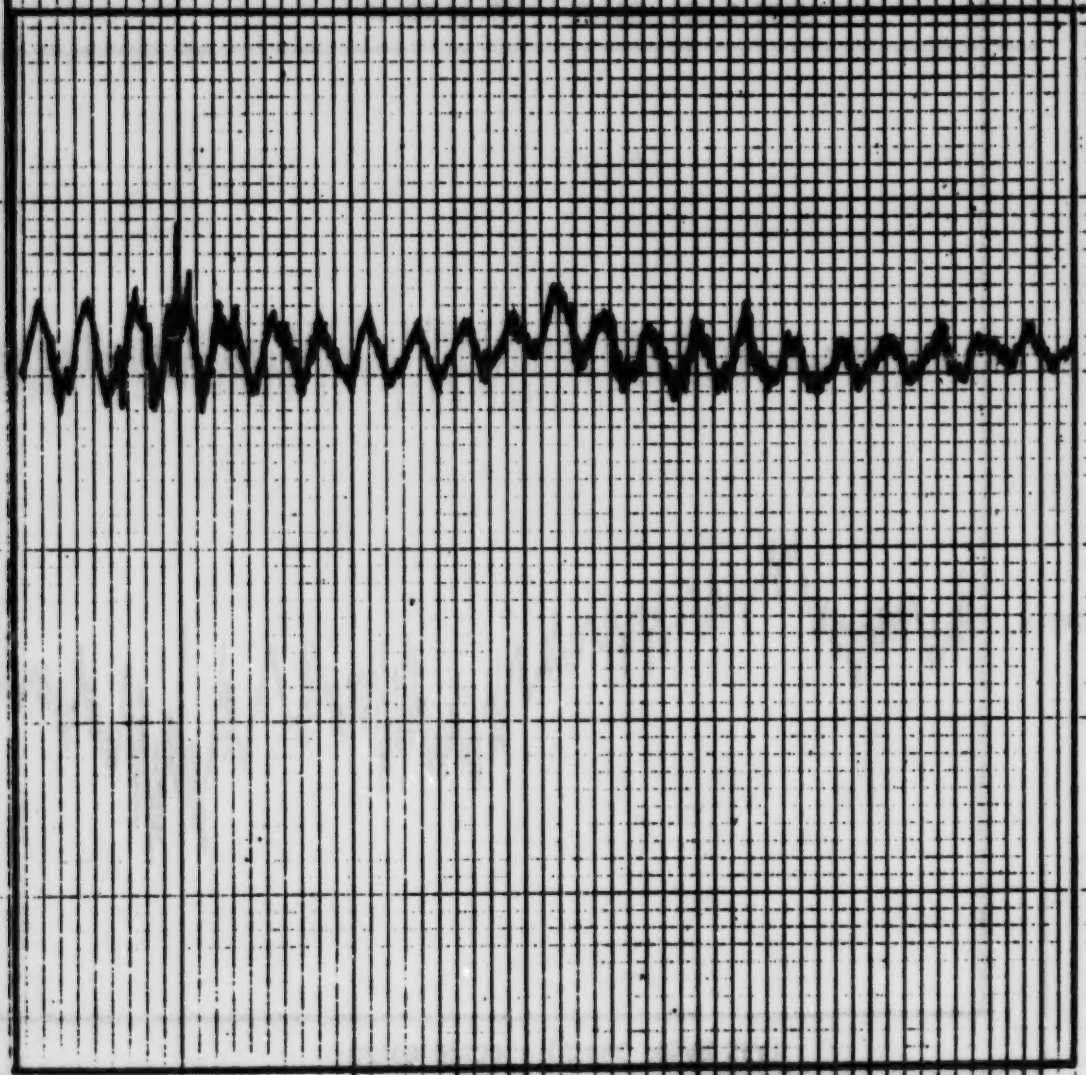

FIGURE D.5 Time Record for bow vertical accelerometer during impact for ramming test at 02:08:02:30 (USCGC POLAR SEA)

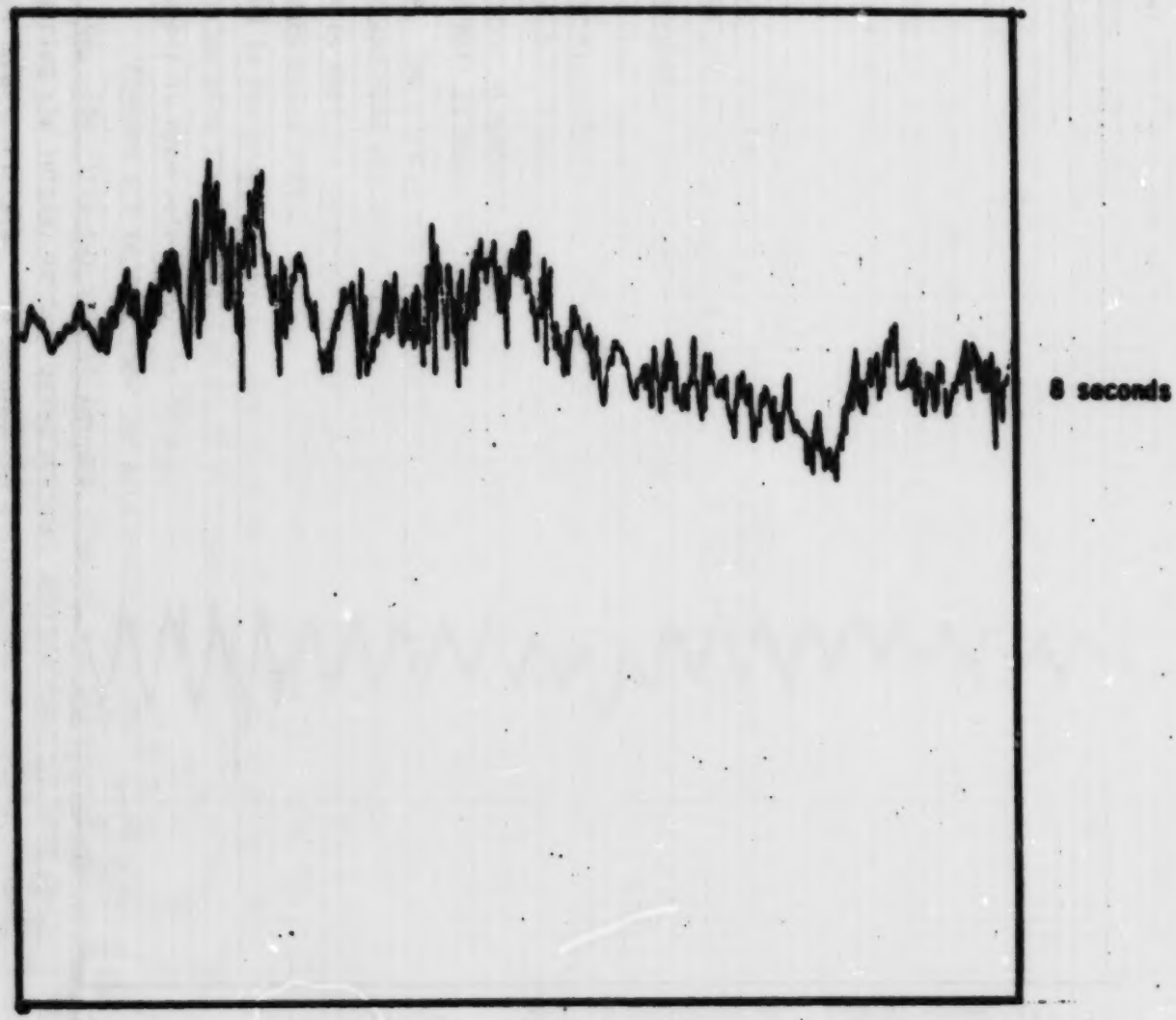

FIGURE D.6 Time Record for bow vertical accelerometer when ship was stuck for ramming test at 02:08:02:30 (USCGC POLAR SEA)

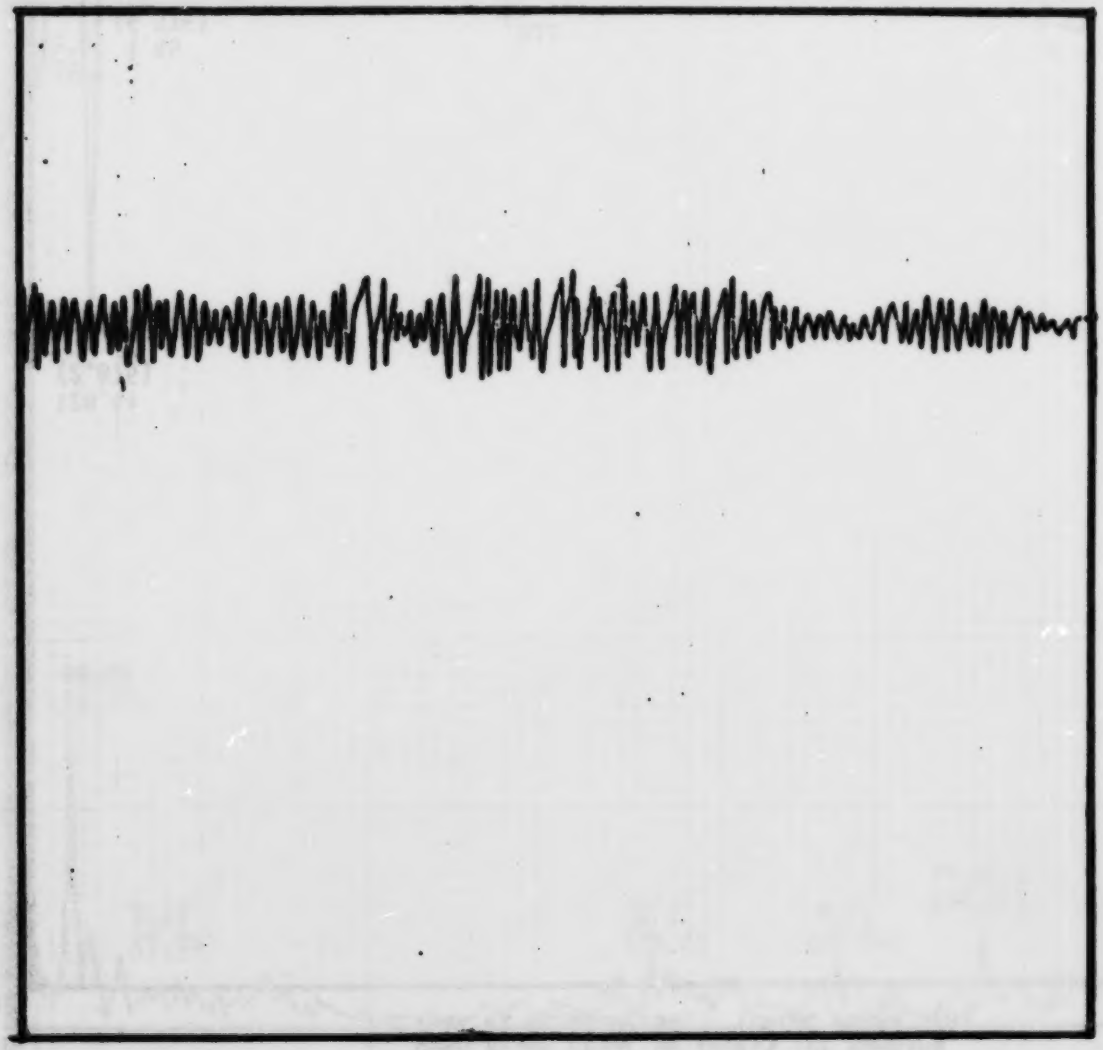

FIGURE D.7 Bow Vertical Acceleration Spectrum in Open Water Prior to Impact for Ramming Test at 02:08:02:30. (USCGC POLAR SEA)

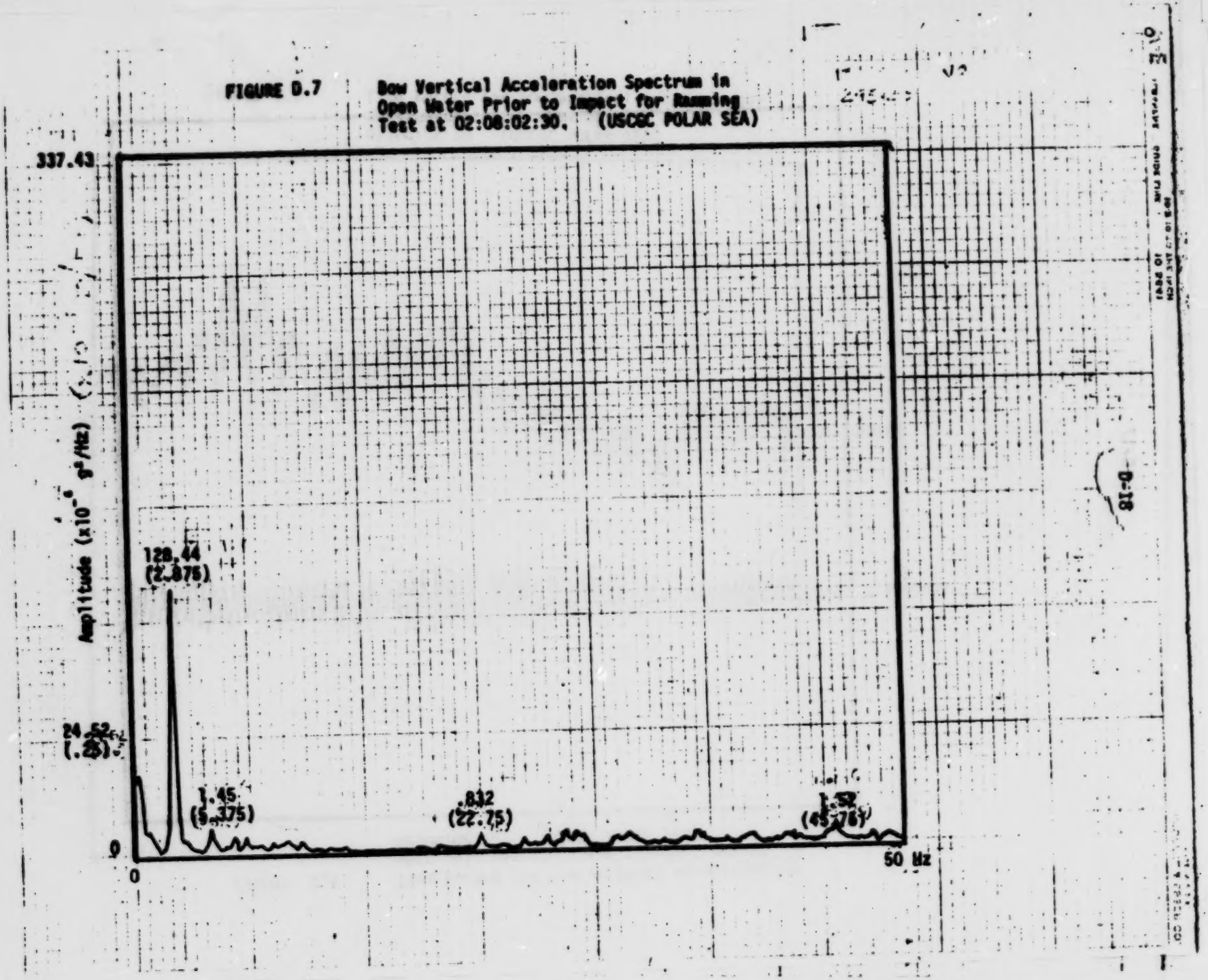

FIGURE D.8 Bow vertical Acceleration Spectrum during Impact for Ramming Test at 02:08:02:30. (USCGC POLAR SEA).

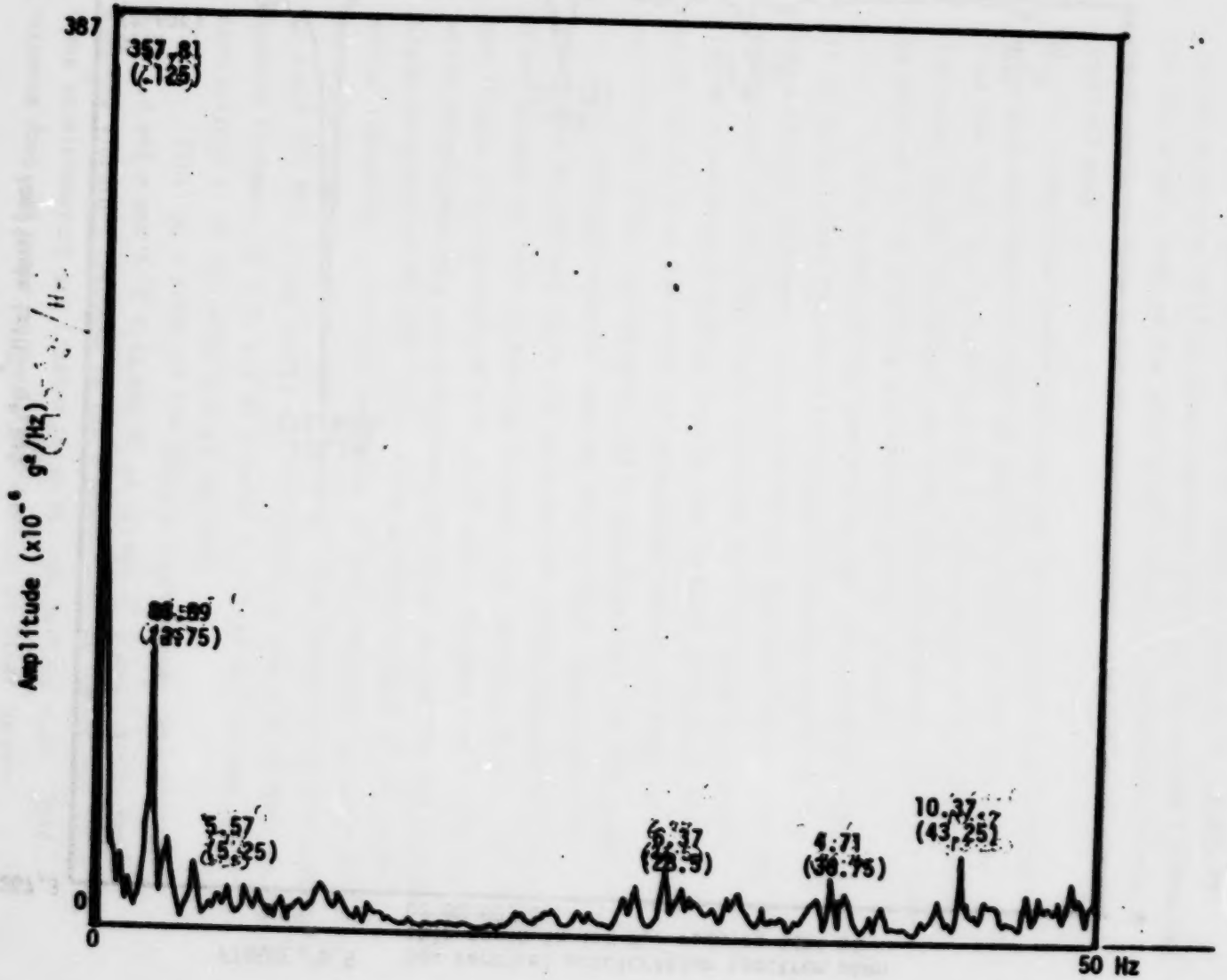

FIGURE D.9 Bow vertical acceleration spectrum when ship stuck in ice for ramming test at 02:08:02:30

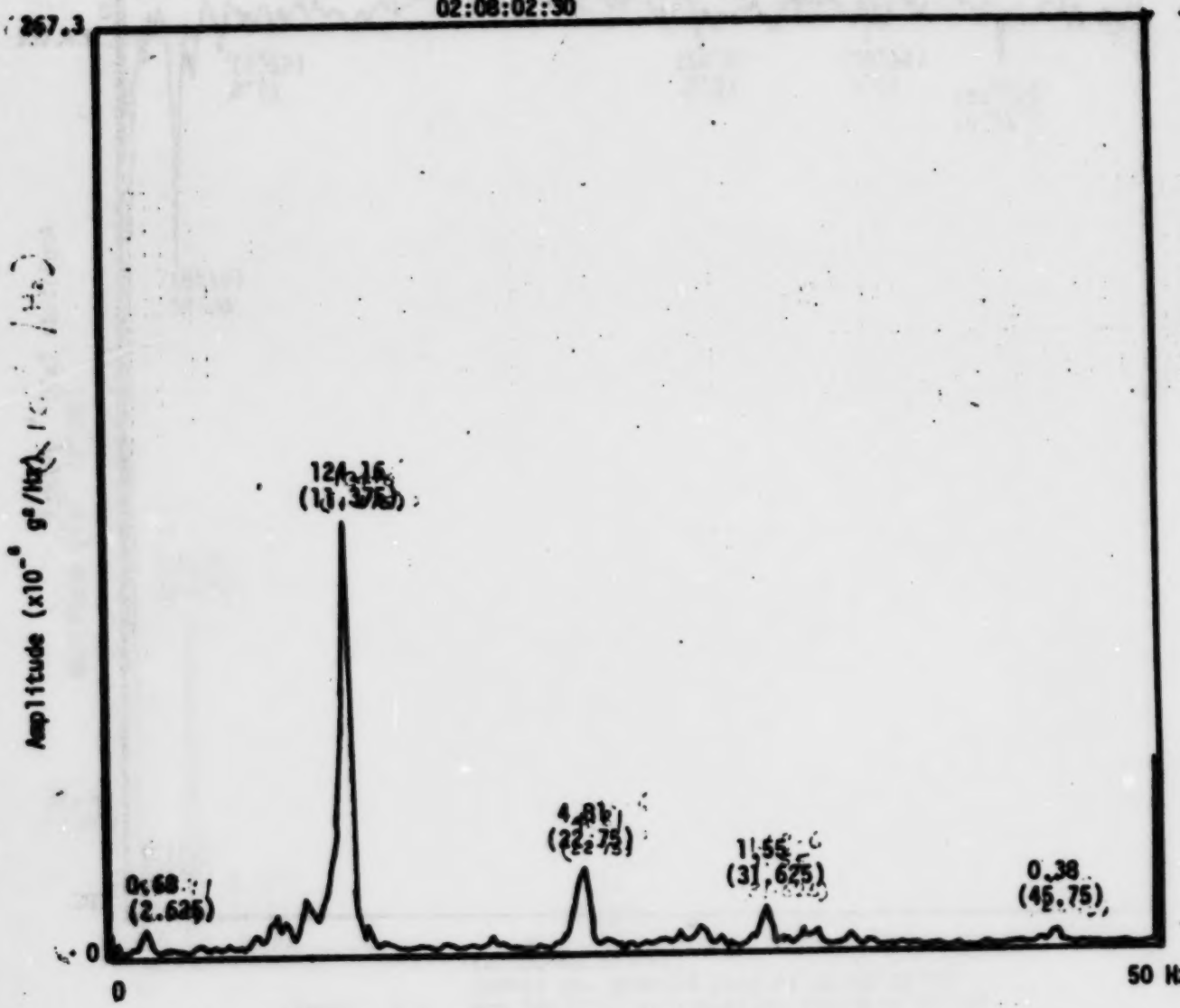

12 Hz, with about 3 significant spikes. The peaks at about 0.125 - 0.25 Hz are associated with ice impact and those at about 9 to 12 Hz are undoubtly related to the propeller. The peaks at about 4.5 - 4.875 Hz detected by the transverse accelerometer and the peaks at about 2.75 - 2.875 Hz picked up by the vertical accelerometers might be the resonant vibration in the primary mode of the ship's hull since the fundamental frequency of the hull is 4.13 Hz for the transverse mode, and 2.74 Hz for the vertical mode.

Magnitude comparisons for the bow and stern accelerometers show that bow vibration level at about 0.125 Hz is more pronounced than the stern level, particularly in the vertical direction. This indicates the bow vibrations are local and low dominant frequency must be related to ice crushing and failing against the bow.

From examining the spectra for the stern accelerometers it is obvious that the vibration energy is mainly induced by the propeller and machinery, since most of the dominant frequencies are spread over 10 Hz. The stern vibration level is usually stronger in the transverse direction than in the vertical direction, this might result from the stern colliding with broken ice floes as well as the effect of the wake, abaft the propellers, on the rudder.

The accelerometer records clearly show *sympathetic hull vibrations* at various shaft and or propeller blade frequencies. A very clear example of this is Ramming in Level Ice (Oblique, 9 kns, Ice: max 4' avg. 3') Figures 6.10 a to 6.10h where frequency of 11.375 Hz - which corresponds to a shaft frequency of close to 180 RPM and a propeller blade frequency of 680 RPM - is evident in each of the eight sensor recordings. Various harmonics of this frequency are also evident, particularly at the after accelerometers. This frequency (corresponding to about 170 RPM of the shaft) and its harmonics are also evident in the Ramming incidents at 5.33 kns of Figures 6.11 a to 6.11 h, and again particularly so at the after end of the ship.

Finally, a study of the *Oblique Impact* cases (viz Figures 6.13 c,d,and e and 6.17 c,d, and e) at speeds of 6 and 7 knots shows a *marked* vibratory response in the midships area at 336.25 and 337.5 Hz. These accelerometers are located above the gas turbine room. This response does not occur at *head-on collisions* or other speeds.

It is probably due to the physcial properties of the resilient mountings of the gas turbines. An examination of the mountings may prevent failure or unacceptable movement at some future date

'Open-Water'

Figures 6.18 a-h and 6.19 a-h shows the acceleration spectra for POLAR SEA in 'open-water' conditions. It is important to point out that the 'open-water' conditions examined here were those just prior to the ramming and it did not truly represent an ice-free open-water condition. Therefore, it was anticipated that the accelerometers would pick up some vibrations due to impact against broken ice. For the case considered here, the concentration of ice rubbles was low and the level of vibration induced by ice impact is believed to be relatively small as compared with that induced by machinery and propellers.

From Figures 6.18 and 6.19, it is interesting to note the presence of two significant acceleration peaks at 2.875 and 11.375 Hz registered by all accelerometers. The first is related to the shaft speed (about 173 RPM), while the latter is undoubtly the propeller induced vibration. It is also noted that none of the higher frequency components (above 20 Hz) that were dominant for the stern accelerometers were detected by the bow accelerometers. The frequency components at 22.75, 34.375, 37.375 and 45.5 Hz could simply be the harmonics of the shaft speed (2.875 Hz). This can be seen from Figures 6.18g,h and 6.19g,h. The acceleration spike at 0.125 Hz appearing in each power spectrum for the horizontal accelerometer is associated with encountering ice rubbles before impact. The level of such vibration is generally lower than that in the impact cases.

D.3 CONCLUSIONS

The large number of acceleration profiles generated from the full scale vibration data indicated that the vibrations of the hull structure are predominantly a combination of rigid body modes (i.e. sway, yaw, heave and pitch) and the first flexural mode (i.e. 2-node).

The above observations indicate that any mathematical model developed to predict ice-induced hull response must take into account the coupling between the rigid body modes and the flexural modes. Conversely, a method of extracting forces (or excitations) from measured responses must adopt a unified approach, incorporating both the rigid body modes and the flexural modes.

Acceleration Spectra

Spectrum analysis has been performed for various types of operation including open-water turning, crash reversal, backing in level ice, continuous ice transit and ramming level ice/pressure ridges. The spectrum analysis was generally performed in the 0 - 50 Hz range. In some cases, however, the 0 - 500 Hz range was also examined.

Comprehensive analysis of the acceleration spectra generated the following comments:

- Impact induced rigid body accelerations are generated at frequencies below 0.5 Hz and flexural vibration accelerations occur up to about 3.0 Hz.
- In continuous icebreaking operations, the accelerometer records show sympathetic hull vibrations at side-cusp encounter frequencies that were in the range of 0.5 to 2 Hz. These cusp-breaking related frequency components are usually larger in the transverse direction and far more pronounced at the bow than at the stern.
- Hull vibrations at various shaft and or propeller blade frequencies are evident, particularly at the after end of the ship.

- Vertical hull vibration, at its fundamental frequency i.e. in the neighbourhood of 2.74 Hz, is noticeable during ice ramming operations.

- In open-water operations, the level of vibration at the stern is usually an order of magnitude higher than that at the bow. However, in ice-transitting operation, the opposite trend is evident, particularly in ramming incidents.

APPENDIX E

METHOD OF EXTRACTING FORCE SPECTRA FROM MEASURED RESPONSE SPECTRA

E.1 BASIC THEORETICAL AND PHYSICAL CONSIDERATIONS

A ship structure is more or less elastic and is, in general, excited in a random manner by the sea. Just as ship strength calculations have necessarily grown up on the basis of empiricism, so has the specification of sea ice conditions. In terms of the motion of, and stresses in, a given ship hull nine-tenths ice cover could mean very different things in the Bering Sea and in the St. Lawrence Seaway. As time goes on, however, the specification of ice conditions becomes ever more consistent in statistical terms and the concept of probability density (which is, at present, used in the description of ocean wave climate specifications) can be used to describe the ice conditions in the operating environment. However, at present, little or no information exists on the time history or frequency content of ice-induced forces on ship hulls. In an attempt to remedy this, and to lay the framework for analyzing further descriptive data that might be available in the future, we use the concept of the Mean Square Spectral Density Functions (or the Power Spectral Density Functions) as used in engineering dynamics [4]. Therefore, it seems unlikely at the moment that anything more sophisticated than some form of mean square spectral density of the ice force will be useful in this context. As the mean square spectral density is directly related to the process of statistics, once again the probability density function can be used to analyze vibratory response data when large quantities of full scale data become available.

To relate a measured response of acceleration or strain for instance to the corresponding random excitation due to surrounding ice field, we have a standard, well-defined problem to solve. The aim is to determine the input for a suitably measured output. In general, the problem is one of transient response to passage through discrete ice floes randomly distributed in the spatial variables. The analysis must account for frequency of impacts, ice properties and impact location on the hull.

Consider a ship moving with nearly constant velocity through a broken ice field with a set of accompanying 'equilibrium axes'. These axes move with the velocity of the ship, but do not perform any other motion so that the ship deflects and distorts about them, so to speak. The actual departures from the mean position within the axes, then, are close to being periodic in time but of some complex shape which depends not only on the form of the ship structure, but also on the characteristics of the ice field it is passing through.

Mode Shapes: Consider a purely symmetric motion of the ship hull following impact at the bow-stem in otherwise calm water. The motion would quickly subside due to the presence of damping within the hull structure and to the damping action of water. In the case where one could suppress both forms of damping, the free vibration would continue indefinitely. These free, undamped vibrations could be performed in one or more specific and unchanging shapes (or 'modes'), each shape being identified with a specific natural frequency. Figure E.1 shows the lowest mode shapes for an imaginary ship, (a) being those for the ship in vacuo and (b) being those for the ship in water. In (b) the water contributes to the mass distribution of the vessel and to the stiffness distribution. Of course the modes will become less and less like those of a non-uniform free-free beam as the order of the mode increases.

The modal shapes of either set are all essentially 'different'. In mathematical terms, the differences of identity between any two modes within either set are expressed by their 'orthogonality'. Modal analysis is only made possible by the possession of orthogonality relations between the modes of the set employed.

It appears that either set of mode shapes, (a) or (b) can be employed. Most of the early investigations were based on the use of the latter (see [1], [2], and [3]).

While this approach may indeed have some merit, there seems to be positive advantage in using the dry modes.

FIGURE E.1
DRY AND WET VIBRATORY MODES OF SHIP HULL

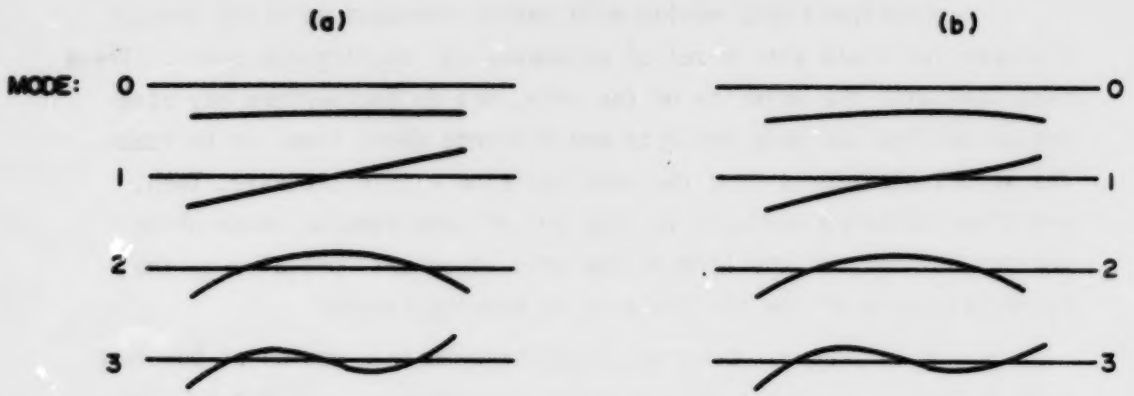

FIGURE E.2

SPECTRAL DENSITY FUNCTIONS, DEFINITION SKETCH

(a) "NARROW BAND" SYSTEM RESPONSE

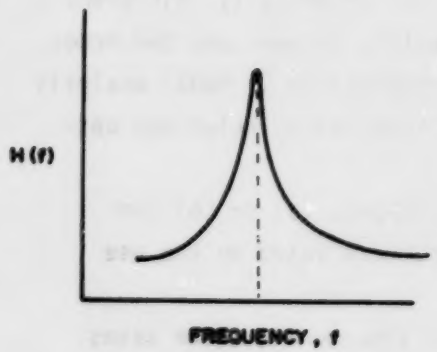

(b) "WIDE BAND" EXCITATION

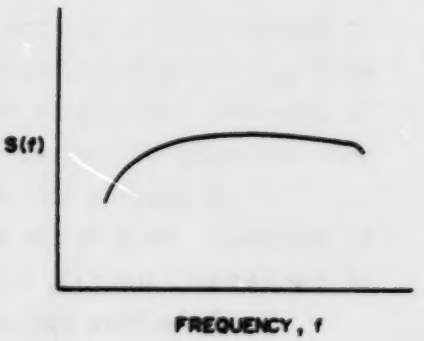

Set (a) does not possess a defect that is inherent in set (b). To determine wet modes accurately one has to have prior knowledge of the fluid's properties, and one has also to adopt some suitable hydrodynamic theory to find the fluid actions; it might be 'strip theory' for instance. This hydrodynamic theory must necessarily be empirical. The wet mode shapes are to this extent empirical and the empiricism is reflected in the orthogonality relations between them. Again, the shapes of the wet modes, and hence the orthogonality relations, are to some extent dependent on ship speed. In the present study, the wet modes will be employed, as the computation of the hydrodynamic effects are included in the basic algorithm (section B.2).

Symmetry and Antisymmetry: If it is assumed that a ship possesses a plane of port-and-starboard symmetry, then it follows that the vessel's dry modes may be divided into two groups - those with symmetric and those with antisymmetric shapes. Further if, the hull is assumed to be prismatic in form then the lowest symmetric modes are essentially bending modes. In defining those modes account may or may not be taken of rotatory inertia and of shear deformation. The dry symmetric modes present no difficulty in principle and have been calculated for an actual ship. (The two lowest are of course rigid body modes and are not treated in their entirety in the present study).

The dry antisymmetric modes of a symmetric ship present more difficulty. Since the hull is assumed to be prismatic, the words 'bending' and 'torsion' are relevant; the modes are found to be combinations of horizontal bending and torsion. (They are sometimes referred to as 'coupled bending and torsion modes'). The orthogonality relations between the antisymmetric modes are much more complex than those between the symmetric modes.

Generalized Forces: It is well known that any deflection of a linear system must be expressible as the sum of suitable deflections in appropriate modes. Generally speaking it is far simpler to trace the variations in the periodically fluctuating intensities of distortions in the separate modes (and to regard the total distortion at any instant as their sum) that it is to try to keep track of the overall shape.

By expressing the distortion of a ship's hull as a sum of distortions in its modes, we have at time t,

$$\vec{v}(x, y, z, t) = \sum_{r=0}^{\infty} q_r(t)\vec{\phi}_r(x, y, z)$$

Where $\vec{v}(x, y, z, t)$ is the deflection from its mean position of some point placed at (x, y, z) with respect to the equilibrium axes. The quantity $q_r(t)$ is the rth generalized co-ordinate that depends only on time and $\vec{\phi}_r(x, y, z)$ is a characteristic function that defines the rth mode of the dry hull.

Every generalized co-ordinate $q_r(t)$ has an associated:

- °inertia coefficient a_r
- °hydrodynamic damping coefficient b_r (and possibly, structural damping coupling coefficient b_{rs})
- °stiffness coefficient c_r (though those associated with undistorted displacements, as with the '0' and '1' modes of symmetric displacement, vanish).

Further, every coordinate $q_r(t)$ has an associated generalized disturbing force:

$$Q_r = \Phi_r e^{i\omega_e t}$$

where ω_e is frequency of encounter.

In theory at least, the apparatus for calculating all the coefficients a_r, b_r (and possibly the b_{rs}) and the c_r exists. It is in the calcualation of the amplitudes Φ_r of the generalized forces that it becomes necessary to invoke some suitable hydrodynamic theory (or even, conceivably, to use the results of model tests).

To the extent that motions in the modes are not coupled, the response in any given mode may be regarded as that of a simple oscillator having but one degree of freedom, when it is excited sinusoidally. (The analogy must not be pressed too far however because, apart from the possibility of coupling, the fluid's contributions to the 'mass', the

'damping' and the 'stiffness' depends partly on the excitation frequency). The 'oscillator' will have a characteristic frequency akin to a natural frequency and display a phenomenon akin to 'resonance'. It is to be expected that, near resonance, the effects of modal damping will be most marked.

Referring to symmetric distortions, intuition suggests that motions in modes $\vec{\phi}_0$ and $\vec{\phi}_1$ will be damped very heavily by the appropriate contributions from the generalized force amplitudes Φ_0 and Φ_1. It also seems likely that distortions in higher modes will be limited mainly by structural damping. When it is recalled that in the higher modes (which, incidentally, between them account for all stresses), the Q-factors may be well over 100, the significance of this becomes apparent.

Component Response: Once the overall response problem is formulated and solved, there remains the strength analysis of units such as bulkheads, frames, grillages, panels and so forth. It may be said, in general, that these units, being mostly 'high frequency' structures are likely to be subject to an essentially static form of loading so that inertia effects will be small. But the overall response is what determines the intensity and form of the fluctuating loads applied to them. It is possible, however, that units with large compressive loads will have low natural frequencies; in this event, dynamic analysis may still be necessary.

E.2 DERIVATION OF FORCE FROM RESPONSE BASED ON MODAL ANALYSIS

As discussed earlier, the displacement response of a linear, elastic structure can be expressed in terms of the principal modes of motion as:

$$u(x, y, z, t) = \sum_{n=1}^{\infty} q_n(t)\phi_n(x, y, z) \qquad (E.1)$$

This equation states that the total response is the sum of the responses in an infinite number of modes. The response in the nth mode consists of a constant shape ϕ_n, the amplitude of which varies with time according to the generalized displacement q_n. Assuming that positive damping exists and is in phase with the velocity, the equation of motion for a linear structure is:

$$m\ddot{u} + c_s\dot{u} + ku = f(x, y, z, t) \qquad (E.2)$$

where c_s is the *structural damping* coefficient.

Structural damping is a property by which energy is dissipated within the material due to the cyclic variation of stresses. Literature shows that the energy dissipated per cycle is:

- independent of the frequency
- proportional to the square of the strain amplitude.

This implies that the shape of the hysterisis curve for the material remains unchanged with amplitude and the enclosed area is independent of the strain rate. By equating the energy dissipated per cycle by linear damping to that dissipated by structural damping, one can derive an equivalent linear damping coefficient, which will have the form α/ω, where α depends on the material.

Substituting (E.1) in (E.2), multiplying both sides by ϕ_r and integrating over the volume v, the Lagrange equations of motion for each mode is obtained:

$$\ddot{q}_n + \frac{\alpha}{m\omega} + \omega_n^2 q_n = Q_n(t)/M_n \qquad (E.3)$$

Where $Q_n(t)$ = the generalized force
M_n = the generalized mass
ω_n = the nth principal frequency.

In arriving at equation (E.3), we make use of the orthogonality relationships:

$$\int_v \phi_n \phi_r \, dv \begin{cases} = 0, & n \neq r \\ \neq 0, & n = r \end{cases} \qquad (E.4)$$

Also,
$$Q_n(t) = \int f(x, y, z, t)\, \phi_n(x, y, z)\, dv \qquad (E.5)$$

$$M_n = \int \phi_n^2 (x, y, z)\, dm \qquad (E.6)$$

If we assume, for the moment, the applied force to be harmonic, then the expression for the generalized force can be written as:

$$Q_n(t) = \exp(i\omega t) \int_v F(x, y, z)\, \phi_n (x, y, z)\, dv \qquad (E.7)$$

which we will write for convenience as:

$$Q_n(t) = \exp i\omega t \;\; w_o w_n \qquad (E.8)$$

where $w_o = \int F(x, y, z)\, dv$ is the amplitude of total applied force on the structure,

$w_n = \frac{1}{w_o}\int F(x, y, z)\, \phi_n(x, y, z)\, dv$ is the mode participation of load.

The steady-state solution of equation (E.3) is:

$$q_n = \frac{w_o w_n}{M_n \omega_n^2} \frac{\exp i(\omega t - \theta_n)}{\sqrt{(1-(\omega/\omega_n)^2)^2 + \zeta^2}} \qquad \text{(E.9)}$$

Where ζ is the structural damping factor, $\alpha/m\omega_n$.

The displacement response from equation (E.1) is then:

$$u(x, y, z, t) = w_o \exp(i\omega t) \sum_{n=1}^{\infty} \frac{w_n \phi_n \exp(-i\theta_n)}{M_n \omega_n^2 [(1-(\omega/\omega_n)^2)^2 + \zeta^2]^{\frac{1}{2}}} \qquad \text{(E.10)}$$

We are interested in the mean-square values of the force and response, defined by:

$$\bar{u}^2 = \frac{1}{T}\int_o^T u^2 dt \quad \text{and} \quad \bar{F}^2 = \frac{1}{T}\int_o^T f^2 dt \qquad \text{(E.11)}$$

Using the above definition, we have:

$$\bar{u}^2 = \bar{F}^2 \sum_n \sum_m \frac{w_n w_m \phi_n \phi_m \cos(\theta_n - \theta_m)}{M_n M_m \omega_n^2 \omega_m^2 [(1-(\omega/\omega_n)^2)^2+\zeta^2]^{1/2}[(1-(\omega/\omega_m)^2)^2 + \zeta^2]^{1/2}}$$

Now, for small damping, all contributions to the response is small except near resonance so that, equation (E.12) can be approximately written as:

$$\overline{u^2} = \overline{F^2} \sum_{n=1}^{\infty} \frac{\omega_n^2 \, \phi_n^2}{M_n^2 \, \omega_n^4 \, [(1-(\omega/\omega_n)^2)^2 + \zeta^2]} \qquad \text{(E.13)}$$

At this stage, it is necessary to invoke the concept of a frequency spectrum for the forces induced by the random ice field. Using the principles of analyzing random vibrations[4] we can press ahead to derive a reasonably "convenient" expression relating the mean square value of the excitation to the displacement response spectra.

If there is a spectrum of excitation frequencies, we can define a spectral density $F(\omega)$ of the exciting forces. The contribution to the mean-square value of excitation in the frequency range $\Delta\omega$ is (see Figure E.2).

$$\overline{\Delta F^2} = F(\omega) \, \Delta\omega$$

so that

$$\overline{F^2} = \int_0^{\infty} F(\omega) \, d\omega \qquad \text{(E.14)}$$

Now, the expression for the mean square response in terms of the spectral density of the excitation is obtained from equations (E.13)and (E.14)as:

$$\overline{u^2} = \int_0^{\infty} F(\omega) \, |H(\omega)|^2 = \int_0^{\infty} U'(\omega) \, d\omega \qquad \text{(E.15)}$$

Where:

$$|H'(\omega)|^2 = \sum \frac{\omega_n^2 \, \phi_n^2}{M_n^2 \, \omega_n^4 \, [(1-(\omega/\omega_n)^2)^2 + \zeta^2]} \qquad \text{(E.16)}$$

= the reciprocal of the square of the generalized transfer function of the structure.

In other words, the spectral density of the response is given by:

$$U(\omega) = F(\omega)|H(\omega)|^2 \quad \text{so that} \quad F(\omega) = U(\omega)/|H(\omega)|^2$$

Therefore, the spectral density of the excitation is:

$$F(\omega) = U(\omega) \Big/ \sum_{n=1}^{\infty} \frac{\omega^2{}_n \phi^2{}_n}{M^2{}_n \omega^4{}_n \left[\left(1 - \frac{\omega^2}{\omega_n^2}\right)^2 + \zeta^2 \right]} \tag{E.17}$$

Similarly, it can be shown that the spectral density of the excitation (or the force) in terms of the spectral density of the measured acceleration is:

$$F(\omega) = \ddot{U}(\omega) \Big/ -\omega^4 \sum_{n=1}^{\infty} \frac{\omega^2{}_n \phi^2{}_n}{M^2{}_n \omega^4{}_n \left[\left(1 - \frac{\omega^2}{\omega_n^2}\right)^2 + \zeta^2 \right]} \tag{E.18}$$

If the damping ζ is small, the generalized transfer function will undergo a large change near the resonant frequency ω_n. Even if the variation in spectral density $F(\omega)$ is of lesser extent in this neighbourhood (i.e. ω approaching ω_n), $U(\omega)$ in equation (E17)or $\ddot{U}(\omega)$ in equation(E.18)will very likely show significant changes. (See Figure E.2 (a) and (b). Therefore, the mean square value of the excitation has

no other simpler form than

$$\overline{F^2} = \int_0^\infty (\omega)\,d\omega = \int_0^\infty \frac{U(\omega)\,d\omega}{\sum_{n=1}^{\infty} \frac{\omega^2{}_n \phi^2{}_n}{M^2{}_n \omega^4{}_n \left[\left(1-\frac{\omega^2}{\omega^2_n}\right)^2 + \zeta^2\right]}} \qquad \text{(E.19)}$$

However, if our interest is restricted to a finite number of frequencies and mode shapes of the hull structure, and in the particular case where the response spectra show significant magnitudes only around the natural frequencies ω_n, equation (E.19) can be approximated with good accuracy by the by the expression:

$$\overline{F^2} = \sum_{n=1}^{N} \frac{M^2{}_n \omega^4{}_n}{\omega^2{}_n \phi^2{}_n} \int_{\omega_n - \Delta\omega}^{\omega_n + \Delta\omega} U(\omega) \left[\left(1-\frac{\omega^2}{\omega^2_n}\right)^2 + \zeta^2\right] d\omega \qquad \text{(E.20)}$$

Once the mean square excitation (or force) is determined $\sqrt{\overline{F^2}}$ will give a numerical value of force which is representative of the particular ice environment and the ship speed which produced the measured response $U(\omega)$. It will also be possible to transform the computed force spectra into a *time series* using an inverse Fourier transform.

Summary and Limitations of the Method

A method is outlined above, based on the principles of linear elastic system dynamics, which may be used to calculate either a "root-mean-square" force or a force time history, if the following conditions are satisfied:

- An acceleration or deflection time series of finite length must be available.
- A spectrum analyzer with adequate resolution for the frequency range of interest is required, which can be used to generate the required response spectrum.

- Mass and stiffness distribution of the ship hull must be known.
- Natural frequencies and mode shapes of the hull structure have to be pre-calculated for the particular symmetric response to be studied (i.e. vertical, horizontal or longitudinal).
- The structural damping factor must be known for the particular ship.
- The *spatial distribution of the external force must be known.*

It can be seen that the last requirement puts a serious limitation on the applicability of the method. Any computational scheme based on the above method can be implemented only for the cases where the external ice loads may be assumed to be *concentrated at a given location on the hull.* Alternatively, if it is confirmed (from visual records) that the case in question is one in which the vessel is in *a priori* assumption on the most likely force distribution. This can be done, for example, in the case of the vessel in a continuous icebreaking mode. This assumed force distribution will necessarily have to be a function of the ice properties and the ship speed.

The above derivation of force spectra shows that the method is based on a given set of symmetric modal functions and the associated frequencies (say, for example, vertical vibration). This implies that the transfer function is capable of faithfully translating a measured response spectra into a force spectra, only if the response spectra is free of components which represent other modes of structural vibration (for instance, horizontal and longitudinal). It has been seen, however, that it is a difficult task to isolate purely symmetric response spectra for purposes of analysis, and also that measured spectra contained 'spikes' which cannot be identified with one set of calculated mode shapes alone (see Section D.2 of Appendix D). In such cases where coupling between the independent symmetric modes is evident, the method will have to be modified to include linear superposition of the modal functions representing each of the constituent types of vibration.

Finally, the present formulation of force spectra takes into account the rigid body motions only in so far as the mode shapes and frequencies are concerned. The transfer function, as represented by equation (E.16), is not applicable to the case of $n = 0$ since the hydrodynamic inertial and damping characteristics in the rigid body modes are dependent on frequency. In addition, the fact that the forward speed of the ship which causes dynamic coupling between the rigid body modes is missing from the formulation, precludes the use of the same transfer function to represent these modes. It may be pointed out, at this stage, that incorporation of the rigid body motions into the present formulation is rendered difficult (if not impossible) by the fact the equations of motion (in surge, heave and pitch for instance) are nonlinear in character. This is illustrated below:

$$(m + A_{11})\ddot{X}_1 = T - F_1 \tag{E.21}$$

$$(m + A_{33})\ddot{X}_3 + B_{33}\dot{X}_3 + C_{33}X_3 + A_{35}\ddot{X}_5 + B_{35}\dot{X}_5 + C_{35}X_5 = F_3 \tag{E.22}$$

$$(I_5 + A_{55})\ddot{X}_5 + B_{55}\dot{X}_5 + C_{55}X_5 + A_{53}\ddot{X}_3 + B_{53}\dot{X}_3 + C_{53}X_3 = F_5 - T(\overline{KG} - d_p) \tag{E.23}$$

In the above equations -

X_1, X_3 and X_5 = Motions in surge, heave and pitch respectively

F_1, F_3 and F_5 = External ice interaction forces plus any hydrodynamic forces not accounted for in the equations.

m, I_5 = Mass and Moment of Inertia of ship

A_{ij}, B_{ij} = added-mass and damping coefficients

T = Propeller thrust, a function of the form $a + b\dot{X}_1 + c\dot{X}_1^2$

$\overline{KG}$ = Location of the c.g. relative to the keel

d_p = Location of axis of propeller relative to the keel.

The added mass and damping coefficients are:

$$A_{33} = \int a_{33} dx' \qquad \text{(E.24)}$$

$$B_{33} = \int b_{33} dx' \qquad \text{(E.25)}$$

$$A_{35} = -\int a_{33} x' dx' - \frac{\dot{X}_1}{\omega^2} B_{33} \qquad \text{(E.26)}$$

$$B_{35} = -\int b_{33} x' dx' + \dot{X}_1 A_{33} + m X_1 \qquad \text{(E.27)}$$

$$A_{53} = -\int a_{33} x' dx' + \frac{\dot{X}_1}{\omega^2} B_{33} \qquad \text{(E.28)}$$

$$B_{53} = -\int b_{33} x' dx' - \dot{X}_1 A_{33} - m\dot{X}_1 \qquad \text{(E.29)}$$

$$A_{55} = \int a_{33} x'^2 dx' + \frac{\dot{X}_1^2}{\omega^2} A_{33} \qquad \text{(E.30)}$$

$$B_{55} = \int b_{33} x'^2 dx' + \frac{\dot{X}_1^2}{\omega^2} B_{33} \qquad \text{(E.31)}$$

In equations (E.24)to(E.31)above, a_{33} and b_{33} are the two-dimensional sectional added mass and damping coefficients for heave. All integrals are over the length of the ship and the sectional hydrodynamic coefficients have to be evaluated either by the Frank close-fit method or the Lewis-form method. Added mass in surge is not of significant magnitude, and can be assumed to be 8% of the ship mass.

It can be seen that introduction of the propeller thrust and cross-coupled damping coefficients such as B_{35} (equation (E.22)), which are dependent on the forward speed of the ship, render the equations of motion nonlinear, so that direct closed-form solutions are not possible. Hence transfer functions for rigid body motions of pitch and heave, and similarly for yaw and sway, have to be formulated in the time domain and perhaps solved numerically so that the forces are derived independent of the vibratory responses.

E.3 EXAMPLE CALCULATION

Vibration of a Uniform Free-Free beam due to Non-Periodic Excitation

For the free-free beam of uniform cross section and mass density excited by a lateral force at the end $x = 0$, we can make use of tables which contain a tabulation of the first n normal modes, their derivatives, and various integrals pertinent to the beam problem. Tables by Young and Felgar [4] is a useful reference in this context.

For this problem we have:

$$M_n = \int \phi_n^2 \, dm = \mu \int \phi_n^2 \, (x) dx = \mu l = \text{total mass}$$

$$\omega_n = \frac{1}{l} \int \phi_n \, (0) \, dx = \frac{2}{l} \cdot l = 2$$

Also $$\omega_n = (\beta_n l)^2 \left[\left(\frac{EI}{m l^4} \right) \right]^{\frac{1}{2}} \text{, where } \beta_n l = (2n + 1) \frac{\pi}{2}$$

$$n = 1, 2, \ldots\ldots \infty$$

If we consider a sinusoidally varying force of the type

$f(t) = F_0 \sin \omega t$, then the generalized equations of motion is:

$$\ddot{q}_n + \frac{\alpha}{m\omega} \dot{q}_n + \omega_n^2 \, q_n = \frac{F_0 \sin \omega t}{M_n} \int \phi_n (0) \, dx$$

The steady-state solution is then:

$$q_n = \frac{\omega_0 \, \omega_n \qquad \sin(\omega t - \theta_n)}{M_n \, \omega_n^2 \sqrt{\left(1 - \frac{\omega^2}{\omega_n^2}\right)^2 + \xi^2}} \qquad \text{(E.32)}$$

where $\omega_0 = \int F_0 dx = F_0 l$

Expressing the lateral displacement $u(x,t)$ by the equation,

$$u(x,t) = q_T + q_R \left(1 - \frac{2x}{l}\right) + \sum_{n=1}^{\infty} q_n \phi_n \qquad \text{(E.33)}$$

where q_T and q_R are generalized coordinates for the rigid body translation and rotation, respectively, we will investigate the acceleration at any point as a quantity of interest.
Acceleration,

$$\frac{\partial^2 u}{\partial t^2} = \ddot{q}_T + \ddot{q}_R \left(1 - \frac{2x}{l}\right) + \sum \ddot{q}_n \phi_n \qquad \text{(E.34)}$$

If we represent the rigid body accelerations $\ddot{q}_T$ and $\ddot{q}_R$ by their mode shapes and frequencies only, (that is, we assume the transfer functions to be of unit magnitudes), then equation (E.34) can be re-written as:

$$\frac{\partial^2 u}{\partial t^2} = F_o/m \sin \omega t + \frac{F_o l^2}{4I}\left(1 - \frac{2x}{l}\right)\sin \omega t + \sum \ddot{q}_n \phi_n \qquad \text{(E.35)}$$

where F_o/m and $\frac{F_o l^2}{4I}$ are respectively the amplitudes of acceleration in the rigid body modes of translation and rotation. In equation (E.35) above, $\ddot{q}_n$ are obtained by differentiating the expression (E.33) with respect to time and I is the mass moment of inertia about an axis through the center.

If we now determine the mean square value of the acceleration time history (E.35) over a long time interval T and follow the procedure outlined in section E.2, the force spectra can be obtained.

E.4 Need for Experimental Validation of Transfer Function

It is seen from the two previous sections (E.2 and E.3) that the method of deriving force spectra from response spectra is based on a linear transfer function of the ship structure in which the elastic, inertial and damping characteristics of the structure is included. The elastic and inertial parameters which govern the mode shapes and frequencies are computed separately by a numerical method (such as that in GBRP). The first order validity of that method was investigated as discussed in Section B.2. The selection of structural damping factor is at the moment arbitary, as not enough experimental data are available in the literature to relate it to the frequency of vibration. Incorporation of generalized damping which depends on forward speed imparts the equation of vibratory motion with time-dependent coefficients (if not nonlinearity) as the forward speed is not a constant. This renders spectral formulation of the transfer function difficult. (Note, however, that the contribution from generalized damping becomes significant at frequencies close to those of the rigid-body modes).

Although the derivation of the transfer function is based on well-established methods in structural dynamics, the fact that it involves all the above ship-related particulars, the calculation or choice of some of which have only been partially verified, points out the necessity for validation of the transfer function. The only rational way of performing this validation involves the use of simultaneously measured responses and excitations. This is standard practice in seakeeping where in the wave environment and ship motions are independently measured. A fairly exhaustive search on ship structural dynamics literature did not reveal a measured set of response and force spectrum usable for present purposes. It is, therefore, concluded that a well-planned series of experiments involving a scaled structural model under controlled conditions will be required to validate the transfer function derived in Section E.2.

E.5 SOFTWARES AND INPUT DATA FOR COMPUTATION

Based on the theory described above, a computer program written in HP extended BASIC was developed for calculating the spectral density of the ice force from the measured response spectrum. The flow chart of this computer code, 400FSC, was detailed in Figure E.3 and the program listing is appended in Annex 8.

In addition the measured acceleration spectrum, the input data required for computation consists of the following:

(1) principal frequencies,
(2) mode shapes,
(3) distributed masses,
(4) location of sensor, and
(5) position of ice impact.

The first three parameters representing the vibratory characteristics of the ship structure were obtained using the General Bending Response Program (GBRP) [6]. Details of the analyses for the horizontal and vertical modes of vibration can be seen in Appendix B of this report. The readers are reminded that the GBRP program does not calculate the frequencies for the rigid body modes ("minus-one" and zeroth modes) therefore the principal frequencies for these two modes were computed separately.

For the vertical vibration, the rigid body modes correspond to the heave and pitch respectively. They can be calculated by:

$$f_h = \frac{1}{2\pi}\sqrt{\frac{K_h}{M + M_a}} \qquad \text{Rigid Body Mode (Heave)} \qquad (E.36)$$

$$f_p = \frac{1}{2\pi}\sqrt{\frac{K_p}{I + I_a}} \qquad \text{Rigid Body Mode (Pitch)} \qquad (E.37)$$

FIGURE E.3

FLOW CHART - ICE FORCE SPECTRAL DENSITY

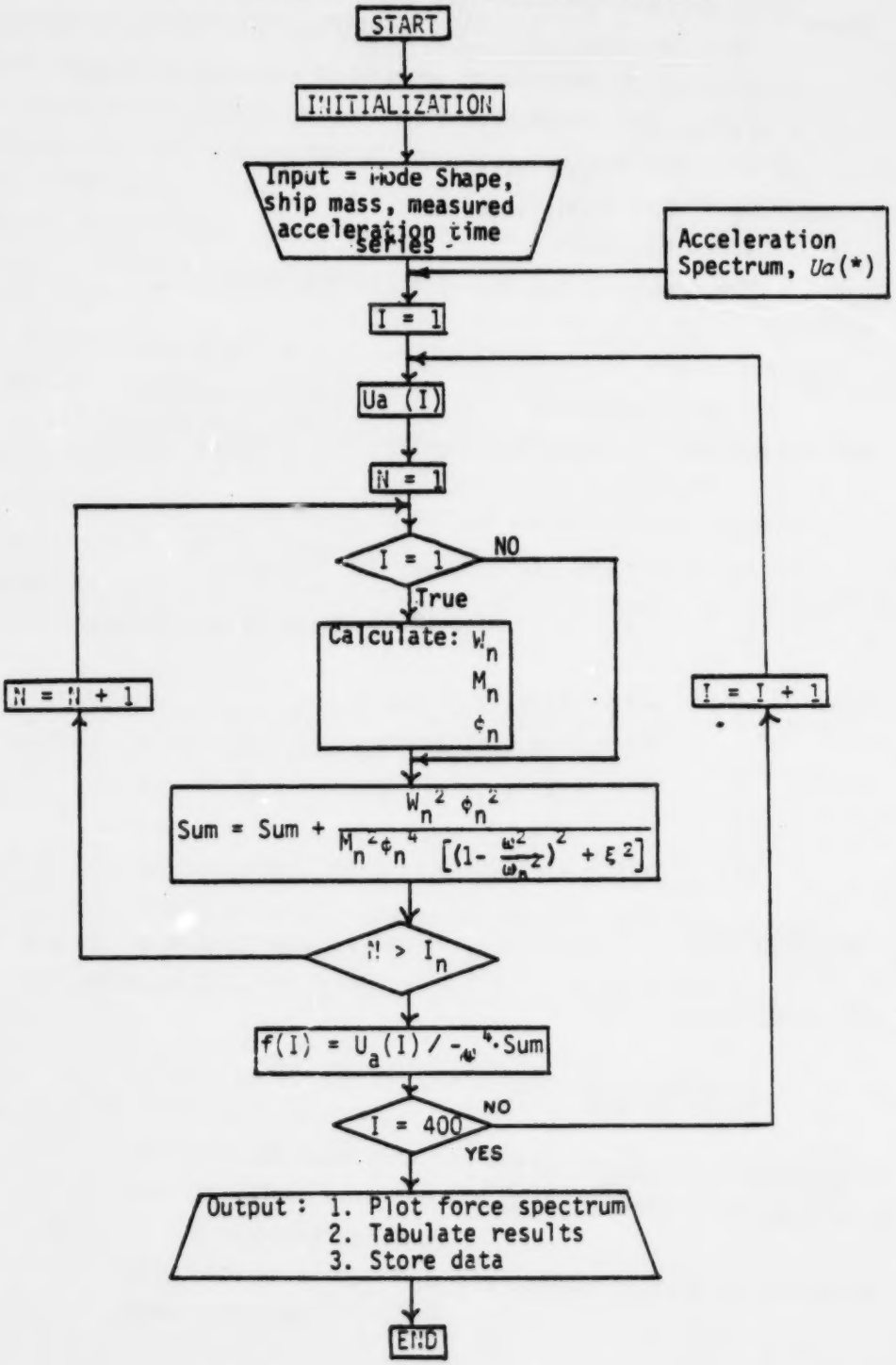

Where K_h , K_p = hydrostatic restoring coefficients in heave and pitch respectively
I = moments of inertia of the ship in pitch
I_a = added mass in pitch
M = ship mass
M_a = ship added mass

The moment of inertia of POLAR SEA in pitch was calculated by (After POPOV [7]):

$$I = 0.07\, MC\omega p L^2 \tag{E.38}$$

and the hydrostatic restoring coefficients in heave and pitch were by:

$$K_h = \rho g\, C\omega p LB \quad (= \text{tons per ft. immersion}) \tag{E.39}$$
$$K_p = \rho g\, I\omega p \quad (= \text{moments to change trim 1 radian})$$

Where ρg is weight density of sea water,
$C\omega p$ is waterplane coefficient,
L is ship length,
B is ship beam, and
$I\omega p$ is moment of inertia of waterplane.

For the purpose of computation, it was assumed that $M_a = .2m$ and $I_a = .2I$, therefore the rigid body (heave and pitch) modes were calculated to be:

$$f_h = 0.1618 \quad (1/\text{sec})$$

and $$f_p = 0.186 \quad (1/\text{sec})$$

For the horizontal vibration, the zero-node and one-node modes correspond to the sway and yaw respectively. However, the associated frequencies will be zero as there is no hydrostatic restoring force moment in the sway and yaw. For the purpose of computation, the frequencies of zero-node and one-node were set to be 0.00001 and 0.0001Hz respectively. The principal frequencies and its associated mode shapes for the horizontal and vertical vibrations were shown in Figures E.4 and E.5.

The spectrum analysis on the acceleration signal was performed by a spectrum analyser (Model 446) supplied by Nicolet Scientific Corporation. It produces the quadrature (real/imaginary) data of the response spectrum and stored under a data code. Data transmission from the analyser to the HP 9845B desktop computer was achieved via the HP-IB interface. Therefore, two additional softwares were developed, during the course of this study, for transmitting and interpreting the spectrum data.

The software code, 400-Q, performs data transmission from the analyser to HP 9845B computer. Operating functions include:

(1) Set up test information file (test date, event, sensor I.D., calibration constants, and so on.)
(2) Set up mass storage and reset HP-IB interface.
(3) Transfer control status to analyser and data information to HP 9845B computer.
(4) Record on floppy disc with a designated file name.

The software code, 400-RI, performs data interpretation and graphics. Its functions include:

(1) Retrieve spectrum data (in hexidecimal) and convert into numeric value, both for the real and imaginary components of the response spectrum.
(2) Calculate power spectrum and convert it into acceleration power spectrum.

FIGURE E.4

MODE SHAPES AND NATURAL FREQUENCIES FOR VERTICAL VIBRATION (USCGC POLAR SEA)

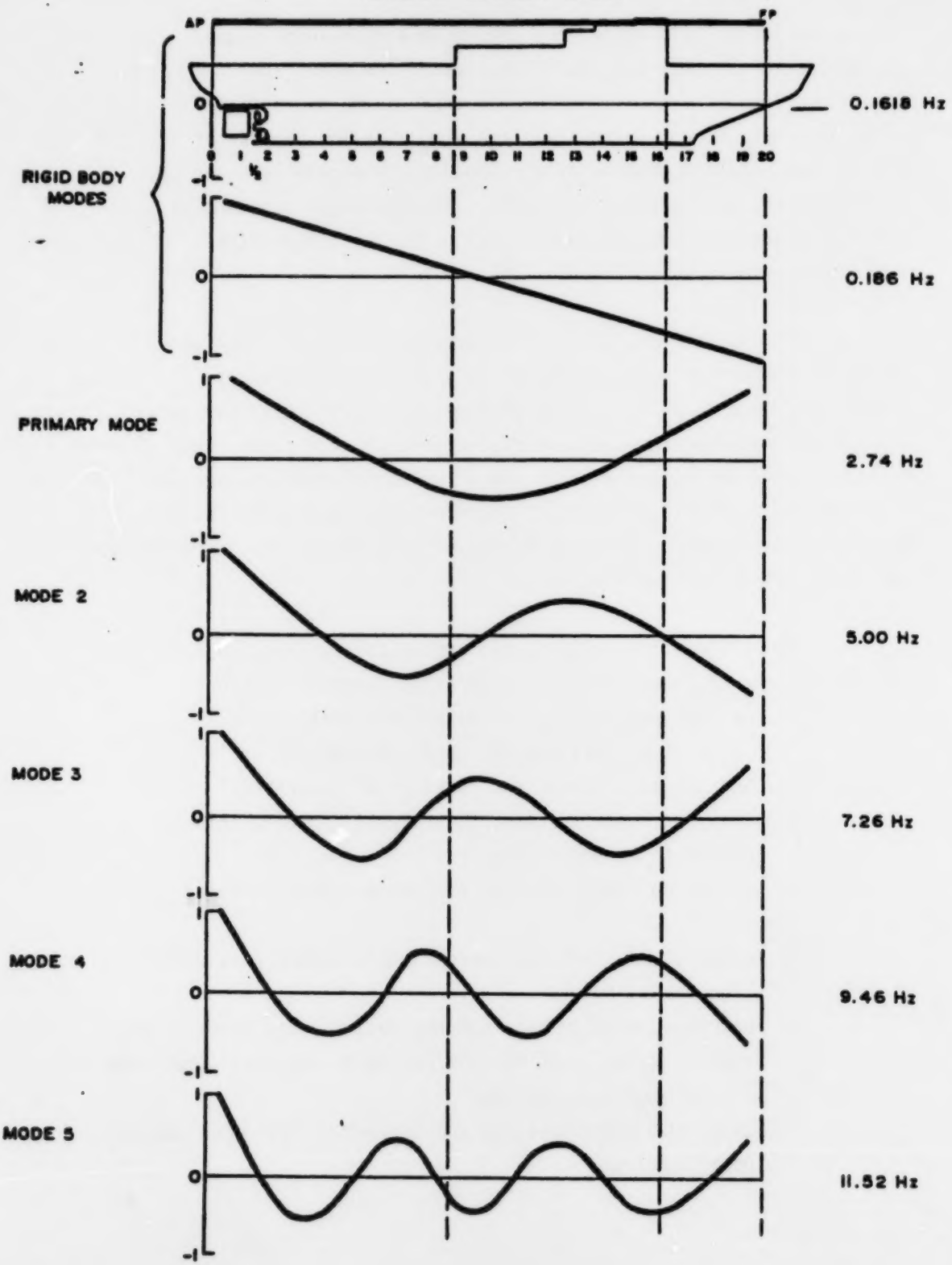

FIGURE E.5

MODE SHAPES AND NATURAL FREQUENCIES FOR HORIZONTAL VIBRATION (USCGC POLAR SEA)

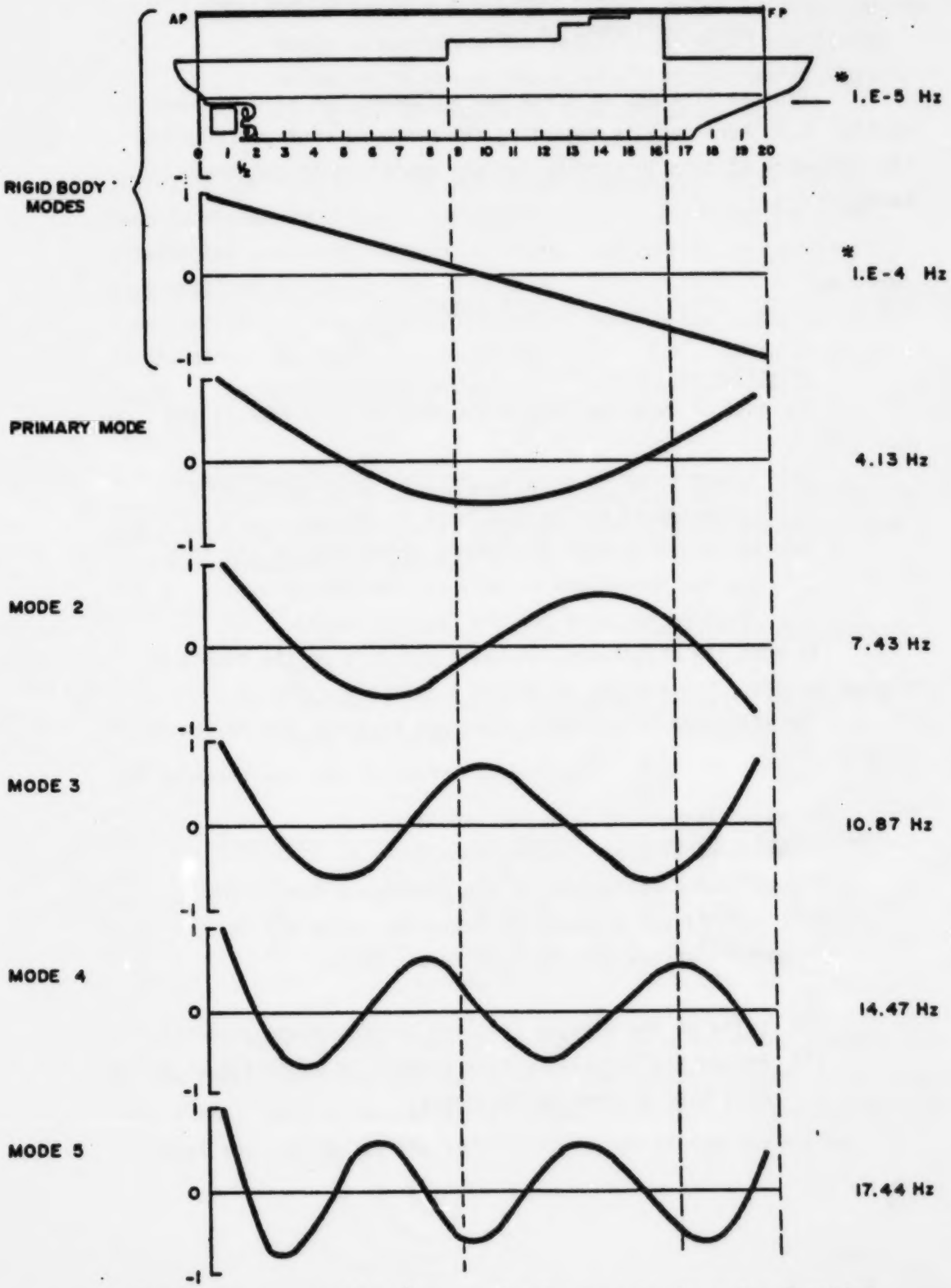

*Small non-zero number for use in the inverse transfer function

(3) Plot and print acceleration power spectrum.
(4) Store formatted quadrature (real/imaginary) spectrum data (performed in Step 1).

Program listings of these two softwares can also be found in section E.9. More details regarding the hardware configuration and the procedure of data interpretation are explained in the instruction manual [8].

E.6 SELECTION OF CASES AND DATA REDUCTION

Selection of Cases

The task of reducing full scale data on ship impacts was done to:

(a) select cases of ship impact that the assumption of concentrated excitation force is valid,
(b) establish initial pre-impact conditions of the ship and ice conditions as well as location of impact required as input for the computer model.

To meet the objectives, emphasis was laid on the events of ramming impacts. The aim was to obtain 8 suitable cases.

The selection of suitable cases was based on the following criteria:

- establishment of data availability,
- evidence of clear, sharp impact
- confidence estimation of the pre-impact conditions
- clear, visual evidence of heave and surge and in particular sway for oblique impact cases.

The review of the voyages involved a three-stage process:

(1) Review trafficability data summary to establish an initial data base of ramming incidents.

(2) Review video tape records of the voyages to establish the impact scenario and the initial pre-impact conditions.
(3) Review oscillograph traces of all accelerometer signals during the corresponding time period of impact.

Review of the trafficability data summary shows that POLAR SEA was ramming rather thick level ice (sometimes pressure ridge ice cover) between the period of February 7 - 10th. A total of 19 incidents were obtained as the initial data base. Further reviews of the video tape records and the oscillograph traces reduced the number of cases to the target 8. These are listed in Table E.1 . Elimination was based on the forementioned criteria.

Data Reduction

Once the cases were generated, a decision was made on the time over which the sample would be taken for the spectrum analysis. The basic requirements are outlined as:

(1) a time window over which the assumption of concentrated force be valid
(2) a suitable frequency resolution that will include the rigid body modes.

The analyser has the following capability:

Frequency Range	Time Window	Frequency Resolution
100 *Hz*	4 sec	0.25 *Hz*
50	8	0.125
20	20	0.050
10	40	0.025

A ramming impact can be considered as a two-stage process. In the first stage, at the beginning of the impact (head-on or oblique), only a small part of the ship side impact with ice, and the interaction is local and limited to the contacting region of the two masses.

TABLE E.1

USCGC POLAR SEA - FULL SCALE RAMMING TESTS

DATE-TIME GROUP MN:DAY:HR:MIN	ACTIVITY (ICE THICKNESS)	IMPACT POSITION	VIDEO TAPES	MAGNETIC TAPE		TEST # USED IN '400 FSC'
				#	COUNT	
02:07:23:34	Ramming Level Ice (max 4', Aug 3')	Head-on	3-6	1-9	2468	
02:08:02:06	Transit Ramming in Level Ice (Aug. 3½')	Head-on	3-6	1-9	3572	
02:08:02:16	Ramming Level Ice (max 4½',Aug3½')	Oblique	3-6	1-9	3666	
02:08:02:23	Ramming Level Ice/P.R. (Max. 4', Aug. 3½')	Oblique (6 knots)	3-6	1-9	3737	F8-0
02:08:23:30	Ramming Level Ice (Max. 4', Aug. 3½')	Oblique (9 knots)	3-6	1-9	3797	F8-1
02:08:23:50	Transit Ramming (Max. 2')	Oblique	3-6	1-9	4494	F8-2
02:09:06:09	Ramming Level Ice (Max. 4', Aug 3')	Head-on (5.33 kn)	3-7	1-10	3115	F9-0
02:09:06:20	Transit Ramming (Max. 4', Aug 3')	Head-on (9 knots)	3-7	1-10	3232	F9-1
02:09:06:26	Transit Ramming	Oblique (7 knots)	3-7	1-10	3310	F9-2
02:09:09:57	Ramming Level Ice (Max 4')	Head-on	3-7			
02:09:10:10	Ramming Level Ice (Max 4')	Head-on	3-7	N/A		
02:09:10:06	Ramming Level Ice (Max 4')	Head-on	3-7			
02:09:13:50	Transit Ramming (Max 3', Aug. 2')	Head-on (12 knots)	3-7	1-11	1748	F9-4
02:09:13:57	Transit Ramming	Oblique	3-7	1-11	1817	
02:09:14:00	Ramming Level Ice (Max. 3')	Head-on (4 knots)	3-7	1-11	1833	F9-5

The ice edge breaks and ice field bends. This process results in the ice field ahead of the contact area failing in the form of cusps. As the ship moves ahead the process is repeated with the new ice edge, while the already broken edge of the ice moves aft creating other loading points on the hull. At this stage, therefore, the assumption that the exciting force is a concentrated force (i.e. a point load) is not strictly valid. From comprehensive analysis of previous full scale data it is knwon that the first stage lasts about 1 second although the whole process, until the ship comes to a stop, may take up to 2 minutes. For the assumption to be valid, therefore, the time window needs to be small; 1 second or less. However, the spectrum analyser's frequency resolution at a one second time window is 1.25 Hz, which is very coarse and cannot take into account components of rigid body motions which are in the 0 to 0.2 Hz range. The final decision regarding the duration of the time window was a compromise between the two extremes. The window was set to 8 secs. thus giving a frequency resolution of 0.125 Hz over a frequency range of 0 to 50 Hz.

Once the case was located on tape, the expected amplitude of the input signal in millivolts was selected on the analyzer. The analyzing system was the following:

- °Step 1. The transient acceleration signal was captured and analyzed to produce a frequency spectrum.
- °Step 2. The spectrum data (real and imaginary) was then transmitted to the HP 9845B desktop computer via HP-IB interface (use program 400-Q).
- °Step 3. HP 9845B then performed data interpretation to convert the hexidecimal data into numeric format and stored data on a floppy disk for the later use of force spectrum calculation. (use program 400-RI).

This analyzing procedure was repeated on every acceleration signal for all the ramming cases selected.

Upon completion of data transmission and interpretation, the force spectrum calculation program, 400 FSC, was then used to compute the spectral density of the excitation force. From the preliminary analysis, it has been noted that there exists a common dominant frequency between the impact incident and the open water conditions immediately prior to the impact. Simply by substracting the open water spectrum from the impact spectrum, it is possible to obtain a power spectrum that is mainly due to the ice impact. This scheme was incorporated in the program. The readers are reminded that we have assumed a 'numeric' cut-off frequency of 15 *Hz* in the force spectrum calculation. That is, only the first 120 spectrum data points were used in the program for deriving the spectrum of the ice force. The reason is that there is no confident mode shape available for frequency range greater than 15 *Hz* and using the present mode shapes to extrapolate the high frequency end would simply result enormous errors in the final results. The GBRP program can provide mode shapes for high frequency range, however, with the present idealization of the 20 - section lumped mass model, the accuracy of the calculated mode shapes for higher frequency range has not been validated. This is not the deficiency of the GBRP program but the lumped mass model was simply not appropriate for frequencies above 15 Hz.

Outputs of athwartship and vertical accelerometers have been analyzed with the force spectrum calculation program and the results have been presented in tabular form as well as graphical form.

E.7 PRESENTATION AND DISCUSSION OF RESULTS

E.7.1 Presentation of Results

The results of this analysis mainly consists of two parts:

1) acceleration spectrum of every accelerometer for each selected ramming test (during impact and open-water prior to impact), and
2) force spectra derived from the corresponding vertical and transverse accelerometers.

Both the acceleration and force spectra are given in tabulated and graphical form. A typical output is shown in Figure E.4. A complete set of the spectrum output of ramming test F8-0 (81:02:08:02:23) can be found in Annex 7, Volume III. For other ramming tests, only the computed force spectra were included.

It is important to note that the accelerometer package installed by ARCTEC INC. at the mid-ship is gyro-stabilized which measured accelerations relative to the space-fixed frame. Since the theory developed in Section E.2. was based on a ship-fixed coordinate system, its acceleration spectra could not be used to derive force spectra. Hence, it was excluded in the discussion of the force spectrum analysis.

Figures E.5 a-n and E.6 a-n show the 400-line (50 Hz range) response (acceleration) spectra of POLAR SEA for ramming test F8-0 and F9-1, while Figures E.7 a-l and E.8a-l illustrate their corresponding acceleration spectra of open-water condition immediately prior to the impact. The number of lines in a spectrum is a function of the sampling memory and anti-aliasing filter of the analyzer. Briefly, the analyzer used had a sampling memory of 1024 points and a maximum anti-aliasing filter value of 1/2.56 of the sampling rate, thus producing 400 lines. (More details of memory, sampling rates, band widths, etc. are given in references [8] and [9].)

1)	Longitudinal accelerometers	2X, 3X, 5X and 7X (not applicable for force spectrum analysis)
2)	Transverse accelerometers	1Y, 2Y, 5Y, and 7Y
3)	Vertical accelerometers	1Z, 2Z, 5Z, and 7Z

FIGURE E.4(a)

TYPICAL OUTPUT

ARCTEC CANADA LIMITED

FORCE SPECTRUM CALCULATION PROGRAM

```
Subject :POLAR SEA -F.S. TEST -4' max L.I. OBL.RAM. AT 9 Kt
Vessel  : USCGC POLAR SEA                  Test Time:FEB 9 1981 (06:20)
Sensor  : ACC. 1Z                          Cal.Factor:1.2500('g/v)
FreqRange:    50 (Hz)                      Force Unit: L.ton*L.ton/Hz
Vib. Mode: Vertical Bending                File Name: F91Z1
* Location of applied conc. load is at section # 18.5
* Location of accelerometer is at section 20
* Cut-off frequency for force calculation is 15 (Hz)
-------------------------------------------------------------------------------

  Mean      Square= 9.027900E+03(L.ton*L.ton)
  Root Mean Square= 9.501526E+01(L.ton)
-------------------------------------------------------------------------------
```

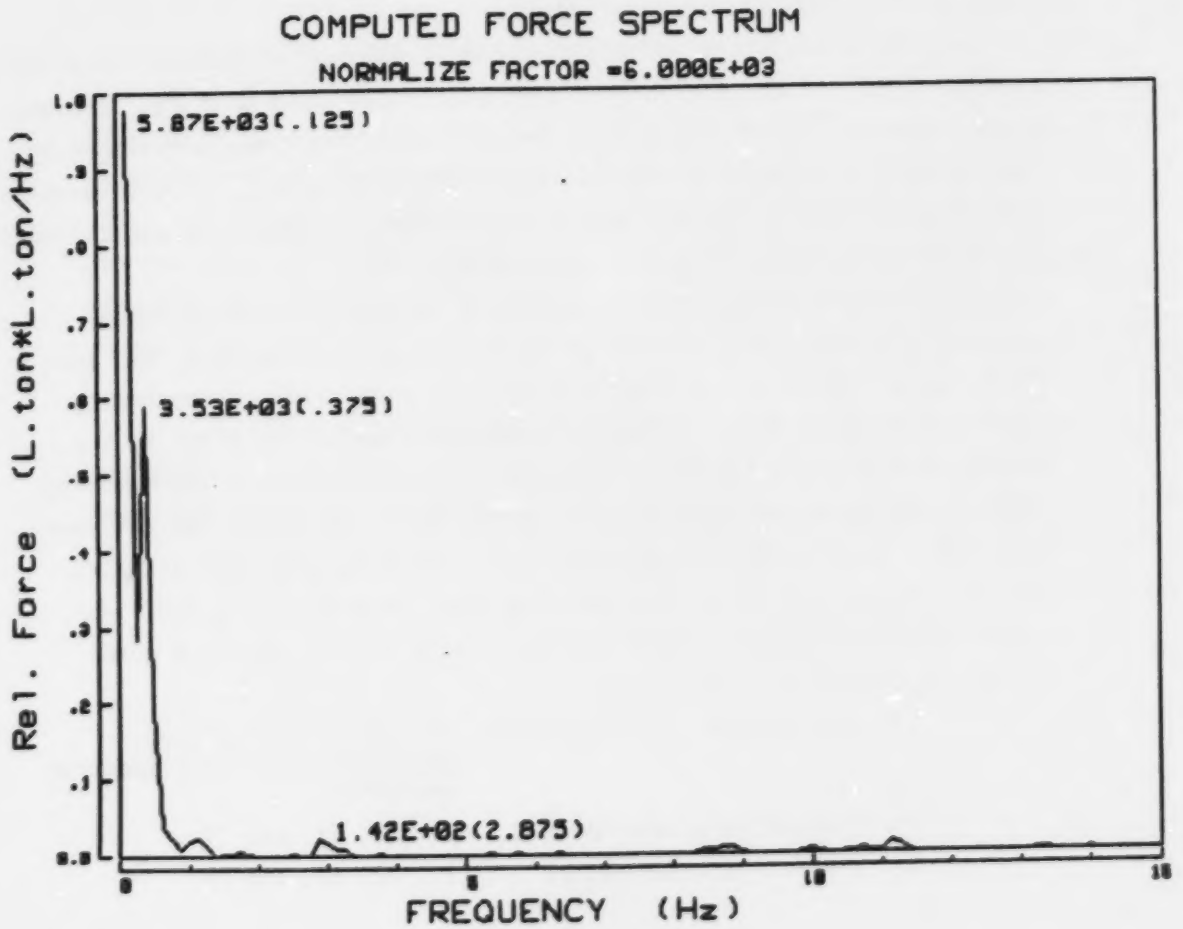

FIGURE E.4(b)

TYPICAL OUTPUT

ARCTEC CANADA LIMITED

FORCE SPECTRUM CALCULATION PROGRAM

```
Subject :POLAR SEA -F.S. TEST -4' max L.I. OBL.RAM. AT 9 Kt
Vessel  : USCGC POLAR SEA                 Test Time:FEB 9 1981 (06:20)
Sensor  : ACC. 1Z                         Cal.Factor:1.2500('g/v)
FreqRange:    50 (Hz)                     Force Unit: L.ton*L.ton/Hz
Vib. Mode: Vertical Bending               File Name: F91Z1
* Location of applied conc. load is at section # 18.5
* Location of accelerometer is at section 20
* Cut-off frequency for force calculation is 15 (Hz)
```

Mean Square= 9.027900E+03(L.ton*L.ton)
Root Mean Square= 9.501526E+01(L.ton)

COMPUTED FORCE SPECTRUM

Hz	Amplitude	Hz	Amplitude	Hz	Amplitude	Hz	Amplitude
.125	5.8686E+03	.250	1.7019E+03	.375	3.5328E+03	.500	1.1749E+03
.625	2.3092E+02	.750	1.3321E+02	.875	6.1120E+01	1.000	1.2834E+02
1.125	1.4478E+02	1.250	6.7167E+01	1.375	7.9815E+00	1.500	2.3192E+01
1.625	2.3555E+01	1.750	3.9043E+01	1.875	2.3412E+01	2.000	4.8831E-01
2.125	6.3220E+00	2.250	2.9473E-01	2.375	5.9070E+00	2.500	1.0945E+01
2.625	8.5960E+00	2.750	2.8180E-01	2.875	1.4172E+02	3.000	1.0352E+02
3.125	5.5829E+01	3.250	5.1506E+01	3.375	4.5197E-01	3.500	8.3157E+00
3.625	4.9005E+00	3.750	1.6920E+01	3.875	7.2927E+00	4.000	2.2215E+00
4.125	5.3712E-01	4.250	7.7551E-01	4.375	1.6448E+00	4.500	4.3553E+00
4.625	4.3220E+00	4.750	2.6529E+00	4.875	1.2679E+00	5.000	2.0102E-02
5.125	6.3077E+00	5.250	3.9938E-01	5.375	1.9618E+01	5.500	4.8191E+00
5.625	6.3840E+00	5.750	2.3499E+01	5.875	9.0099E+00	6.000	3.3854E+00
6.125	5.3626E+00	6.250	3.4065E+00	6.375	1.3916E+01	6.500	3.0669E+00
6.625	3.7169E+00	6.750	1.2467E+00	6.875	1.0800E+00	7.000	1.9202E+00
7.125	8.4854E-01	7.250	6.7578E-04	7.375	4.6875E-03	7.500	3.6345E+00
7.625	4.2966E+00	7.750	1.7191E+00	7.875	4.6467E-01	8.000	6.0651E+00
8.125	5.0897E+00	8.250	2.2494E+00	8.375	1.5383E+01	8.500	3.3998E+01
8.625	2.8216E+01	8.750	5.7053E+01	8.875	4.4381E+01	9.000	1.6763E+01
9.125	6.1053E+00	9.250	6.4060E-01	9.375	1.8273E+00	9.500	4.4704E-01
9.625	1.5772E+00	9.750	1.1578E+00	9.875	1.7399E+01	10.000	3.4423E+01
10.125	2.3567E+01	10.250	9.4558E+00	10.375	4.7907E+00	10.500	1.2139E+01
10.625	1.7932E+01	10.750	3.9667E+01	10.875	2.1137E+01	11.000	2.4897E+01
11.125	8.0885E+01	11.250	7.2859E+01	11.375	2.2066E+01	11.500	4.9019E-01
11.625	3.3620E+00	11.750	7.0698E+00	11.875	3.4081E+00	12.000	2.7115E-01
12.125	3.8618E+00	12.250	6.2621E+00	12.375	3.2182E+00	12.500	1.1422E+00
12.625	1.0816E-01	12.750	1.4160E+00	12.875	3.8686E+00	13.000	2.8966E+00
13.125	7.7060E+00	13.250	1.6551E+01	13.375	1.1282E+01	13.500	1.6683E+00
13.625	8.3823E-01	13.750	1.9170E+00	13.875	6.3723E-01	14.000	1.3914E+01
14.125	7.9888E+00	14.250	1.0510E-01	14.375	1.1199E+00	14.500	1.7175E-01
14.625	3.8410E-01	14.750	1.9649E+00	14.875	3.8073E+00	15.000	2.2670E-01

Figure E.5

RESPONSE SPECTRA FOR RAMMING TEST F8-0

(a)

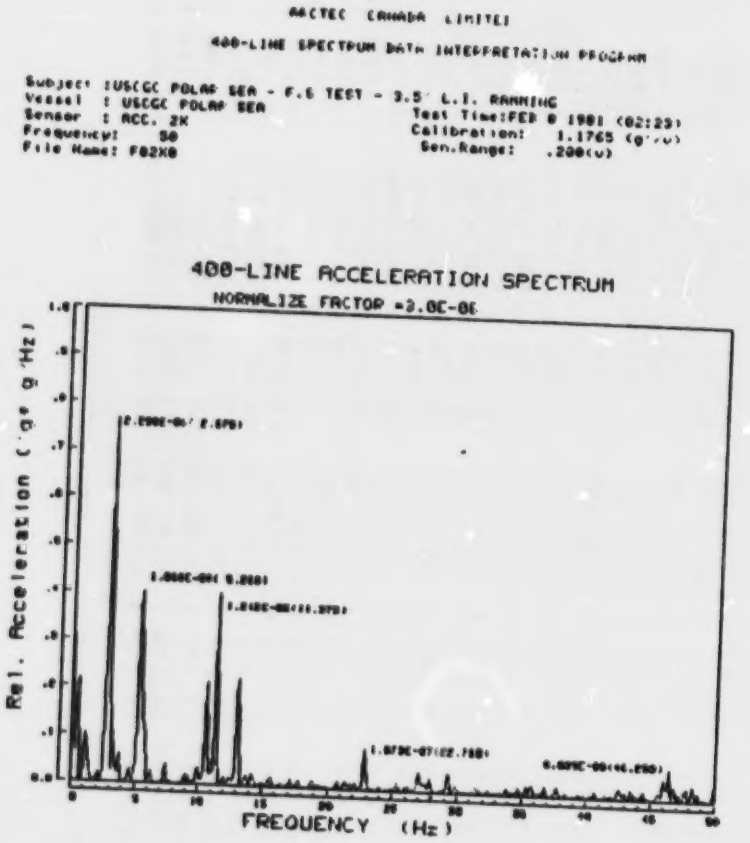

(b)

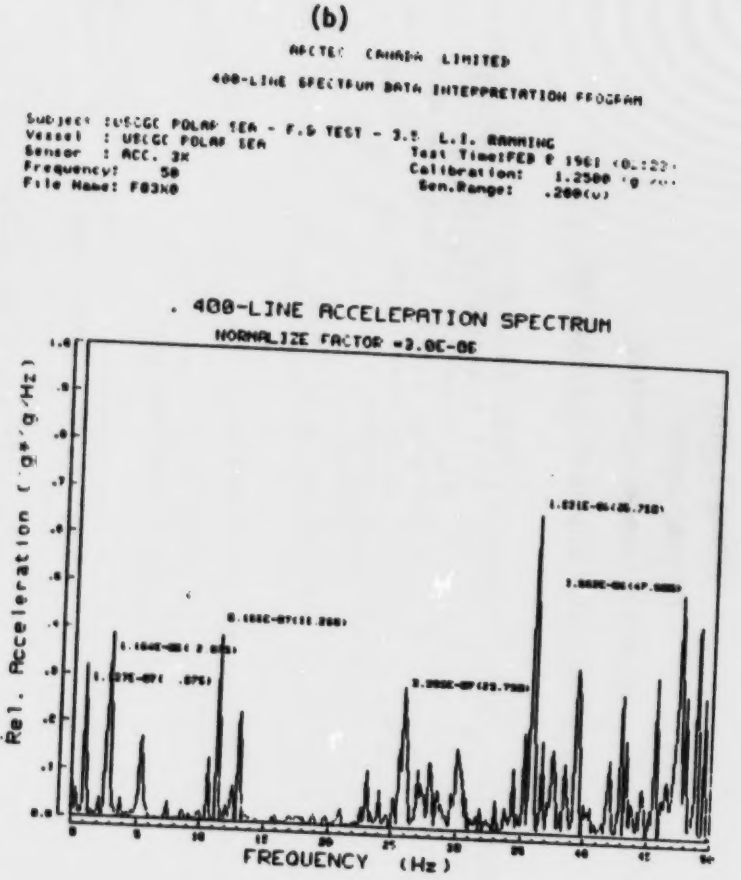

Figure E.5

RESPONSE SPECTRA FOR RAMMING TEST F8-0

(c)

ARCTEC CANADA LIMITED

400-LINE SPECTRUM DATA INTERPRETATION PROGRAM

Subject :USCGC POLAR SEA - F.S TEST - 3.5' L.I. RAMMING
Vessel : USCGC POLAR SEA
Sensor : ACC. 5X
Frequency: 50
File Name: F85X0
Test Time:FEB 8 1981 (02:23
Calibration: 1.1940 (g' v)
Sen.Range: .100(v)

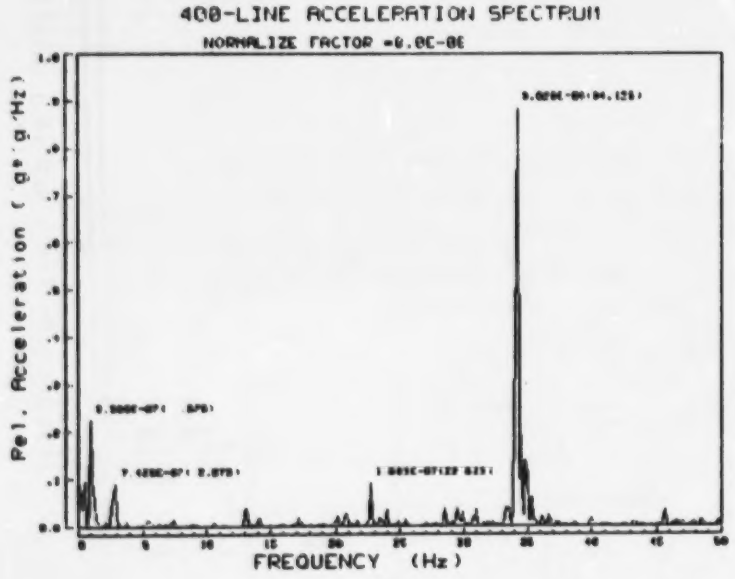

(d)

ARCTEC CANADA LIMITED

400-LINE SPECTRUM DATA INTERPRETATION PROGRAM

Subject :USCGC POLAR SEA - F.S TEST - 3.5 L.I. RAMMING
Vessel : USCGC POLAR SEA
Sensor : ACC. 7X
Frequency: 50
File Name: F87X0
Test Time:FEB 8 1981 (02:23:
Calibration: 1.1834 (g'/v)
Sen.Range: .500(v)

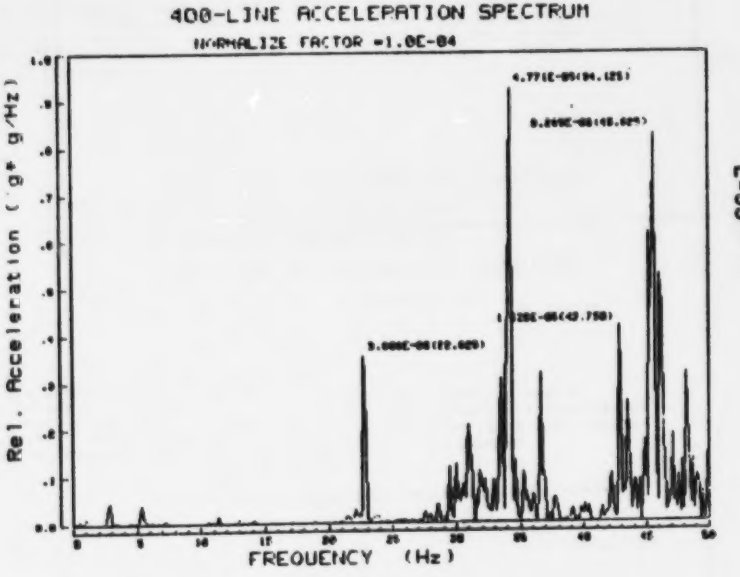

Figure E.5
RESPONSE SPECTRA FOR RAMMING TEST F8-0

(e)

ARCTEC CANADA LIMITED

400-LINE SPECTRUM DATA INTERPRETATION PROGRAM

Subject :USCGC POLAR SEA - F.S TEST - 3.5' L.I. RAMMING
Vessel : USCGC POLAR SEA
Sensor : POW SWAY
Frequency: 50
File Name: F81Y0
Test Time:FEB 8 1981 (02:23)
Calibration: 1.1940 (g'/v)
Sen.Range: .200(v)

400-LINE ACCELERATION SPECTRUM

NORMALIZE FACTOR =1.0E-05

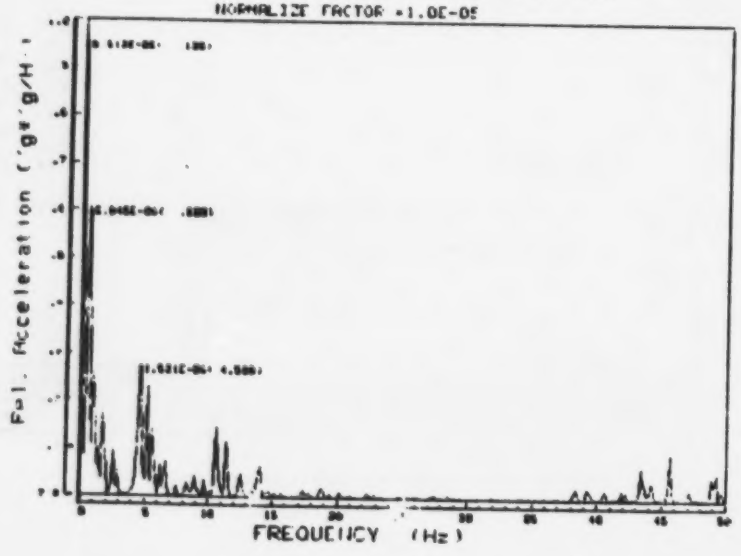

(f)

ARCTEC CANADA LIMITED

400-LINE SPECTRUM DATA INTERPRETATION PROGRAM

Subject :USCGC POLAR SEA - F.S TEST - 3.5' L.I. RAMMING
Vessel : USCGC POLAR SEA
Sensor : ACC. 2Y
Frequency: 50
File Name: F82Y0
Test Time:FEB 8 1981 (02:23)
Calibration: 1.2739 (g'/v)
Sen.Range: .200(v)

400-LINE ACCELERATION SPECTRUM

NORMALIZE FACTOR =6.0E-06

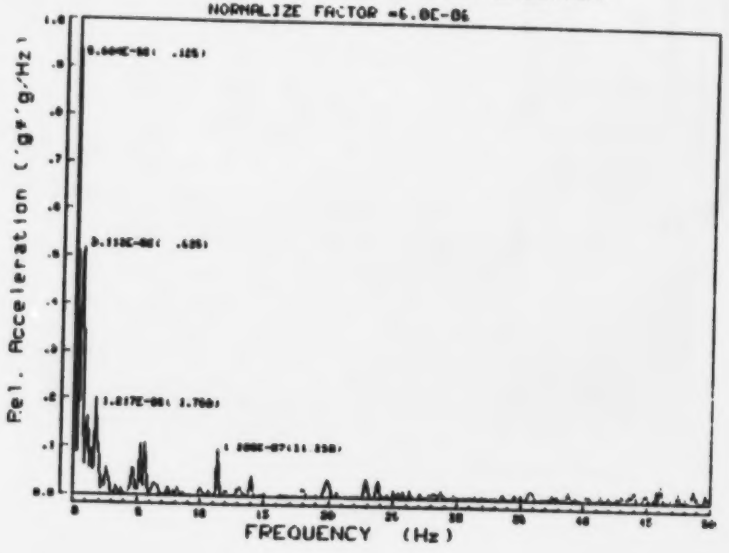

Figure E.5
RESPONSE SPECTRA FOR RAMMING TEST F8-0

(g)

ARCTEC CANADA LIMITED

400-LINE SPECTRUM DATA INTERPRETATION PROGRAM

Subject :USCGC POLAR SEA - F.S TEST - 3.5' L.I. RAMMING
Vessel : USCGC POLAR SEA
Sensor : ACC. 5Y
Frequency: 50
File Name: F05Y0
Test Time:FEB 8 1981 (02:23)
Calibration: 1.2270 (g'/v)
Sen.Range: .100(v)

400-LINE ACCELERATION SPECTRUM

NORMALIZE FACTOR =5.0E-06

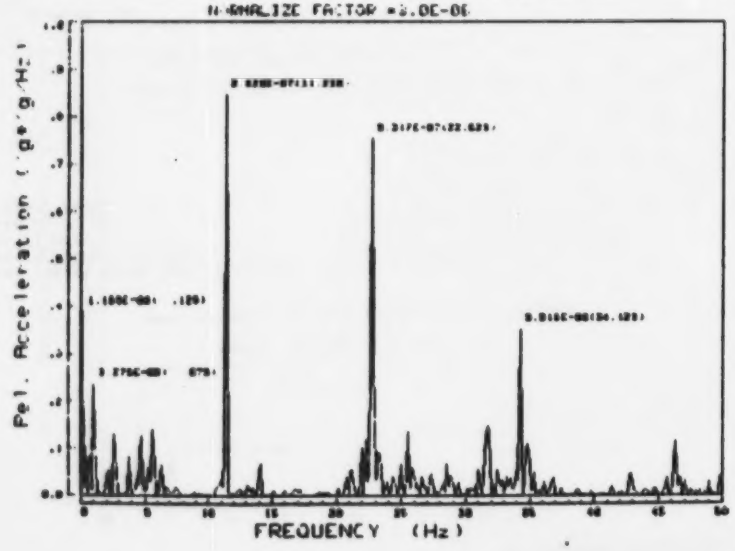

(h)

ARCTEC CANADA LIMITED

400-LINE SPECTRUM DATA INTERPRETATION PROGRAM

Subject :USCGC POLAR SEA - F.S TEST - 3.5' L.I. RAMMING
Vessel : USCGC POLAR SEA
Sensor : ACC. 7Y
Frequency: 50
File Name: F07Y0
Test Time:FEB 8 1981 (02:23)
Calibration: 1.2270 (g'/v)
Sen.Range: .500(v)

400-LINE ACCELERATION SPECTRUM

NORMALIZE FACTOR =6.0E-05

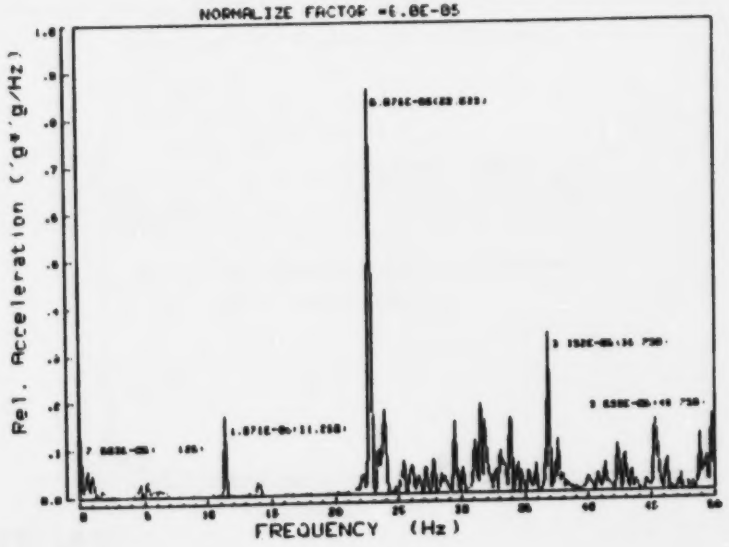

Figure E.5
RESPONSE SPECTRA FOR RAMMING TEST F8-0

(1)

ARCTEC CANADA LIMITED

400-LINE SPECTRUM DATA INTERPRETATION PROGRAM

Subject :USCGC POLAR SEA - F.6 TEST - 3.5' L.I. RAMMING
Vessel : USCGC POLAR SEA
Sensor : ACC. 3Y
Frequency: 50
File Name: F83Y0
Test Time:FEB 6 1981 (02:23)
Calibration: 1.2195 (g'/v)
Sen.Range: .200(v)

400-LINE ACCELERATION SPECTRUM
NORMALIZE FACTOR =9.0E-06

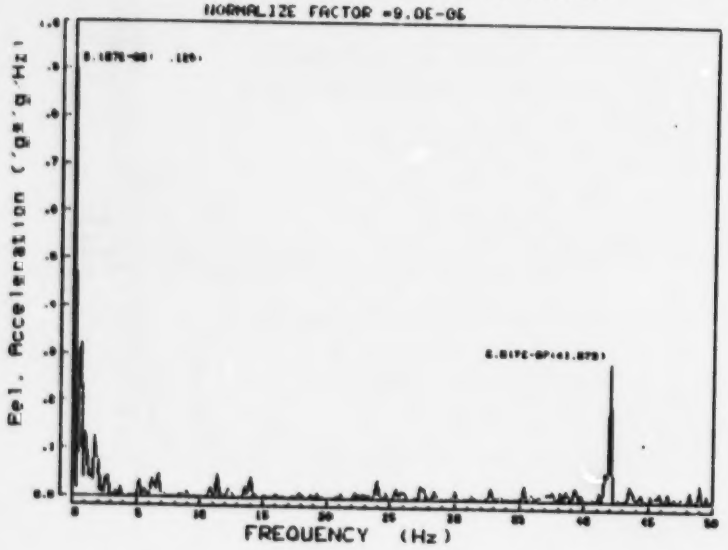

(j)

ARCTEC CANADA LIMITED

400-LINE SPECTRUM DATA INTERPRETATION PROGRAM

Subject :USCGC POLAR SEA - F.6 TEST - 3.5' L.I. RAMMING
Vessel : USCGC POLAR SEA
Sensor : ACC. 6Y
Frequency: 50
File Name: F86Y0
Test Time:FEB 6 1981 (02:23)
Calibration: 1.2422 (g'/v)
Sen.Range: .200(v)

400-LINE ACCELERATION SPECTRUM
NORMALIZE FACTOR =4.0E-06

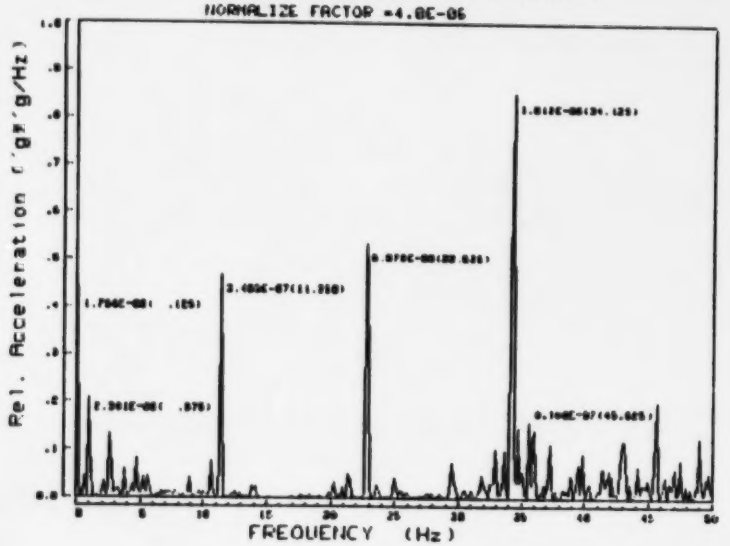

Figure E.5
RESPONSE SPECTRA FOR RAMMING TEST F8-0

(k)

ARCTEC CANADA LIMITED

400-LINE SPECTRUM DATA INTERPRETATION PROGRAM

Subject :USCGC POLAR SEA - F.S TEST - 3.5' L.I. RAMMING
Vessel : USCGC POLAR SEA
Sensor : BOW HEAVE
Frequency: 50
File Name: F8120
Test Time:FEB 6 1981 (02:23)
Calibration: 1.2500 (g/V)
Sen.Range: .200(V)

400-LINE ACCELERATION SPECTRUM

NORMALIZE FACTOR =4.0E-04

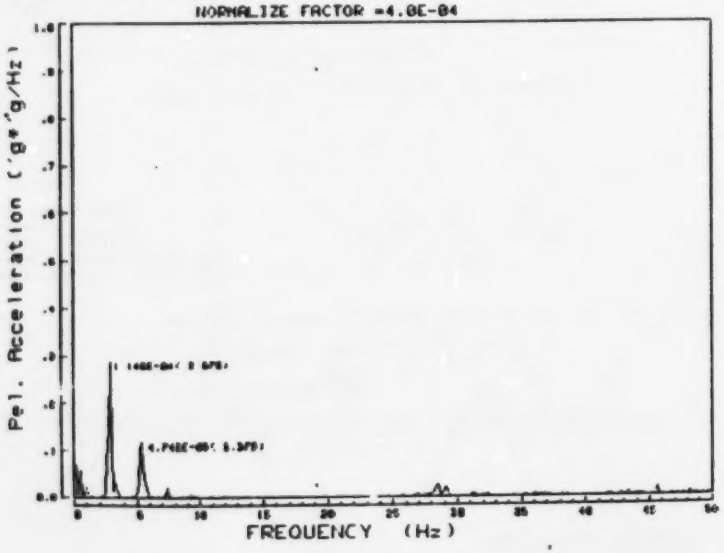

(l)

ARCTEC CANADA LIMITED

400-LINE SPECTRUM DATA INTERPRETATION PROGRAM

Subject :USCGC POLAR SEA - F.S TEST - 3.5' L.I. RAMMING
Vessel : USCGC POLAR SEA
Sensor : ACC. 22
Frequency: 50
File Name: F8220
Test Time:FEB 6 1981 (02:23)
Calibration: 1.2500 (g/V)
Sen.Range: .200(V)

400-LINE ACCELERATION SPECTRUM

NORMALIZE FACTOR =2.0E-05

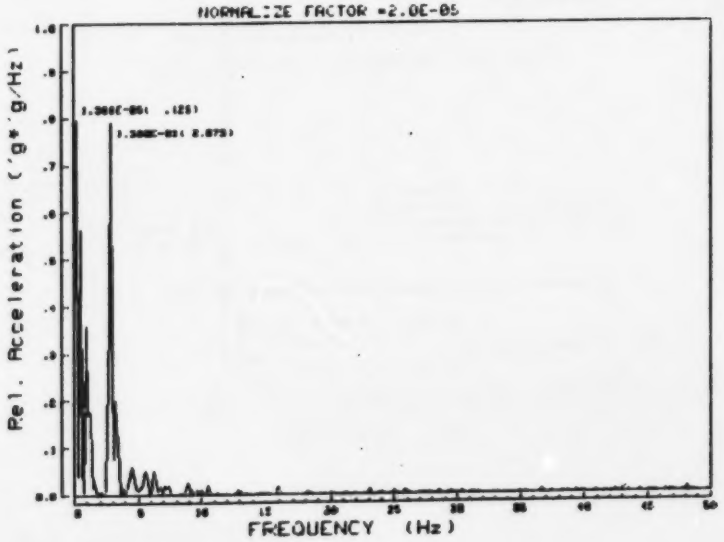

Figure E.5
RESPONSE SPECTRA FOR RAMMING TEST F8-0

(m)

ARCTEC CANADA LIMITED

400-LINE SPECTRUM DATA INTERPRETATION PROGRAM

Subject :USCGC POLAR SEA - F.6 TEST - 3.5' L.I. RAMMING
Vessel : USCGC POLAR SEA — Test Time:FEB 8 1981 (02:23)
Sensor : ACC. 52 — Calibration: 1.2422 (g'/v)
Frequency: .50 — Sen.Range: .200(v)
File Name: F8520

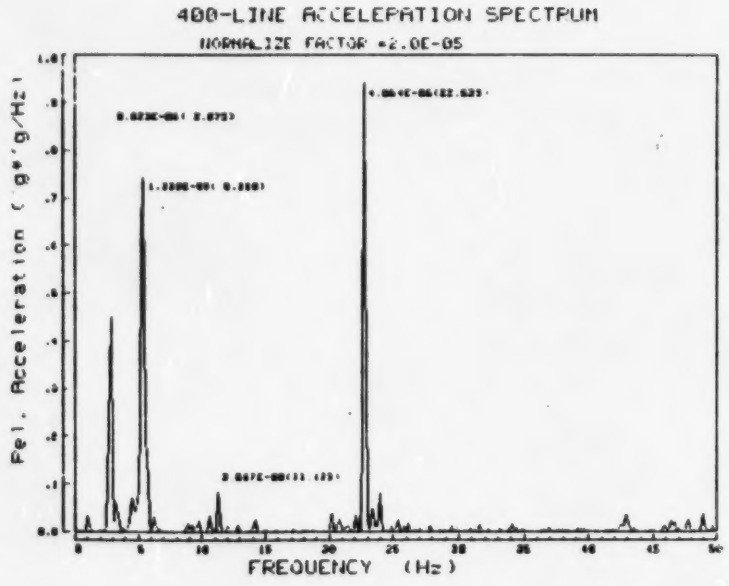

(n)

ARCTEC CANADA LIMITED

400-LINE SPECTRUM DATA INTERPRETATION PROGRAM

Subject :USCGC POLAR SEA - F.6 TEST - 3.5' L.I. RAMMING
Vessel : USCGC POLAR SEA — Test Time:FEB 8 1981 (02:23)
Sensor : ACC. 72 — Calibration: 1.2345 (g'/v)
Frequency: 50 — Sen.Range: .500(v)
File Name: F8720

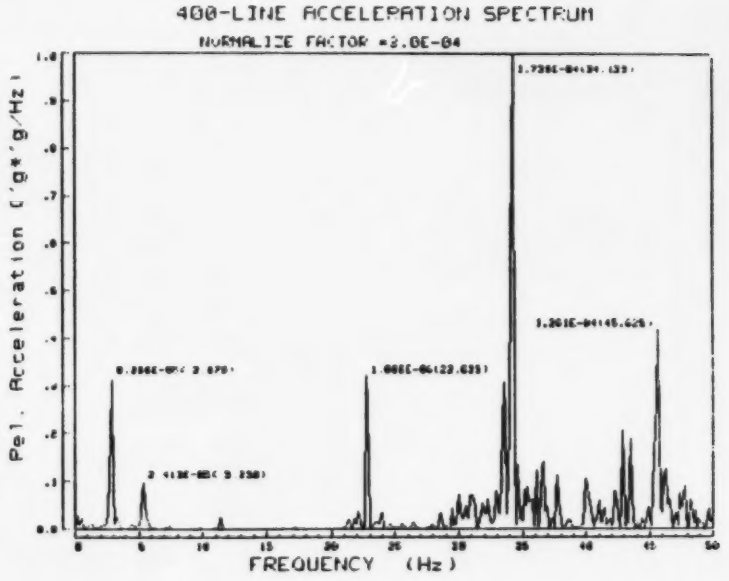

FIGURE E.6

RESPONSE SPECTRA FOR RAMMING TEST F9-1

(a)

ARCTEC CANADA LIMITED

400-LINE SPECTRUM DATA INTEPPRETATION PROGRAM

Subject :POLAR SEA -F.S. TEST -4' max L.I. OBL.RAM. AT 9 Kt
Vessel : USCGC POLAR SEA
Sensor : ACC. 2X
Frequency: 50
File Name: F92X1
Test Time:FEB 9 1981 (06:20)
Calibration: 1.1765 (g'/v)
Sen.Range: .200(v)

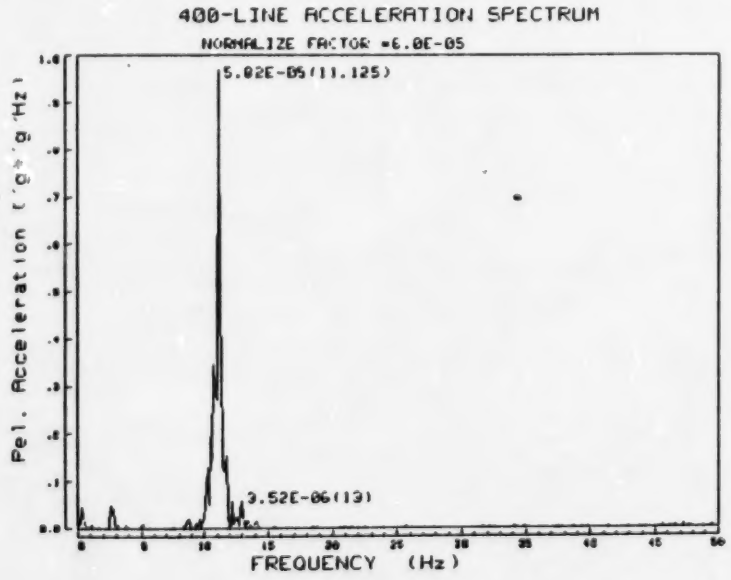

(b)

ARCTEC CANADA LIMITED

400-LINE SPECTRUM DATA INTERPRETATION PROGRAM

Subject :POLAR SEA -F.S. TEST -4 max L.I. OBL.RAM. AT 9 Kt
Vessel : USCGC POLAR SEA
Sensor : ACC. 3X
Frequency: 50
File Name: F93X1
Test Time:FEB 9 1981 (06:20)
Calibration: 1.2500 (g'/v)
Sen.Range: .200(v)

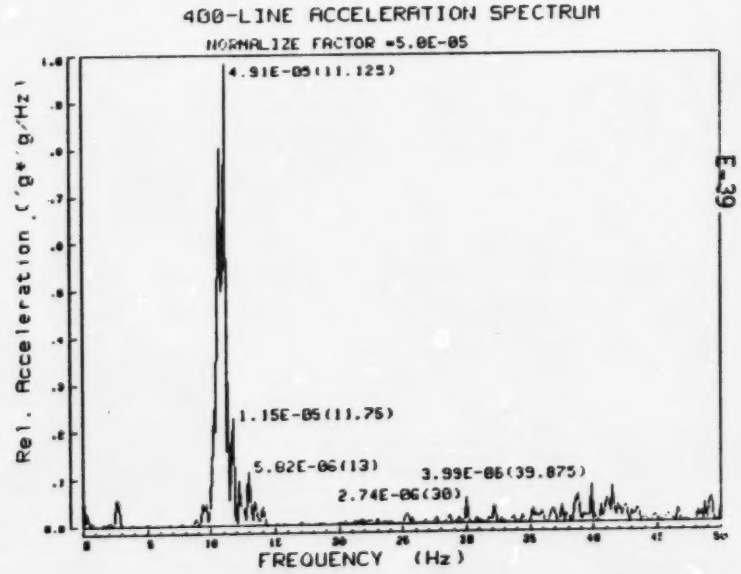

FIGURE E.6

RESPONSE SPECTRA FOR RAMMING TEST F9-1

(c)

ARCTEC CANADA LIMITED

400-LINE SPECTRUM DATA INTERPRETATION PROGRAM

Subject :POLAR SEA -F.S. TEST -4' max L.I. OBL.RAM. AT 9 Kt
Vessel : USCGC POLAR SEA — Test Time:FEB 9 1981 (06:20)
Sensor : ACC. 5X — Calibration: 1.1940 (g''v)
Frequency: 50 — Sen.Range: .200(v)
File Name: F95X1

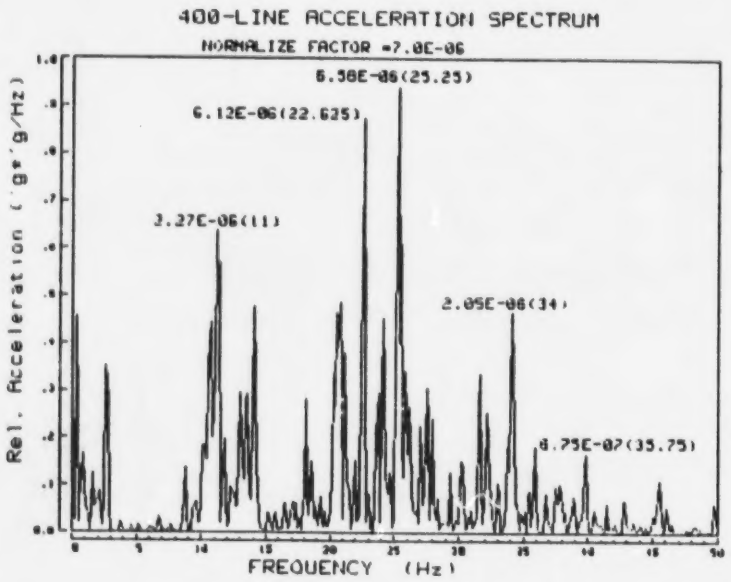

(d)

ARCTEC CANADA LIMITED

400-LINE SPECTRUM DATA INTERPRETATION PROGRAM

Subject :POLAR SEA -F.S. TEST -4' max L.I. OBL.RAM. AT 9 Kt
Vessel : USCGC POLAR SEA — Test Time:FEB 9 1981 (06:20)
Sensor : ACC. 7X — Calibration: 1.1834 (g''v)
Frequency: 50 — Sen.Range: .500(v)
File Name: F97X1

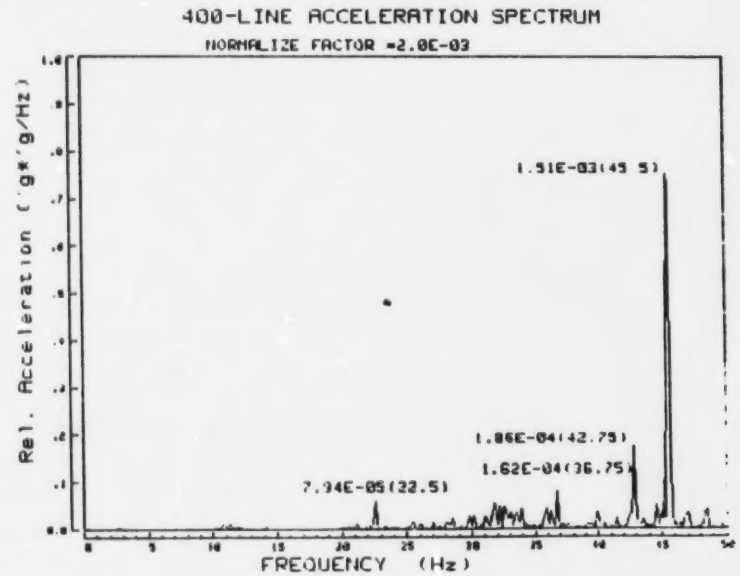

FIGURE E.6

RESPONSE SPECTRA FOR RAMMING TEST F9-1

(e)

ARCTEC CANADA LIMITED

400-LINE SPECTRUM DATA INTERPRETATION PROGRAM

Subject :POLAR SEA -F.S. TEST -4' max L.I. OBL.RAM. AT 9 kt
Vessel : USCGC POLAR SEA
Sensor : ACC. 1Y
Frequency: 50
File Name: F91Y1
Test Time:FEB 9 1981 (06:20)
Calibration: 1.1940 (g'/v)
Sen.Range: .200(v)

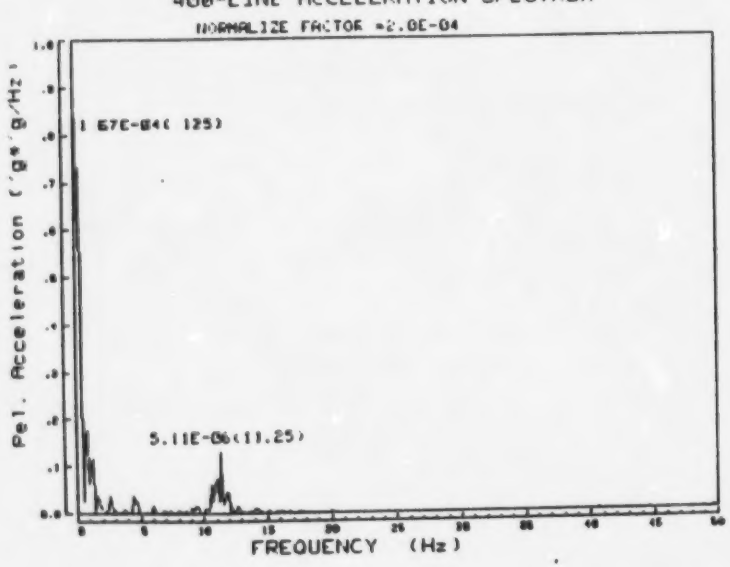

(f)

ARCTEC CANADA LIMITED

400-LINE SPECTRUM DATA INTERPRETATION PROGRAM

Subject :POLAR SEA -F.S. TEST -4' max L.I. OBL.RAM. AT 9 kt
Vessel : USCGC POLAR SEA
Sensor : ACC. 2Y
Frequency: 50
File Name: F92Y1
Test Time:FEB 9 1981 (06:20)
Calibration: 1.2739 (g'/v)
Sen.Range: .200(v)

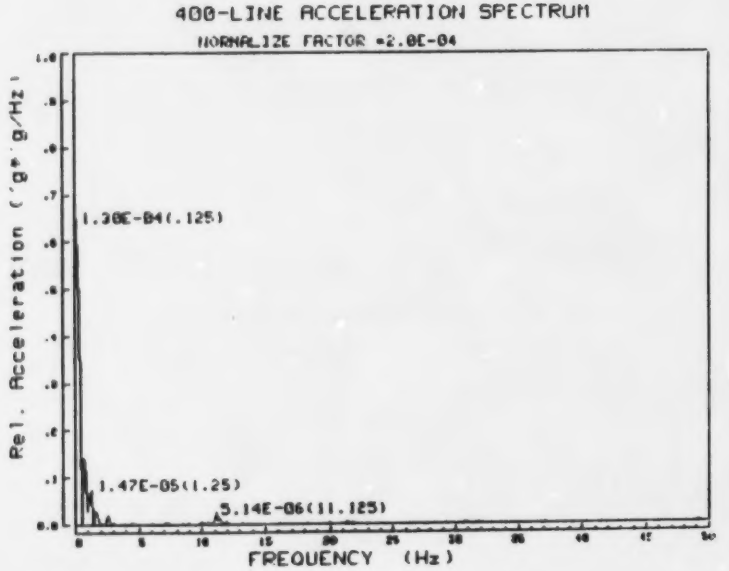

FIGURE E.6

RESPONSE SPECTRA FOR RAMMING TEST F9-1

(g)

ARCTEC CANADA LIMITED

400-LINE SPECTRUM DATA INTERPRETATION PROGRAM

Subject :POLAR SEA -F.S. TEST -4 max L.I. OBL.RAM. AT 9 kt
Vessel : USCGC POLAR SEA
Sensor : ACC. SY
Frequency: 50
File Name: F95Y1
Test Time:FEB 9 1981 (06:20)
Calibration: 1.2270 (g*/v)
Sen.Range: .200(v)

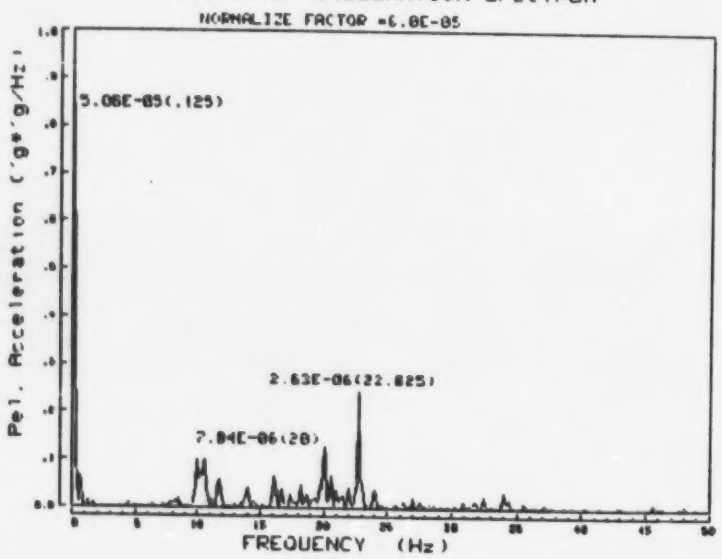

(h)

ARCTEC CANADA LIMITED

400-LINE SPECTRUM DATA INTERPRETATION PROGRAM

Subject :POLAR SEA -F.S. TEST -4' max L.I. OBL.RAM. AT 9 kt
Vessel : USCGC POLAR SEA
Sensor : ACC. 7Y
Frequency: 50
File Name: F97Y1
Test Time:FEB 9 1981 (06:20)
Calibration: 1.2270 (g*/v)
Sen.Range: .500(v)

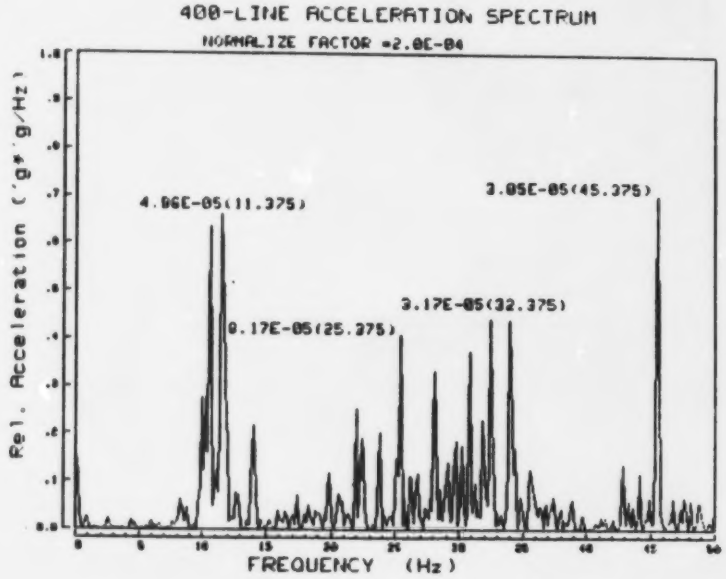

FIGURE E.6

RESPONSE SPECTRA FOR RAMMING TEST F9-1

(i)

ARCTEC CANADA LIMITED

400-LINE SPECTRUM DATA INTERPRETATION PROGRAM

Subject :POLAR SEA -F.S. TEST -4' max L.I. OBL.RAM. AT 9 Kt
Vessel : USCGC POLAR SEA — Test Time:FEB 9 1981 (06:20)
Sensor : ACC. 3Y — Calibration: 1.2195 (g'/v)
Frequency: 50 — Sen.Range: .200(v)
File Name: F93Y1

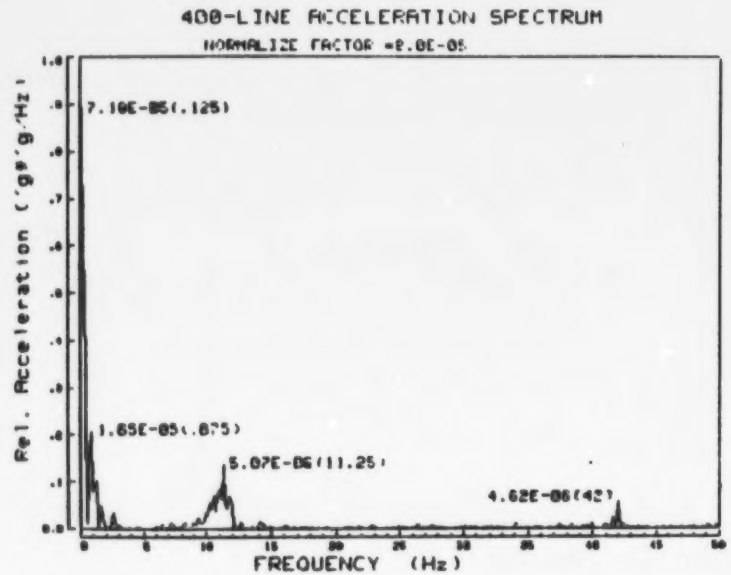

(j)

ARCTEC CANADA LIMITED

400-LINE SPECTRUM DATA INTERPRETATION PROGRAM

Subject :POLAR SEA -F.S. TEST -4' max L.I. OBL.RAM. AT 9 Kt
Vessel : USCGC POLAR SEA — Test Time:FEB 9 1981 (06:20)
Sensor : ACC. 6Y — Calibration: 1.2422 (g'/v)
Frequency: 50 — Sen.Range: .200(v)
File Name: F96Y1

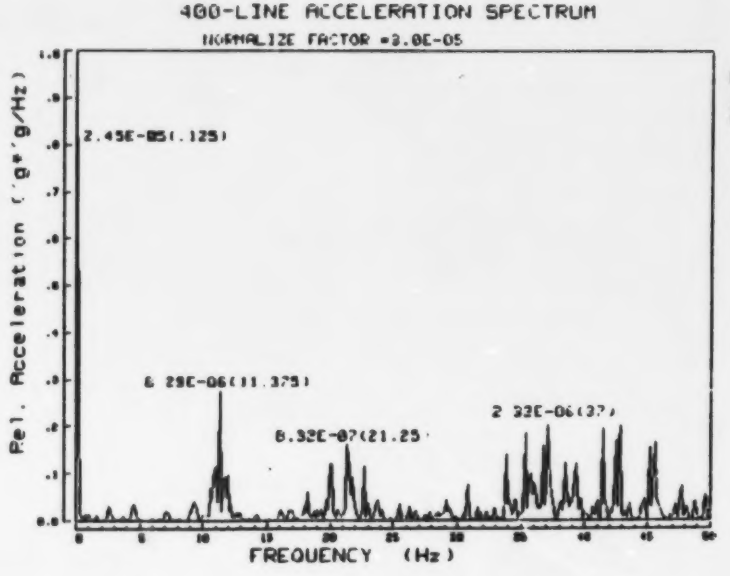

FIGURE E.6
RESPONSE SPECTRA FOR RAMMING TEST F9-1

(k)

ARCTEC CANADA LIMITED

400-LINE SPECTRUM DATA INTERPRETATION PROGRAM

Subject :POLAR SEA -F.S. TEST -4' max L.I. OBL.RAM. AT 9 kt
Vessel : USCGC POLAR SEA
Sensor : ACC. 12
Frequency: 50
File Name: F9121
Test Time:FEB 9 1981 (06:20)
Calibration: 1.2500 (g'/v)
Sen.Range: .200(v)

400-LINE ACCELERATION SPECTRUM

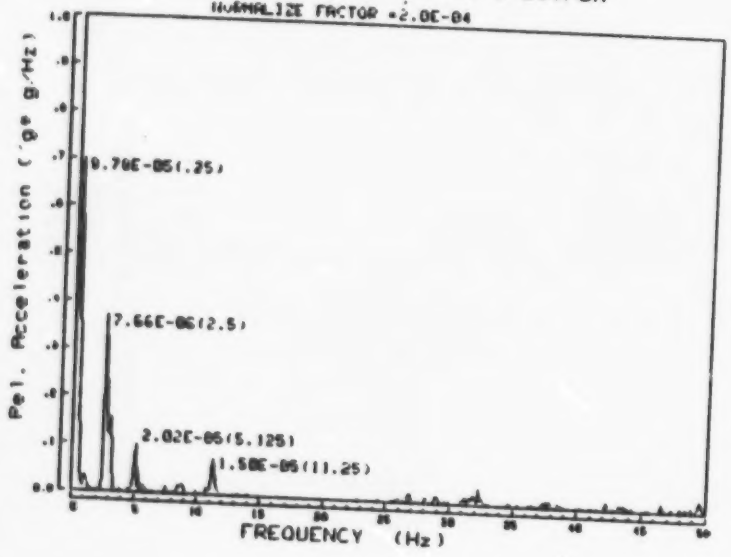

(l)

ARCTEC CANADA LIMITED

400-LINE SPECTRUM DATA INTERPRETATION PROGRAM

Subject :POLAR SEA -F.S. TEST -4' max L.I. OBL.RAM. AT 9 kt
Vessel : USCGC POLAR SEA
Sensor : ACC. 22
Frequency: 50
File Name: F9221
Test Time:FEB 9 1981 (06:20)
Calibration: 1.2500 (g'/v)
Sen.Range: .200(v)

400-LINE ACCELERATION SPECTRUM

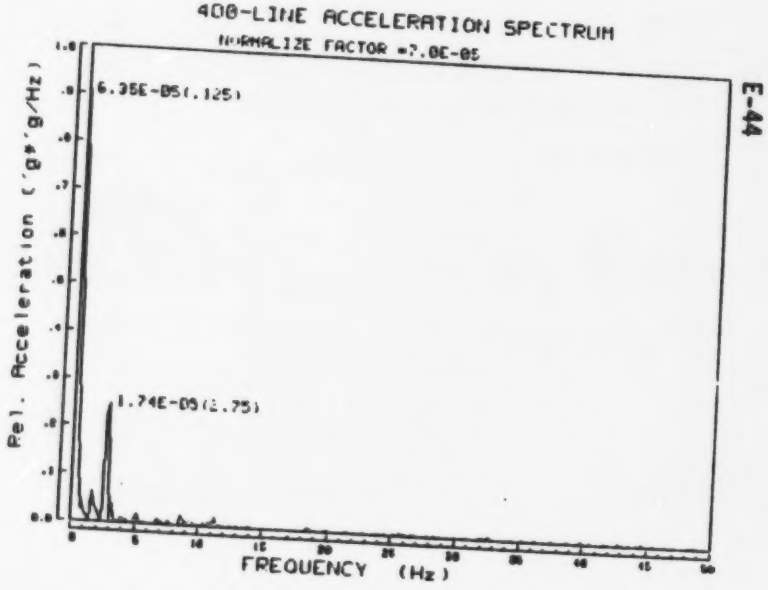

FIGURE E.6

RESPONSE SPECTRA FOR RAMMING TEST F9-1

(m)

ARCTEC CANADA LIMITED

400-LINE SPECTRUM DATA INTERPRETATION PROGRAM

Subject :POLAR SEA -F.S. TEST -4' max L.I. OBL.RAM. AT 9 Kt
Vessel : USCGC POLAR SEA
Sensor : ACC. S2
Frequency: 50
File Name: F9S2I
Test Time:FEB 9 1981 (06:20)
Calibration: 1.2422 (g'/v)
Sen.Range: .200(v)

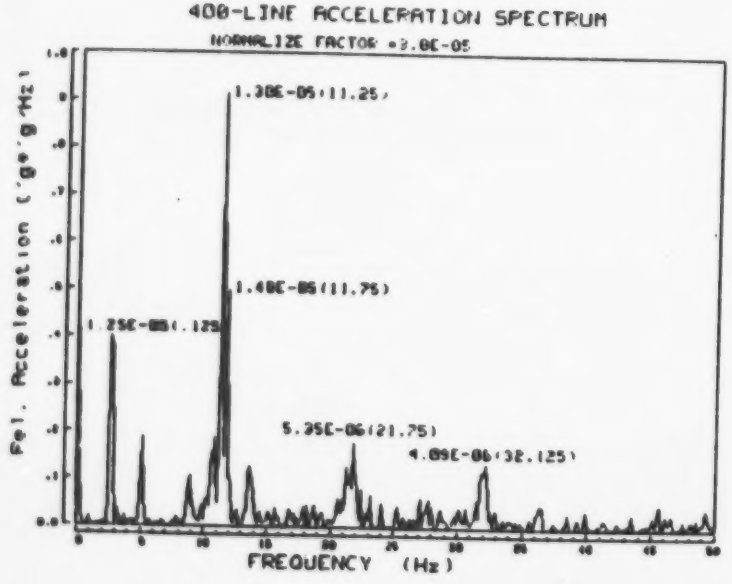

(n)

ARCTEC CANADA LIMITED

400-LINE SPECTRUM DATA INTERPRETATION PROGRAM

Subject :POLAR SEA -F.S. TEST -4' max L.I. OBL.RAM. AT 9 Kt
Vessel : USCGC POLAR SEA
Sensor : ACC. T2
Frequency: 50
File Name: F9T2I
Test Time:FEB 9 1981 (06:20)
Calibration: 1.2345 (g'/v)
Sen.Range: .500(v)

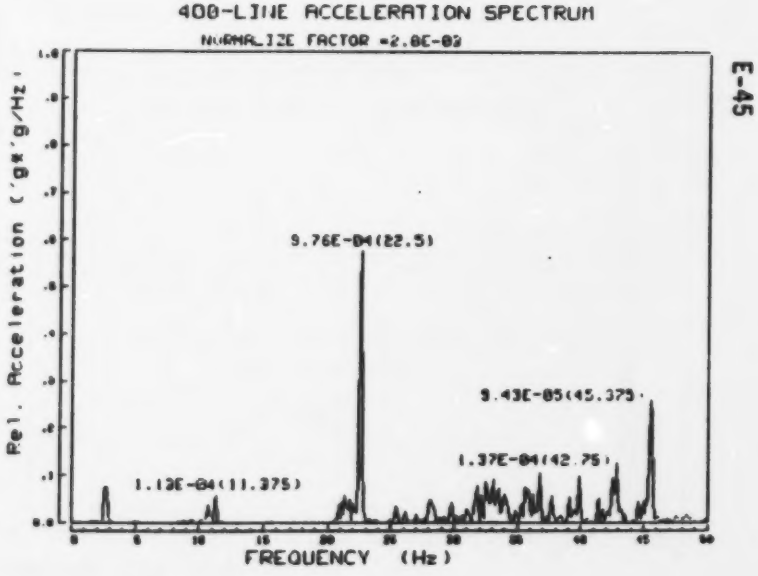

FIGURE E.7
"OPEN-WATER" RESPONSE SPECTRA FOR RAMMING TEST F8-0

(a)

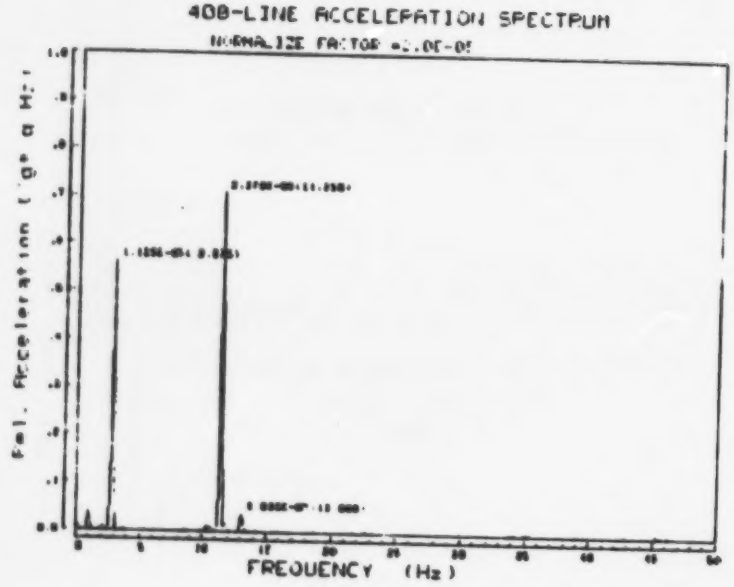

(b)

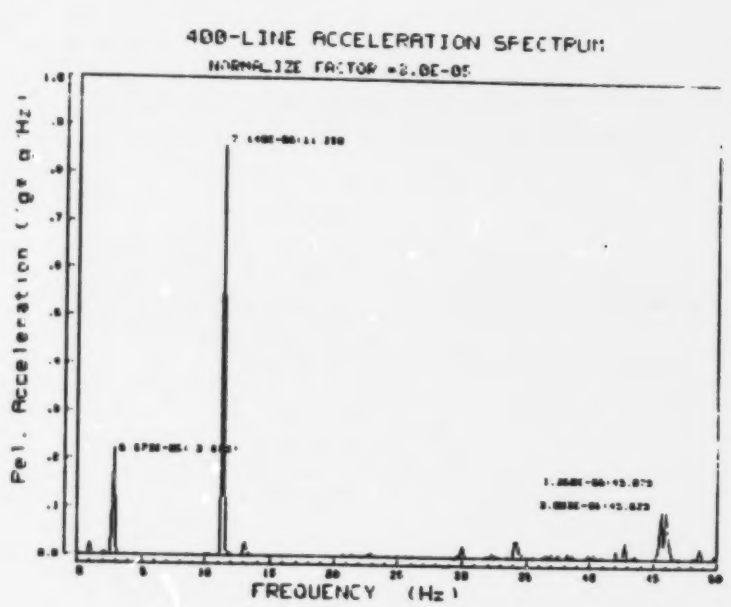

FIGURE E.7

"OPEN-WATER" RESPONSE SPECTRA FOR RAMMING TEST F8-0

(c)

ARCTEC CANADA LIMITED

400-LINE SPECTRUM DATA INTERPRETATION PROGRAM

Subject :USCGC POLAR SEA - F.8 TEST - 3.5' L.I. RAMMING HEAD-ON:BEFORE IMPA
Vessel : USCGC POLAR SEA
Sensor : ACC. 5
Frequency: 50
File Name: F85.0
Test Time:FEB 8 1981 (02:23)
Calibration: 1.1940 (g'/V)
Sen.Range: .100 (V)

400-LINE ACCELERATION SPECTRUM

NORMALIZE FACTOR =5.0E-04

Pol. Acceleration (g² g/Hz)

FREQUENCY (Hz)

(d)

ARCTEC CANADA LIMITED

400-LINE SPECTRUM DATA INTERPRETATION PROGRAM

Subject :USCGC POLAR SEA - F.8 TEST - 3.5' L.I. RAMMING HEAD-ON:BEFORE IMPACT
Vessel : USCGC POLAR SEA
Sensor : ACC. 7
Frequency: 50
File Name: F87.0
Test Time:FEB 8 1981 (02:2
Calibration: 1.1634 (g
Sen.Range: .500

400-LINE ACCELERATION SPECTRUM

NORMALIZE FACTOR =7.0E-04

Pol. Acceleration (g² g/Hz)

FREQUENCY (Hz)

FIGURE E.7
"OPEN-WATER" RESPONSE SPECTRA FOR RAMMING TEST F8-0

(e)

ARCTEC CANADA LIMITED

400-LINE SPECTRUM DATA INTERPRETATION PROGRAM

Subject :USCGC POLAR SEA - F.I TEST - 3.5 K.I. RAMMING HEAD-ON:BEFORE IMPACT
Vessel : USCGC POLAR SEA
Sensor : ACC. Z
Frequency: 50
File Name: F8I+0
Test Time:FEB 6 1981 <02:23>
Calibration: 1.1940 (g'/v)
Sen.Range: .200

400-LINE ACCELERATION SPECTRUM

NORMALIZE FACTOR =2.0E-05

Pol. Acceleration (g**2/Hz)

FREQUENCY (Hz)

(f)

ARCTEC CANADA LIMITED

400-LINE SPECTRUM DATA INTERPRETATION PROGRAM

Subject :USCGC POLAR SEA - F.I TEST - 3.5 K.I. RAMMING HEAD-ON:BEFORE IMPACT
Vessel : USCGC POLAR SEA
Sensor : ACC. Z
Frequency: 50
File Name: F8I+0
Test Time:FEB 6 1981 <02:23>
Calibration: 1.2739 (g'/v)
Sen.Range: .200

400-LINE ACCELERATION SPECTRUM

NORMALIZE FACTOR =2.0E-05

Pol. Acceleration (g**2/Hz)

FREQUENCY (Hz)

FIGURE E.7

"OPEN-WATER" RESPONSE SPECTRA FOR RAMMING TEST F8-0

(g)

ARCTEC CANADA LIMITED

400-LINE SPECTRUM DATA INTERPRETATION PROGRAM

Subject :USCGC POLAR SEA - F.8 TEST - 3.5 K.I. RAMMING HEAD-ON(BEFORE IMPACT
Vessel : USCGC POLAR SEA
Sensor : ACC. SY
Frequency: 50
File Name: F8T0

Test Time:FEB 8 1981 (02:25)
Calibration: 1.2270 (g'sec)
Sen.Range: .100(v)

400-LINE ACCELERATION SPECTRUM

NORMALIZE FACTOR =1.0E-05

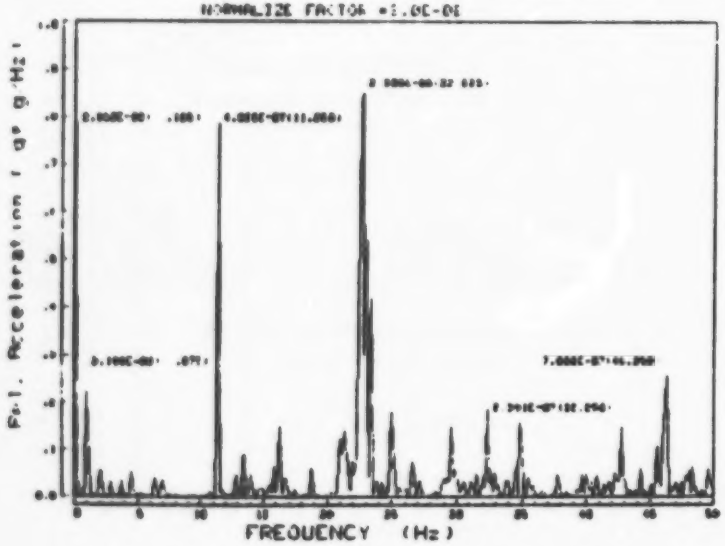

(h)

ARCTEC CANADA LIMITED

400-LINE SPECTRUM DATA INTERPRETATION PROGRAM

Subject :USCGC POLAR SEA - F.8 TEST - 3.5 K.I. RAMMING HEAD-ON(BEFORE IMPACT
Vessel : USCGC POLAR SEA
Sensor : ACC. TY
Frequency: 50
File Name: F8Ty0

Test Time:FEB 8 1981 (02:33)
Calibration: 1.2270 (g'sec)
Sen.Range: .500(v)

400-LINE ACCELERATION SPECTRUM

NORMALIZE FACTOR =1.0E-05

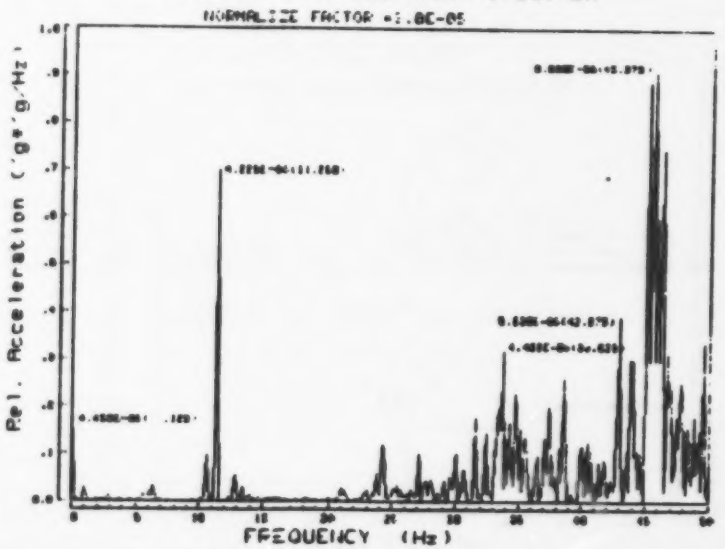

FIGURE E.7

"OPEN-WATER" RESPONSE SPECTRA FOR RAMMING TEST F8-0

(1)

400-LINE SPECTRUM DATA INTERPRETATION PROGRAM

Subject :USCGC POLAR SEA - F.I TEST - 3.0 K.I. RAMMING HEAD-ON(BEFORE IMPACT
Vessel : USCGC POLAR SEA
Sensor : BOW HEAVE
Frequency: 50
File Name: F8120
Test Time:FEB 6 1981 (02:23)
Calibration: 1.2500 (g/v)
Sen.Range: .200(v)

400-LINE ACCELERATION SPECTRUM

NORMALIZE FACTOR =6.0E-04

Rel. Acceleration ('gn'g/Hz)

FREQUENCY (Hz)

(J)

400-LINE SPECTRUM DATA INTERPRETATION PROGRAM

Subject :USCGC POLAR SEA - F.I TEST - 3.0 K.I. RAMMING HEAD-ON(BEFORE IMPACT
Vessel : USCGC POLAR SEA
Sensor : ACC. 22
Frequency: 50
File Name: F8220
Test Time:FEB 6 1981 (02:23)
Calibration: 1.2500 (g/v)
Sen.Range: .200(v)

400-LINE ACCELERATION SPECTRUM

NORMALIZE FACTOR =6.0E-05

Rel. Acceleration ('gn'g/Hz)

FREQUENCY (Hz)

FIGURE E.7

"OPEN-WATER" RESPONSE SPECTRA FOR RAMMING TEST F8-0

(k)

ARCTEC [illegible]

400-LINE SPECTRUM DATA INTERPRETATION PROGRAM

Subject :USCGC POLAR SEA - F.6 TEST - 3.5 L.I. RAMMING HEAD-ON:BEFORE IMPACT
Vessel : USCGC POLAR SEA
Sensor : ACC. 52
Frequency: 50
File Name: F67z0
Test Time:FEB 6 1981 (02:25)
Calibration: 1.2422 (g'/v)
Sen.Range: .200(v)

400-LINE ACCELERATION SPECTRUM

NORMALIZE FACTOR =4.0E-05

Pel. Acceleration ('g**2/g Hz')

FREQUENCY (Hz)

(l)

ARCTEC CANADA LIMITED

400-LINE SPECTRUM DATA INTERPRETATION PROGRAM

Subject :USCGC POLAR SEA - F.[illegible] TEST - 3.5' L.I. RAMMING HEAD-ON:BEFORE IMPACT
Vessel : USCGC POLAR SEA
Sensor : ACC. 72
Frequency: 50
File Name: F67z0
Test Time:FEB 0 1981 (02:[illegible])
Calibration: 1.2345 g [illegible]
Sen.Range: .500[illegible]

400-LINE ACCELERATION SPECTRUM

NORMALIZE FACTOR =9.8E-04

Pel. Acceleration ('g**2/g/Hz')

FREQUENCY (Hz)

FIGURE E.8

"OPEN-WATER" RESPONSE SPECTRA FOR RAMMING TEST F9-1

(a)

ARCTEC Canada LIMITED

400-LINE SPECTRUM DATA INTERPRETATION PROGRAM

Subject :POLAR SEA -F.S. TEST -4' aa> L.I. OBL.RAM. AT 9 Kt<BEFORE IMPACT>
Vessel : USCGC POLAR SEA
Sensor : ACC. 2...
Frequency: 50
File Name: F9L 1
Test Time:FEB 9 1981 (06:20)
Calibration: 1.1765 (g'/v)
Sen.Range: .200(v)

400-LINE ACCELERATION SPECTRUM

NORMALIZE FACTOR =7.8E-05

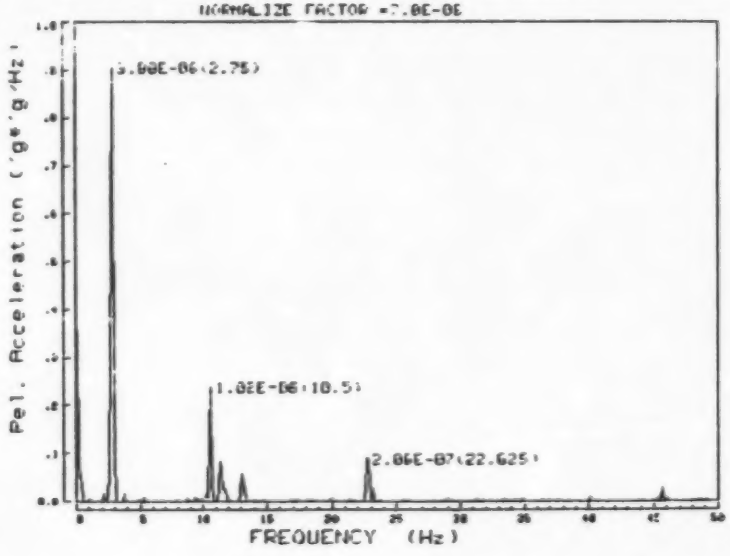

(b)

ARCTEC Canada LIMITED

400-LINE SPECTRUM DATA INTERPRETATION PROGRAM

Subject :POLAR SEA -F.S. TEST -4 aa L.I. OBL.RAM. AT 9 Kt<BEFORE IMPACT>
Vessel : USCGC POLAR SEA
Sensor : ACC. 3X
Frequency: 50
File Name: F9L1
Test Time:FEB 9 1981 (06:20)
Calibration: 1.2500 (g'/v)
Sen.Range: .200(v)

400-LINE ACCELERATION SPECTRUM

NORMALIZE FACTOR =5.8E-05

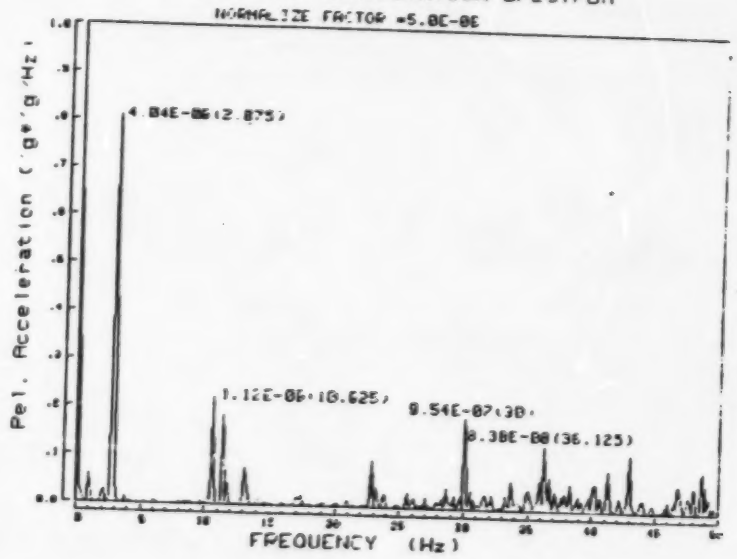

FIGURE E.8

"OPEN-WATER" RESPONSE SPECTRA FOR RAMMING TEST F9-1

(c)

ARCTEC CANADA LIMITED

400-LINE SPECTRUM DATA INTERPRETATION PROGRAM

Subject :POLAR SEA -F.S. TEST -4 ** L.I. OBL.RAM. AT 9 kt (BEFORE IMPACT)
Vessel : USCGC POLAR SEA
Sensor : ACC. 6X
Frequency: 50
File Name: F95.1
Test Time:FEB 9 1981 (06:20)
Calibration: 1.1940 (g'/v)
Sen.Range: .200(v)

400-LINE ACCELERATION SPECTRUM

NORMALIZE FACTOR =4.0E-06

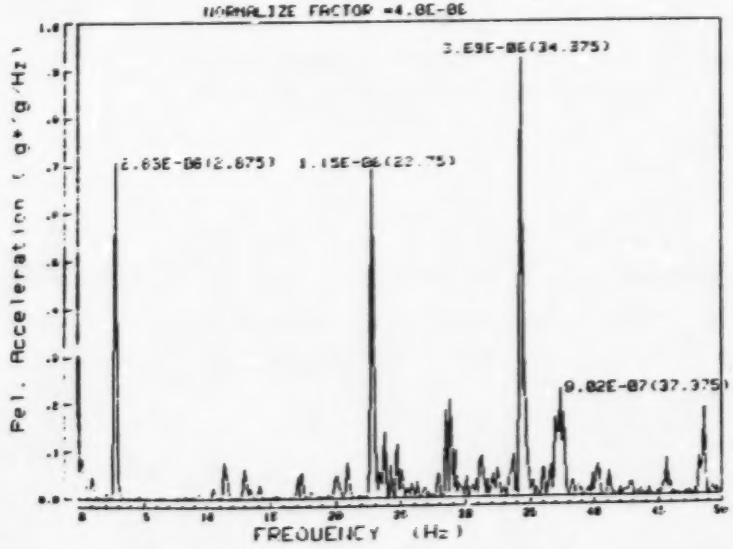

(d)

ARCTEC CANADA LIMITED

400-LINE SPECTRUM DATA INTERPRETATION PROGRAM

Subject :POLAR SEA -F.S. TEST -4 ** L.I. OBL.RAM. AT 9 kt (BEFORE IMPACT)
Vessel : USCGC POLAR SEA
Sensor : ACC. 7X
Frequency: 50
File Name: F97.1
Test Time:FEB 9 1981 (06:20)
Calibration: 1.1634 (g'/v)
Sen.Range: .500(v)

400-LINE ACCELERATION SPECTRUM

NORMALIZE FACTOR =2.0E-04

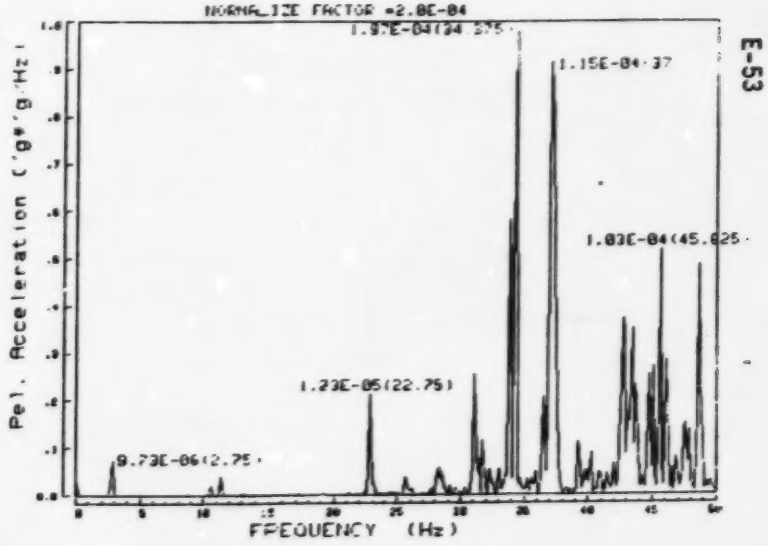

FIGURE E.8

"OPEN-WATER" RESPONSE SPECTRA FOR RAMMING TEST F9-1

(e)

ARCTEC CANADA LIMITED

400-LINE SPECTRUM DATA INTERPRETATION PROGRAM

Subject :POLAR SEA -F.S. TEST -4' max L.I. OBL.RAM, AT 9 kt(BEFORE IMPACT)
Vessel : USCGC POLAR SEA
Sensor : ACC. 1V
Frequency: 50
File Name: F91-1
Test Time:FEB 9 1981 (06:20)
Calibration: 1.1940 (g/v)
Sen.Range: .200(v)

400-LINE ACCELERATION SPECTRUM

NORMALIZE FACTOR =2.0E-05

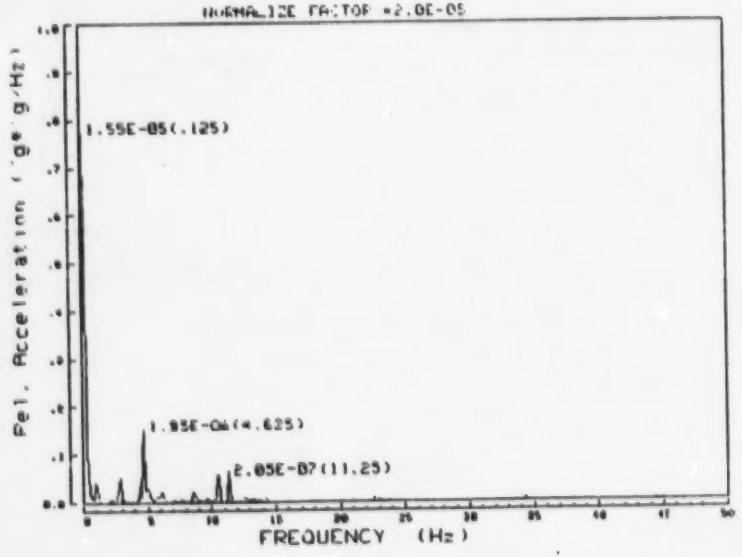

(f)

ARCTEC CANADA LIMITED

400-LINE SPECTRUM DATA INTERPRETATION PROGRAM

Subject :POLAR SEA -F.S. TEST -4' max L.I. OBL.RAM, AT 9 kt(BEFORE IMPACT)
Vessel : USCGC POLAR SEA
Sensor : ACC. 2Y
Frequency: 50
File Name: F92-1
Test Time:FEB 9 1981 (06:20)
Calibration: 1.2739 (g/v)
Sen.Range: .200(v)

400-LINE ACCELERATION SPECTRUM

NORMALIZE FACTOR =6.0E-06

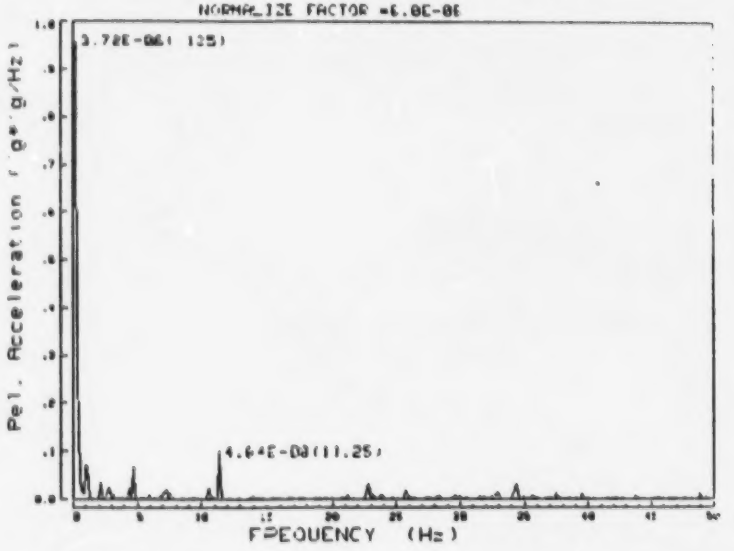

FIGURE E.8

"OPEN-WATER" RESPONSE SPECTRA FOR RAMMING TEST F9-1

(g)

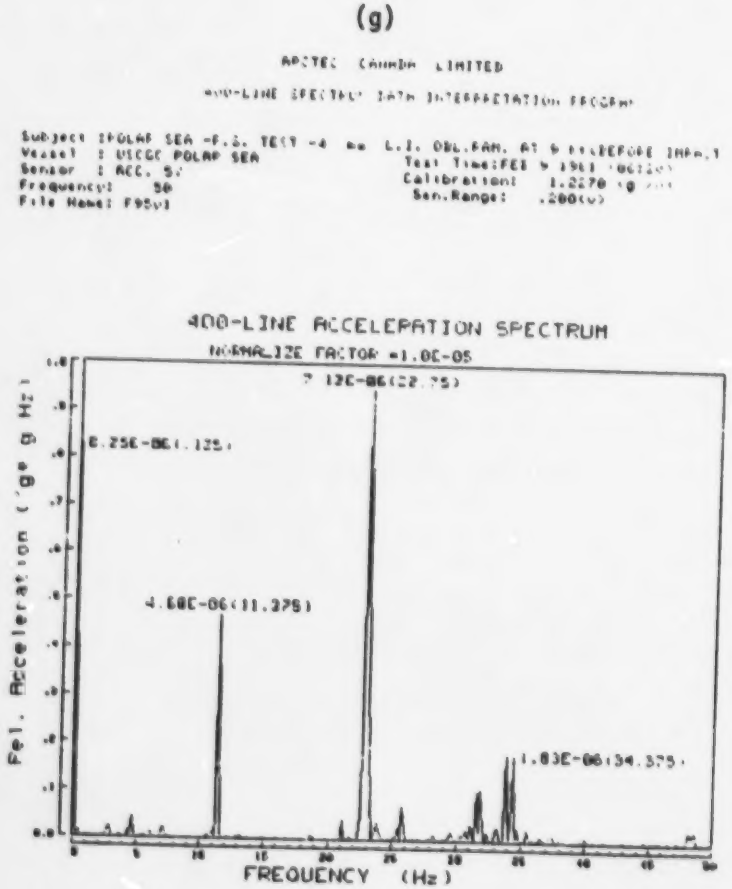

(h)

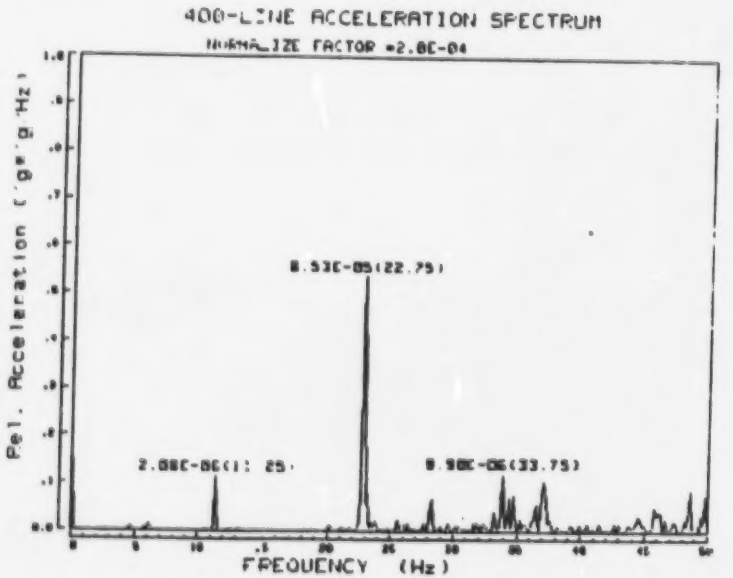

FIGURE E.8
"OPEN-WATER" RESPONSE SPECTRA FOR RAMMING TEST F9-1

(i)

ARCTEC CANADA LIMITED

400-LINE SPECTRUM DATA INTERPRETATION PROGRAM

Subject :POLAR SEA -F.S. TEST -4 ram L.I. OBL.RAM. AT 9 kt(BEFORE IMPACT)
Vessel : USCGC POLAR SEA
Sensor : ACC. 12
Frequency: 50
File Name: F9121
Test Time:FEB 9 1981 (06:20)
Calibration: 1.2500 (g /V)
Sen.Range: .200(V)

400-LINE ACCELERATION SPECTRUM

NORMALIZE FACTOR =4.0E-04

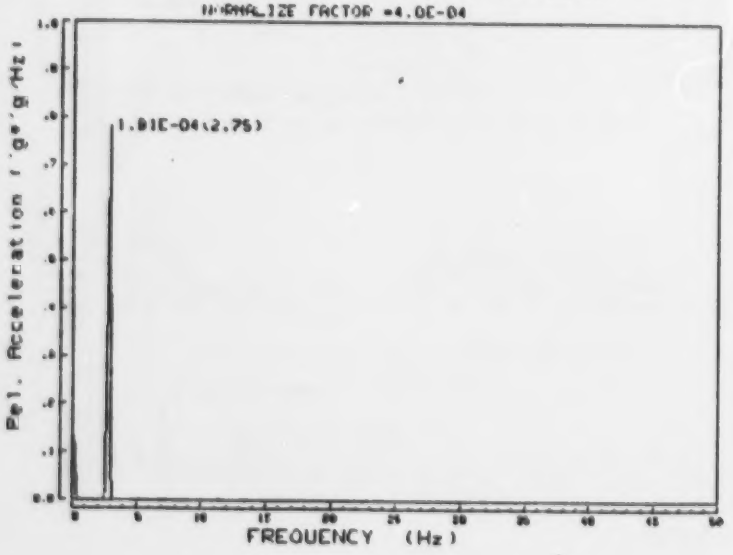

(j)

ARCTEC CANADA LIMITED

400-LINE SPECTRUM DATA INTERPRETATION PROGRAM

Subject :POLAR SEA -F.S. TEST -4 ram L.I. OBL.RAM. AT 9 kt(BEFORE IMPACT)
Vessel : USCGC POLAR SEA
Sensor : ACC. 22
Frequency: 50
File Name: F9221
Test Time:FEB 9 1981 (06:20)
Calibration: 1.1500 (g /V)
Sen.Range: .200(V)

400-LINE ACCELERATION SPECTRUM

NORMALIZE FACTOR =4.0E-05

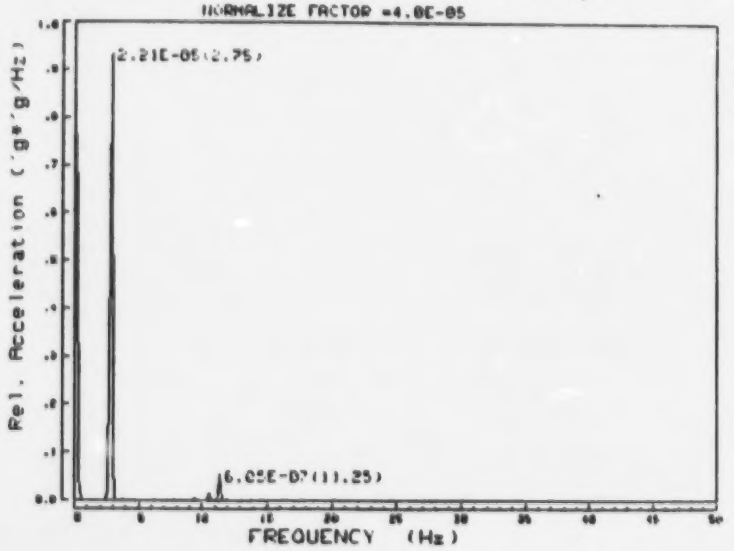

FIGURE E.8

"OPEN-WATER" RESPONSE SPECTRA FOR RAMMING TEST F9-1

(k)

APCTEL (Canada) LIMITED

400-LINE SPECTRUM DATA INTERPRETATION PROGRAM

Subject :POLAR SEA -F.S. TEST -4 aa L.I. OBL.RAM. AT 9 kt(BEFORE IMPACT)
Vessel : USCGC POLAR SEA Test Time:FEB 9 1981 (0C:20)
Sensor : ACC. 52 Calibration: 1.2422 (g'/v)
Frequency: 50 Sen.Range: .200(v)
File Name: F9121

400-LINE ACCELERATION SPECTPUM

NORMALIZE FACTOR =2.0E-05

1.35E-05(2.75)

5.23E-06(22.75)

2.91E-06(25.75)

Rel. Acceleration (g*g/Hz)

FREQUENCY (Hz)

(l)

APCTEL (Canada) LIMITED

400-LINE SPECTRUM DATA INTERPRETATION PROGRAM

Subject :POLAR SEA -F.S. TEST -4 aa: L.I. OBL.RAM. AT 9 kt(BEFORE IMPACT)
Vessel : USCGC POLAR SEA Test Time:FEB 9 1981 (0C:20)
Sensor : ACC. 72 Calibration: 1.2345 (g/v)
Frequency: 50 Sen.Range: .500(v)
File Name: F9121

400-LINE ACCELERATION SPECTPUM

NORMALIZE FACTOR =7.0E-04

6.59E-04(34.375)

2.83E-04(2.875)

2.03E-04(37.375)

1.28E-05(22.75)

Rel. Acceleration (g*g/Hz)

FREQUENCY (Hz)

FIGURE E.9

COMPUTED FORCE SPECTRA FOR RAMMING TEST FB-0

(a)

ARCTEC CANADA LIMITED

FORCE SPECTRUM CALCULATION PROGRAM

Subject :USCGC POLAR SEA - F.S TEST - 3.8' L.I. RAMMING
Vessel : USCGC POLAR SEA — Test Time:FEB 8 1991 (02:23)
Sensor : ACC 1V — Cal.Factor: 1.194('g/v)
FreqRange: 50 (Hz) — Force Unit: L.ton=L.ton/Hz
Vib. Mode: Horizontal Bending — File Name: FB1V0
• Location of applied conc. load is at section 0 10.5
• Location of accelerometer is at section 20
• Cut-off frequency for force calculation is 15 (Hz)

Mean Square= 1.207214E+03(L.ton=L.ton)
Root Mean Square= 3.474099E+01(L.ton)

COMPUTED FORCE SPECTRUM

HARMONIC FACTOR =2.000E+02

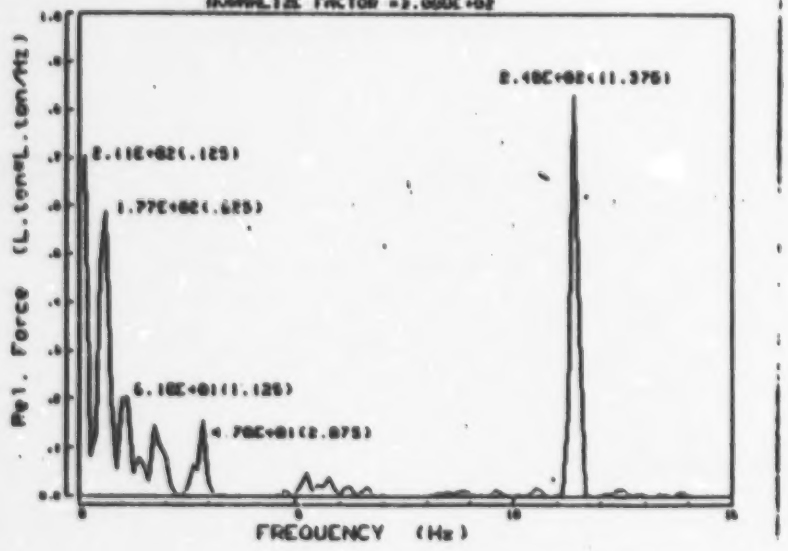

(b)

ARCTEC CANADA LIMITED

FORCE SPECTRUM CALCULATION PROGRAM

Subject :USCGC POLAR SEA - F.S TEST - 3.8' L.I. RAMMING
Vessel : USCGC POLAR SEA — Test Time:FEB 8 1991 (02:23)
Sensor : ACC. 2V — Cal.Factor: 1.194('g/v)
FreqRange: 50 (Hz) — Force Unit: L.ton=L.ton/Hz
Vib. Mode: Horizontal Bending — File Name: FB2V0
• Location of applied conc. load is at section 0 10.5
• Location of accelerometer is at section 16.4
• Cut-off frequency for force calculation is 15 (Hz)

Mean Square= 1.094194E+03(L.ton=L.ton)
Root Mean Square= 3.307868E+01(L.ton)

COMPUTED FORCE SPECTRUM

HARMONIC FACTOR =2.000E+02

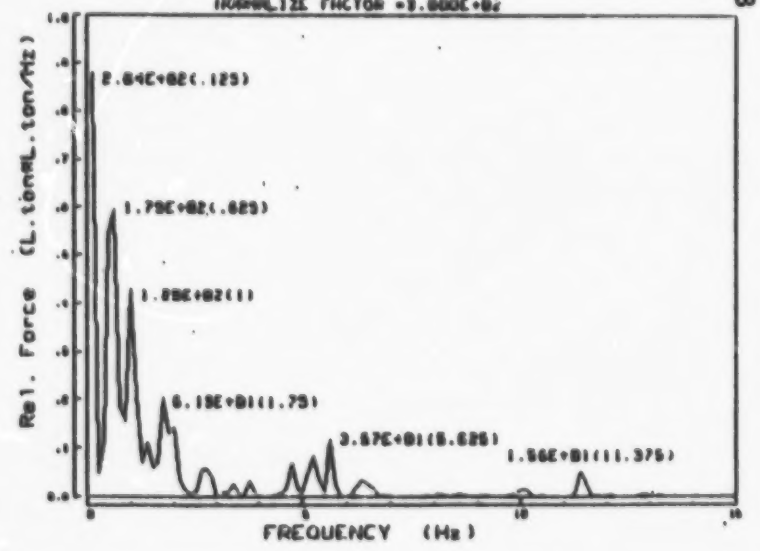

FIGURE E.9

COMPUTED FORCE SPECTRA FOR RAMMING TEST F8-0

(c)

ARCTEC CANADA LIMITED

FORCE SPECTRUM CALCULATION PROGRAM

Subject :USCGC POLAR SEA - F.8 TEST - 3.5' L.I. RAMMING
Vessel : USCGC POLAR SEA
Sensor : ACC. SY
FreqRange: 50 (Hz)
Vib. Mode: Horizontal Bending
Test Time:FEB 8 1981 (02:23)
Cal.Factor:1.2278('g/v)
Force Unit: L.tonsL.ton/Hz
File Name: F8SY0
* Location of applied conc. load is at section 0 10.5
* Location of accelerometer is at section 7.6
* Cut-off frequency for force calculation is 15 (Hz)

Mean Square= 7.938996E+02(L.tonsL.ton)
Root Mean Square= 2.817622E+01(L.ton)

COMPUTED FORCE SPECTRUM

NORMALIZE FACTOR =0.000E+00

7.83E+02(.125)

8.03E+01(2.625)

8.38E+01(11.375)

Rel. Force (L.tonsL.ton/Hz)

FREQUENCY (Hz)

(d)

ARCTEC CANADA LIMITED

FORCE SPECTRUM CALCULATION PROGRAM

Subject :USCGC POLAR SEA - F.8 TEST - 3.5' L.I. RAMMING
Vessel : USCGC POLAR SEA
Sensor : ACC. SY
FreqRange: 50 (Hz)
Vib. Mode: Horizontal Bending
Test Time:FEB 8 1981 (02:23)
Cal.Factor:1.2278('g/v)
Force Unit: L.tonsL.ton/Hz
File Name: F8SY0
* Location of applied conc. load is at section 0 10.5
* Location of accelerometer is at section 7
* Cut-off frequency for force calculation is 15 (Hz)

Mean Square= 1.480140E+03(L.tonsL.ton)
Root Mean Square= 3.782520E+01(L.ton)

COMPUTED FORCE SPECTRUM

NORMALIZE FACTOR =7.000E+00

6.86E+02(.125)

1.87E+02(1)

4.12E+01(11.375)

3.58E+01(10.5)

Rel. Force (L.tonsL.ton/Hz)

FREQUENCY (Hz)

FIGURE E.9

COMPUTED FORCE SPECTRA FOR RAMMING TEST F8-0

(e)

ARCTEC CANADA LIMITED

FORCE SPECTRUM CALCULATION PROGRAM

Subject :USCGC POLAR SEA - F.S TEST - 3.5' L.I. RAMMING
Vessel : USCGC POLAR SEA — Test Time:FEB 8 1981 (02:23)
Sensor : ACC 12 — Cal.Factor: 1.250('g/v)
FreqRange: 50 (Hz) — Force Unit: L.tonsL.ton/Hz
Vib. Mode: Vertical Bending — File Name: F8120
* Location of applied conc. load is at section 0 18.5
* Location of accelerometer is at section 20
* Cut-off frequency for force calculation is 15 (Hz)

Mean Square= 5.278088E+03(L.tonsL.ton)
Root Mean Square= 4.773603E+01(L.ton)

COMPUTED FORCE SPECTRUM

NORMALIZE FACTOR =0.000E+02

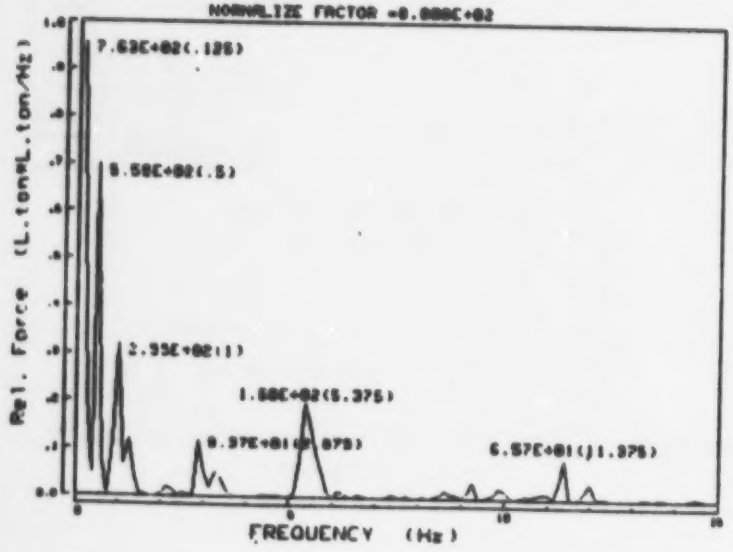

(f)

ARCTEC CANADA LIMITED

FORCE SPECTRUM CALCULATION PROGRAM

Subject :USCGC POLAR SEA - F.S TEST - 3.5' L.I. RAMMING
Vessel : USCGC POLAR SEA — Test Time:FEB 8 1981 (02:23)
Sensor : ACC. 22 — Cal.Factor: 1.250('g/v)
FreqRange: 50 (Hz) — Force Unit: L.tonsL.ton/Hz
Vib. Mode: Vertical Bending — File Name: F8220
* Location of applied conc. load is at section 0 18.5
* Location of accelerometer is at section 16.4
* Cut-off frequency for force calculation is 15 (Hz)

Mean Square= 3.110502E+03(L.tonsL.ton)
Root Mean Square= 5.577187E+01(L.ton)

COMPUTED FORCE SPECTRUM

NORMALIZE FACTOR =0.000E+02

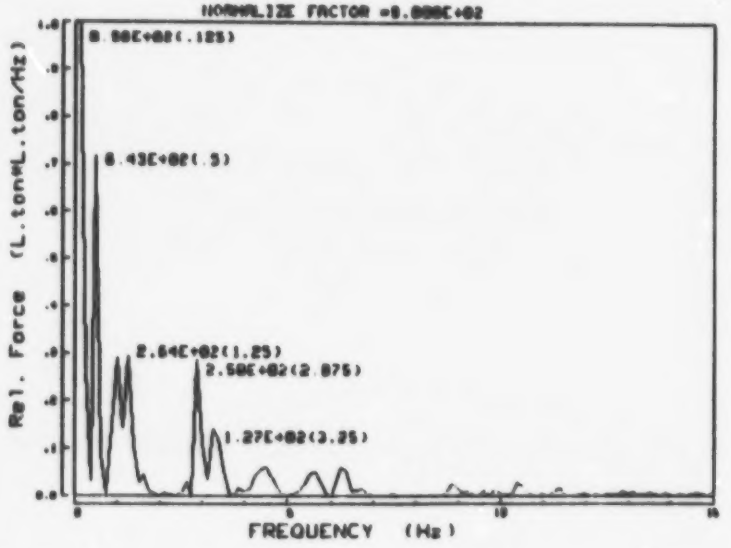

FIGURE E.9

COMPUTED FORCE SPECTRA FOR RAMMING TEST F8-0

(g)

ARCTEC CANADA LIMITED

FORCE SPECTRUM CALCULATION PROGRAM

Subject :USCGC POLAR SEA - F.S TEST - 3.5' L.I. RAMMING
Vessel : USCGC POLAR SEA — Test Time:FEB 8 1981 (02:23)
Sensor : ACC. 32 — Cal.Factor: 1.242('g/v)
FreqRange: 50 (Hz) — Force Unit: L.tons(L.ton/Hz)
Vib. Mode: Vertical Bending — File Name: F8S20
* Location of applied conc. load is at section 0 18.5
* Location of accelerometer is at section 7.6
* Cut-off frequency for force calculation is 15 (Hz)

Mean Square= 5.453298E+03(L.tons(L.ton)
Root Mean Square= 6.953878E+01(L.ton)

COMPUTED FORCE SPECTRUM

NORMALIZE FACTOR =5.000E+02

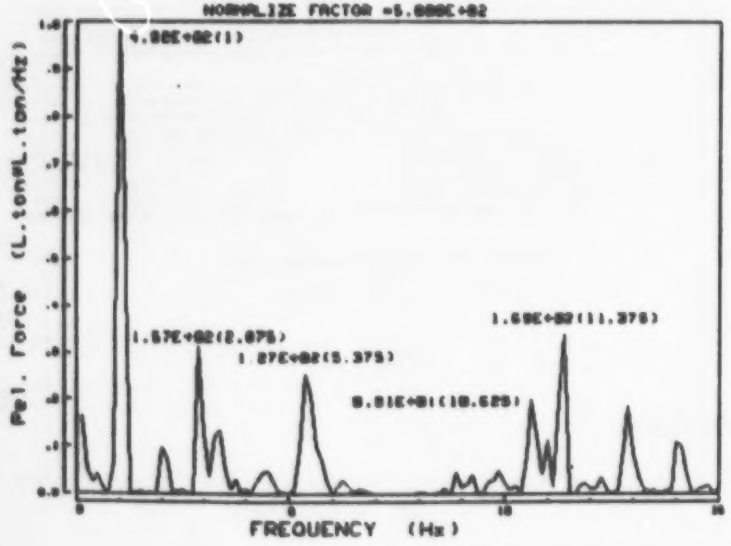

(h)

ARCTEC CANADA LIMITED

FORCE SPECTRUM CALCULATION PROGRAM

Subject :USCGC POLAR SEA - F.S TEST - 3.5' L.I. RAMMING
Vessel : USCGC POLAR SEA — Test Time:FEB 8 1981 (02:23)
Sensor : ACC. 72 — Cal.Factor: 1.238('g/v)
FreqRange: 50 (Hz) — Force Unit: L.tons(L.ton/Hz
Vib. Mode: Vertical Bending — File Name: F8P20
* Location of applied conc. load is at section 0 18.5
* Location of accelerometer is at section 2
* Cut-off frequency for force calculation is 15 (Hz)

Mean Square= 1.786803E+03(L.tons(L.ton)
Root Mean Square= 4.131457E+01(L.ton)

COMPUTED FORCE SPECTRUM

NORMALIZE FACTOR =4.000E+02

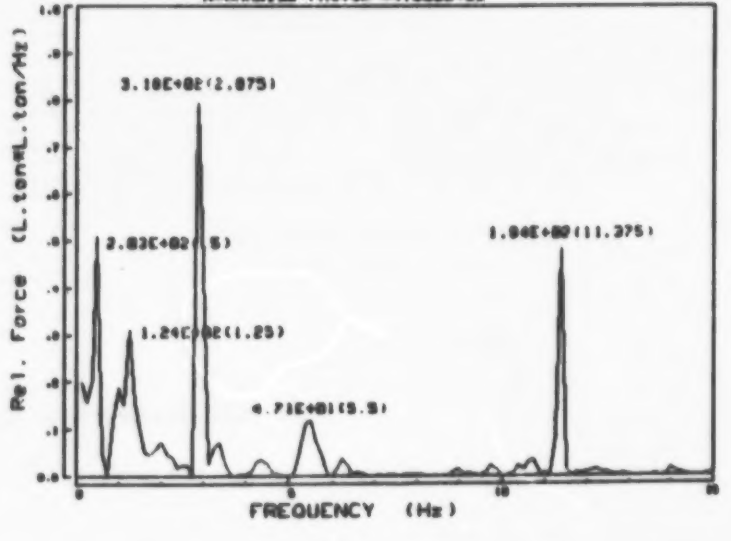

FIGURE E.10

COMPUTED FORCE SPECTRA FOR RAMMING TEST F9-1

(a)

ARCTEC CANADA LIMITED

FORCE SPECTRUM CALCULATION PROGRAM

Subject :POLAR SEA -P.S. TEST -4' aaa L.I. OBL.RAM. AT 9 Kt
Vessel : USCGC POLAR SEA — Test Time:FEB 9 1981 (06:20)
Sensor : ACC. 1V — Cal.Factor:1.1940('g/v)
FreqRange: 50 (Hz) — Force Unit: L.ton&L.ton/Hz
Vib. Mode: Horizontal Bending — File Name: F91V1
* Location of applied conc. load is at section 0 18.5
* Location of accelerometer is at section 20
* Cut-off frequency for force calculation is 15 (Hz)

Mean Square= 1.827718E+04(L.ton&L.ton)
Root Mean Square= 1.013761E+03(L.ton)

COMPUTED FORCE SPECTRUM

NORMALIZE FACTOR =4.000E+03

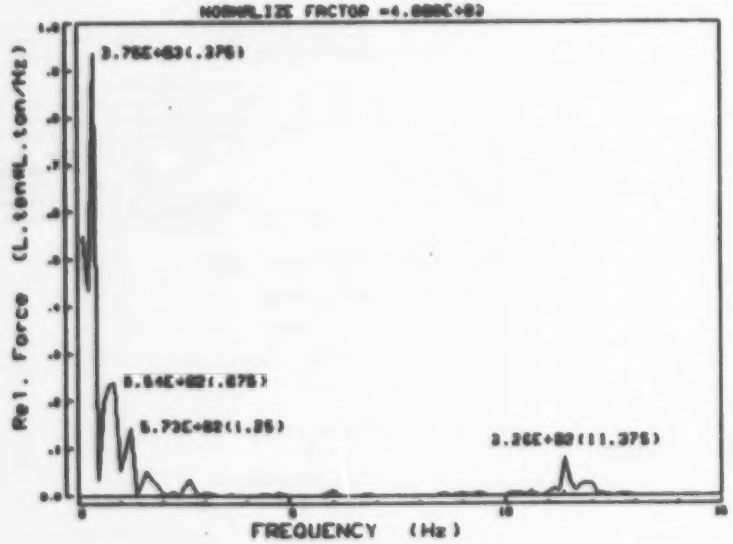

(b)

ARCTEC CANADA LIMITED

FORCE SPECTRUM CALCULATION PROGRAM

Subject :POLAR SEA -P.S. TEST -4' aaa L.I. OBL.RAM. AT 9 Kt
Vessel : USCGC POLAR SEA — Test Time:FEB 9 1981 (06:20)
Sensor : ACC. 2V — Cal.Factor:1.2939('g/v)
FreqRange: 50 (Hz) — Force Unit: L.ton&L.ton/Hz
Vib. Mode: Horizontal Bending — File Name: F92V1
* Location of applied conc. load is at section 0 18.5
* Location of accelerometer is at section 16.4
* Cut-off frequency for force calculation is 15 (Hz)

Mean Square= 1.639188E+04(L.ton&L.ton)
Root Mean Square= 1.280277E+03(L.ton)

COMPUTED FORCE SPECTRUM

NORMALIZE FACTOR =4.000E+03

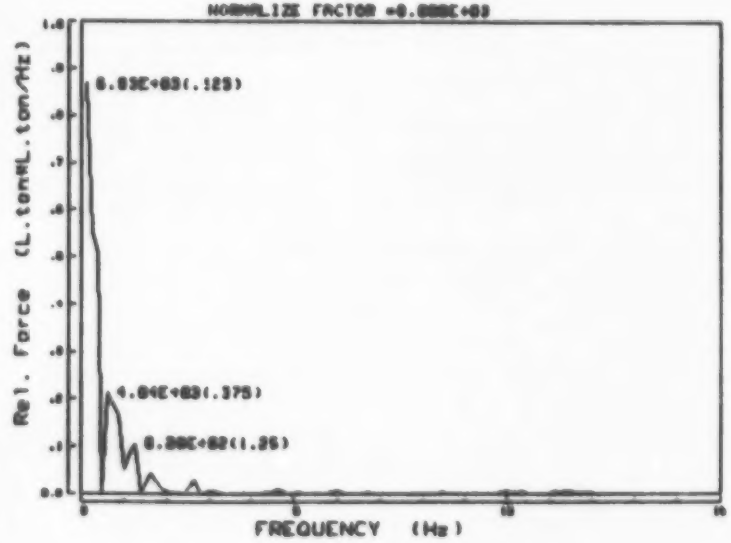

FIGURE E.10

COMPUTED FORCE SPECTRA FOR RAMMING TEST F9-1

(c)

ARCTEC CANADA LIMITED

FORCE SPECTRUM CALCULATION PROGRAM

Subject :POLAR SEA -F.S. TEST -4' aan L.I. BBL.RAM. AT 9 Kt
Vessel : USCGC POLAR SEA — Test Time:FEB 9 1981 (06:20
Sensor : ACC. PY — Cal.Factor:1.2270('g/v)
FreqRange: 50 (Hz) — Force Unit: L.tonsL.ton/Hz
Vib. Mode: Horizontal Bending — File Name: F9PY1
• Location of applied conc. load is at section 0 18.5
• Location of accelerometer is at section 7.6
• Cut-off frequency for force calculation is 15 (Hz)

Mean Square= 1.2838386E+04(L.tonsL.ton)
Root Mean Square= 1.0968386E+02(L.ton)

COMPUTED FORCE SPECTRUM

NORMALIZE FACTOR =1.488E+04

1.27E+04(.126)

Rel. Force (L.tonsL.ton/Hz)

FREQUENCY (Hz)

(d)

ARCTEC CANADA LIMITED

FORCE SPECTRUM CALCULATION PROGRAM

Subject :POLAR SEA -F.S. TEST -4' aan L.I. BBL.RAM. AT 9 Kt
Vessel : USCGC POLAR SEA — Test Time:FEB 9 1981 (06:20)
Sensor : ACC. PY — Cal.Factor:1.2270('g/v)
FreqRange: 50 (Hz) — Force Unit: L.tonsL.ton/Hz
Vib. Mode: Horizontal Bending — File Name: F9PY1
• Location of applied conc. load is at section 0 18.5
• Location of accelerometer is at section 2
• Cut-off frequency for force calculation is 15 (Hz)

Mean Square= 1.8769096E+04(L.tonsL.ton)
Root Mean Square= 1.2987826E+02(L.ton)

COMPUTED FORCE SPECTRUM

NORMALIZE FACTOR =4.888E+03

3.68E+03(.125)

1.01E+03(11.5)

1.18E+03(10.625)

Rel. Force (L.tonsL.ton/Hz)

FREQUENCY (Hz)

FIGURE E.10

COMPUTED FORCE SPECTRA FOR RAMMING TEST F9-1

(e)

ARCTEC CANADA LIMITED

FORCE SPECTRUM CALCULATION PROGRAM

Subject :POLAR SEA -F.S. TEST -4' aer L.I. OBL.RAM. AT 9 Kt
Vessel : USCGC POLAR SEA — Test Time:FEB 9 1981 (06:20)
Sensor : ACC. 12 — Cal.Factor:1.2000('g/v)
FreqRange: 50 (Hz) — Force Unit: L.ton<L.ton/Hz
Vib. Mode: Vertical Bending — File Name: F9121
• Location of applied conc. load is at section @ 10.5
• Location of accelerometer is at section 20
• Cut-off frequency for force calculation is 15 (Hz)

Mean Square= 9.827900E+03(L.ton<L.ton)
Root Mean Square= 9.901526E+01(L.ton)

COMPUTED FORCE SPECTRUM

NORMALIZE FACTOR =6.000E+03

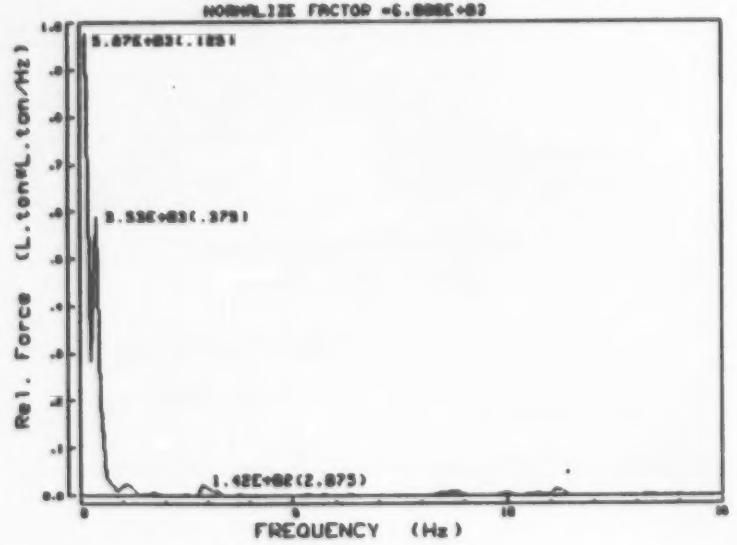

(f)

ARCTEC CANADA LIMITED

FORCE SPECTRUM CALCULATION PROGRAM

Subject :POLAR SEA -F.S. TEST -4' aer L.I. OBL.RAM. AT 9 Kt
Vessel : USCGC POLAR SEA — Test Time:FEB 9 1981 (06:20)
Sensor : ACC. 22 — Cal.Factor:1.2000('g/v)
FreqRange: 50 (Hz) — Force Unit: L.ton<L.ton/Hz
Vib. Mode: Vertical Bending — File Name: F9221
• Location of applied conc. load is at section @ 10.5
• Location of accelerometer is at section 16.4
• Cut-off frequency for force calculation is 15 (Hz)

Mean Square= 4.289250E+03(L.ton<L.ton)
Root Mean Square= 6.487073E+01(L.ton)

COMPUTED FORCE SPECTRUM

NORMALIZE FACTOR =1.000E+03

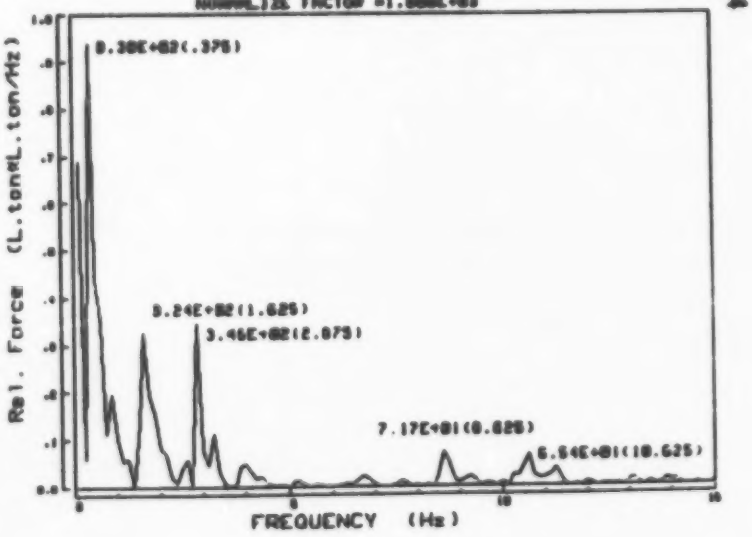

FIGURE E.10
COMPUTED FORCE SPECTRA FOR RAMMING TEST F9-1

(g)

ARCTEC CANADA LIMITED

FORCE SPECTRUM CALCULATION PROGRAM

Subject :POLAR SEA -F.S. TEST -4' max L.I. OBL.RAM. AT 9 Kt
Vessel : USCGC POLAR SEA — Test Time:FEB 9 1981 (06:20)
Sensor : ACC. SZ — Cal.Factor:1.2422('g/v)
FreqRange: 50 (Hz) — Force Unit: L.ton<L.ton/Hz
Vib. Mode: Vertical Bending — File Name: F9S2I
• Location of applied conc. load is at section 0 10.5
• Location of accelerometer is at section 7.6
• Cut-off frequency for force calculation is 15 (Hz)

Mean Square= 6.678432E+03(L.ton<L.ton)
Root Mean Square= 8.167271E+01(L.ton)

COMPUTED FORCE SPECTRUM

NORMALIZE FACTOR =1.400E+03

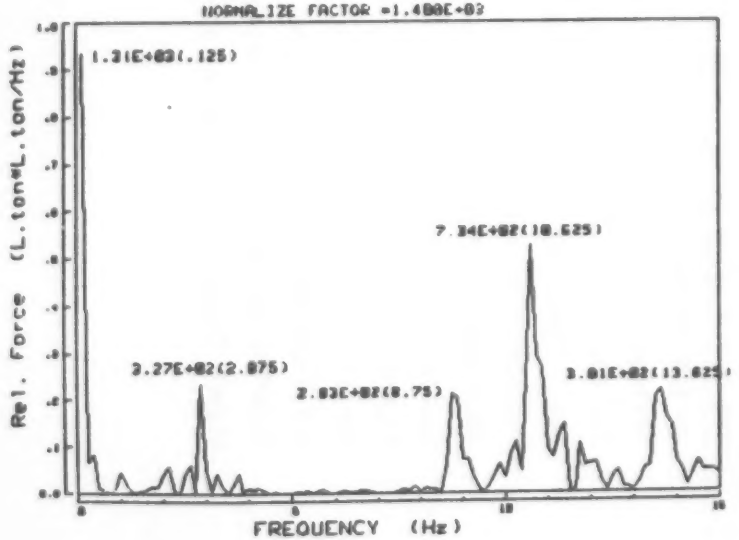

(h)

ARCTEC CANADA LIMITED

FORCE SPECTRUM CALCULATION PROGRAM

Subject :POLAR SEA -F.S. TEST -4 max L.I. OBL.RAM. AT 9 Kt
Vessel : USCGC POLAR SEA — Test Time:FEB 9 1981 (06:20)
Sensor : ACC. SZ — Cal.Factor:1.2345('g/v)
FreqRange: 50 (Hz) — Force Unit: L.ton<L.ton/Hz
Vib. Mode: Vertical Bending — File Name: F9S2I
• Location of applied conc. load is at section 0 10.5
• Location of accelerometer is at section 2
• Cut-off frequency for force calculation is 15 (Hz)

Mean Square= 8.269237E+03(L.ton<L.ton)
Root Mean Square= 9.093534E+01(L.ton)

COMPUTED FORCE SPECTRUM

NORMALIZE FACTOR =4.000E+03

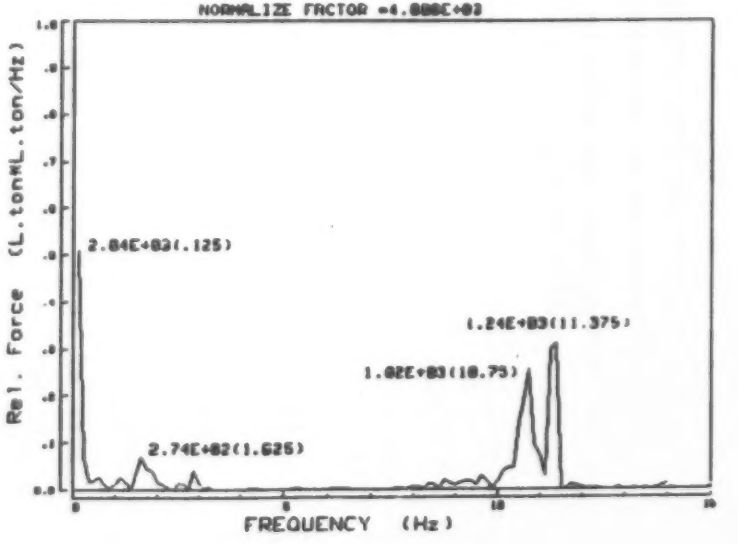

Table E.2 lists the root mean square (RMS) value of the exciting forces determined by the mathematical model from the response occurring at each vertical and horizontal accelerometer. These values are plotted and presented in Figures E.11 to E.18.

E.7.2 Discussion of Results

Acceleration Spectra

Figures E.5 a-n and E.6 a-n show the acceleration spectra for POLAR SEA ramming level ice obliquely in two incidents. The corresponding acceleration spectra for the open-water immediately prior to the impact are shown in Figures E.7 a-l and E.8 a-l. Magnitude comparison of the corresponding spectra before and at impact for each ramming case indicates that the lower frequency components (below 2 Hz) that were most dominant during impact were not detected by any accelerometer before impact. This is particularly evident from those spectra for the bow accelerometers. These lower frequency components must be associated with the ice breaking (local ice crushing, bending and failing, side cusp encounters). Such lower frequency components in the "impact" spectra (Figures E.5 a-n and E.6 a-n) are usually distributed in such a manner that there is always one sharp spike below 0.4 Hz and may be two to three less significant spikes between 0.4 to 2 Hz. The latter spikes, as discussed in Section D.2.4 are considered to be caused by the side-cusp encounters. The one at the lowest resolution must be related to the impact against ice. These low frequency spikes in the "impact" spectra were not registered as the most significant by the aft accelerometers but the most dominant frequencies were found in the middle (9-20 Hz) and higher (above 20 Hz) frequency ranges (see Figures E.5g,h,j,m and n, and Figures E.6g,h,j,m and n). It is believed that the aft accelerometers see little accelerations due to the largely attenuated impact, but are subjected to the vibrations of the stern induced by machinery, stearing hydraulics and propeller. It is also noted that none of the higher frequency components (above 30Hz) that were most dominant

TABLE E.2

ROOT-MEAN-SQUARE ICE FORCE FOR USCGC POLAR SEA

(Unit in L.Tons)

DERIVED FROM ACCELERO-METER NUMBER \ TEST	F8-0	F8-1	F8-2	F9-0	F9-1	F9-2	F9-4	F9-5
Acc. 1Y	34.74	306.71	119.12	80.96	101.38	179.44	118.21	60.18
Acc. 2Y	33.08	332.53	138.74	94.53	128.03	228.63	153.44	85.11
Acc. 3Y	36.64	242.63	89.67	64.08	106.56	166.68	109.67	59.73
Acc. 5Y	28.17	260.72	147.10	42.24	109.68	179.46	148.69	39.44
Acc. 6Y	37.10	147.08	79.67	54.49	77.20	122.00	96.54	40.13
Acc. 7Y	37.53	133.17	84.50	30.25	125.58	122.16	66.84	31.50
Acc. 1Z	47.74	135.74	81.80	99.43	95.02	128.20	70.41	52.07
Acc. 2Z	55.77	184.34	121.84	116.79	64.88	146.12	92.39	84.37
Acc. 5Z	49.53	89.66	49.21	29.97	81.67	79.71	33.91	44.65
Acc. 7Z	41.31	109.53	58.89	56.30	90.94	94.96	63.90	51.42

NOTE: Further details of the Force Spectra are given in Annex 7, Volume III.

FIGURE E.11 RMS ICE FORCE PROFILE FOR TEST F8-0
USCGC POLAR SEA

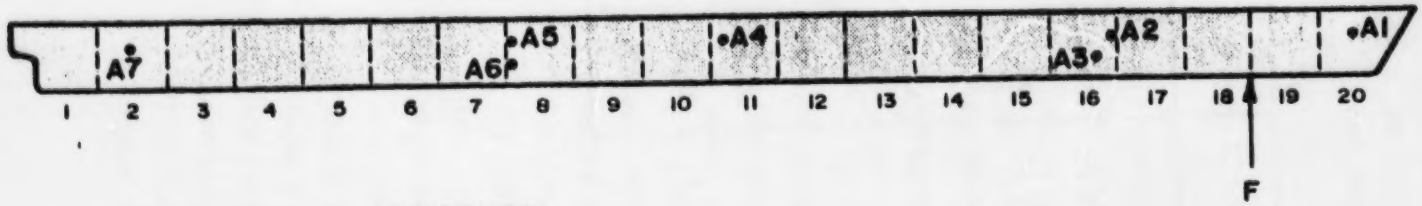

● —— HORIZONTAL

▲ - - - - VERTICAL

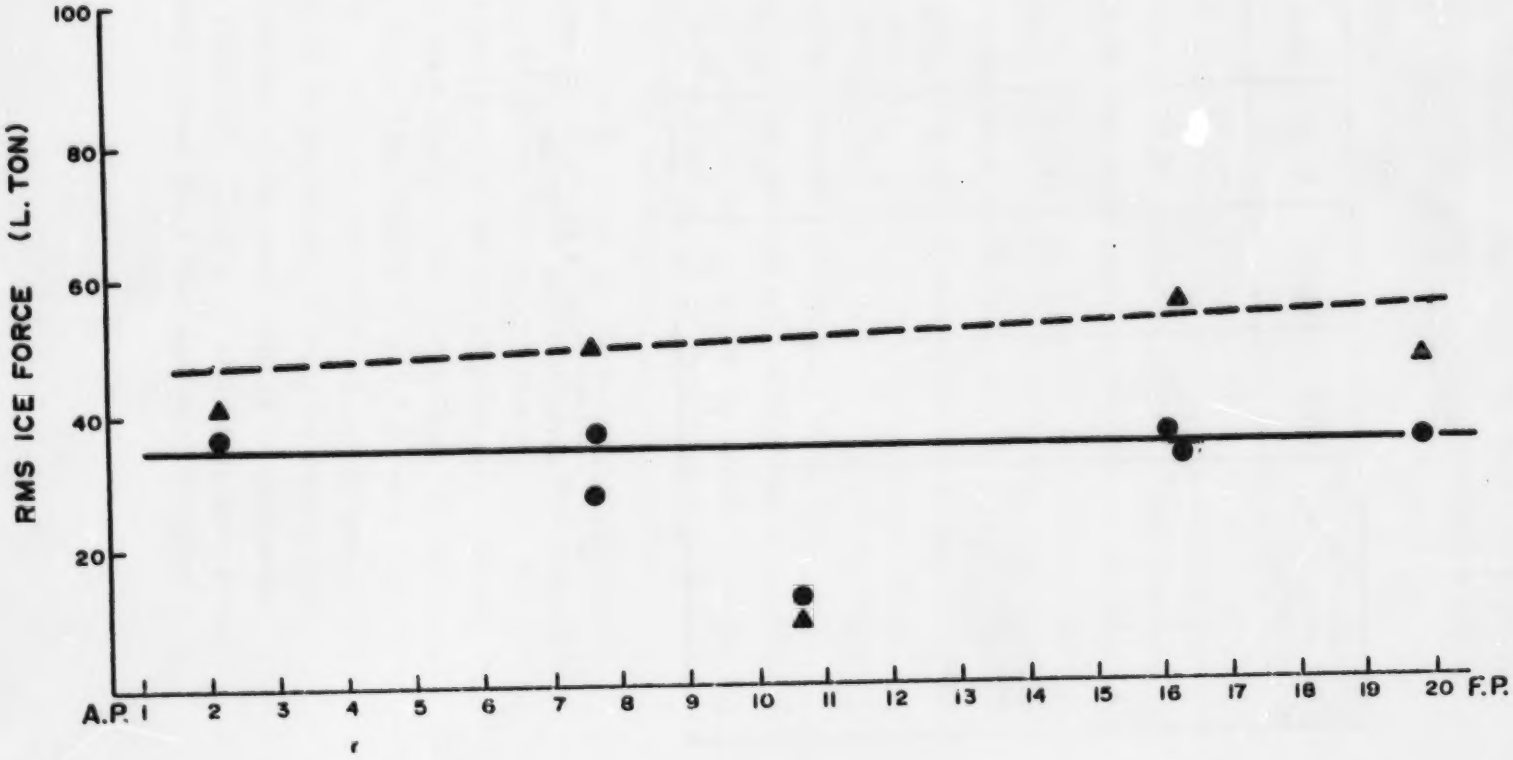

FIGURE E.12 RMS ICE FORCE PROFILE FOR TEST F8-1
USCGC POLAR SEA

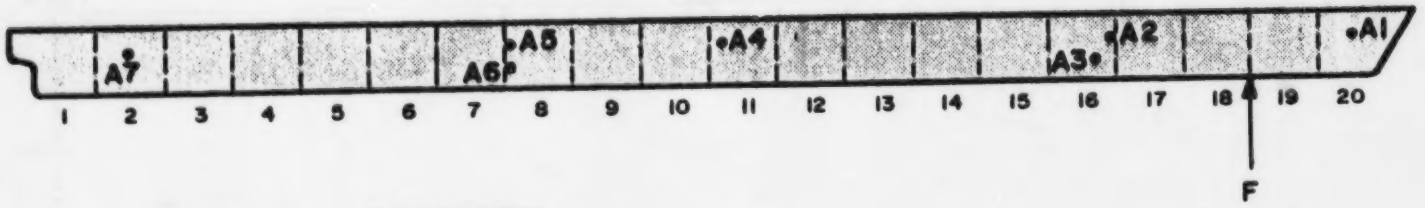

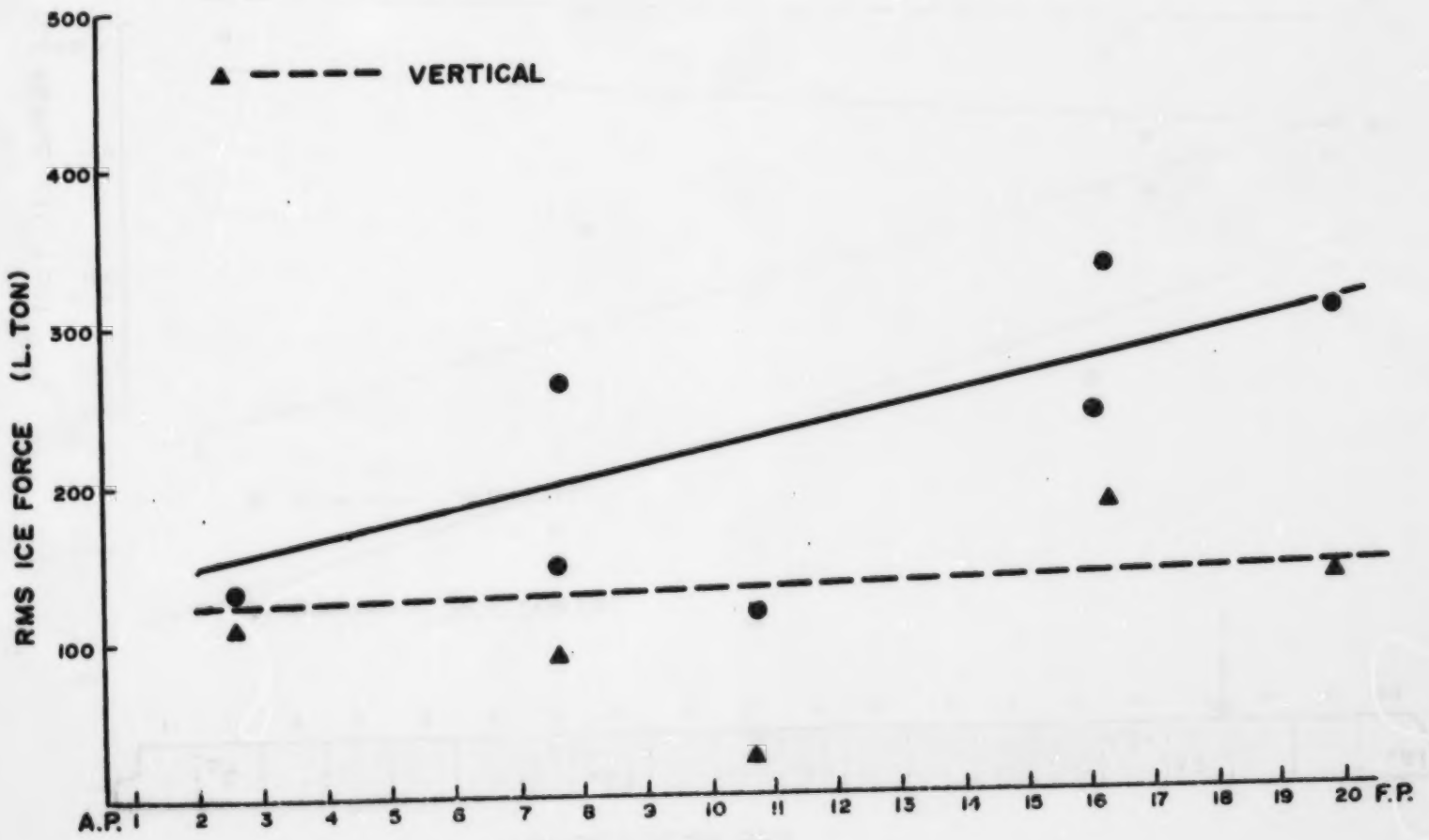

FIGURE E.13 RMS ICE FORCE PROFILE FOR TEST F8-2
USCGC POLAR SEA

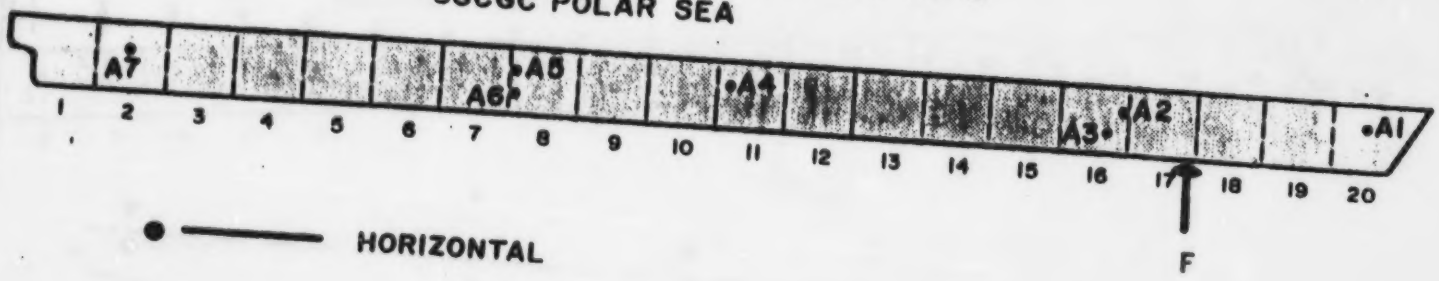

HORIZONTAL

VERTICAL

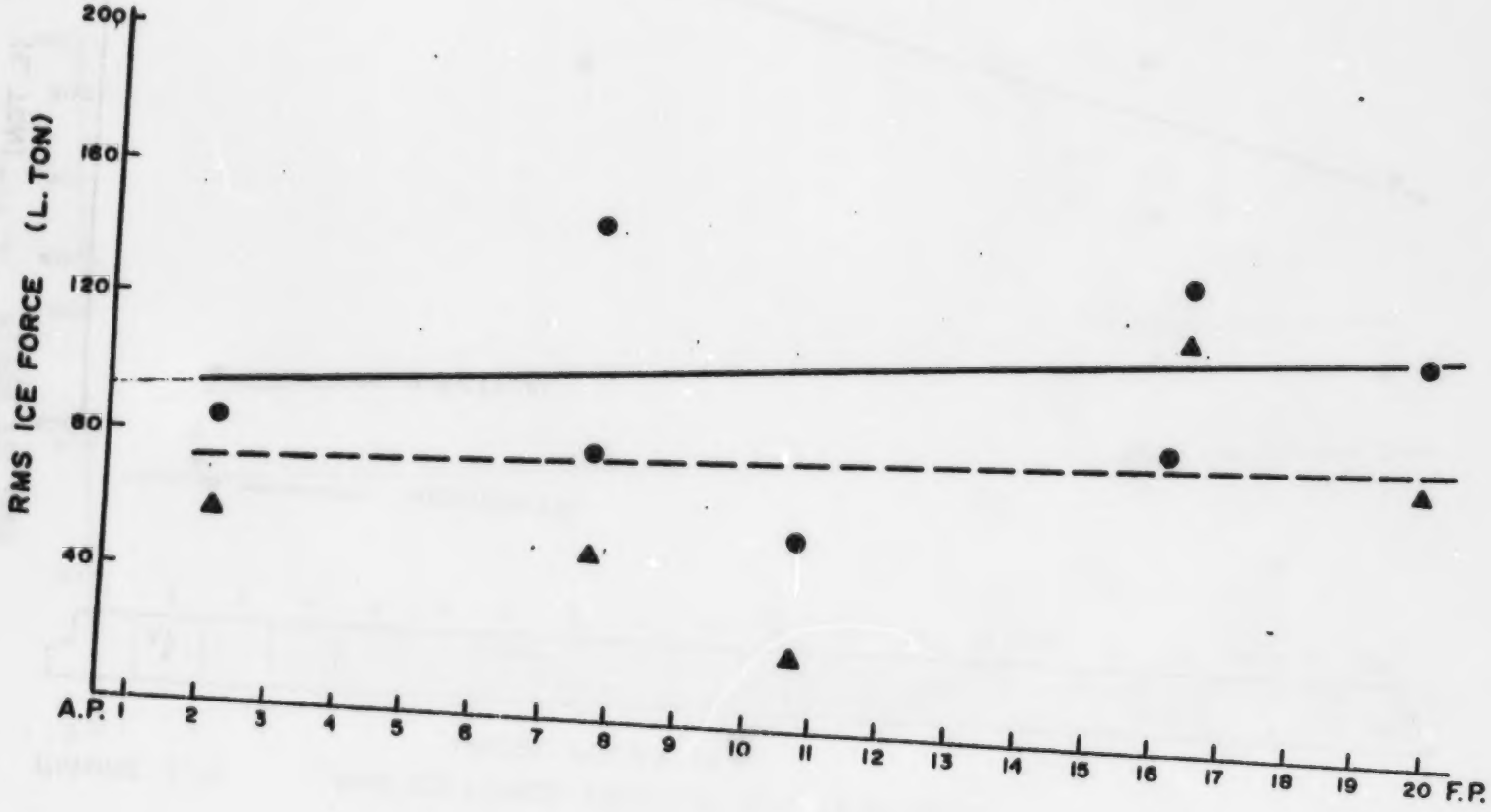

FIGURE E.14 RMS ICE FORCE PROFILE FOR TEST F9-O
USCGC POLAR SEA

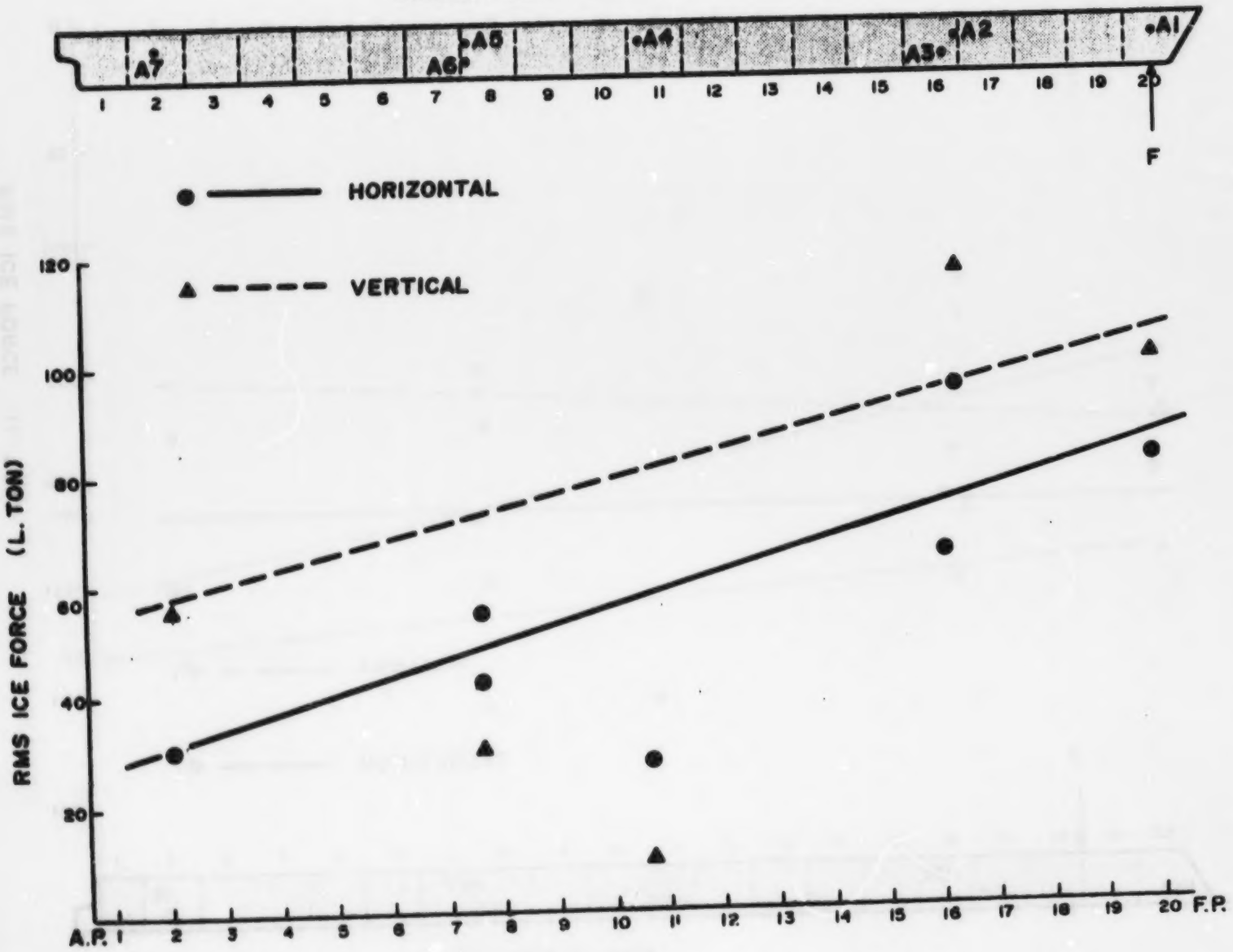

FIGURE E.15 RMS ICE FORCE PROFILE FOR TEST F9-1
USCGC POLAR SEA

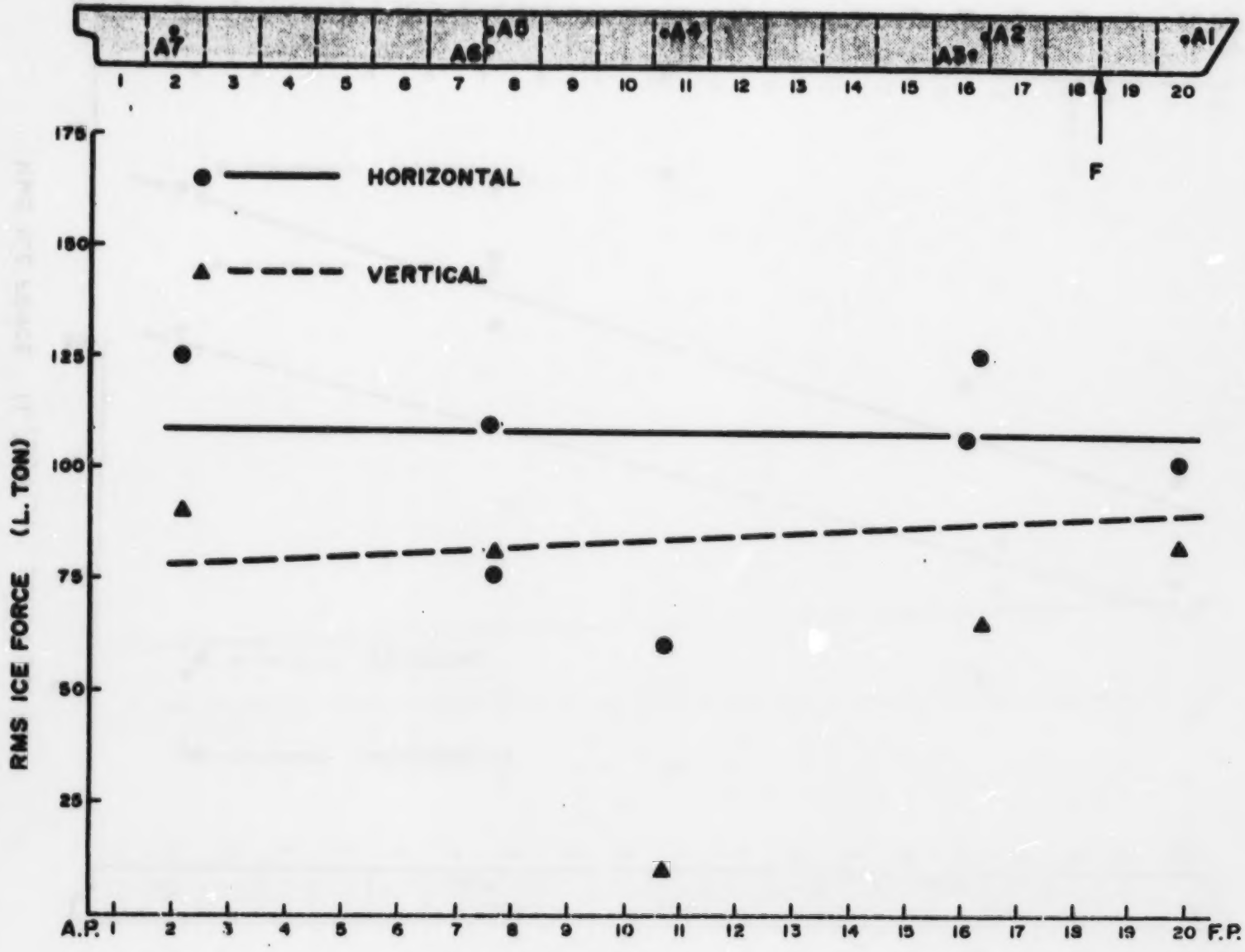

FIGURE E.16 RMS ICE FORCE PROFILE FOR TEST F9-2
USCGC POLAR SEA

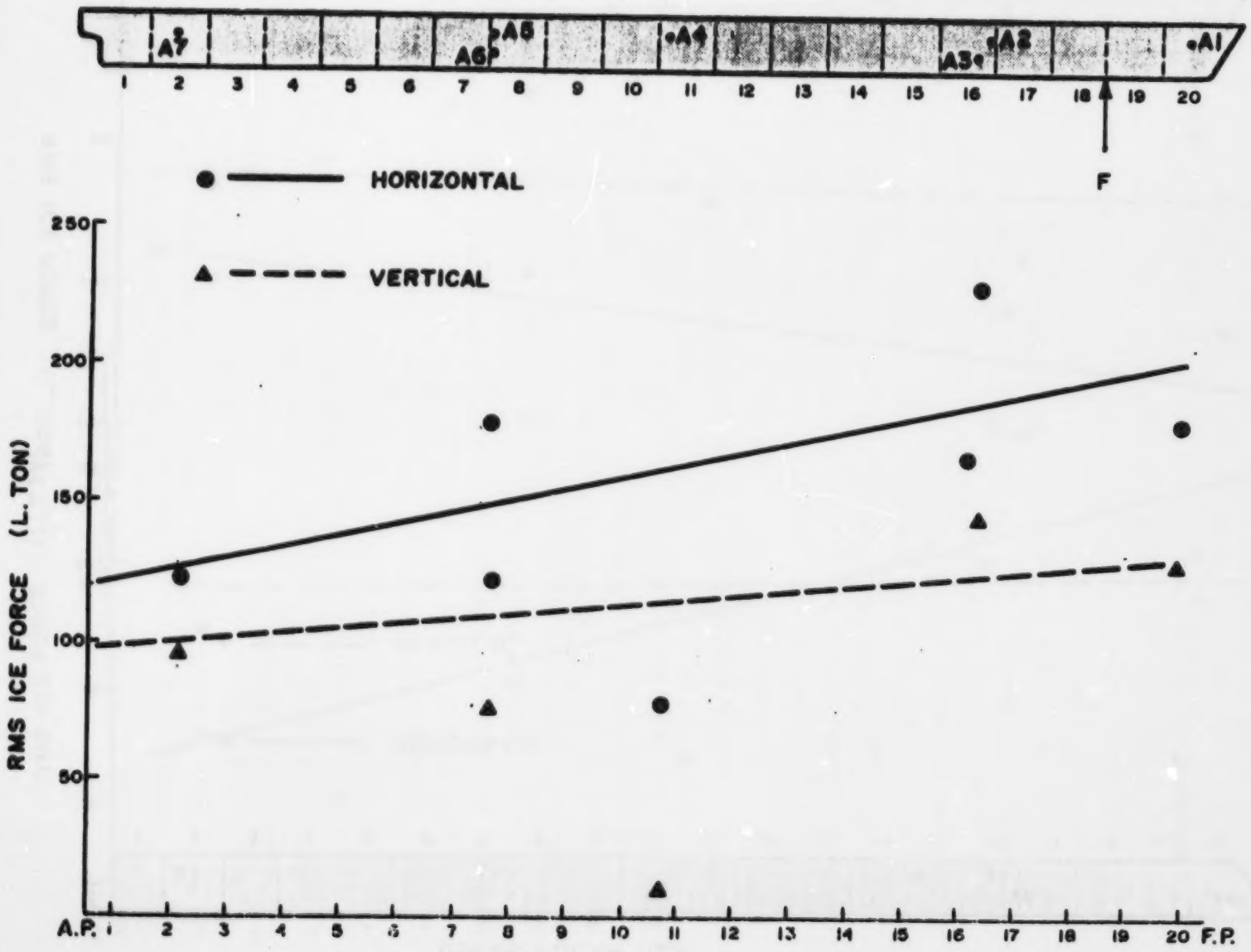

FIGURE E.17 RMS ICE FORCE PROFILE FOR TEST F9-4
USCGC POLAR SEA

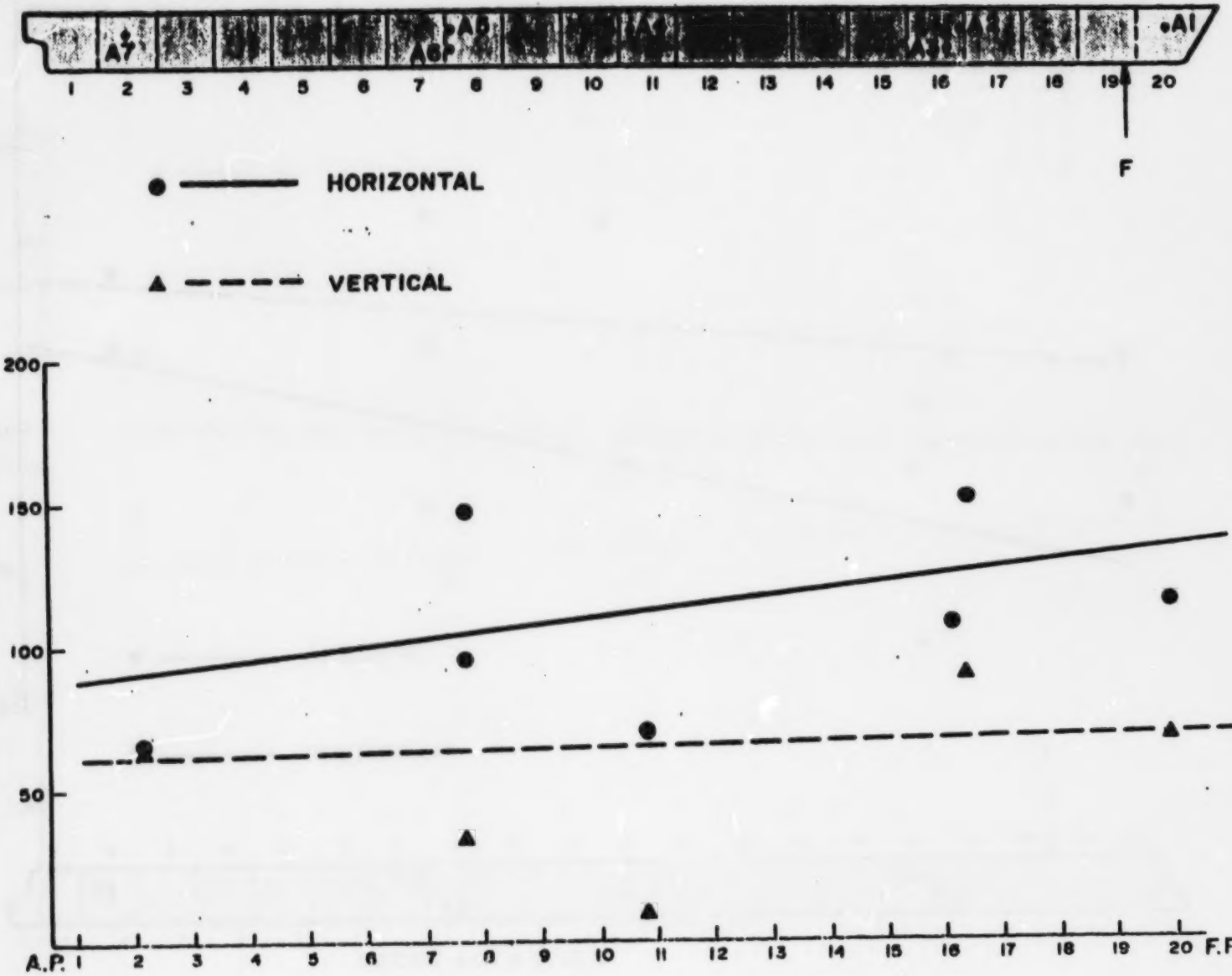

FIGURE E.18 RMS ICE FORCE PROFILE FOR TEST F9-5
USCGC POLAR SEA

● —— HORIZONTAL

▲ - - - - VERTICAL

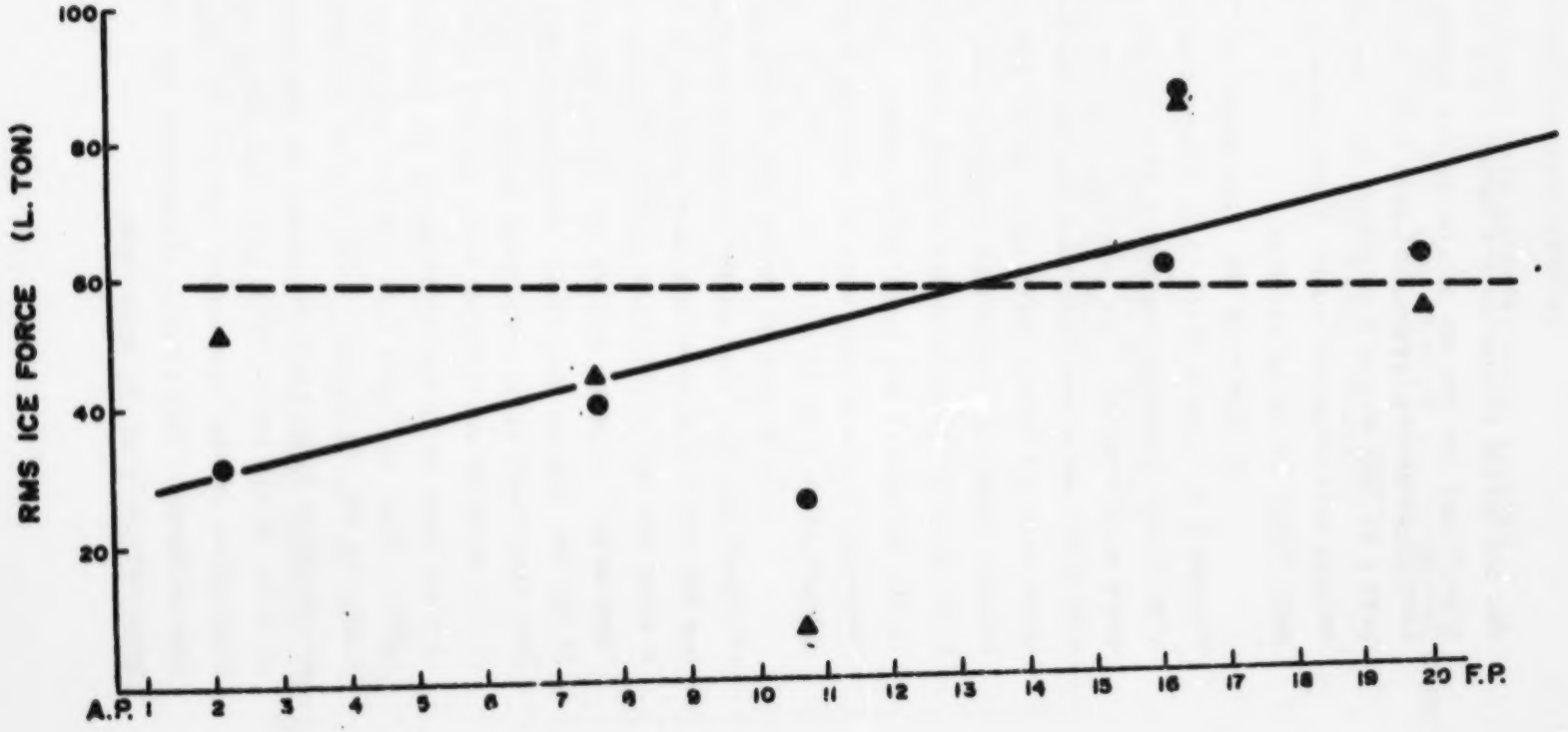

for the bottom accelerometers number 3 and number 6 were found significant for the top accelerometers number 2 and number 5. This can be seen by comparing Figure E.5f with E.5i, Figure E.5g with E.5j, Figure E.6f with E.6i, and Figure E.6g with E.6j. The difference is particularly obvious between accelerometers number 6 and number 5, as accelerometer 6 was located much closer to the machineries.

In examining the 'open-water' or "before impact" spectra Figures E.7a-l and E.8a-l) it is interesting to note the presence of two significant frequency components at 2.875 and 11.375 Hz recorded in every accelerometer. The previous component is caused by the shaft speed (173 RPM), while the latter one must be the propeller induced vibration which resulted from a shaft speed of 173 RPM with a four-blade propeller. However, magnitude comparison indicates that the level of vibration at 2.875 Hz is at least an order of magnitude higher in the vertical mode than in the horizontal and longitudinal modes. This can be readily explained as resonance as the primary mode of vertical vibration of the ship hull was calculated as 2.74 Hz.

To be able to relate the resonances at the lowest mode-forms of vibration, the "open-water" acceleration spectra up to 25 Hz for the bow and stern accelerometers were enlarged in a different scale to allow viewing the less significant spikes. Figures E.19 a-f show the enlarged "open-water" response spectra for accelerometers 1Z, 7Z, 1Y, 7Y, 2X and 7X for the ramming test F8-0. Response spectra in Figures E.19 a and b show that there exist resonance peaks at 2.875, 5.375, 7.375, 9,875 and 11.375 Hz which are situated very near the mode-forms of vibration in the vertical mode up to the fifth mode. As for the horizontal acceleration spectra shown in Figure E.19 c and d, resonance peaks appeared at 4.625, 7.625, 10.375, 14.25 and 17.875 Hz also situated close to the mode-forms of vibration up to the fifth mode. In the longitudinal mode, resonances at 8.75, 16.125 and 22.75 Hz were also noted in Figures E.19 e and f. Examination of the "open-water" spectra for other cases also show the same evidence. This clearly illustrates that the ship hull did vibrate sympathetically at its mode-forms.

FIGURE E.19 (a)

ARCTEC CANADA LIMITED

400-LINE SPECTRUM DATA INTERPRETATION PROGRAM

Subject :USCGC POLAR SEA - F.S TEST - 3.5' L.I. RAMMING (BEFORE IMPACT)
Vessel : USCGC POLAR SEA
Sensor : BOW HEAVE
Frequency: 50
File Name: F81z0
Test Time:FEB 8 1981 (02:23)
Calibration: 1.2500 (g'/v)
Sen.Range: .200(v)

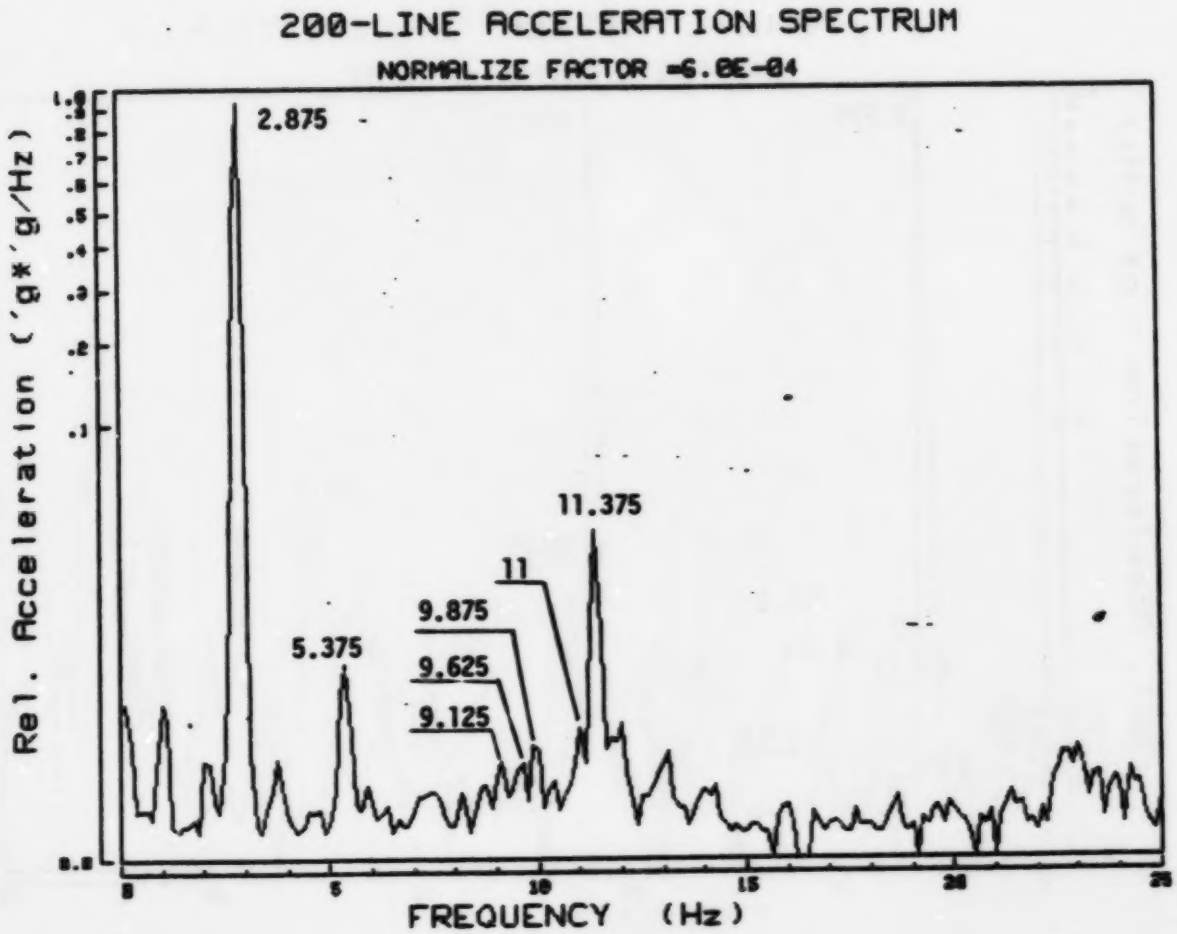

FIGURE E.19 (b)

ARCTEC CANADA LIMITED

400-LINE SPECTRUM DATA INTERPRETATION PROGRAM

Subject :USCGC POLAR SEA - F.S TEST - 3.5' L.I. RAMMING (BEFORE IMPACT)
Vessel : USCGC POLAR SEA
Sensor : ACC. 7Z
Frequency: 50
File Name: F87z0
Test Time:FEB 8 1981 (02:28)
Calibration: 1.2345 (g'/v)
Sen.Range: .500(v)

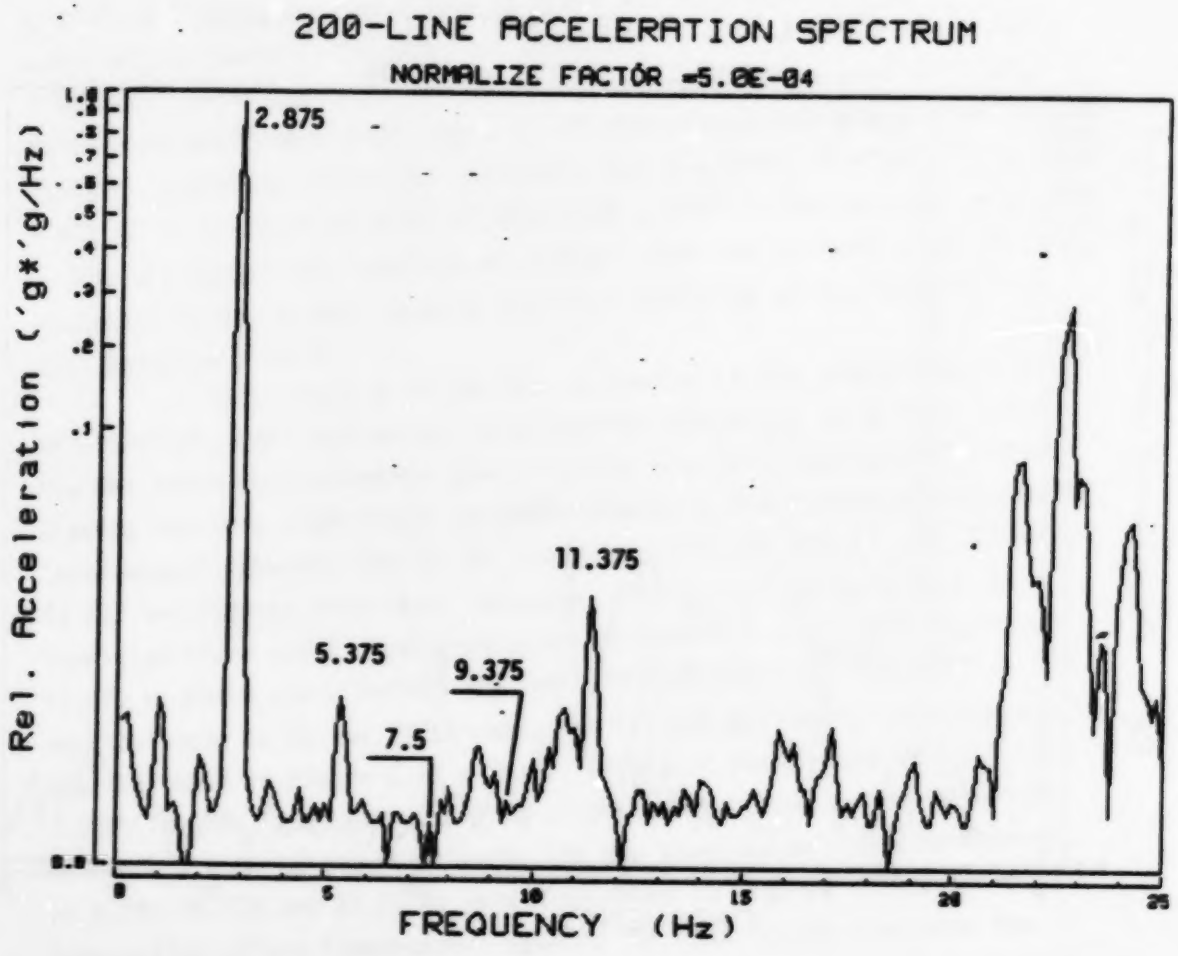

FIGURE E.19 (c)

ARCTEC CANADA LIMITED

400-LINE SPECTRUM DATA INTERPRETATION PROGRAM

Subject :USCGC POLAR SEA - F.S TEST - 3.5' L.I. RAMMING (BEFORE IMPACT)
Vessel : USCGC POLAR SEA Test Time:FEB 8 1981 (02:23)
Sensor : BOW SWAY Calibration: 1.1940 (g'/v)
Frequency: 50 Sen.Range: .200(v)
File Name: F81y0

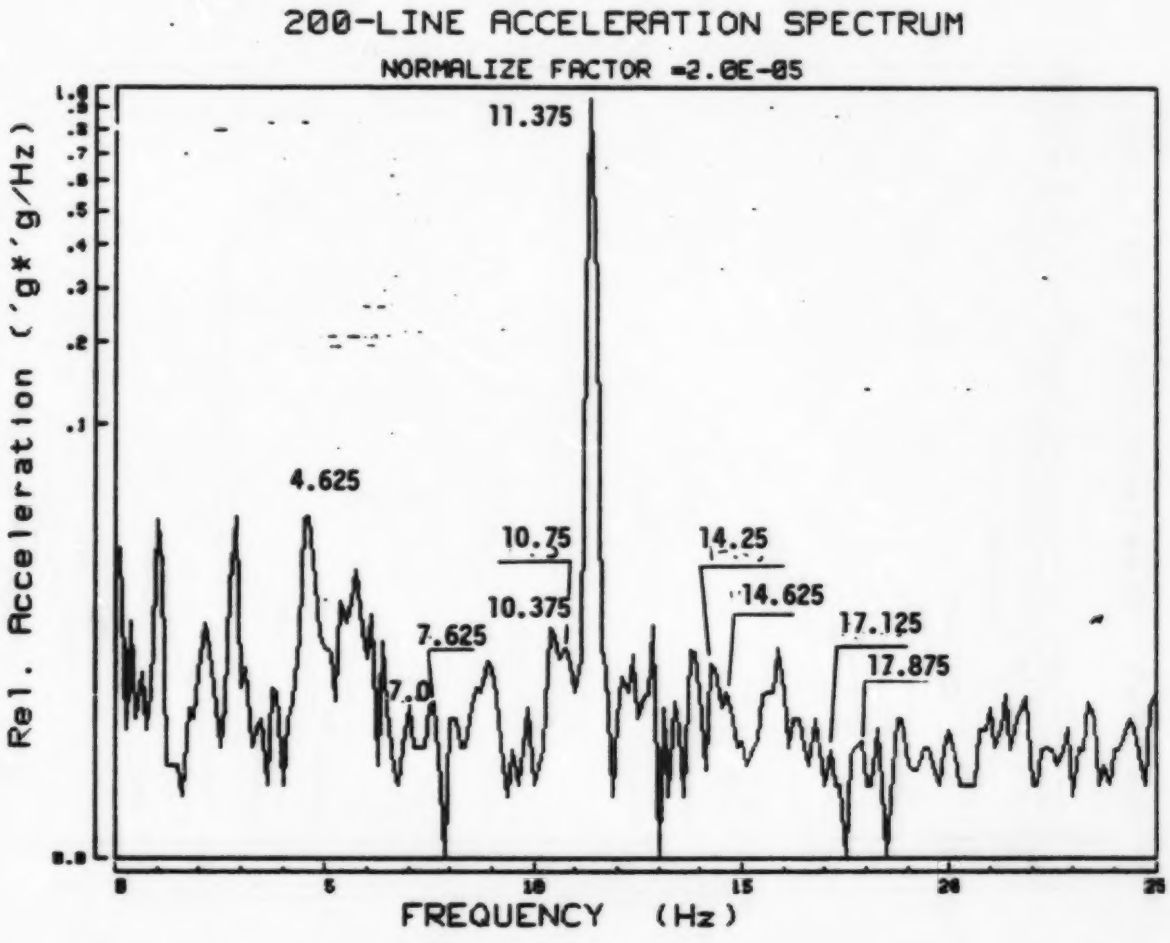

FIGURE E.19 (d)

ARCTEC CANADA LIMITED

400-LINE SPECTRUM DATA INTERPRETATION PROGRAM

Subject :USCGC POLAR SEA - F.S TEST - 3.5' L.I. RAMMING (BEFORE IMPACT)
Vessel : USCGC POLAR SEA
Sensor : ACC. 7Y
Frequency: 50
File Name: F87y0
Test Time:FEB 8 1981 (02:23)
Calibration: 1.2270 (g'/v)
Sen.Range: .500(v)

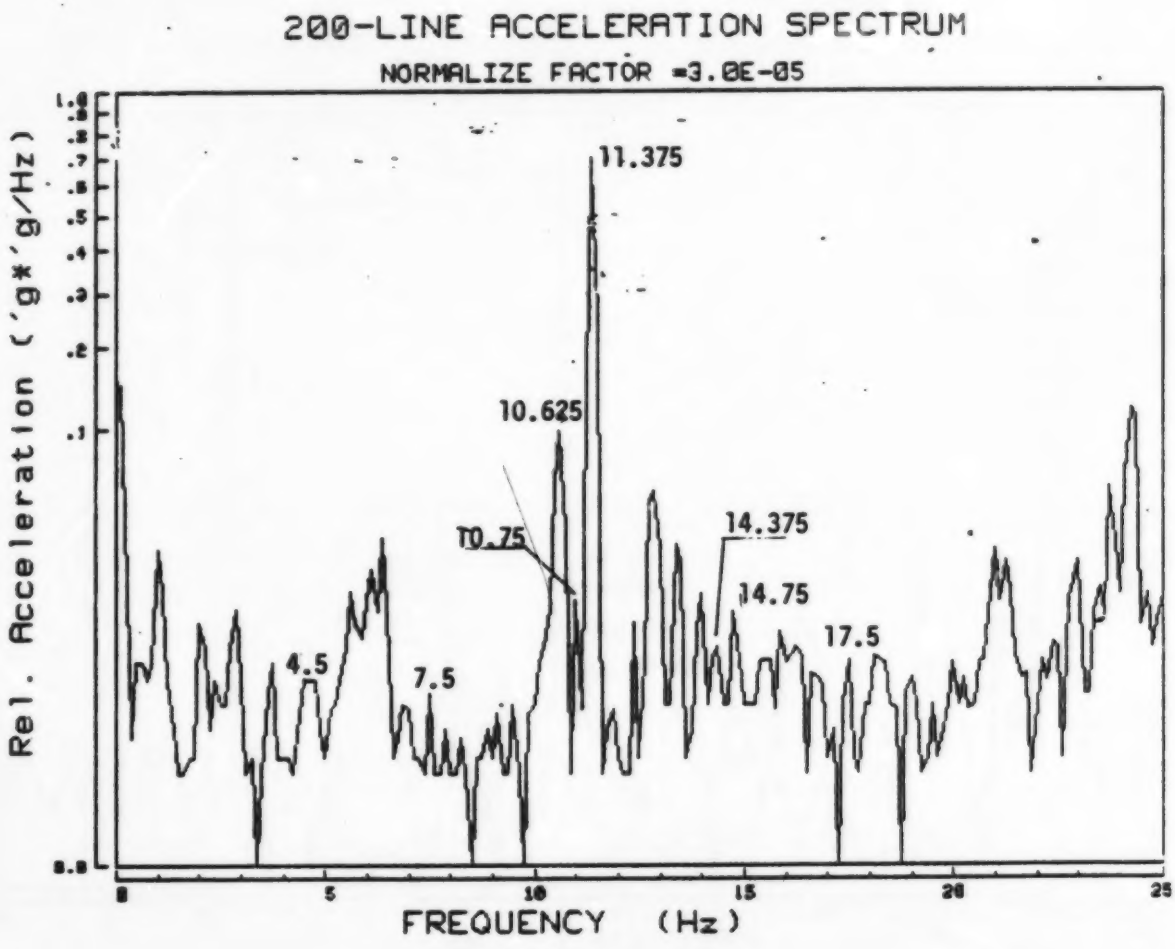

FIGURE E.19 (e)

ARCTEC CANADA LIMITED

400-LINE SPECTRUM DATA INTERPRETATION PROGRAM

Subject :USCGC POLAR SEA - F.S TEST - 3.5' L.I. RAMMING (BEFORE IMPACT)
Vessel : USCGC POLAR SEA
Sensor : ACC. 2X
Frequency: 50
File Name: F82x0
Test Time:FEB 8 1981 (02:23)
Calibration: 1.1765 (g'/v)
Sen.Range: .200(v)

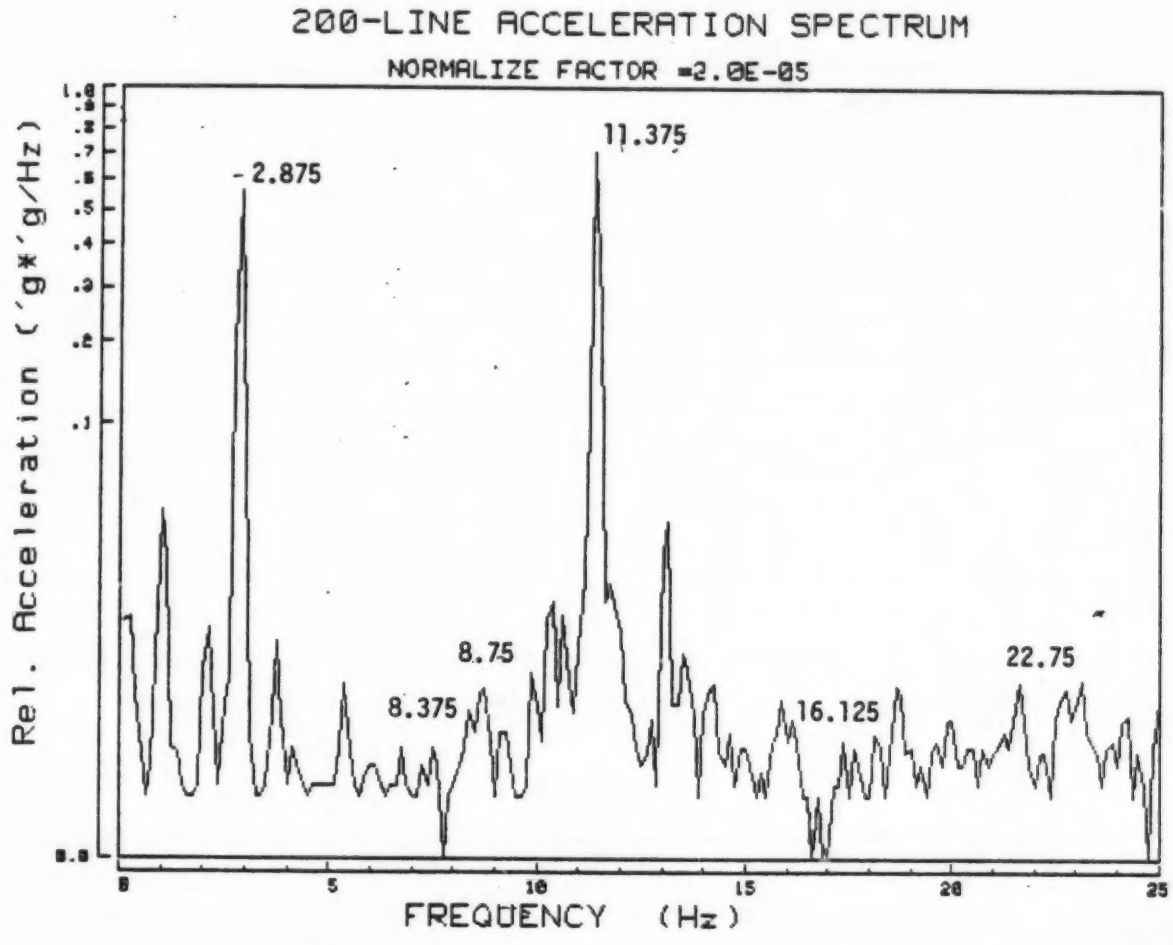

FIGURE E.19 (f)

ARCTEC CANADA LIMITED

400-LINE SPECTRUM DATA INTERPRETATION PROGRAM

Subject :USCGC POLAR SEA - F.S TEST - 3.5′ L.I. RAMMING (BEFORE IMPACT)
Vessel : USCGC POLAR SEA
Sensor : ACC. 7X
Frequency: 50
File Name: F87x0
Test Time:FEB 8 1981 (02:23)
Calibration: 1.1834 (g′/v)
Sen.Range: .500(v)

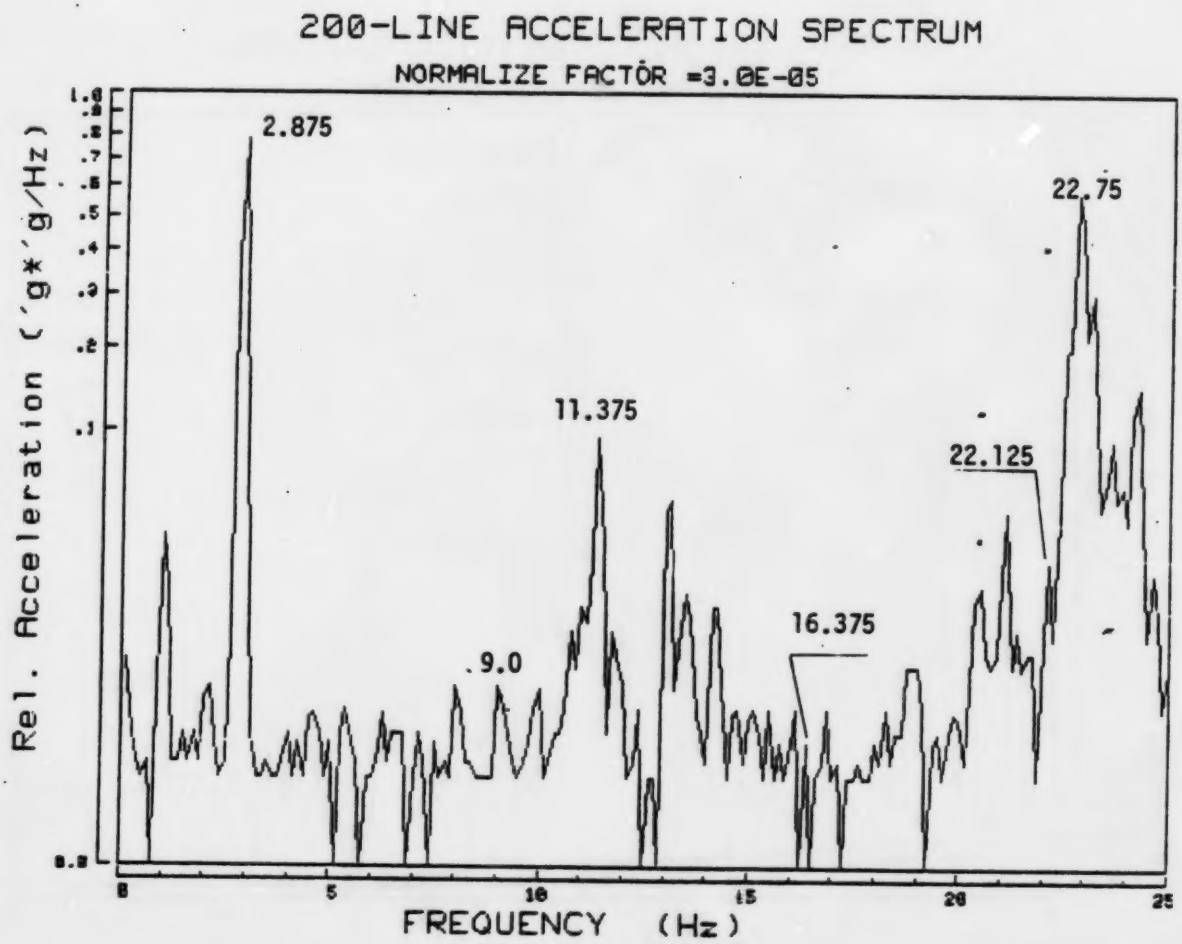

Force Spectra

It is important to point out that the response (acceleration) spectrum used in the force spectrum computation, was obtained by substracting the response spectrum in open-water before impact from that during impact. This was done to remove the propeller, machinery and hydraulic-gear induced vibrations and to obtain an acceleration spectrum that is primarily ice related. The substraction was performed in the complex plane.

Careful examination of the computed force spectra (see Figures E.9 a-h and E.10 a-h as well as results in Annex 7) indicate that the spectra usually have one to four sharp peaks in the frequency range from 0.125 to 2 Hz, then randomly die down and peak again around 10 - 12 Hz. In certain cases, several small spikes also occur between 2 and 10 Hz.

In the low frequency range (below 2 Hz), the sharp peaks can be related to ice interactions during the ramming process. Firstly, to be able to relate some of these frequencies to the ice encounters ,it is necessary to estimate the distance between the cusps in a typical ice field (Figure E.20). Under our hypothetical system, a ship will encounter an ice cusp every half of the cusp length due to unsymmetric failure of the ice allowing cusps on opposite sides to be misaligned. Figure E.21 shows experimental data on ice cusp width as a function of ice thickness and using the approximation

$$L_c = 3\, W_c$$

representing the length between ice cusps. The frequency of cusp encounters has been estimated using this data for various ice thicknesses and ship speeds and is shown in Table E.3.

It has been noted that there are, in general, fewer spikes on the spectra for the aft accelerometers than those for the forward accelerometers. This is because the stern sees little effect of the cusp breaking. Combining this information with the previous data on frequency of cusp encounters, it becomes logical that the cusp breaking accounts for the spikes between 0.5 and 1.5 Hz, while the spike at 0.125 Hz could be resulted from ice crushing during the initial contact.

FIGURE E.20

IDEALIZED SHIP TRACK

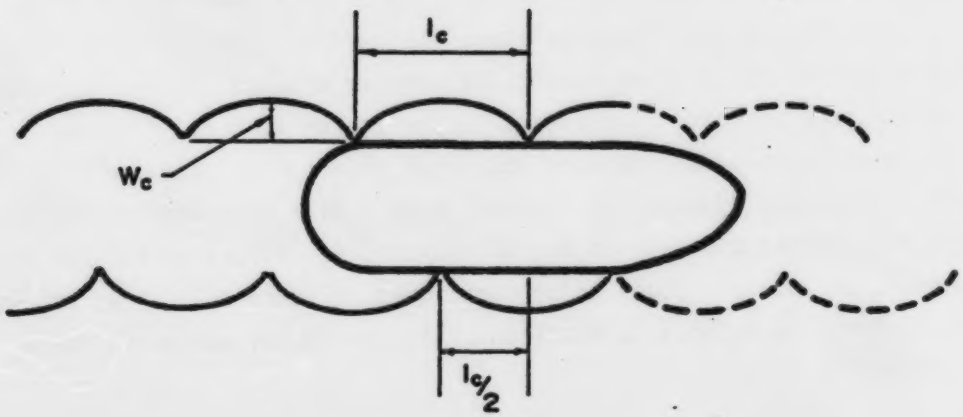

$l_c = 1.0\ W_c \rightarrow 4.0\ W_c$

.WE ASSUME $l_c = 3.0\ W_c$

FIGURE E.21

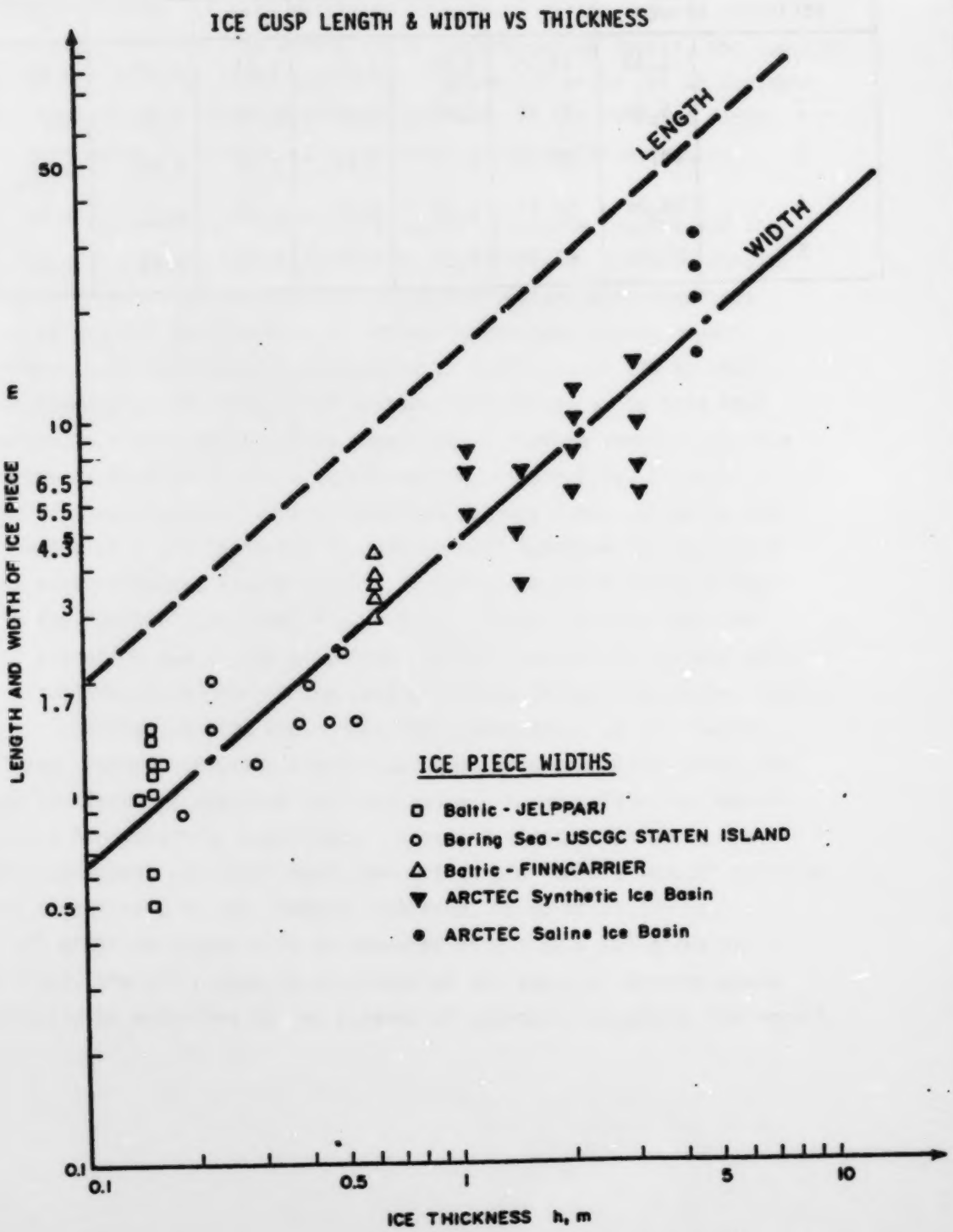
ICE CUSP LENGTH & WIDTH VS THICKNESS
LENGTH
WIDTH
LENGTH AND WIDTH OF ICE PIECE m
50
10
6.5
5.5
4.3
3
1.7
1
0.5
0.1
0.1
0.5
1
5
10
ICE THICKNESS h, m
ICE PIECE WIDTHS
Baltic - JELPPARI
Bering Sea - USCGC STATEN ISLAND
Baltic - FINNCARRIER
ARCTEC Synthetic Ice Basin
ARCTEC Saline Ice Basin

TABLE E.3

ESTIMATES OF FREQUENCY OF CUSP ENCOUNTERS

ICE THICKNESS (ft)	CUSP DEPTH Wc	CUSP LENGTH Lc	SHIP SPEED (IN KNOTS)					
			4	6	8	10	12	14
1	5.58	16.74	0.81	1.21	1.61	2.02	2.42	2.82
2	9.84	29.52	0.46	0.69	0.91	1.14	1.37	1.60
3	14.11	42.33	0.32	0.48	0.64	0.80	0.96	1.12
4	18.04	54.12	0.29	0.37	0.50	0.62	0.75	0.87
5	21.33	63.98	0.21	0.32	0.42	0.53	0.63	0.74

The force spikes above 2 Hz that were dominant as shown in Figures E.9a, E.9h, E.10 d, E.10g and E.10h were very much in doubt, those at 2.875 and 11.375 Hz in Figures E.9a and E.9h in particular. The frequencies at 2.875 and 11.375 Hz as discussed earlier, are related to shaft speed and propeller noise. If such machinery/propulsion system induced vibration were completely removed from acceleration spectra during impact, the spectral density of ice force at these particular frequencies would not be dominant at all. However, the presence of dominant peaks in the computed force spectra were noted to situate at these machinery/propulsion induced frequencies.

Examination of the "before impact" response spectra and the impact response spectra revealed that the magnitudes of spectral density at certain frequencies, detected by the accelerometers were sometimes noted to be greater for the case of before impact than during impact. The difference is particularly noticeable at 2.875 and 11.375 Hz which are associated with the propulsion system. For instance, in test F8-0 the acceleration peak at 11.375 Hz appearing in "before impact" spectrum for the bow transverse (Y-dir.) accelerometer, Figure E.7e, is about 13 times of that shown in "impact" spectrum, Figure E.5e. As well, the peak situated at 2.875 Hz in the "before impact" spectrum for the stern vertical accelerometer, Figure E.7(1), is approximately 4 times of that shown in the "impact" spectrum, Figure E.5n. These indicate that the level of vibration due to the propulsion system induced, in certain part of the structure, is higher in the case of before impact than during impact.

Bearing in mind that since the subtraction of the "before impact" and "impact" response spectra was done in the complex plane, the resulted acceleration spectrum that was assumed to be solely ice induced will always have positive magnitudes. Thus, in a situation where the frequency component was found most dominant in the "before impact" spectrum but less significant in the "impact" spectrum, (e.g. at 11.375 Hz, 1.88×10^{5} g^2/Hz in Figure E.7e as compared with 1.50×10^{6} g^2/Hz in Figure E.5e), the difference in magnitude of the spectral density would automatically be accounted for as a level of vibration caused by ice impact.

As in this case, the magnitude of the acceleration peak resulted after subtraction will still be greater than that seen in the "impact" spectrum because of the two-order of magnitude difference between the two peaks. However, judging from the fact that the bow tranverse accelerometer (Acc 1Y) never detected such a high level of frequency response during impact (as compared with Figure E.5e). This clearly indicates that the present method of removing the propulsion system induced vibration from the "impact" response spectrum needs further refinement. Few comments have therefore been made on force spectra for the frequency ranges above 2 Hz.

On the other hand, such propulsion induced vibration did not seem to contribute to the spectrum below 2 Hz, the previous discussion on the force peaks between 0 and 2 Hz will still be applicable.

Figures E.11 to E.18 show the root-mean-square ice force profiles for the 8 selected ramming cases. The solid and broken lines in each figure represent the best-fit line for the horizontal (Y-direction) and vertical (Z-direction) force component respectively.

According to the theory discussed in section E.2, it is possible to determine for any point in the structure the excitation force from the measured response of the structure. Therefore, the ice force profile would ideally be a straight level line. That is, the root-mean-square ice forces derived from any one of the tranverse accelerometers would be essentially the same or very much in the same order of magnitude. The same can be said for the vertical force components.

The accuracy of the force spectrum calculation program depends on the assumption that the excitation force is a concentrated force. This is not so for the 8-second window of time transient chosen. It also depends on the estimates of the points of impact obtained from the video review and the frequency of vibration (ω) calculated by the GBRP. The accuracy of the GBRP depends on parameters such as ship's mass, inertia, stiffness, etc. Sensitivity analyses required to provide error estimates have not been carried out on the above parameters. A study of Figures E.11 to E.18, however, shows fair agreement in the derived force for four of the eight cases studied (viz: Figures E.11, 13, 15 and 17) with the remainder varying from reasonable (Figures E.12 and 16) to poor, thus giving an idea of the accuracy of the program.

E.8 References

1. Henderson, F.M. and Cuthill, E., "Description and Usage of General Bending Response Code 1 (GBRCL)", DTNSRDC Report 1925, David Taylor Model Basin, Washington, D.C., July 1965.

2. McGoldrick, R., "Ship Vibrations, " DTNSRDC Report 1451, David Taylor Model Basin, Washington, D.C., December 1960.

3. Bishop, R.E.D., Eatock-Taylor, R. and Jackson, K.L., "On the Structural Dynamics of Ship Hulls in Waves", Trans. RINA, Vol.115, 1973.

4. Crandall, S.H. *Random Vibration*, M.I.T., Press, Cambridge, Mass. 1963.

5. Young, D. and R.P. Felgar, "Tables of Characteristic Functions Representing Normal Modes of a Beam", University of Texas Publication No.4913, July 1949.

6. Golden, M.E. and Henderson, F.M., "An Updated Guide to the Use of General Bending Response Program (GBRP)," David W.Taylor Naval Ship Research and Development Center, Report 4601, April 1965.

7. Popov, Yu. N., "Strength of Ships Navigating in Ice", Sudostroenic, Leningrad, 1968.

8. Nicolet Scientific Corporation, "Instruction Manual For Model 446 Mini-Ubiquitous FFT Computing Spectrum Analyzer."

9. Brüel and Kjaer, "Frequency Analysis", by R.B. Randall, B. Tech., B.A.

POOR

QUALITY

ORIGINAL